FINAL REPORT

Environmentally Benign Multi-Component Delay System with Tunable Propagation Characteristics

SERDP Project WP-2519

JANUARY 2020

Matthew Puszynski
Innovative Materials & Processes LLC

SERDP
DOD ▪ EPA ▪ DOE

Page Intentionally Left Blank

Page Intentionally Left Blank

REPORT DOCUMENTATION PAGE

Form Approved
OMB No. 0704-0188

1. REPORT DATE *(DD-MM-YYYY)*	2. REPORT TYPE	3. DATES COVERED *(From - To)*
22-01-2020	SERDP Final Report	25-06-2015 – 24-06-2019

4. TITLE AND SUBTITLE

Environmentally Benign Multi-Component Delay System with Tunable Propagation Characteristics

5a. CONTRACT NUMBER
W912HQ-15-C-0022

5b. GRANT NUMBER

5c. PROGRAM ELEMENT NUMBER

6. AUTHOR(S)
Matthew Puszynski
Dan Perkins
Dr. Jan Puszynski

5d. PROJECT NUMBER
WP-2519

5e. TASK NUMBER
Task 14

5f. WORK UNIT NUMBER

7. PERFORMING ORGANIZATION NAME(S) AND ADDRESS(ES)

Innovative Materials and Processes, LLC
8420 Blackbird Court
Rapid City, SD 57702

8. PERFORMING ORGANIZATION REPORT NUMBER

WP-2519

9. SPONSORING / MONITORING AGENCY NAME(S) AND ADDRESS(ES)

Strategic Environmental Research and Development Program
4800 Mark Center Drive, Suite 16F16
Alexandria, VA 22350-3605

10. SPONSOR/MONITOR'S ACRONYM(S)
SERDP

11. SPONSOR/MONITOR'S REPORT NUMBER(S) WP-2519

12. DISTRIBUTION / AVAILABILITY STATEMENT
DISTRIBUTION STATEMENT A. Approved for public release: distribution unlimited.

13. SUPPLEMENTARY NOTES

14. ABSTRACT
This report describes the results generated by Innovative Materials and Processes, LLC (IMP) related to the development of an environmentally benign gasless pyrotechnic delay formulation for use in pyrotechnic applications. The work is sponsored by the Strategic Environmental Research and Development Program (SERDP) under project WP-2519 (Contract W912HQ-12-C-0022). The project has focused on the replacement of lead, chromate, and perchlorate-based compounds from current pyrotechnic delay applications. The new system consists of fuel and oxidizer components that were reviewed by the Army Public Health Center and have been found to have a reduced environmental impact. An aluminum-silicon-strontium molybdate based pyrotechnic gasless delay formulation with a tunable inverse burn rate (IBR) in the range between 1.33 and 11 seconds per inch was developed. The material has been characterized within M201A1, M213, and M228 fuze assemblies and yielded the required delay times. Two alternative lead-free M42 primers have been successfully been tested to replace the legacy lead-based primers currently in production.

15. SUBJECT TERMS Gasless pyrotechnic delay, environmentally benign, variable inverse burn rate, sub-assembly test fixture, M201A1 fuze assembly, M213/M228 fuze assembly

16. SECURITY CLASSIFICATION OF:			17. LIMITATION OF ABSTRACT	18. NUMBER OF PAGES	19a. NAME OF RESPONSIBLE PERSON
a. REPORT	b. ABSTRACT	c. THIS PAGE			Matthew Puszynski
UNCLASS	UNCLASS	UNCLASS	UNCLASS	203	19b. TELEPHONE NUMBER *(include area code)* (720)935-0671

Standard Form 298 (Rev. 8-98)
Prescribed by ANSI Std. Z39.18

Page Intentionally Left Blank

Table of Contents

List of Figures

List of Tables

List of Acronyms

ºF	Degrees Fahrenheit
ºC	Degrees Celsius
ADP	Ammonium Dihydrogen Phosphate
Al	Aluminum
ARDEC	Armament Research Development and Engineering Center
ASTM	American Society for Testing and Materials
B	Boron
$BaCrO_4$	Barium chromate
BET	Brunauer–Emmett–Teller
Bi_2O_3	Bismuth trioxide
cc	Cubic centimeter
D.E.	Diatomaceous earth
DoD	Department of Defense
DSC	Differential scanning calorimeter
EBA&D	Ensign-Bickford Aerospace and Defense
EDS	Energy Dispersive X-ray Spectrometry
EPA	Environmental Protection Agency
ESD	Electrostatic Discharge
Fe_2O_3	Iron oxide
g	Gravity
g	Gram
HMX	Octogen
ID	Internal diameter
IMP	Innovative Materials and Processes, LLC
in	Inch
inHg	Inches Mercury
J g^{-1}	Jules per gram
K	Kelvin
KIO_4	Potassium periodate
ksi	Kilo pound per square inch
lb_f	Pound force
mg	Milligram
MIL-SPEC	Military Specification
µL	Microliter
mL	Milliliter
Ni	Nickel
NiCr	Nickel chrome
OD	Outer diameter
R&D	Research and Development
RDT&E	Research, Development, Testing, and Evaluation
s	Seconds
SAT	Sub-assembly test
SDSM&T	South Dakota School of Mines and Technology
s/in	Seconds per inch
SERDP	Strategic Environmental Research and Development Program
SHS	Self-propagating high temperature synthesis
Si	Silicon
$SrMoO_4$	Strontium molybdate
SiO_2	Silicon oxide
TGA	Thermal gravimetric analysis
TOI	Threshold of Ignition
VDC	Volts Direct Current
W/m·K	Watts per meter Kelvin
wt%	Weight percent
XRD	X-ray diffraction crystallography
ZPP	Zirconium potassium perchlorate
Zr	Zirconium

Key Words

Gasless pyrotechnic delay, environmentally benign, variable inverse burn rate, sub-assembly test fixture, M201A1 fuze assembly, M213/M228 fuze assembly.

Acknowledgments

Innovative Materials and Processes, LLC would like to acknowledge the financial support of the SERDP Weapons and Platform Program for SERDP Project WP-2519 under contract W912HQ-C-15-0022.

1. Abstract

To find a replacement for currently used, but environmentally hazardous, delay mixtures consisting of potassium perchlorate, barium chromate (containing hexavalent chromium), and lead compounds, a collaborative R&D project between Innovative Materials and Processes, LLC (IMP) and Ensign-Bickford Aerospace & Defense Company (EBA&D) was funded by the Strategic Environmental Research and Development Program (SERDP) under the project WP-2519 (Contract W912HQ-12-C-0022).

The main technical objective of this R&D project was focused on the development of a multi-component environmentally benign pyrotechnic delay system with burn-rate tunability within the required temperature range (-65 ^{o}F to 160 ^{o}F). The project focused on M201A1 and the M213/M228 fuze assemblies used by the Department of Defense (DoD). M201A1 fuzes require a 1 to 2.3 s burn time from ignition of the M39A1C primer to ignition of an internal output charge. The M213/M228 fuzes have a burn time specification range of 4 to 5.5 s from initiation of the M42 primer to ignition of the C70 detonator. All reactants and additives involved in the selected delay systems were evaluated as prescribed in ASTM E2552-16.

Based on the thermodynamic analyses and preliminary experimental results collected prior to the submission of the proposal, IMP proposed the use of $SrMoO_4$ as the oxidizer in the new delay formulation. The key advantage of this replacement is that $SrMoO_4$ is a very similar oxidant to $BaCrO_4$, while meeting all environmental standards. The proposed binary fuel of Si and Al, as well as SiO_2 and Diatomaceous Earth powders, also meet the environmental standards. The technical approach undertaken in this project included: 1) fundamental understanding of thermodynamic and kinetic properties of the proposed gasless reacting system; 2) mathematical modeling of combustion front propagation in the actual device geometry; 3) measurements of burn rates and determination of performance characteristics of the system understudy at different temperatures; and 4) testing of M201A1 and M213/M228 fuzes.

The comprehensive data generated in this R&D project include the effect of the pyrotechnic reactive system stoichiometry, binary fuel ratio, and fuel particle size on inverse burn rate. The developed formulations are demonstrated in two different fuze applications. The proposed gasless reacting system has shown tunable inverse burn rates between 1.33 and 11 seconds per inch in fuze assembles. The environmentally benign delay formulation was characterized in the M201A1 fuze assembly at -65 ^{o}F, 70 ^{o}F, and 160 ^{o}F with an average burn time of 1.76, 1.66, and 1.56 seconds with standard deviations of 0.05, 0.06, and 0.05 seconds, respectively. This formulation has also been successfully demonstrated in M213/M228 fuzes.

Material sensitivity characterization (electrostatic discharge, impact, and friction) and, the long-term chemical compatibility of the pyrotechnic delay; as well as, the determination of reaction kinetics and two-dimensional (2-D) modeling of combustion front propagation in various cylindrical geometries using the COMSOL software is presented. All necessary kinetic parameters, like activation energy, were measured during this R&D project. Using this data, a heat flow model was generated using Solidworks Simulation Software. This model demonstrates the flow of heat through the M213/M228 fuze system and identifies locations within this specific fuze body's geometry and material that presents propagation concerns. These analyses provided

more in-depth understanding of the fuze system and its limitations. Finally, the use of resonant acoustic mixing (RAM) technology has been the key aspect of making this project successful. The use of this technology has been widely documented and this contribution provides substantial evidence of its viability as a mixing technique.

IMP and EBA&D companies contributed to this project with both environmentally benign M42 primers and C70 detonators. Two primer systems were investigated as potential replacements for the legacy lead styphnate primer. Both metastable interstitial composite (MIC) and DBX-1 based primer systems demonstrated excellent results. Also, IMP investigated improvement of the M67 fragmentation grenade's entire firing train to obtain an environmentally benign system, by removing the lead styphnate and lead azide components of the C70 detonator replacing it with DBX-1. The successful results provided the first ever fully an environmentally benign explosive train that resides in the M67 grenade system.

Based on the performed experimental and modeling studies as well as successful testing in the fuze hardware, it can be concluded that the new environmentally acceptable delay material exhibits a wide range of tunability and meets required military performance standards. Therefore it could be considered for qualification tests in selected military applications, requiring replacement of the currently used delay mixtures.

2. Objectives

The technical objective of the proposed R&D project was focused on the development of a multi-component environmentally benign pyrotechnic delay system with inverse burn-rate tunability within the required temperature range (-65 ^{o}F to 160 ^{o}F). This new delay formulation will be tested and characterized in the M201A1 and M213/M228 fuze assemblies to meet the application specific burn times.

This project focused on M201A1 and the M213/M228 fuze assemblies used by the Department of Defense (DoD). M201A1 fuzes require a 1 to 2.3 s burn time ignited by an M39A1C primer to ignition of an internal output charge. The M213/M228 fuzes have a burn time specification range of 4 to 5.5 s from initiation of the M42 primer to ignition of the C70 detonator. In addition to the development of the environmentally benign delay formulation, IMP selected and tested M42 primers, M213/M228 fuzes, and C70 detonators that would meet the environmental and performance standards. All reactants and additives involved in the selected delay systems were evaluated as prescribed in ASTM E2552-16.

The main objective of the proposed R&D work was the replacement of the currently used, but environmentally hazardous, delay mixtures consisting of potassium perchlorate, barium chromate (containing hexavalent chromium), and lead compounds. Based on the thermodynamic analyses of different reacting systems, IMP's expertise in the area of self-propagating high temperature synthesis (SHS) and gasless delays (5-10 ml/g)[1], as well as, preliminary experimental results collected prior to the submission of the proposal, IMP proposed the use of $SrMoO_4$ as the oxidizer in the new delay formulation. The key advantage of this replacement is that $SrMoO_4$ is a very similar oxidant to $BaCrO_4$, while meeting all environmental standards. The proposed binary fuel of Si and Al, also meet the environmental standards.[2]

This report addresses the milestones/tasks 1-14. A list of the tasks associated with this project are presented in Table 2.1.

Table 2.1. *Tasks associated with period of performance for the development of an Environmentally Benign Multi-Component Delay System with Tunable Propagation Characteristics project.*

Task #	Task	Expected Completion Date	Completed
1	Chemical compatibility testing	12/2017	03/2018
2	Development of optimized formulations meeting the burn rate specifications from 4 - 12 s/in at -65 ^{o}F, 70 ^{o}F, and 160 ^{o}F	12/2017	04/2017
3	Optimization of mixing, dosing, and loading procedures	06/2018	02/2018
4	Manufacturing and testing of ten fully assembled M201A1 delay elements	06/2016	06/2016
5	Submit Technical Report to SERDP	06/2016	06/2016
6	Determination of reaction kinetics and thermal conductivity	06/2017	10/2017
7	Manufacturing and testing of a minimum of thirty fully assembled M201A1 delay elements at -65 ^{o}F, 70 ^{o}F, and 160 ^{o}F	06/2017	12/2016
8	Development of environmentally acceptable input transition and output charges	01/2018	10/2017
9	Development of Mathematical Model	06/2018	06/2018
10	Submit Technical Report to SERDP	06/2017	06/2017
11	Basic Technology Assessment for Scale-Up	06/2018	10/2018
12	ESD, BAM Friction, and BAM Impact Characterization	06/2018	07/2017
13	Manufacturing and Testing of Sixty Fully Assembled M228 and M213 Delay Elements at -65 °F, 70 °F and 160 °F	06/2018	04/2019
14	Submit Technical Report to SERDP	06/2018	06/2019

3. Background

Pyrotechnic delay systems are widely used in devices by both the civilian sector and the DoD for the generation of consistent time delays. Commonly used pyrotechnic delays include T-10 (boron/barium chromate) primarily used in CAD/PAD applications, nickel zirconium delays (nickel, zirconium, barium chromate, and potassium perchlorate) used in the M201A1 fuze system,

tungsten delays (tungsten, barium chromate, and potassium perchlorate) used in the M213/M228 fuze systems, and manganese delays (manganese, lead chromate, and barium chromate) also used in the M213/M228 fuze systems.

Chromates, perchlorates, and lead are all considered environmental contaminants by the Environmental Protection Agency (EPA). The National Institute of Occupational Safety and Health (NIOSH) considers all chromium (VI) compounds to be occupational carcinogens and OSHA has established a permissible level of 0.5 $\mu g/m^3$, [6] which is 100 times less than lead which is 50 $\mu g/m^3$.[5] Currently the levels of perchlorates, chromium, and lead in the soil and drinking water are monitored by the EPA with permissible levels being set as low as Maximum Contaminant Level (MCL) 0.1 mg/L[7] for chromium (VI).

The hardware selected for this development effort included the M201A1 delay fuzes that are initiated by a M39A1 lead thiocyanate based primer and used in smoke grenade applications that require a delay burn time between 1 to 2.3 seconds. The M213/M228 delay fuzes initiated with a M42 lead styphnate based primer and are utilized in the M67 fragmentation grenade and the training counterpart. Both the M213 and M228 fuzes require a delay burn time between 4 and 5.5 seconds.

The team for this work effort included IMP and EBA&D. IMP was responsible for R&D and deliverable manufacturing, while EBA&D was responsible for the technology scale up assessment and testing of the deliverable items.

4. Materials and Methods

4.1. Raw Materials

Several reactants were used during the course of this R&D project. The information on raw powders purchased and used for the development of the environmentally benign delay formulations are presented in Table 4.1.

Table 4.1. *Materials associated with the development of the environmentally benign delay formulations.*

Material	Manufacturer	Part #	Lot #	Particle Size (μm)
Aluminum (Al)	Valimet	H-2	14-5016	2-3 (per manufacturer)
Aluminum (Al)	Valimet	H-3	15-6030	3-4.5 (per manufacturer)
Aluminum (Al)	Valimet	H-5	15-6053	4.5-7 (per manufacturer)
Ammonium Dihydrogen Phosphate (ADP)	Acros	193701000	0297702	Not Measured
Diatomaceous Earth (DE)	Atlantic Equipment Engineers	MIL-D-20550B	1502518	21

Iron (III) Oxide (Fe_2O_3)	Atlantic Equipment Engineers	A-A-59280	1506516	10-15
Silicon (Si)	Elkem	Si99 0-45µm	95612-3	1-45 (per manufacturer)
Silicon (Si)	Atlantic Equipment Engineers	Si100	1210528	1-5 (per manufacturer) 1-66 (measured)
SiO_2	Alfa Aesar	42737	I20W038	85-115 m^2/g (per manufacturer)
Strontium Molybdate ($SrMoO_4$)	NOAH Technologies Corporation	15015	60536/0.0	-200 Mesh
Strontium Molybdate ($SrMoO_4$)	Alfa Aesar	40238	I27X015	-200 Mesh
Zirconium Powder	Alfa Aesar	00418	N02B033	-325 Mesh

4.2. Environmental and Toxicology Data[2]

All data in this section was collected and analyzed by the Army Public Health Command. Research, development, testing, training, and use of substances potentially less hazardous to human health and the environment is vital to military readiness. Safeguarding the health of military personnel, civilians, and the environment is a key element of this effort. Reduction of impact to health and environment early in the Research, Development, Testing, and Evaluation (RDT&E) phase can save significant time and effort. Residues of pyrotechnics, propellants, explosives, and incendiaries, (that cost the DoD billions of dollars and are part of mission essential activities) have been found in soil, air, surface, and ground water samples, creating environmental problems and interfering with training activities.

Table 4.2. *Categorization Criteria used in the Development of Environmental Safety and Occupational Health Severity.* [2]

	Low	**Moderate**	**High**
PERSISTENCE	Readily biodegrades (<28 days)	Degradation ½ life: water <40 days , soil <120 days	Degradation ½ life: water >40 days soil > 120 days
TRANSPORT	Water sol. < 10 mg/L log K_{OC} > 2.0	Water sol. 10-1000 mg/L log K_{OC} 2.0-1.0	Water sol. > 1000 mg/L log Koc <1.0
BIOACCUMULATION	log K_{OW} <3.0	log K_{OW} 3.0-4.5	log K_{OW} >4.5
TOXICITY	No evidence of carcinogenicity/ mutagenicity; Subchronic LOAEL > 200 mg/kg-d	Mixed evidence for carcinogenicity/mutagenicity (B2, 2); Subchronic LOAEL 5-200 mg/kg-d	Positive corroborative evidence for carcinogenicity /mutagenicity; LOAEL < 5 mg/kg-d
ECOTOXICITY	Acute LC_{50}/LD_{50} >1 mg/L or 1500 mg/kg; Subchronic EC_{50} >100 µg/L or LOAEL >100 mg/kg-d	Acute LC_{50}/LD_{50} 1-0.1 mg/L or 1500-150 mg/kg; Subchronic EC_{50} 100-10 µg/L or LOAEL – 10-100 mg/kg-d	Acute LC_{50}/LD_{50}<100 µg/L or <150 mg/kg; Subchronic LOAEL <10 mg/kg-d

Notes:
mg/L - milligrams per liter
LOAEL - lowest-observed adverse effect level
LC_{50} – concentration expected to result in 50 percent lethality to a population of test animals.
mg/kg-d - milligrams per kilogram per day
µg/L - micrograms per liter

Table 4.3. *Physical properties of reactants and products associated with the environmentally benign delay formulations.* [2]

Compound (Chemical formula)	Molar Mass (g/mol)	Melting Point (ºC)	Boiling Point (ºC)	Aqueous solubility (mg/L) @ 25ºC	log K_{OW}	log K_{OC}	Henry's Law Constant (atm-m^3/mol) @ 25ºC	Vapor Pressure mmHg @ 25°C
SiO_2	60.08[a]	1720[b]	2230[b]	Insoluble[a]	n/a	n/a	n/a	n/a
Si	28.09[a]	1412[a]	2680[a]	Insoluble[a]	n/a	n/a	n/a	n/a
Fe_2O_3	159.69[a]	1462[a] (dec)	ND	Insoluble[a]	n/a	n/a	n/a	n/a
Fe_3O_4	231.54[a]	1597[a]	ND	Insoluble[a]	n/a	n/a	n/a	n/a
Zr	91.22[d]	1857[d]	3577[d]	Insoluble[d]	n/a	n/a	n/a	n/a
Al	26.98[a]	660[a]	2518[a]	Insoluble[a]	n/a	n/a	n/a	n/a
Al_2O_3	101.96[p]	2030[q]	2977[q]	Insoluble[q]	n/a	n/a	n/a	n/a
$[NH_4][H_2PO_4]$	115.03[a]	190[a] (dec)	n/a	3.7E+05[a]	n/a	n/a	n/a	n/a
$Al_4O_{12}Si_3$	384.17[r]	1810[s]	ND	Insoluble[s]	n/a	n/a	n/a	n/a
$SrMoO_4$	247.56[v]	1040[b]	Dec	Nearly insoluble	ND	ND	ND	n/a
$SrAl_2O_4$	205.58[w]							
SrO	103.63[a]	2430[a]	n/a	0.0695@ 20°C[1]	n/a	n/a	n/a	n/a
$MoSi_2$	153.86[t]		n/a	Insoluble[u]				

Notes Table 4.3:
dec = decomposes
ND=No data
n/a=Not applicable
a=Dean 1992
b=NIOSH 2015
c = CIDP 2013
d = O'Neil 2006
e = HSDB 2002
f = HSDB 2005d
g = NIOSH 2016
h = CIDP 2017
i = Fisher 2015
j = HSDB 2005e
k = Koutsospyros et al. 2006
l = HSDB 2006b
m = PubChem 2017b
n = PubChem 2017d
o = HSDB 2006c
p = Budavari 1996
q = HSDB 2011
r = PubChem 2015
s = Sigma-Aldrich 2015
t = PubChem2017g
u = ESPI 2007

Table 4.4. *Toxicity data of reactants and products associated with the environmentally benign delay formulations.* [2]

Compound (Chemical formula)	Acute Oral LD_{50} (mg/kg)	Chronic Oral LOAEL (mg/kg-d)	Inhalation LC_{50} (g/m^3-h)	Dermal	Ocular	Genotoxicity	Carcinogenicity
SiO_2	>5000[d]	ND	>200[d]	ND	ND	Negative[d]	Negative[d]
Si	3160[e] (rat)	ND	ND	Irritant[e]	Irritant[e]	Negtive[e]	Negative[e]
Fe_2O_3	>10,000[f]	ND	ND	ND	ND	Negative[f]	Negative[f]
Fe_3O_4	500[g]	ND	Irritant[g]	Irritant[g]	ND	ND	ND
Zr	ND	ND	ND	ND	ND	ND	ND
Al	ND	ND	ND	Negative	Negative	ND	ND
Al_2O_3	>5000[r]	ND	ND	Negative	Irritant[r]	Negative	Negative
$[NH_4][H_2PO_4]$	ND	ND	ND	Irritant in dry form[t]	Irritant[a]	ND	ND
$Al_4O_{12}Si_3$	ND	ND	>0.002[a]	ND	Mild irritant	Negative	Negative in humans
$SrMoO_4$	690[v] (adult rats) 140[v] (weanling rats)	ND	ND	Irritant[w]	Irritant[w]	ND	ND
$SrAl_2O_4$	Data not yet available						
SrO							
$MoSi_2$							

Notes to Table 4.4:
ND = No data
a = Moreno et al. 2009
b = HSDB 2008a
c = ATSDR 2012
d = HSDB 2005a
e = HSDB 2002a
f = HSDB 2012
g = HSDB 2005b
h = HSDB 2005c
i = ATSDR 2005
j = HSDB 2003
k = Sax et al. 1989
l = HSDB 2002b
j = HSDB 2005d
k = Sigma-Aldrich 2014
l = HSDB 2005e
m = ATSDR 2005 (WO3)
n = HSDB 2005f
o = PubChem 2017
p = HSDB 2013
q = HSDB 2006
r = ATSDR 2010
s = HSDB 2011
t = Alfa Aesar 2012
u = Sigma-Aldrich 2015
v = CIDP 2017
w = AAA Molybdenum 2017

Table 4.5. *Toxicity Assessment.* [2]

Compound (Chemical formula)	Oral	Inhalation	Dermal	Ocular	Carcinogenicity	Comments
SiO_2	**Low**	**Low**	**Low**	**Low**	**Low**	
Si	**Low**	**Low**	**Low**	**Low**	**Low**	
Fe_2O_3	**Low**	**Low**	**Low**	**Low**	**Low**	
Fe_3O_4	**Mod**	**Low**	**Mod**	**Mod**	**Low**	
Zr	**Low**	**Low**	**Low**	**Low**	**Low**	
Al	**Low**	**Mod**	**Low**	**Low**	**Low**	
Al_2O_3	**Low**	**Low**	**Low**	**Low**	**Low**	
$[NH_4][H_2PO_4]$	**Low**	**Low**	**Low**	**Mod**	**Low**	
$Al_4O_{12}Si_3$	**Low**	**Mod**	**Low**	**Low**	**Low**	
$SrMoO_4$	**Mod**	**Mod**	**Mod**	**Mod**	**Low**	
$SrAl_2O_4$	**Data not yet available**					
SrO						
$MoSi_2$						

Table 4.6. *Ecotoxicity assessment* [2]

Compound (Chemical formula)	Aquatic	Terrestrial Invertebrates	Terrestrial Plants	Mammals	Birds	Comments
SiO_2	Low	Low	Low	Low	Unk	
Si	Low	Low	Low	Low	Unk	
Fe_2O_3	Low	Low	Low	Low	Low	
Fe_3O_4	Low	Low	Low	Mod	Unk	
Zr	Low	Low	Low	Low	Low	
Al	Low	Low	Low	Low	Unk	Moderate toxicity toward shellfish
Al_2O_3	Low	Low	Low	Low	Unk	
$[NH_4][H_2PO_4]$	Low	Low	Low	Low	Unk	
$Al_4O_{12}Si_3$	Low	Unk	Unk	Low	Unk	
$SrMoO_4$	Unk	Unk	Unk	Mod	Unk	
$SrAl_2O_4$	Data not yet available					
SrO						
$MoSi_2$						

Conclusions [2]

The proposed formulation for the gasless delay is entirely composed of solids contained within an isolating tube. The combustion process does not produce excess gases that would result in expansion of the container with potential inhalation exposure. Some of the materials produced represent inhalation hazards, but inhalation exposure is not expected in this application. This limits exposure to the materials of the formulation except during manufacturing and post-ignition degradation. As none of the materials pose a significant dermal contact hazard, occupational exposures are anticipated to be of low hazard. After use, the munitions fragments that remain after the device function are likely to be released to the environment through weathering. The human health and environmental effects of these released compounds are expected to be minimal, as their groundwater transport potential is limited, and the ultimate compounds are ubiquitous in the environment and non-toxic.

Recommendations [2]

Due to the nature of the device in which this delay formulation is to be deployed, inhalation exposure is expected to be non-existent, as zero gas is released from the device. The principal means of compound release to the environment is expected to be by degradation of the delay element through weathering. As all components are found regularly in soils, there are no recommendations for additional toxicity data collection.

4.3. Raw Materials Quality Control Parameters

The quality control parameters were detailed for each of the raw materials used in development of the environmentally benign delay formulation. Analysis was conducted using the following instruments located at South Dakota School of Mines and Technology (SDSM&T):

- Scanning Electron Microscope (SEM); Zeiss Supra40 variable-pressure field-emission SEM with an Oxford AZtecEnergy advanced system for X-ray microanalysis and electron backscattered diffraction.
- Differential Scanning Calorimeter (DSC) with a Thermal Gravimetric Analysis (TGA).
- Particle Size: MicroTrac S3000 Micron particle size analyzer

Instrumentation employed for materials characterization at Ensign Bickford Aerospace and Defense Company (EBA&D):

- DSC/TGA: Netzsch Jupiter 449 F1 Simultaneous DSC/TGA (alumina crucible, 10 °C/min);
- Particle Size: Cilas 1090LD Particle Size Analyzer;
- Surface Area: Micromeretics Gemini VII 2390p Brunauer–Emmett–Teller (BET) Surface Analyzer;
- FTIR: Bruker Tensor 27

The specific surface area was determined for the following raw materials; Aluminum, Diatomaceous Earth (DE), Strontium Molybdate, Silicon Dioxide, and Silicon SI-100. The collected specific surface area data is presented in Table 4.7.

Table 4.7. *BET specific surface area of associated raw materials used in development of formulations. Analysis conducted by EBA&D.*

BET Surface Area	
AL102373	
Sample	**m^2/g**
Aluminum Valimet H-2	
Run 1	1.28
Run 2	1.32
Average	1.3
Diatomaceous Earth	
Run 1	1.17
Run 2	1.4
Average	1.29
Strontium Molybdenum	
Run 1	0.48
Run 2	0.54
Average	0.51
Silicon SI-100	
Run 1	1.33
Run 2	1.46
Average	1.39
Silicon Dioxide	
Run 1	84.56
Run 2	83.62
Average	84.09

Aluminum (Spherical) Variants

Valimet spherical aluminum H-2 SEM image is presented in Figure 4.1. Particle size distribution analysis in Figure 4.2. Results from DSC/TGA under an argon atmosphere are presented in Figure 4.3, and under an air atmosphere in Figure 4.4.

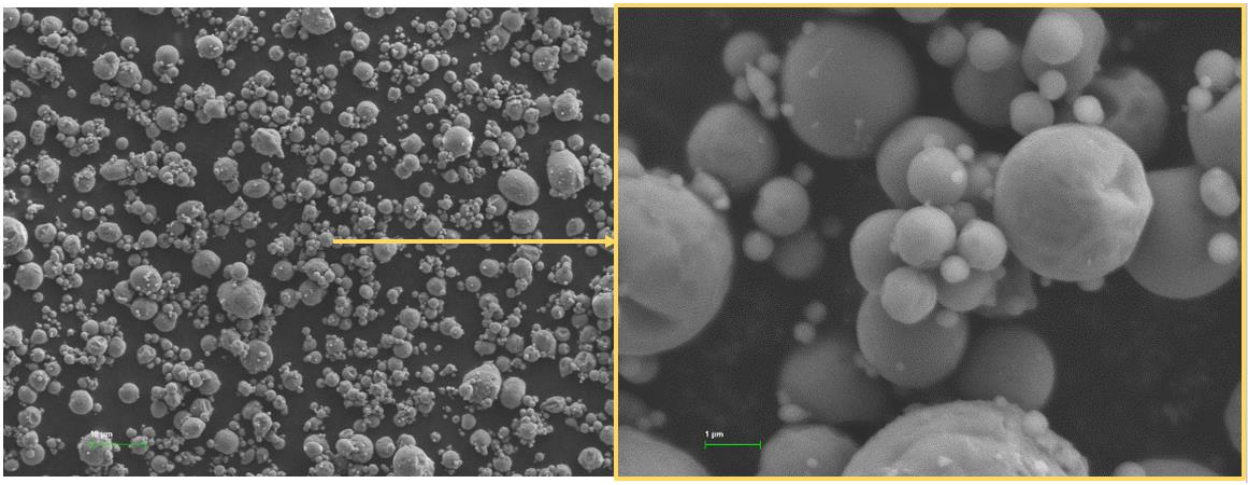

Figure 4.1. *SEM image of Valimet H-2 spherical aluminum 1k magnification with 10k magnification inset.*

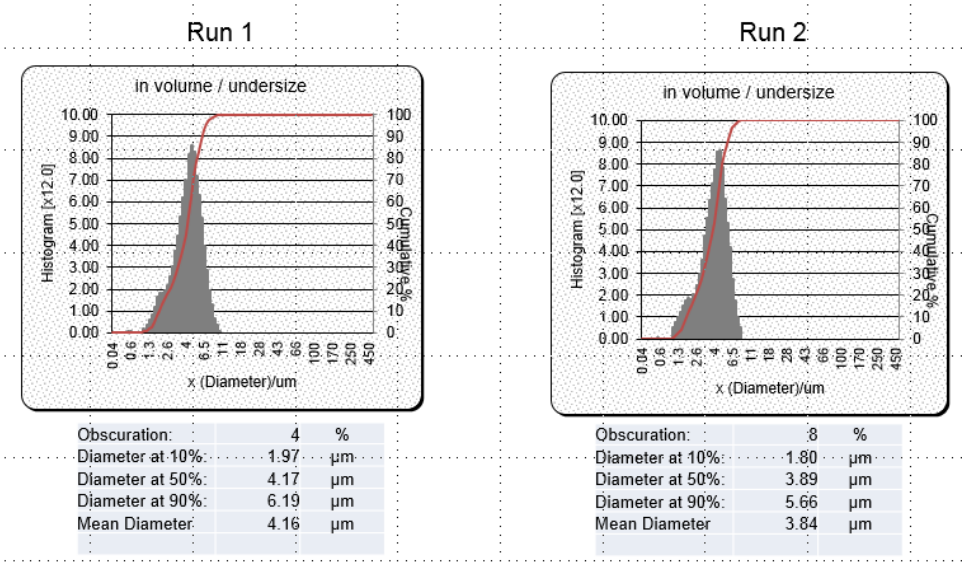

Figure 4.2. *Particle size analysis of Valimet H-2 spherical aluminum analysis completed by EBA&D.*

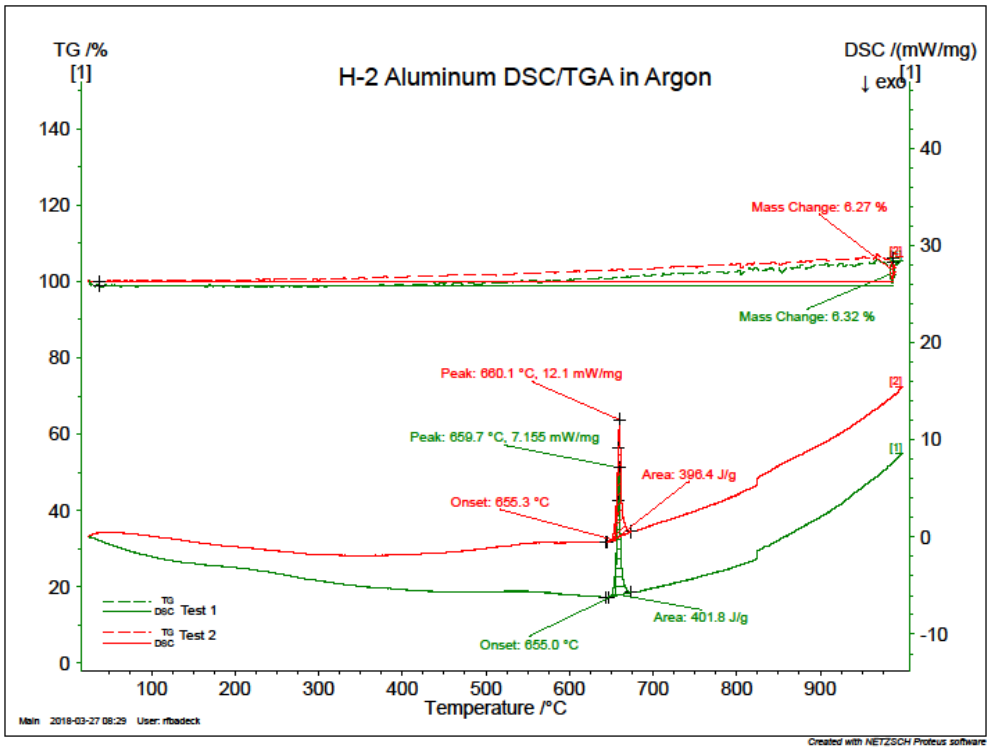

Figure 4.3. *DSC/TGA of Valimet H-2 spherical aluminum under an argon atmosphere, analysis conducted by EBA&D.*

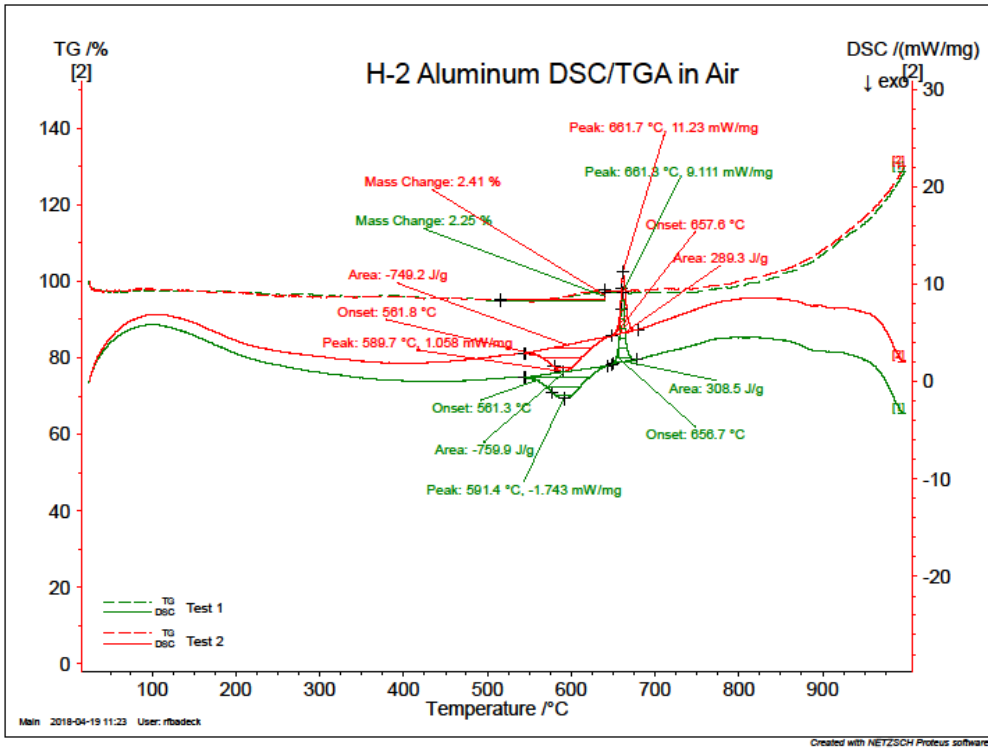

Figure 4.4. *DSC/TGA of Valimet H-2 spherical aluminum under an air atmosphere, analysis conducted by EBA&D.*

SEM image of Valimet H-3 spherical aluminum is presented in Figure 4.5.

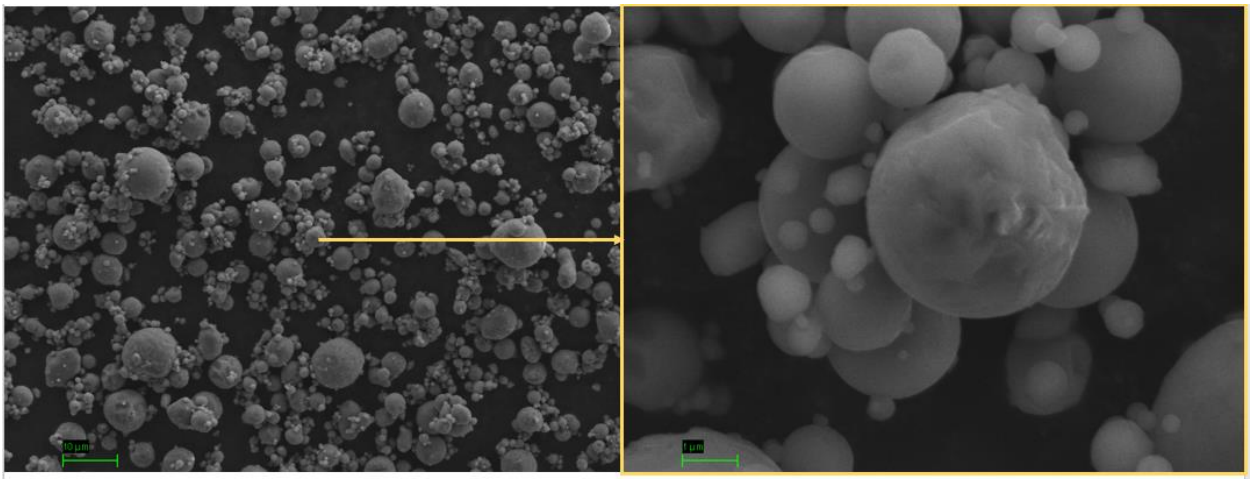

Figure 4.5. *Site 1 SEM image of Valimet H-3 spherical aluminum 1k magnification with 10k magnification inset.*

SEM image of Valimet H-5 spherical aluminum is presented in Figure 4.6.

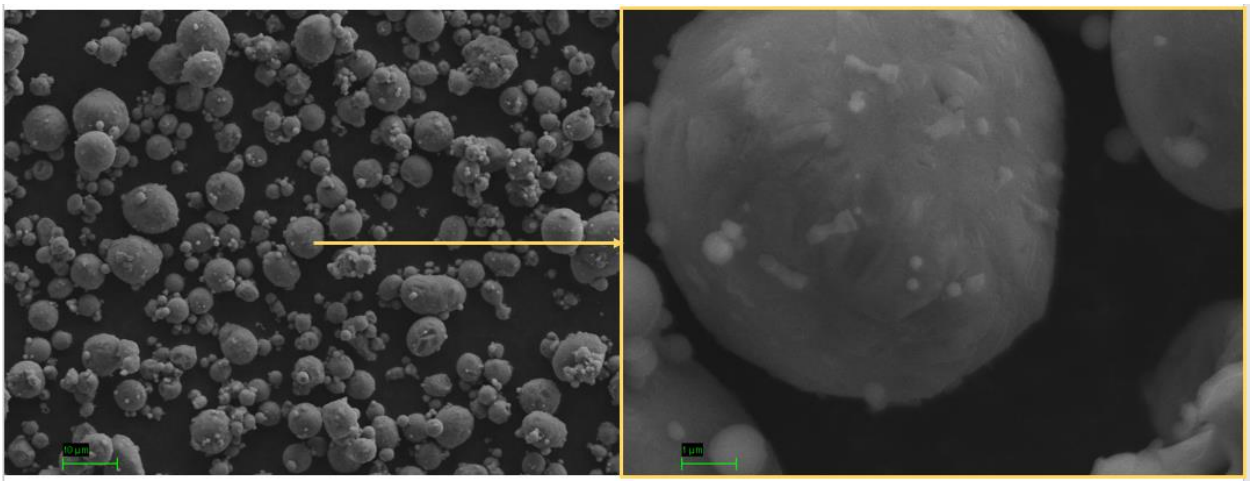

Figure 4.6. *Site 2 SEM image of Valimet H-5 spherical aluminum 1k magnification with 10k magnification inset.*

SEM image of diatomaceous earth MIL- D-20550B SEM can be seen in Figure 4.7. Particle size distribution is shown in Figure 4.8.

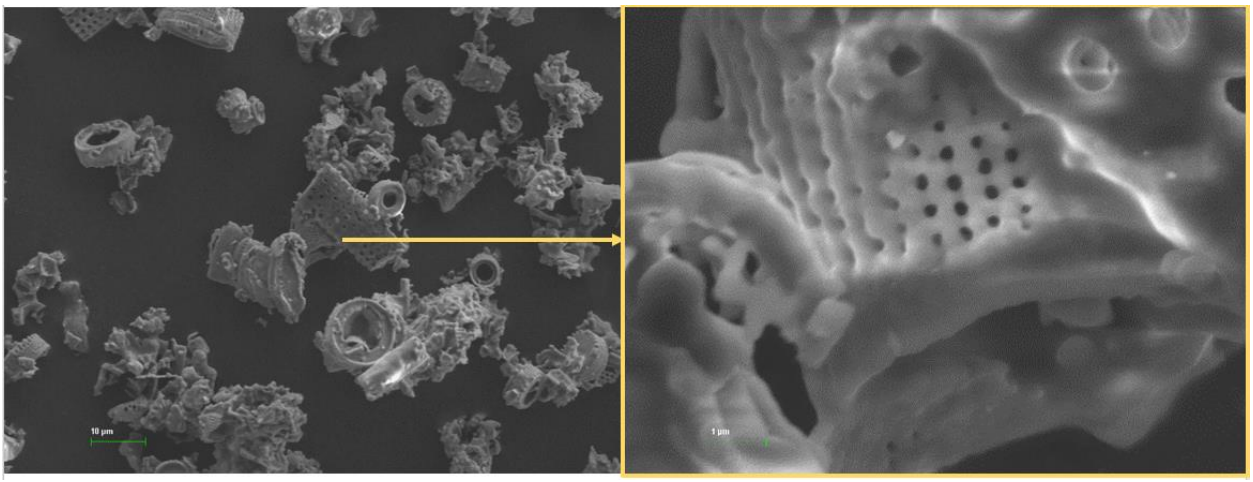

Figure 4.7. *Diatomaceous earth, 1k zoom image with 10k zoom inset.*

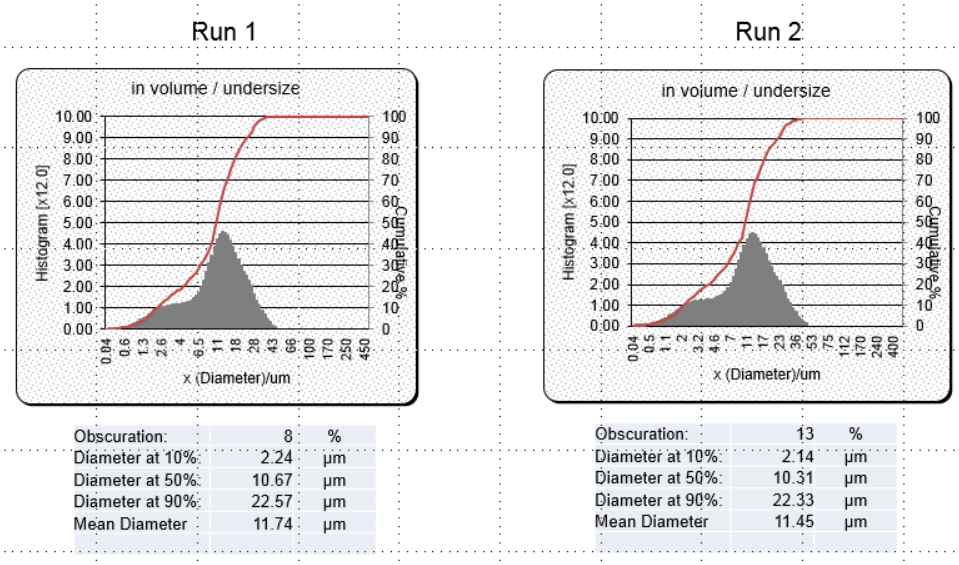

Figure 4.8. *Particle size distribution analysis completed by EBA&D of diatomaceous earth.*

SEM image of silicon metal powder can be seen in Figure 4.9. Particle size distribution is shown in Figure 4.10. Results of DSC/TGA under an argon atmosphere are presented in Figure 4.13, and under an air atmosphere in Figure 4.14. A second manufacturer of silicon was sourced due to quality control issues with previous vendor. The manufacture of silicon now being used is Elkem specifically Si99 0-45 µm. The SEM of this material can be seen in Figure 4.11 and the particle size distribution in Figure 4.12.

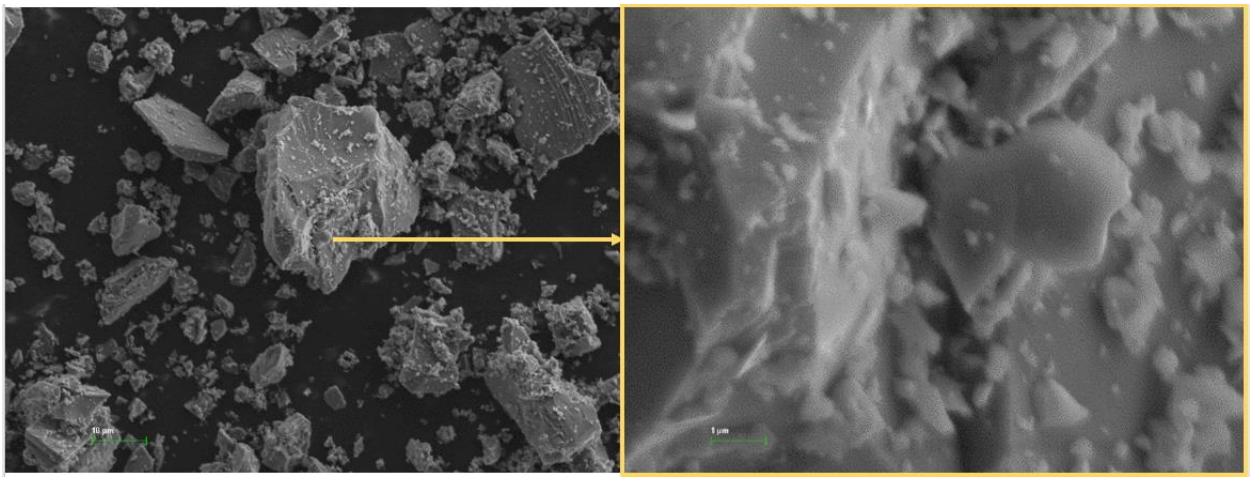

Figure 4.9. *Silicon metal powder 1-5 micron, 1k zoom image with 10k zoom inset.*

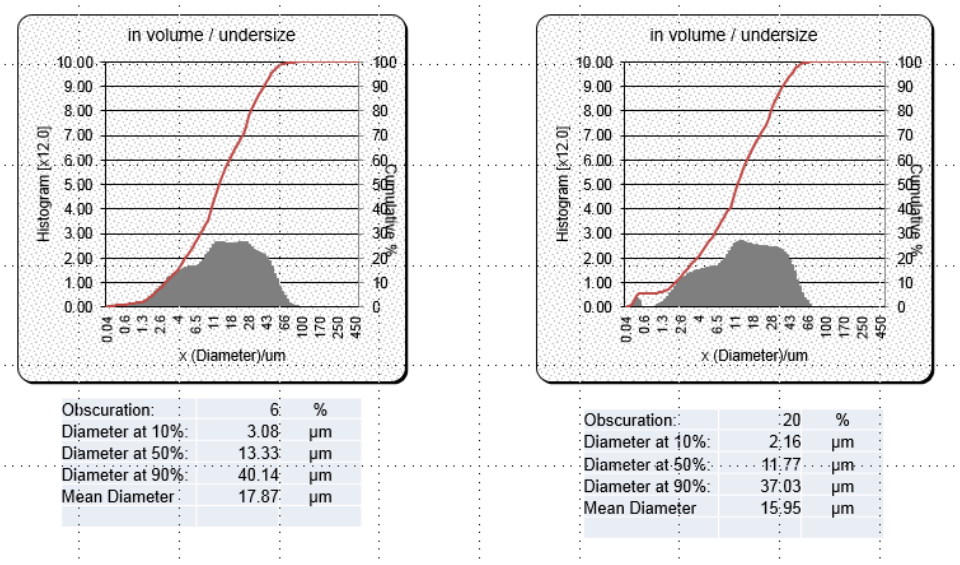

Figure 4.10. *Particle size distribution analysis completed by EBA&D of silicon metal powder.*

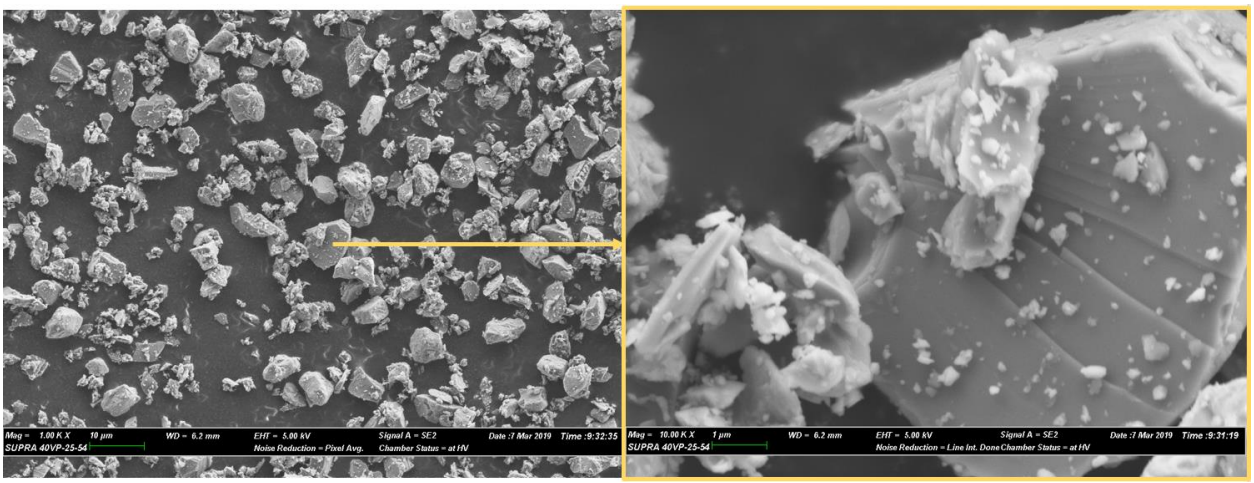

Figure 4.11. SEM of Elkem s*ilicon 0-45 µm, 1k zoom image with 10k zoom inset.*

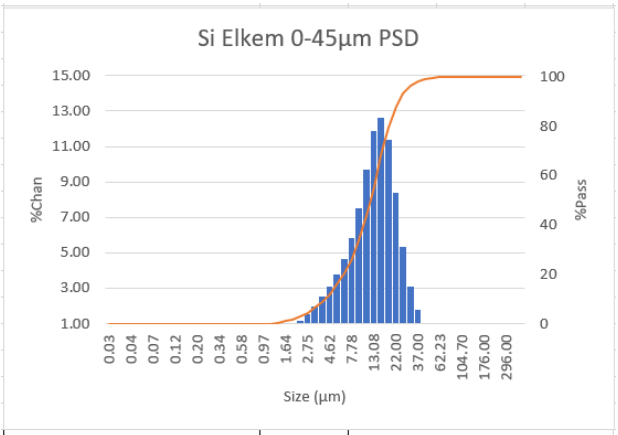

Mean Volume Diameter (um):	13.40
Mean Intensity Diameter(um):	2.685
Mean Area Diameter (um):	8.37
Diamter at 10%	4.14
Diamter at 50%	12.13
Diamter at 90%	23.42

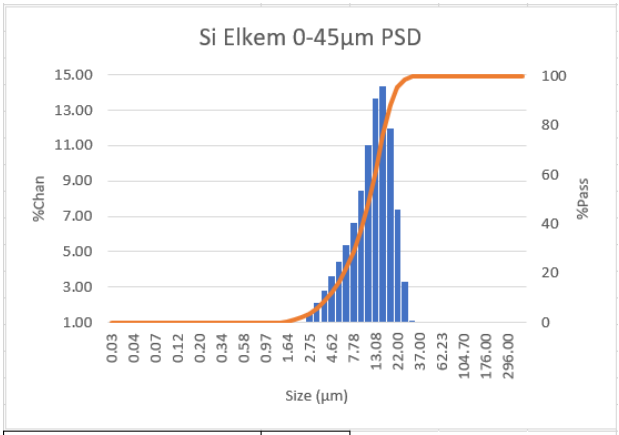

Mean Volume Diameter (um):	13.40
Mean Intensity Diameter(um):	2.685
Mean Area Diameter (um):	8.37
Diamter at 10%	4.14
Diamter at 50%	12.13
Diamter at 90%	23.42

Figure 4.12. *Particle size distribution analysis completed by IMP of Elkem 0-45 µm silicon powder.*

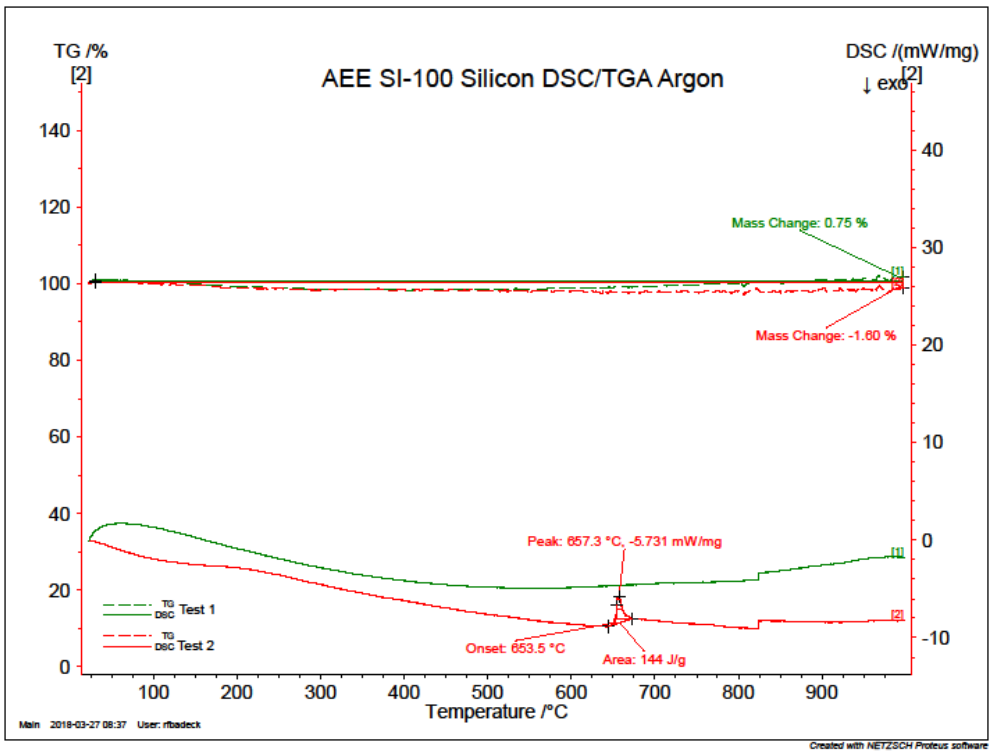

Figure 4.13. *DSC/TGA of silicon metal powder under an argon atmosphere, analysis conducted by EBA&D.*

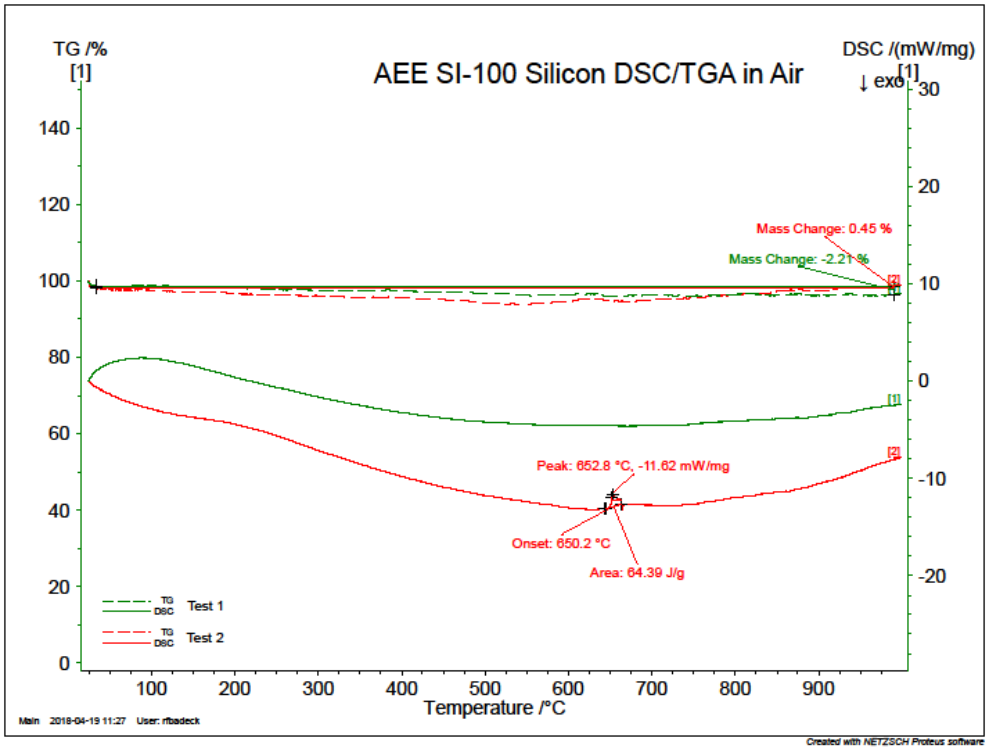

Figure 4.14. *DSC/TGA of silicon metal powder under an air atmosphere, analysis conducted by EBA&D.*

SEM image of fumed silica can be seen in Figure 4.15. Particle size distribution analysis is presented in Figure 4.16.

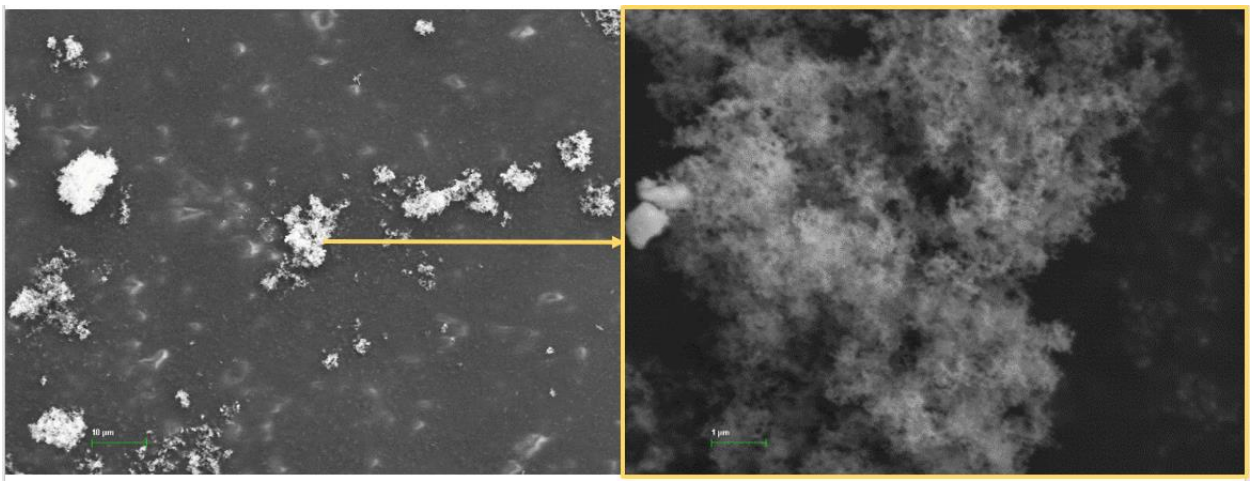

Figure 4.15. *Silicon (IV) oxide, amorphous fumed 85-115 m^2/g, 1k zoom image with 10k zoom inset.*

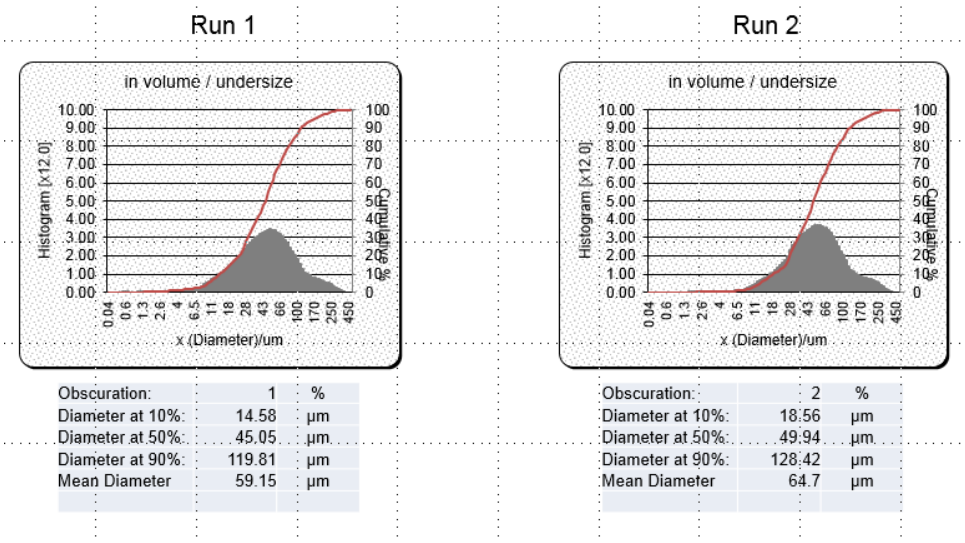

Figure 4.16. *Particle size distribution analysis completed by EBA&D of fumed silica.*

SEM image of strontium molybdate can be seen in Figure 4.17. Particle size distribution is presented in Figure 4.18. DSC/TGA under an argon atmosphere is shown in Figure 4.19, and under an air atmosphere in Figure 4.20. FTIR analysis results can be found in Figure 4.21.

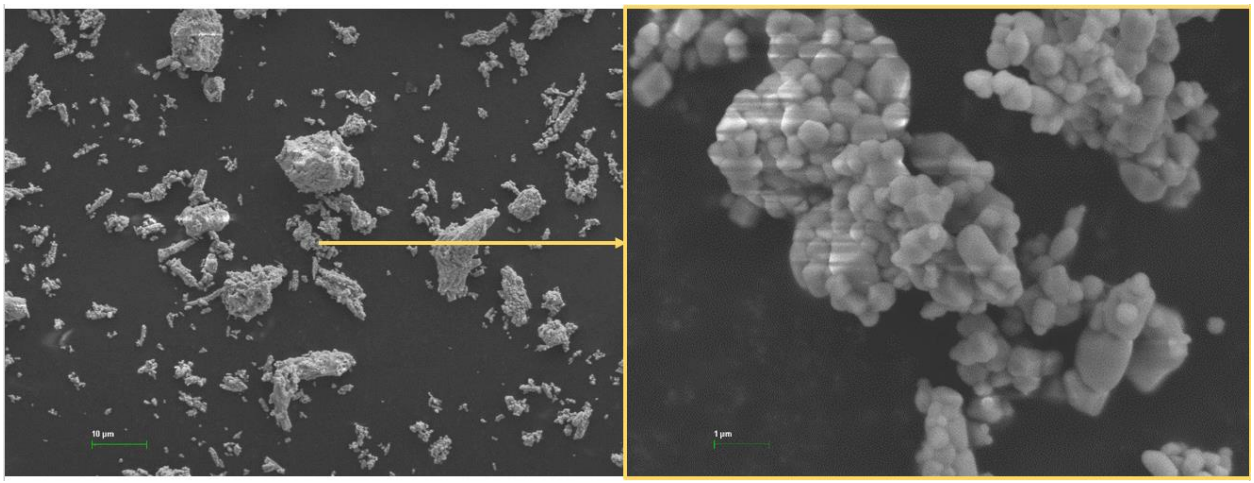

Figure 4.17. *Strontium molybdate 99.9% pure -200 Mesh 1k zoom image with 10k zoom inset.*

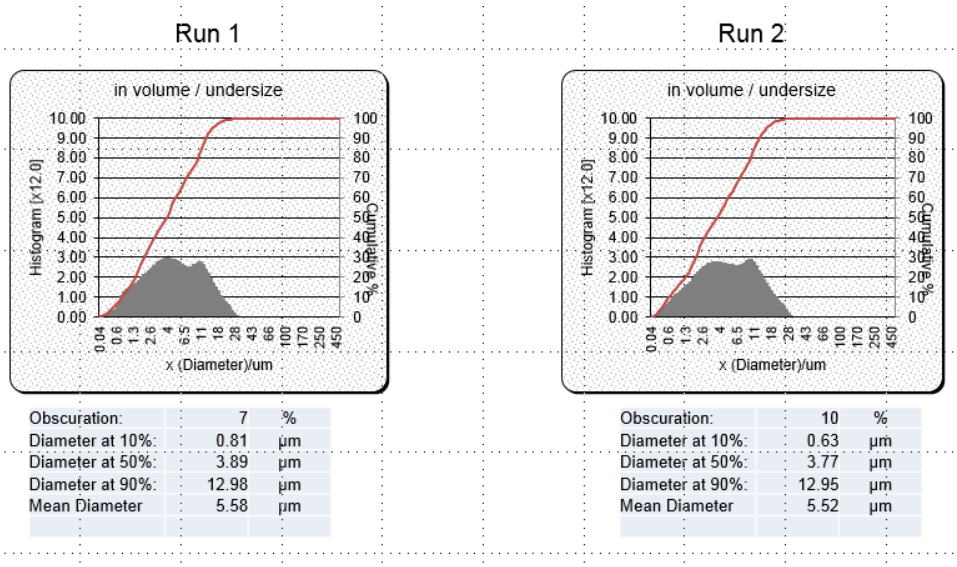

Figure 4.18. *Particle size distribution analysis completed by EBA&D of strontium molybdate.*

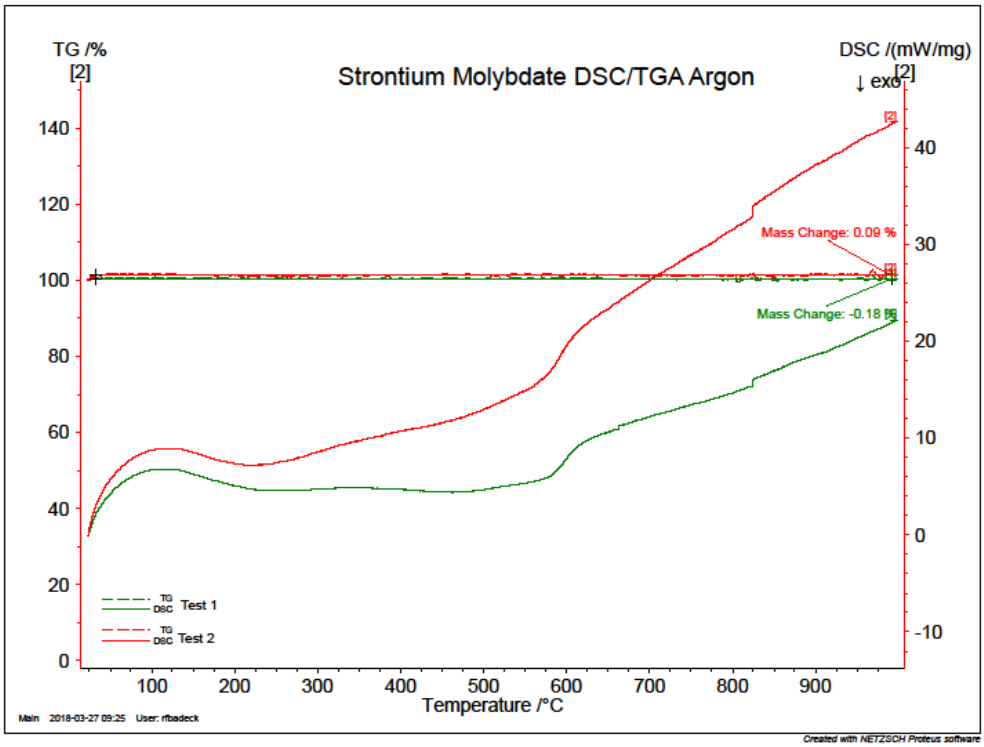

Figure 4.19. *DSC/TGA of strontium molybdate under an argon atmosphere, analysis conducted by EBA&D.*

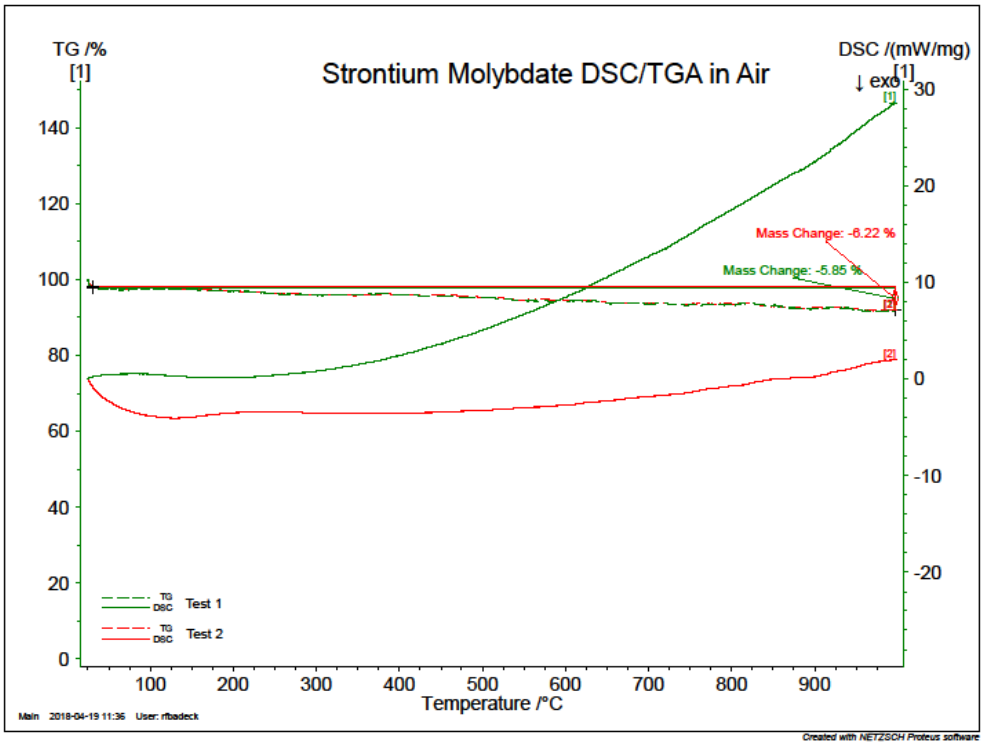

Figure 4.20. *DSC/TGA of strontium molybdate under an air atmosphere, analysis conducted by EBA&D.*

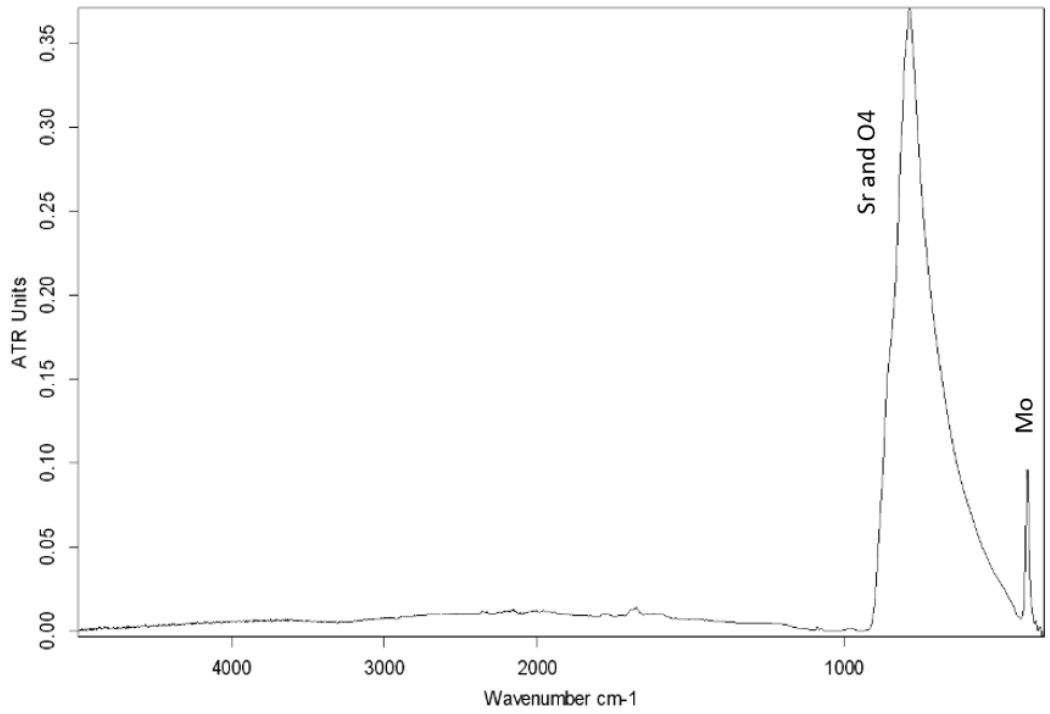

Figure 4.21. *FTIR of strontium molybdate, analysis conducted by EBA&D.*

5. Task 1 – Compatibility Testing

5.1. Methods

Compatibility analysis of the selected environmentally benign delay formulation was conducted using microcalorimeter and differential scanning calorimetry (DSC) techniques. Chemical compatibility analysis of the selected delay formulation constituents was conducted using two methods:

- Long term thermal stability analysis was conducted using microcalorimetry using a TA Instruments TAM IV Microcalorimeter located at IMP R&D Laboratory (Figure 5.1).
- Differential scanning calorimetry and thermogravimetric analysis (DSC/TGA) TA Instruments SDT Q600 located at SDSM&T.

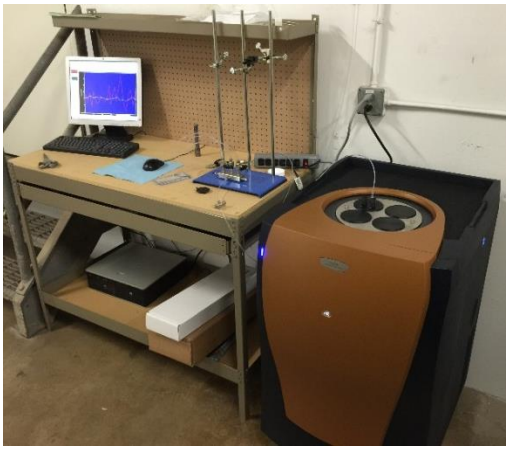

Figure 5.1. *Photograph of TAM IV Microcalorimeter located at IMP.*

The characterization was split into three parts:

- Non-reactive ($SrMoO_4$, diatomaceous earth (DE), SiO_2);
- Fuel (Al, and Si);
- The delay mixture ($SrMoO_4$, Al, Si, SiO_2, and DE).

The microcalorimetry experiments were conducted at 284 °F (140 °C) for 10 days. The DSC experiments were conducted at a heating rate of 10 °C per minute up to 1100 °C under both air and argon atmospheres.

These methods of analysis were performed to observe if any unwanted side reactions exist between the constituents of the delay formulation. Fuels (reactive) and oxidizers (non-reactive) were first characterized separately, and then together, to verify compatibility. The DSC/TGA analysis of the mixtures were conducted at a heating rate of 68 °F (20 °C) per minute up to 2552 °F (1400 °C) under an argon atmosphere. All samples were tested under an argon atmosphere to approximate actual environmental conditions inside the M213/M228 fuze. The tests were conducted with a reference sample of alumina in the reference pan. DSC/TGA analysis consisted of three tests:

- A delay formulation consisting of all constituents as the signal for the experiment;
- A blend of the oxidizer (non-reactive) components of the delay composition ($SrMoO_4$, SiO_2, and DE) as a reference for the experiment;
- A blend of the fuel (reactive) components of the delay composition (aluminum and silicon) also as a reference for the experiment.

Sample preparation: testing of the delay composition in the DSC/TGA consisted of forming a 100 mg pellet of delay composition pressed at 30 ksi to simulate the configuration of the material in the fuze. A 26.6 mg portion of the compressed delay composition was removed from the pellet and used for DSC/TGA characterization. The fuel and inert samples were separately placed in a vile and jar-rolled for 60 minutes to provide homogeneity.

Long term thermal stability analysis was conducted to ensure chemical stability within the delay formulation. The sample used was comprised of the complete delay formulation and was tested for 10 days at 284 °F (140 °C). The sample of delay composition was analyzed by loading a 1.0 g powder sample into the primary ampoule and a 0.5 g silica media into the reference ampoule.

5.2. Results

Compatibility analysis of the environmentally benign delay formulation selected for the use in the M213/M228 fuze system was conducted using a microcalorimeter and DSC/TGA techniques. Illustrated in Figure 5.2, the DSC/TGA produced an endotherm at 650 °C that shows the melting of aluminum. The projected melting point from EBA&D's material characterization was 659 °C. This is apparent in the characterization of both the delay composition and the reactive constituents. Otherwise, no unwanted side reactions were present in the data. The results do not indicate any incompatibility issues related to the environmentally benign delay composition.

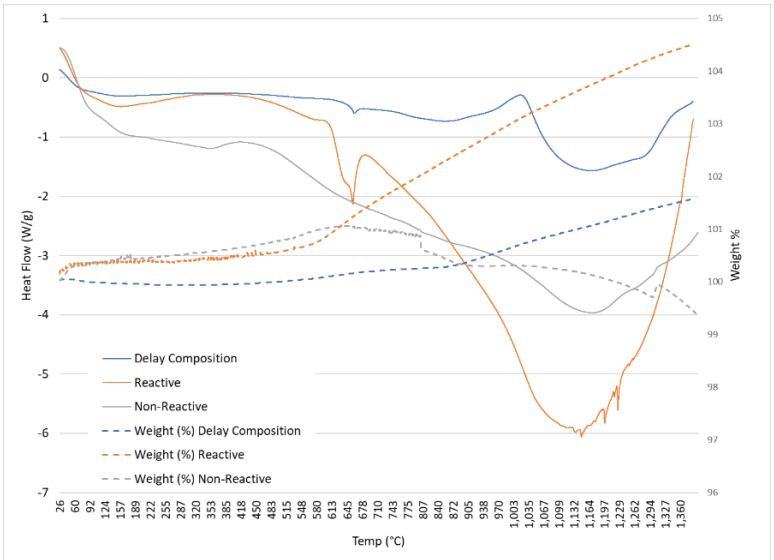

Figure 5.2. *DSC/TGA of the delay composition, fuels (reactive), and oxidizers (non-reactive) materials used in M213/M228 fuzes.*

The microcalorimeter output data shown in Figure 5.3 confirms long term chemical compatibility of the mixture. The chart shows if there are any reactions they are decreasing in rate. And that any reactivity that does occur is not accelerating with time at temperature. The delay was also calculated in accordance with STANAG 4147 Test 2 – The Heat Flow Calorimetry Test[9]. This calculation also shows no compatibility issues.

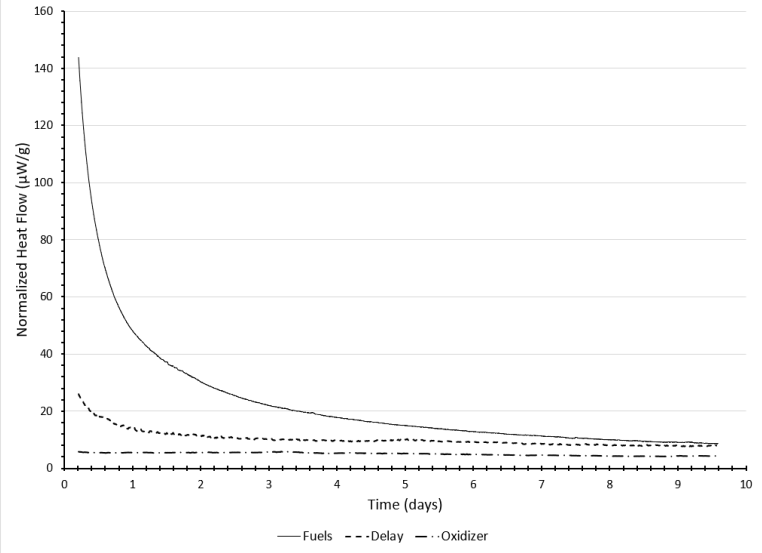

Figure 5.3. *Microcalorimeter report from delay composition compatibility analysis.*

$$D = \frac{2M}{E + S}$$

where:

M = heat generation of the mixture of explosive and test material (J g^{-1})
E = heat generation of the explosive (J g^{-1})
S = heat generation of the test material (J g^{-1})

When D > 3: the test material must be considered as incompatible with the explosive.
When 2 < D < 3: another method should be used to determine compatibility.

The applied data was calculated as:

- Delay Formulation (M) 9.17 J g^{-1},
- Fuel 22.54 (E) J g^{-1},
- Oxidizer (S) 4.34 J g^{-1}.

The calculated D value is 0.68. According to STANAG 4147 the material is considered compatible.

6. Task 2 – Development of optimized formulations meeting the burn rate specifications from 4 - 12 s/in at -65 °F, 70 °F, and 160 °F

6.1. Initial development

Initial development of the environmentally benign delay formulation investigated numerous formulations that met the specifications of this project. Delay formulations were evaluated for their performance characteristics while ensuring compliance with the SERDP strategic goals. The concentration ranges of each component considered for the development of delay formulations are presented in Table 6.1. For all formulations containing aluminum, ADP was added as a pH buffer at a concentration of 5 wt% with respect to aluminum content, to ensure that there was no reaction between the aluminum and water during processing.

Table 6.1. *Compositions of environmentally acceptable delay mixtures.*

Material	Bi_2O_3 (wt%)	$SrMoO_4$ (wt%)	Fe_2O_3 (wt%)	Al (wt%)	Si (wt%)	KIO_4 (wt%)	Bentonite (wt%)	SiO_2 (wt%)
Range	0 - 38	41 - 82	0 - 34	0 - 15	12 - 25	0 – 6	0 - 5	0 - 5

For each delay formulation prepared, composite granules of the material were prepared with the first batch of the material. After drying, initial combustion tests were conducted on each formulation by igniting several of the dried granules. This was performed to verify whether the reaction was self-sustaining, and/or if any visible gases were generated. The mixtures that contained Bi2O3 and/or KIO4 generated visible gas during combustion. Based on this data, the use of these constituents was eliminated from all future gasless delay formulations being prepared and tested. The burn data from the unconfined combustion experiments allowed for the selection of formulations to be tested within the mock delay columns. This section includes additional details for selected formulations that had good performance.

A formulation consisting of: 16.61 wt% Si, 1.85 wt% Al, and 81.54 wt% $SrMoO_4$ were consolidated in 8 layers, with 2 energetic composite granules per layer (approximately 1.3 g of material total), into an open column. The measured results yielded an average burn time of 9.5 s for the delay columns tested at room temperature and 10 s for the delay columns tested at -65 °F. However, it should be noted that the combustion reaction quenched in one of the delay columns tested at the room temperature. The IBR for this delay formulation was too slow for the M201A1 delay and therefore further compositional adjustments were required.

Subsequently, 12 additional delay formulations were prepared in a granular form for characterization. After drying, the self-sustaining combustion characteristics of each mixture was verified through ignition at 70 °F. All 12 mixtures prepared demonstrated self-sustaining combustion characteristics. However, the mixtures with silicon as the sole fuel component were very difficult to ignite and were not tested in mock delay columns. In addition, during the production of reactive granules, it was observed that the granules containing Al/Si/$SrMoO_4$/DE did not have a good structural integrity and broke apart easily even when gently handled. It should also be noted that when some of the $SrMoO_4$ was replaced with iron oxide, the structural integrity of the granules was greatly improved.

Based on the results from the unconfined combustion experiments of the 12 delay formulations, 8 delay formulations were selected for testing within open delay columns. Each of the selected formulations was pressed into six open delay columns for testing. Out of the six columns prepared, three columns were tested at 70 °F and three columns were tested at -65 °F. The IBR of the selected Al-Si-$SrMoO_4$-Fe_2O_3 delay mixtures formulations ranged from 2.5 – 4.37 s/in. The IBR results for the Al-Si-$SrMoO_4$-Fe_2O_3 delay mixtures are summarized in Figure 6.1. The IBR required for the M201A1 is 2 – 4.6 s/in. The IBR for the Al-Si-$SrMoO_4$ mixtures are presented in Figure 6.2 and Figure 6.3 and range from 3.9 – 10.03 s/in. All mock delay columns tested up to this point were consolidated at 12.5 ksi.

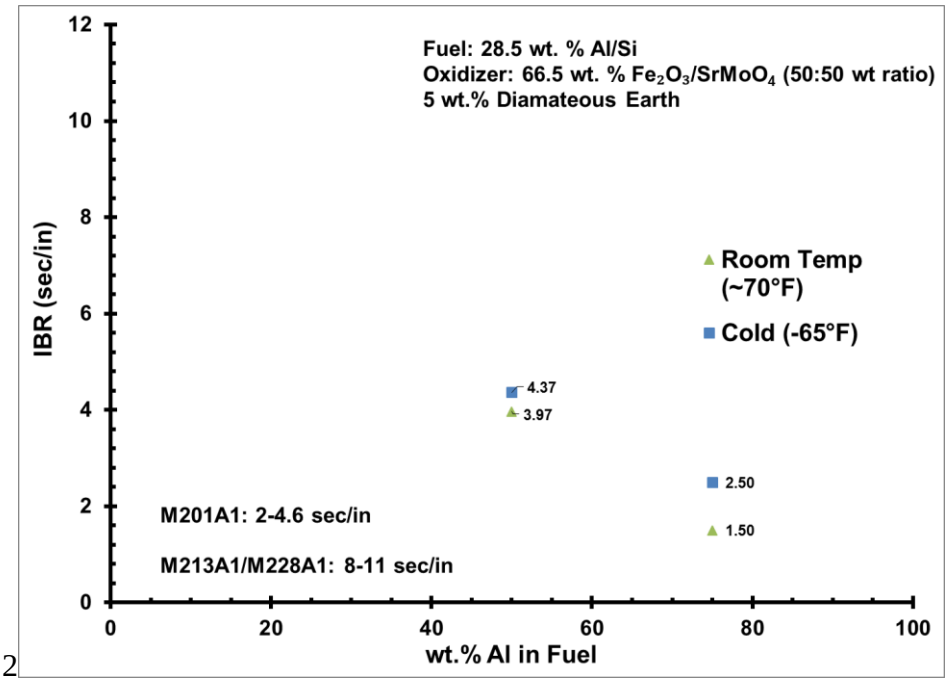

2

Figure 6.1. *IBR of Al-Si-$SrMoO_4$-Fe_2O_3 delay mixtures at a constant fuel concentration of 28.5 wt. % with a varying amount of Al within the fuel mixture tested at 70 °F and -65 °F*

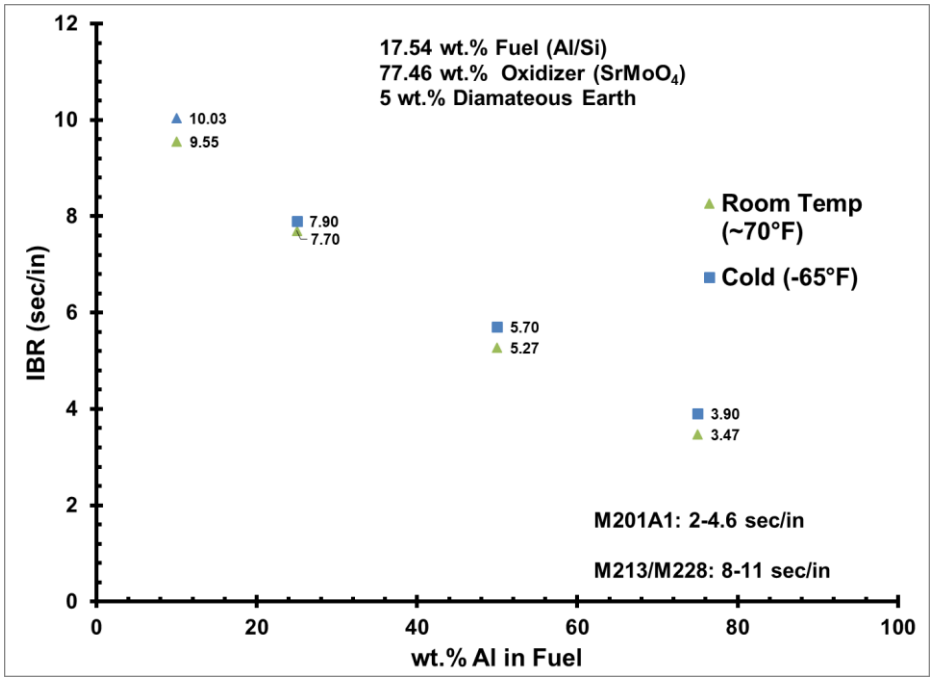

Figure 6.2. *IBR of Al-Si-$SrMoO_4$ delay mixtures at a constant fuel concentration of 17.54 wt. % with a varying amount of Al within the fuel mixture tested at 70 °F and -65 °F.*

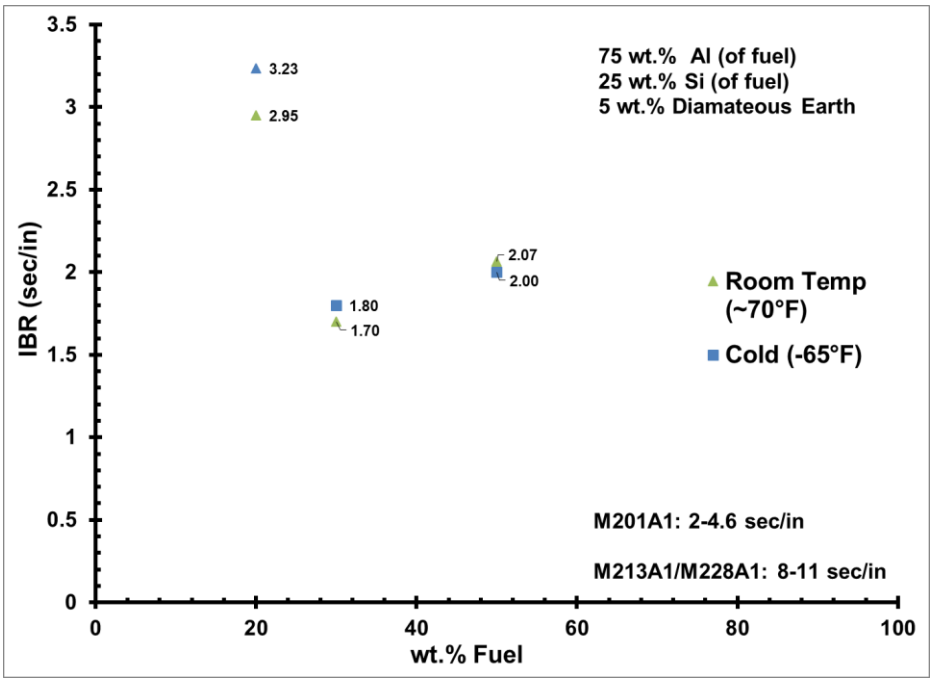

Figure 6.3. *IBR of Al-Si-$SrMoO_4$ delay mixtures with a constant fuel mixture ratio of 75:25 by weight of Al:Si with varying fuel concentrations tested at 70 ^oF and -65 ^oF.*

Several other delay mixtures containing Fe_2O_3 as an oxidizer in addition to strontium molybdate were also tested. The collected data indicated that the material had IBR within the required M201A1 specification of 2.0 to 4.6 s/in. However, when burned, the material released a significant amount of molten material from the delay columns in the form of sparks. The sparking may cause

problems in the enclosed delay system of the M201A1. Delay formulations were prepared in order to determine the minimum iron oxide concentration that did not cause sparking during combustion. The composition of the delay mixture with iron oxide that did not spark during combustion is presented in Table 6.2. The IBR data for this delay mixture at -65 °F and 70 °F is presented in Table 6.3.

Table 6.2. *Composition of delay mixture containing iron oxide without sparking during combustion.*

Component	wt.%
Fe_2O_3	3.33%
$SrMoO_4$	63.18%
Al	12.83%
Si	15.68%
Dia Earth	5.00%

Table 6.3. *IBR data for the delay mixture presented in Table 6.2.*

Temperature (^oF)	Sample Size	Average IBR (sec/in)	Standard Deviation	Coefficient of Variation
-65	10	3.5	0.07	2
70	10	3.4	0.06	1.7

Based on the IBR data gathered up to this point in the mock delay columns, the following two base compositions were selected for moving forward:

- $SrMoO_4$ 77.46 wt%; Al 13.15 wt%; Si 4.38 wt%; DE 5 wt%;
- Fe_2O_3 3.33 wt%; $SrMoO_4$ 63.18 wt%; Al 12.83 wt%; Si 15.68 wt%; DE 5 wt%.

At this stage of the development process, bentonite was identified as a possible inorganic binder that would increase the strength of the composite granules. An environmentally acceptable composite delay mixture was prepared with the following composition: $SrMoO_4$ 63.2 wt%, Al 20.3 wt%, Si 6.8 wt%, DE 4.75 wt%, and bentonite 5 wt%. After dosing and drying, the granules qualitatively demonstrated acceptable strength and could be easily handled without breaking or chipping. The mixture was pressed into delay columns and the IBR of the mixtures was determined using video analysis. At room temperature, this mixture had an average IBR of 2.4 sec/in with a standard deviation of 0.1 sec/in. A second composite delay formulation was also prepared with a lower binder concentration (2.5 wt%). This formulation was used to determine the minimum binder concentration required within the granules in order to maintain acceptable structural strength. In this formulation, the aluminum concentration was also decreased in an attempt to increase the IBR. The second composite delay mixture had a composition of: $SrMoO_4$ 64.9 wt%, Al 13.9 wt%, Si 13.9 wt%, DE 4.8 wt%, and Bentonite 2.5 wt%. At room temperature this mixture had an average IBR of 3.0 sec/in with a standard deviation of 0.19 sec/in. The reduction of the binder concentration by 50% led to granules that could be easily handled but demonstrated chipping around the edges of the granules. This led to the collection of loose fine powder in the storage container and around the pressing fixture; therefore, a binder concentration of 5 wt% was selected.

The environmentally benign delay formulation was loaded into 30 mock aluminum delay columns with 0.1 grams of A-1A ignition mixture on top of the consolidated delay columns. The columns

were split into three groups of 10 mock delay columns and placed into the testing fixtures followed by temperature conditioning for a minimum of 4 h at the required temperature ranges (-65 °F, 70 °F, and 160 °F). The burn time and IBR data are presented in Table 6.4.

Table 6.4. *Burn time and IBR data for one batch of delay columns tested at -65 °F, 70 °F, and 160 °F.*

Temperature (-65°F)				Temperature (70°F)				Temperature (160°F)			
Column #	Height	Burn Time (s)	IBR (s/in)	Column #	Height	Burn Time (s)	IBR (s/in)	Column #	Height	Burn Time (s)	IBR (s/in)
11	0.549	1.74	3.16	1	0.563	1.68	2.99	21	0.549	1.58	2.88
12	0.543	1.72	3.17	2	0.553	1.67	3.02	22	0.565	1.73	3.06
13	0.565	2.07	3.67	3	0.541	1.63	3.01	23	0.553	1.58	2.86
14	0.547	1.59	2.90	4	0.541	1.66	3.07	24	0.542	1.74	3.20
15	0.559	1.70	3.05	5	0.556	1.80	3.24	25	0.566	1.62	2.87
16	0.574	1.95	3.40	6	0.539	1.82	3.38	26	0.538	1.54	2.87
17	0.542	1.81	3.34	7	0.549	1.68	3.06	27	0.546	1.67	3.07
18	0.554	1.82	3.28	8	0.560	1.80	3.22	28	0.563	1.58	2.81
19	0.557	1.81	3.24	9	0.592	1.85	3.13	29	0.543	1.56	2.87
20	0.541	1.70	3.15	10	0.563	1.78	3.16	30	0.565	1.62	2.86
	Average	1.79	3.24		Average	1.74	3.13		Average	1.62	2.94
	Std Dev	0.14	0.21		Std Dev	0.08	0.12		Std Dev	0.07	0.13

The data presented in Table 6.4 indicates that the presented energetic composite delay mixture meets the DoD requirements for the M201A1 when tested in the mock M201A1 aluminum columns.

Further investigation into the effect of composition on the IBR was conducted by preparing three additional delay formulations presented in Table 6.5.

Table 6.5. *Compositions of follow up sets of delay column mixtures tested.*

Constituent	WT%		
	Mix 1	Mix 2	Mix 3
$SrMoO_4$	63.17	63.17	63.17
Al	13.54	5.42	8.13
Si	13.54	21.66	18.95
Diatomaceous earth	4.75	4.75	4.75
Bentonite	5.00	5.00	5.00

A sample of 30 mock delay columns was prepared containing Mix 1 at a consolidation pressure of 12.5 ksi and tested at room temperature. The average burn time and standard deviation for the mock delay columns were 1.725 s and 0.070 s, respectively. This data is consistent with the data that has been collected up to this point for the firing of over 100 columns of this composition with zero no-fires being reported. Based on the current M201A1 drawings provide by SERDP, the consolidation pressure for this mixture was increased to 30 ksi and an additional 30 delay columns were prepared for testing. The increase in consolidation pressure, decreased the height of the delay mixture in the column from an average height of 0.56 in to 0.47 in. This reduction in height decreased the average burn time of the delay columns to 1.57 s. In one test (for the columns pressed at 30 ksi), the A-1A mixture ignited, but the delay mixture did not ignite.

Mix 2 was characterized next and was selected to provide an IBR of 8.5 s/in (similar to the current delay composition that is used). Six composite granules (prepared from Mix 2) were loaded into the mock aluminum delay columns and consolidated in one step at 30 ksi. The height data for each column prepared is presented in control chart form in Figure 6.4. After consolidation, 100 mg of A-1A was added to the top of each column and consolidated at 30 ksi. For this test, 50 columns were prepared and tested at ambient temperature and had an average burn time of 1.91 s; however, 10 columns did not ignite when the A-1A was ignited.

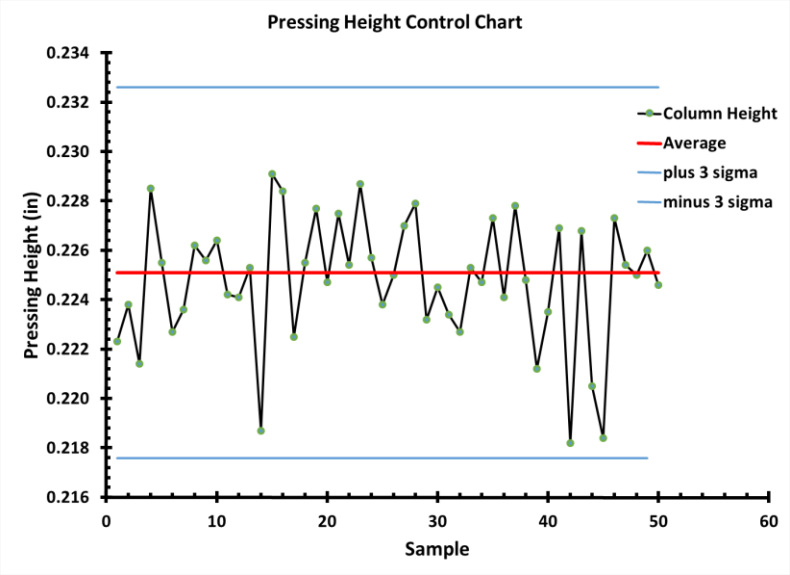

Figure 6.4. *Pressing height control chart for delay Mix 2 (μ=0.225 in, σ=0.003 in).*

Mix 3 was prepared and tested in the same manner as Mix 2, but the consolidation pressure was reduced to 15 ksi. Mix 3 had an average burn time of 1.49 s with a standard deviation of 0.09 s. During the testing of the 50 columns, there was only one column in which the delay mixture did not ignite when the A-1A was ignited. Upon completion of the burn tests for all three mixtures, the columns that did not fire were successfully ignited from the bottom.

Investigation into the no-fires identified two possible root causes. The first possible cause is the amount of A-1A (100 mg) may be too great and is causing the A-1A material to push away from the delay mixture when ignited. This effect may be further increased by the interface that is generated from pressing the delay mixture first, followed by the addition and pressing of the A-1A.

Due to A-1A/delay interface issues, a new consolidation procedure was developed to eliminate the interface between the delay mixture and the A-1A transition charge. The new processing technique used a powder loading technique that that is similar to the current method used for the production of the M201A1 fuze assemblies.

6.2. Delay Mixture Selection

After preparation of the delay formulation, initial mock column combustion tests were conducted. The tests were performed to verify if the reaction was self-sustaining, and/or there were any issues

with combustion front propagation. The data accumulated, formed the basis for the use of these formulations. The burn data from the mock column, combustion experiments allowed for the tuning of formulations prior to be tested within the M213/M228 fuze system.

The developed delay composition can be tuned to a relatively wide range of burn rates by utilizing several key compositional factors:

- Fuel-to-oxidizer ratio (20:80 – 50:50 by weight);
- Ratio of Al/Si in binary fuel (20/80 – 90/10 by weight);
- Particle size of aluminum in the binary fuel (3 – 10 μm).

Figure 6.5 shows the effect of fuel to oxidizer ratio at constant ratio of aluminum-to-silicon in the binary fuel (30:70 by weight) on IBR. These measurements were conducted in an open column configuration and each point indicates the average IBR of ten open delay column tests.

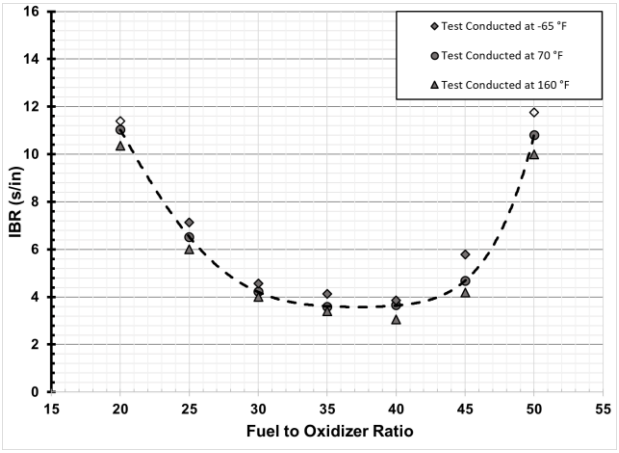

Figure 6.5. *IBR as a function of fuel-to-oxidizer ratio at constant concentration of aluminum in the binary fuel (Al(H-2)/Si=30/70 by weight). Each point indicates the average IBR of ten open delay column tests. Note: Data shown with an empty point failed to maintain combustion propagation.*

As can be observed in this graph, the IBR can be varied at 70 °F from approximately 3.5 to 11 s/in. The IBR at -65 °F and 160 °F are consistently lower and higher, respectively. The effect of aluminum concentration in the binary fuel on IBR is shown in Figure 6.6. This shows that some degree of tunability can also be achieved by this aluminum concentration adjustment.

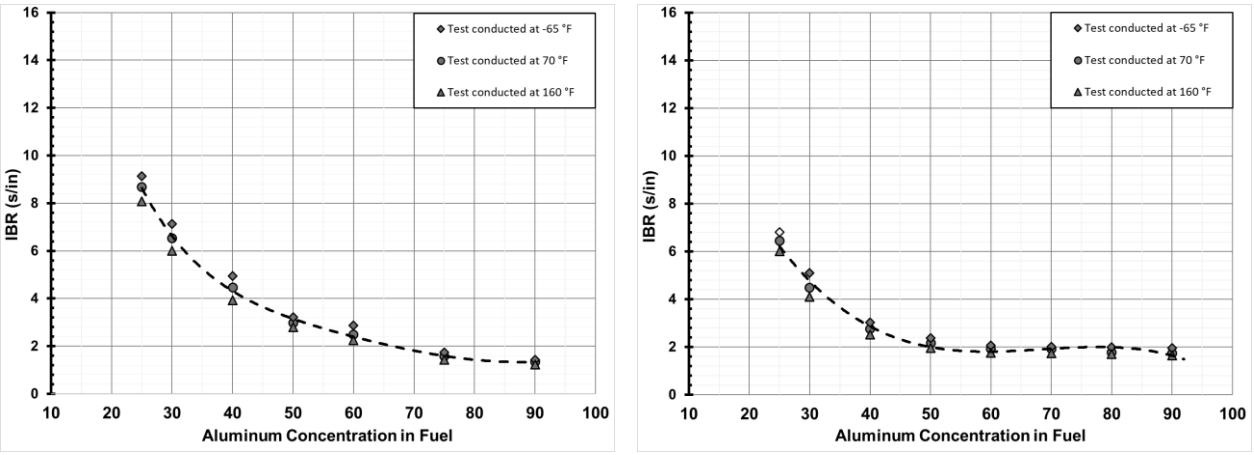

(a) (b)

Figure 6.6. *IBR as a function of fuel-to-oxidizer ratio at constant concentration of aluminum in the binary fuel (Al(H-2)/Si=30/70 by weight): (a) - 25/75 by weight and (b) – 45/55 by weight. Each point indicates the average IBR of ten open delay column tests. Note: Data shown with an empty point failed to maintain combustion propagation.*

The effects of spherical aluminum particle size and its concentration in the binary fuel on IBR were also tested and the results for two different aluminum particles are shown in Figure 6.7.

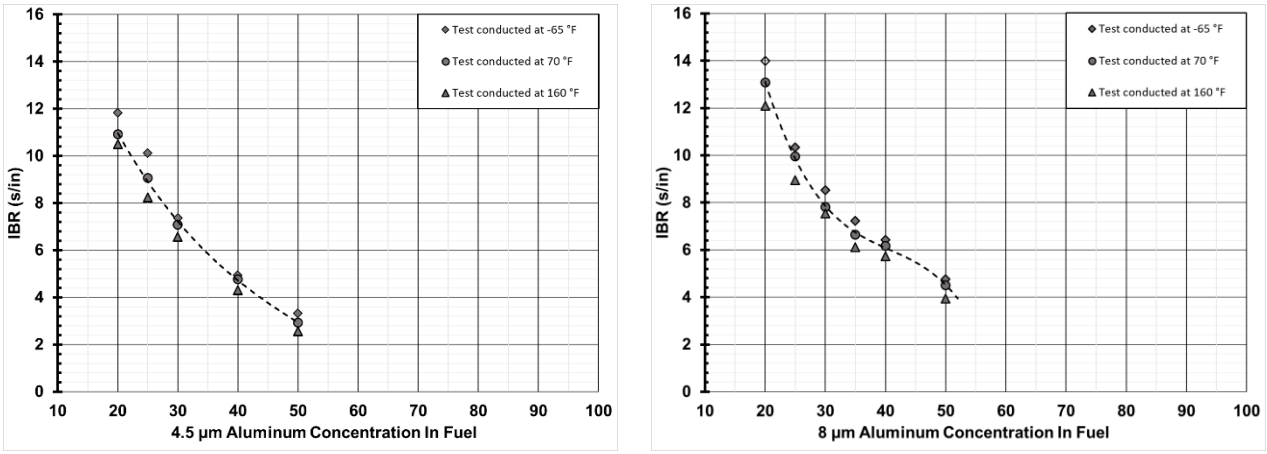

(a) (b)

Figure 6.7. *The effect of aluminum concentration in binary fuel and aluminum average particle size, (a): 4.5 µm and (b): 8 µm, on IBR at constant fuel-to-oxidizer ratio (25/75 by weight). Each point indicates the average IBR of ten open delay column tests. Note: Data shown with an empty point failed to maintain combustion propagation.*

The final down selected delay formulations and their identifiers are presented in Table 6.6. These formulation identifiers are used throughout the report to signify where the down selected formulations were used.

Table 6.6. *List and details of the down selected delay formulations.*

Identifier	Fuel to Oxidizer Ratio	Al to Si Ratio	SiO_2 (wt%)	DE (wt%)	Fuze Type	Comments
IMP-092716-V1	25:75	30:70	5	5	M201A1	• Mixed in Water • ADP 5% with respect to Al • Valimet H-2 Al • AEE 0-45 µm Si • Good results outperformed current production fuze
IMP-050818-V2	25:75	30:70	5	4.7	M213/ M228	• Mixed in Water • ADP 5% with respect to Al • Valimet H-3 Aluminum. • AEE 0-45 µm • Failed to produce quality results • 2 Failed to Fire (propagation issues)
IMP-082118-V3	25:75	35:65	7.5	5	M213/ M228 & M201A1	• Mixed in IPA • Valimet H-2 Al • Elkem 0-45 µm Si • Deliverable quality outperformed current production fuze • Zero miss fires

6.3. Testing and Consolidation Equipment

Fuze testing was conducted at extreme temperatures as specified in MIL-STD-331C Appendix C. The testing of these fuzes was slightly modified from the tests described in MIL-STD-331C due to not having boosters crimped to the fuze housings. The main purpose of this testing procedure was to ensure that the fuze's core temperature has equilibrated to the desired extreme temperature. The procedure used for this test was:

- Fuzes were soaked at -65 °F (-54 °C) for >4 hours,
- Fuzes were maintained at 68 °F (20 °C),
- Fuzes were soaked at +160 °F (71 °C) for >4 hours.
- All fuzes were tested within 70 s of removal from temperature conditioning chamber.

6.4. IMP A-1A Characterization

A-1A used for fuzes and mock delay columns is made to MIL-P-22264A with the following exemptions:

- Zirconium powder was -325 Mesh (44 µm) instead of 1 to 3 µm defined in MIL-Z-399D;
- Sieved using a 30 Mesh (595 µm) sieve instead of a 325-mesh sieve.

This configuration produces similar energy output as A-1A outlined in MIL-STD A-1A, while being more cost effective and safer to handle and produce in lab.

Three experiments were conducted to compare energy output performance of both types of A-1A (IMP and MIL-SPEC). Both experiments were conducted at SDSM&T and were as follows:

- Heat of combustion (reaction conducted under an air atmosphere)
- Heat of reaction (reaction conducted under an argon atmosphere)

The experiments for determination of heat of combustion and heat of reaction were conducted using a Parr instruments 6100 bomb calorimeter.

The data generated clearly demonstrated the similarity of heat of combustion and heat of reaction between the IMP A1-A and MIL SPEC A1-A transition charge (Table 6.7 and Table 6.8).

Table 6.7. *Heat of Combustion, IMP versus MIL-P-22264 A-1A*

Sample ID	Type	Sample Weight (g)	Total Heat (J/g)
408	IMP A-1A	1.1423	7,212.54
412	IMP A-1A	1.0003	8,226.56
413	IMP A-1A	1.1038	7,869.46
414	MIL SPEC A-1A	1.0141	7,685.52

Table 6.8. *Heat of Reaction, IMP versus MIL-P-22264 A-1A*

Sample ID	Type	Sample Weight (g)	Total Heat (J/g)
415	IMP A-1A	1.0926	2,001.13
417	MIL SPEC A-1A	1.0454	2,005.52

6.5. Gas generation determination

Gas generation of the delay formulation was tested at SDSM&T in a specially designed testing fixture. The fixture is demonstrated in Figure 6.8

a b

Figure 6.8. *(a) Gas generation testing fixture used to test gas volume produced by delay formulations. (b) Closed combustion bomb used for ignition A-1A and delay material.*

Supporting FactSage© calculations provided a theoretical amount of gas generated and a predicted adiabatic combustion temperature for the selected delay composition. The software predicted an adiabatic combustion temperature of 2226 K with 8.45 wt% of the products being in the gas phase. The theoretical amount of gas generated at adiabatic conditions is significant. However, large volumes of gas have not been observed during combustion of the delay formulation in the laboratory. Lower reaction temperatures are normally associated with nonadiabatic conditions and rather significant heat losses, therefore, the volume of gas generated during combustion was much lower, as indicated by the data presented in Figure 6.9.

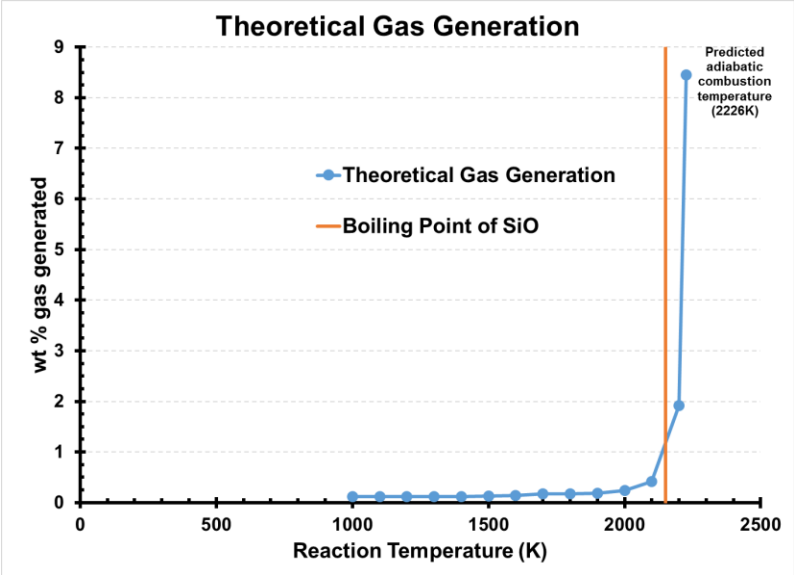

Figure 6.9. *Theoretical gas generation for the selected environmentally benign delay formulation at different reaction temperatures.*

Up to this point, only one A-1A and M213/M228 delay formulation sample was tested with gas generation empirically measured. The delay sample consisted of 25:75 fuel to oxidizer ratio and a 30:70 binary fuel ratio. The testing revealed that the A-1A produced 3.0 ml/g of gas and the delay formulation produced 4.6 ml/g of gas. This is significantly less than observed, during testing at EBA&D, from combustion of the tungsten / barium chromate-based delay currently used in M213/M228 fuzes.

6.6. Consolidation of Delay Formulations

A digital dial indicator mounted on the pneumatic press (pictured in Figure 6.10) allows for accurate measurement of the consolidation height for all delay formulations (mock delay columns and M213/M228 fuzes) for determination of the IBR. The dial indicator is zeroed at the bottom of the delay housing.

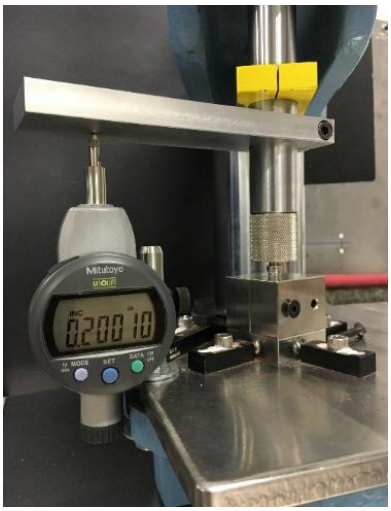

Figure 6.10. *Photograph of IMP developed delay column material consolidation height measurement system.*

6.7. Pressing force verification

This study was focused on understanding the correlation between the force used to consolidate columns and burn rates. The consolidation force was measured using a pressure cell. Testing was conducted in mock delay columns. As can be observed in Figure 6.11, adjusting pressing pressures from 15 to 20 ksi reduces the IBR by 0.21 s/in. It is also apparent that varying consolidation pressures from 25 to 37.5 ksi does not have any effect on IBRs. This data is useful in understanding the limits of operational parameters for manufacturing process development.

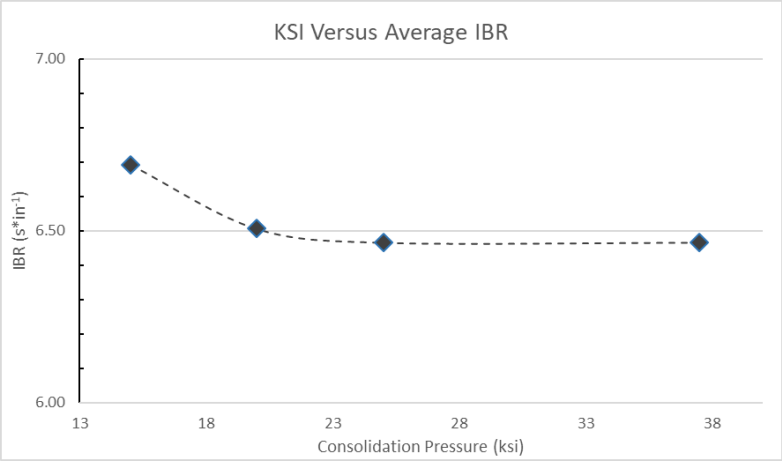

Figure 6.11. *Data demonstrating the correlation between consolidation pressure and IBR.*

6.8. Open Delay Column Manufacture and Testing

For characterization and tuning of the environmentally benign delay compositions, IMP developed a mock delay testing system. This testing system provides an accurate means to tune delay formulations to the desired requirements. Using this analysis method is cost effective and efficient. This method is nondestructive to expensive fuze system hardware and reduces manufacturing times. The mock delay column consists of a 1 in long aluminum tube with an inner diameter of 0.215 in and an outer diameter of 0.3125 in. The column is constructed by attaching an aluminum pressure sensitive tape disk on one end. The mock delay column is then placed into a manufacturing/consolidation die shown in Figure 6.12. A photograph of the mock aluminum tube with the developed consolidation die is shown in Figure 6.13.

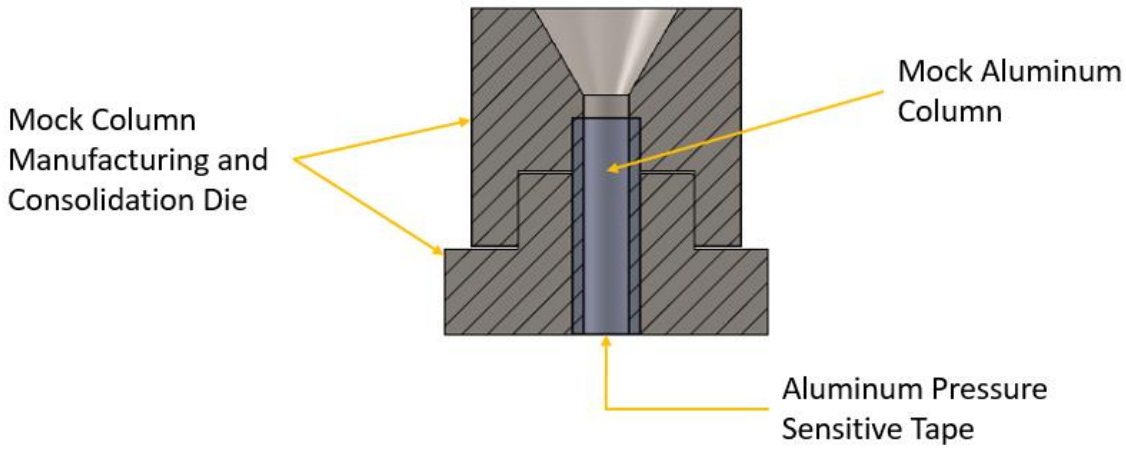

Figure 6.12. *Solidworks Rendering of a mock aluminum delay column within the consolidation die.*

Figure 6.13. *Photograph of mock delay column with the manufacturing and consolidation die.*

Mock delay column loading procedure is as follows:

1. Use a volumetric spoon to measure 30 ± 5 mg A-1A and add it to the mock delay housing;
2. Use a volumetric spoon to measure out the required amount of delay mixture and add it to the mock delay housing repeat for multiple layers (min 3 layers);
3. Use serrated scraping punch to degauss layer surface.
4. Use a volumetric spoon to measure out 60 ± 5 mg A-1A and add it to the mock delay housing;
5. Consolidate the materials using a pneumatic press at a pressure between 20 - 50 ksi;
6. Repeat until all mock delay columns have been prepared for testing.

Once the delay material is consolidated, the mock columns are loaded into the testing fixture as shown in Figure 6.14. This testing fixture consists of a steel outer housing, a steel lid, a zinc sleeve, a 32 BNC solid bare nickel chromium resistance wire (60% nickel, 16% chromium, 24% iron) as the ignition wire threaded through ceramic insulator. A 12 VDC charge is passed across the ignition wire using a BK precision 1692 3-15 VDC switching power supply. The resistance in the ignition wire produces heat to ignite the A-1A charge. Two ThorLabs DET10A photo diodes, connected to the testing assembly with fiber optic cables, are used to measure the burn times by detecting the light produced by the A-1A charges on either end of the delay element.

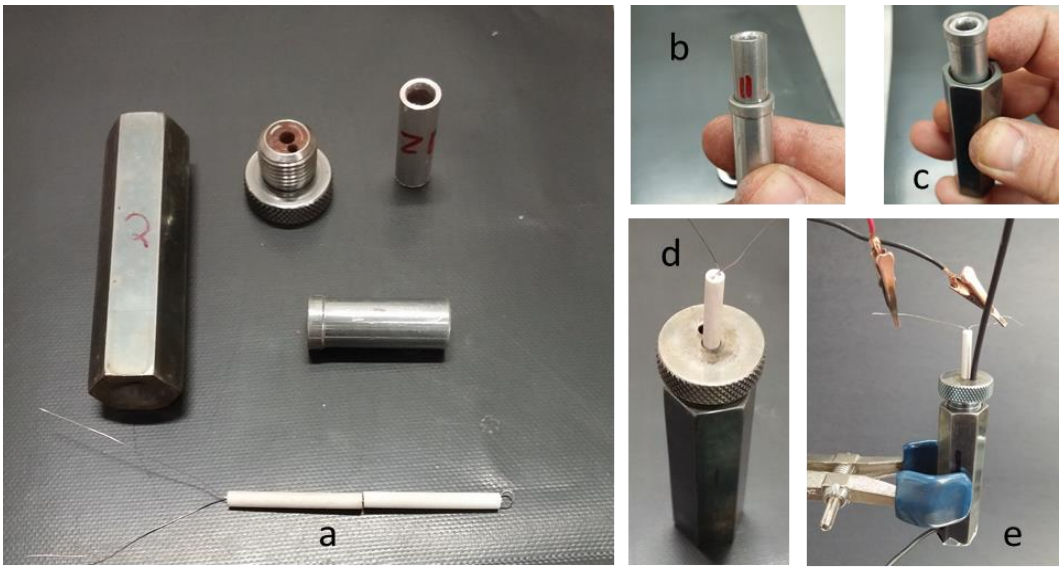

Figure 6.14. *Photographs of mock column burn time measurement setup. a) individual parts (steel housing and lid, mock delay column, zinc sleeve, and NiCr wire igniter), b) mock tube inserted into zinc sleeve, c) delay setup inserted into steel housing, d) assembled test setup, and e) testing setup with electrical leads and fiber optic cables connected.*

7. Task 3 – Optimization of mixing, dosing, and loading procedures

7.1. Mixing

IMP conducted a process analysis to identify critical parameters affecting the mixing process. The study was performed by running the program, pausing it every 30 seconds, opening the mixing vessel, documenting the observation with a photograph, and resuming the program. The Resodyn viewer presents a live feedback mixing profile of logged output channels (example shown in Figure 7.1). The interval study shows the conditions within the mixing vessel throughout this mixing process (see Figure 7.2). The observation study provided a clear correlation between the viewer output log and the slurry mixing consistency. It was observed that a phase change from solid to liquid did not occur until approximately 12 minutes into the program. This correlates with the % power increase on the viewer at that time.

Figure 7.1. *Typical output of the Resodyn viewer for the delay composition mixing process.*

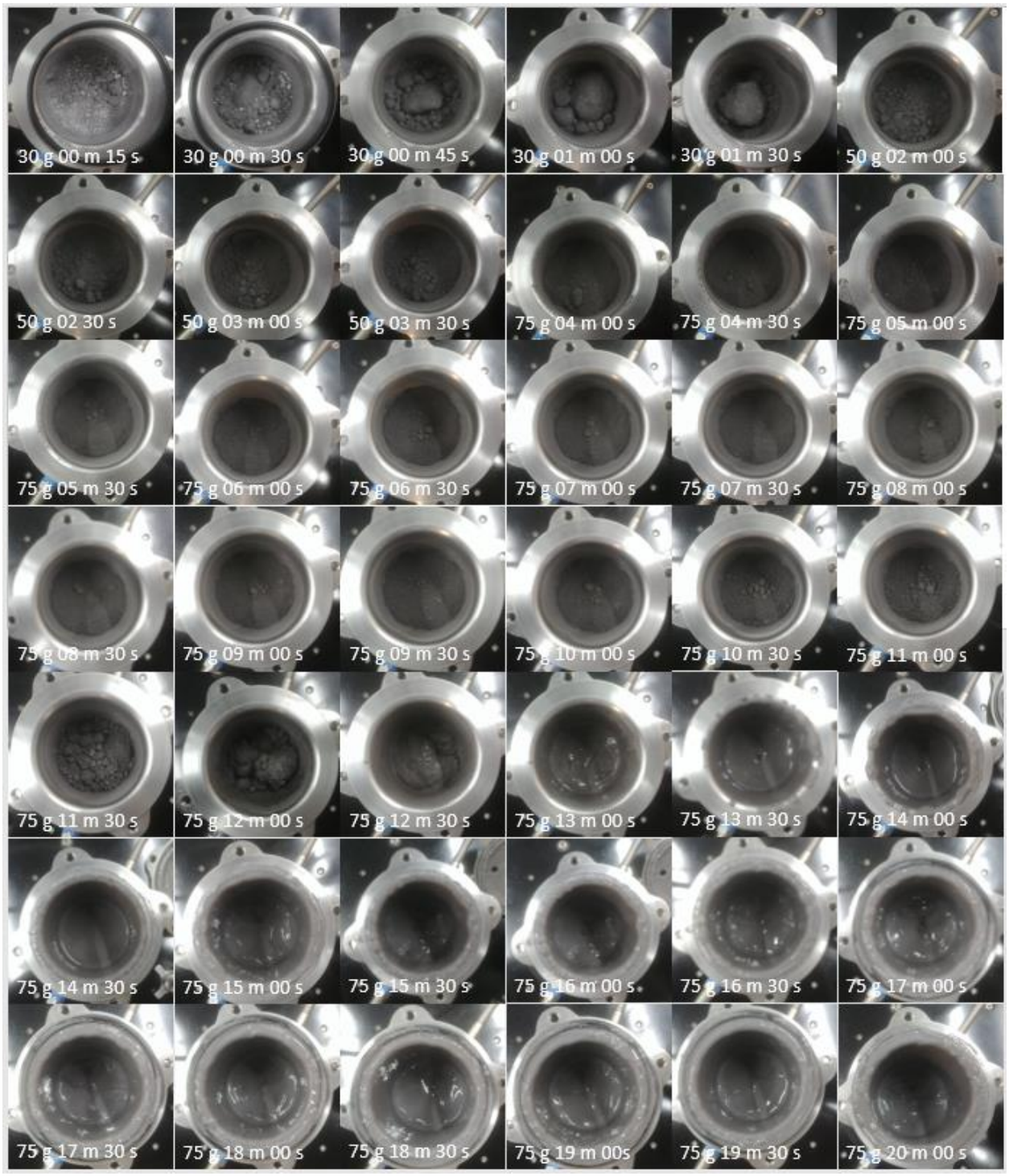

Figure 7.2. *Visual representation of delay mixing process throughout the Resodyn mixing program.*

The results from this study identified locations where the original mixing program had ineffective points.

1. The process showed that the initial interval of 30 g acceleration force was not needed and was eliminated.

2. This study also identified where in the program the vacuum should be applied in order to prevent air entrapment in the slurry. Prior to this study, vacuum was applied to the vessel when the program accelerated to 75 g acceleration force. Following this study, the vacuum is now applied when the phase change occurs at approximately 12 min into the program.
3. Finally, the program was extended to allow longer mixing of the liquid slurry. This process helps ensure all agglomerates are broken down. The time extension also provides an improvement in homogeneity of the resulting slurry formation.

The updated program is visualized in Figure 7.3, illustrating the effect of program adjustments.

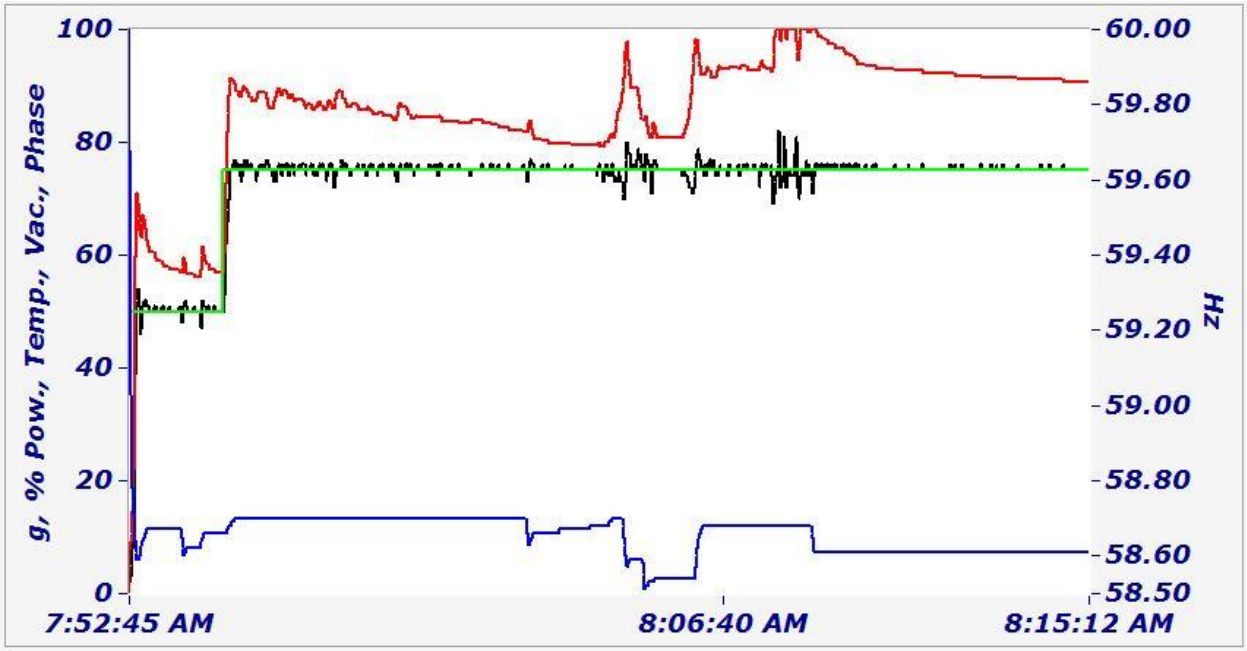

Figure 7.3. *Updated program output of the Resodyn viewer for the delay composition mixing process.*

7.2. Water Mixed Delay Mixture Preparation.

Procedures for the consolidation of the mock delay columns and M213/M228 fuze assemblies were developed and optimized to aid in efficient, repeatable, and consistent production of the fuze system. The production procedures for each fuze type are presented below.

Several mixing procedures were tested using a Resodyn LabRAM resonant acoustic mixer with a jacketed mixing vessel for the preparation of the delay formulation (see Figure 7.4). The procedures included both wet and dry mixing techniques. Based on results, the following wet mixing procedure was developed for the preparation of the delay formulations.

a

b

Figure 7.4. *(a) Resodyn LabRAM mixers with integrated cooling and vacuum systems. (b) Jacketed mixing vessel used for mixing of the environmentally benign delay formulation.*

1. Program the control software to mix the materials using the following procedure: 2 minutes at 50 g acceleration force, and 20 min at 75 g acceleration force;
2. Weigh out the required constituents and add the powders to the Resodyn LabRAM mixing container;
3. Add the required amount of water to the Resodyn LabRAM mixing container to achieve 75% solids loading concentration;
4. Secure the mixing container in the Resodyn LabRAM and start cooling water < 50 °F (10 ^{o}C);
5. Start pre-dispersing step at set-point of 50 g acceleration force for 2 min;
6. Ramp-up set-point to 75 g acceleration force for 20 min.

The drying procedure for the formation of the composite powder used for powder loading is as follows:

1. Pour the mixture onto a tray coated with a conductive Teflon sheet and spread it as thin as possible to facilitate drying;
2. Dry the delay mixture in a convection air dryer for 20-30 minutes under ambient conditions;
3. Sieve the delay mixture using a US #200 (70 µm) sieve;
4. Dry the delay mixture in a convection oven at 212 °F (100^{o}C) for 16 hours;
5. Place delay mixture in desiccator to cool.

7.3. Granule Formation

A method for the automated dosing of the delay formulation slurry for the formation of composite granules or direct loading of the delay columns was investigated. Initial production of the granules was conducted through dosing 35 µL of the prepared composite slurry from a manual displacement pipette onto a conductive Teflon sheet. The granules were then air dried under ambient conditions and then at 302 °F (150 °C) for 2 hours followed by storage in a desiccator for a minimum of 12 h. The granules were then used for the loading of the mock delay columns for characterization. For one batch, each individual granule was weighed after drying to determine a precision range

for the employed dosing technique and to ensure that settling of the material was not occurring during the dosing process. The composite granules were weighed in the order that they were dosed. The weight of each granule, along with the control limits, are presented in Figure 7.5. The control limits were set at plus and minus 3 standard deviations from the mean. The data showed that only two granules were outside the control limits. These granules could have been caused by slurry material sticking to the tip of the pipette after filling from the mixing container. After weighing, the granules were split into batches of 15 (based on dosing number) and then loaded into 30 delay columns. The weight of the 15 granules and consolidation height were compared, and the data is presented in Figure 7.6.

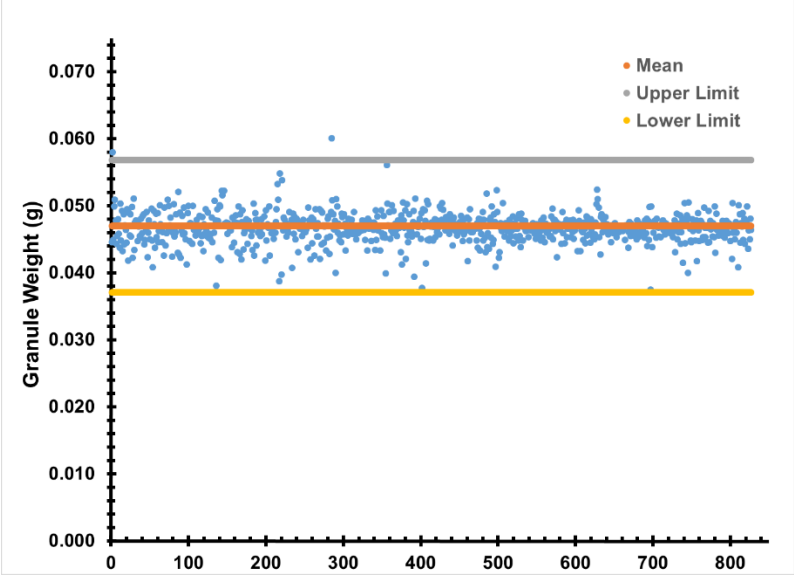

Figure 7.5. *Control chart for the weight of energetic composite delay column granules formed using a manual pipette.*

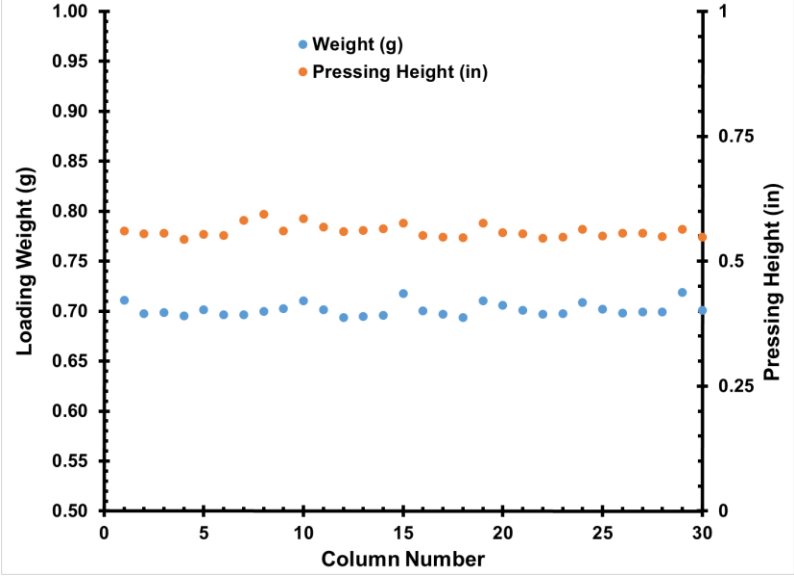

Figure 7.6. *Loading weight and consolidation height of delay columns loaded with the composite energetic delay mixture.*

For the automated formation of the energetic composite granules, the use of an air actuated positive displacement valve was selected. Based on previous experience, IMP selected the VDP150 positive displacement valve produced by Fisnar. A photograph of the valve and controller is shown in Figure 7.7.

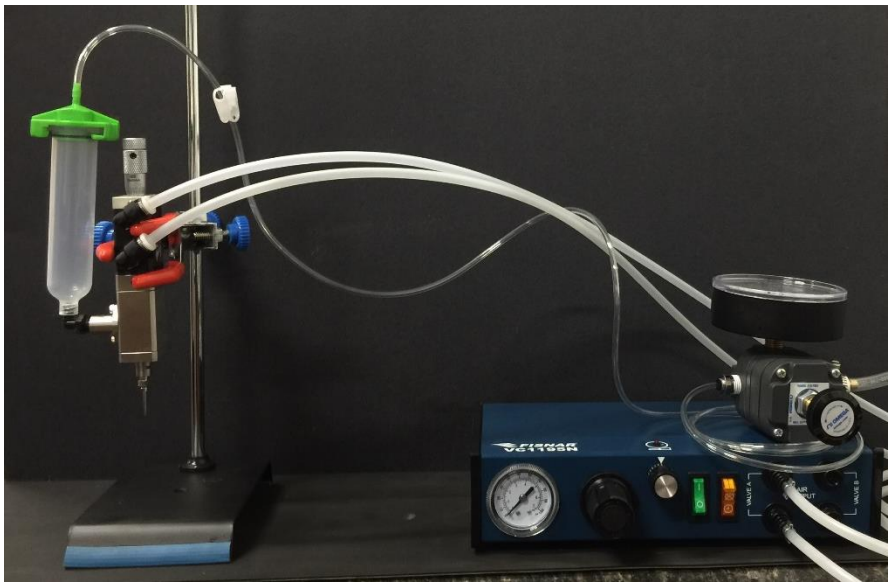

Figure 7.7. *Photograph of Fisnar VDP150 valve with controller and product syringe.*

For the initial granule dosing experiments, the valve was held with a clamp on a ring stand or by hand for determination of valve operating parameters prior to use on a xyz robotic platform.

The dosing experiments were conducted during year 1 of the project as year 2 focused on the powder loading of the delay columns. During the initial experiments, there were problems associated with clogging of the valve during the priming process due to the low viscosity of the composite slurry. The viscosity of the slurry was increased by reducing the water content of the composite slurry. In the next dosing experiment, approximately 300 granules were produced prior to the plugging of the valve. The viscosity of the composite slurry was further increased by reducing the water content to 2.27 g of solids per mL of water. The composite slurry was dosed into approximately 35 µL granules using the VDP150 positive displacement valve. For a selected experiment, 50 g of composite slurry was prepared and approximately 560 granules were produced. After drying, the selected granules were weighed in the order they were dosed. The data is presented in Figure 7.8 The results indicated that some granules fell outside of the plus/minus 3 sigma window. At this time, it is unknown if these slight variations in granule weight will have any effect on the IBR of delay columns produced using a specific number of composite granules. Additionally, it appears that the weight of the granules is decreasing throughout the dosing process.

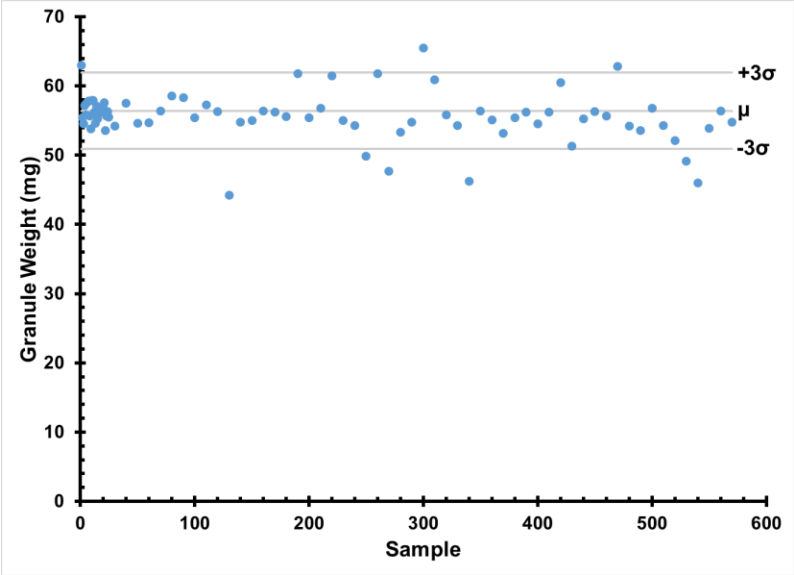

Figure 7.8. *Weights of selected granules after drying for a dosing experiment.*

In addition to the dosing of granules, investigation into the direct dosing and freeze drying of the environmentally benign delay formulation slurry in M201A1 delay columns was conducted. The first dosing experiment consisted of a 100 g batch ($SrMoO_4$: 67.4 wt%; Al: 6.7 wt%; Si: 15.7 wt%; D.E.: 4.8 wt%; SiO_2: 5.0 wt%; and ADP: 0.4 wt%) mixed in 32 mL of water. The prepared mixture was observed to have low viscosity, similar to water, and settling of the constituents during processing was a concern. Before dosing, the mock aluminum delay columns were loaded with dry A-1A (30 mg) as the output charge. Each column was then dosed with 500 µL of the composite slurry using a positive displacement pipette. The VDP150 positive displacement valve was not used for this experiment due to clogging of the valve inlet. The settling of the constituents most likely caused the clogging. Before consolidation, the mock aluminum columns were air dried for 4 hours followed by 70 hours in a desiccator. Due to the structure of the dried material within the mock columns after drying (Figure 7.9), it was necessary to consolidate the columns before the addition of the A-1A transition charge. Initial consolidation of the material occurred at 30 ksi. After the first consolidation step, an X was scribed into the top of the mix to increase the interface between the A-1A transition charge and the environmentally benign delay formulation. Following the addition of 30 mg of A-1A to the mock delay column, a second consolidation step occurred at 30 ksi followed by the combustion characterization of the 10 columns at ambient conditions. After the second consolidation, the material within the 10 columns had an average height of 0.412 inches with a standard deviation of 0.005 in. Ignition of the A-1A transition charge did not lead to combustion of the environmentally benign delay formulation in several of the columns produced from this batch. Failure analysis of the columns indicated that a black crystalline layer had formed on the top of the column, most likely silica and silicon. This layer could have been formed due to segregation of the constituents and inhibited ignition. Also, consolidation of the material within the mock delay columns was not uniform within the material or between columns.

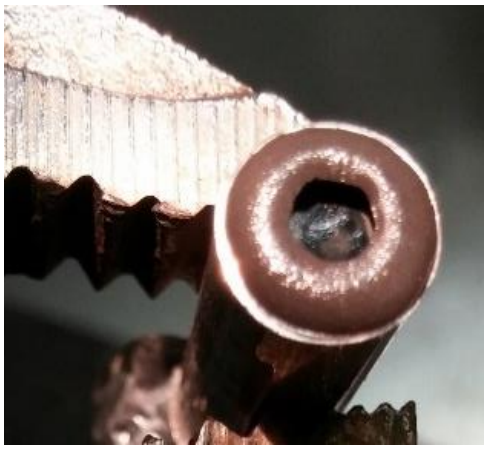

Figure 7.9. *Photograph of mock aluminum delay column dosed with the environmentally benign delay composition after drying.*

To increase the slurry viscosity in the next experiment, the water content was decreased by 0.04 mL per g of material. The viscosity of the slurry was still too low and led to similar results as the first test. Further reduction of the water (by 0.04 mL per g of material) led to the formation of a damp powder after mixing. The prepared material was processed a second time in the Resodyn LabRAM after the addition of addition water (0.02 mL per g of material). The slurry produced had a viscosity that was too low and caused segregation of the constituents during drying.

Slurry loading was attempted a fourth time with the water content being reduced further by 0.015 mL per gram of material. This batch was a 50 g batch ($SrMoO_4$ 67.4 wt%, Al 6.7 wt%, Si 15.7 wt%, D.E. 4.8 wt%, SiO_2 5.0 wt%, and ADP 0.4 wt%) dispersed in 12.25 mL of water. The slurry came out thick, but flowable and could be processed using a positive displacement pipette. In addition to the increased viscosity, freeze-drying of the prepared mock delay columns minimized constituent segregation during the drying process. For freeze-drying, the columns were frozen at 14 °F (-10 °C) for 2.5 h under no vacuum followed by the application of vacuum at 0.44 Torr for 16 hours. The dried samples were then warmed to room temperature under vacuum and consolidation occurred at 30 ksi. Visual inspection of the columns did not indicate any segregation of the constituents and the black layer previously observed on the top of the columns was not evident. The first column to be consolidated still had wet material at the top. The columns were then dried at 194 °F (90 °C) for 2 h followed by storage in a desiccator for 16 h. The columns were then consolidated at 30 ksi and combustion characterization completed. In Table 7.1 the column height, burn time, and IBR data are presented for the first batch of freeze-dried mock delay columns.

Table 7.1. *Consolidation height, burn time, and IBR data for first batch of freeze-dried columns.*

Column	Height (in)	Burn time (s)	Inverse Burn Rate (s/in)
1	Problems during consolidation		
2	0.430	2.332	5.423
3	0.420	2.212	5.264
4	0.438	2.452	5.602
5	0.431	2.500	5.807
6	0.414	2.212	5.348
7	0.433	2.276	5.254
8	0.417	2.180	5.225
9	0.424	2.484	5.853
10	0.421	2.340	5.558
11	0.428	2.172	5.072
12	0.434	2.332	5.379
13	0.295	1.412	4.786
14	0.431	2.268	5.268
15	0.418	2.288	5.468
16	0.423	2.064	4.879
17	0.407	2.044	5.021
18	0.443	2.404	5.427
19	0.409	2.388	5.834
20	0.411	2.244	5.465
Minimum	0.295	1.412	4.786
Maximum	0.443	2.500	5.853
Range	0.148	1.088	1.067
Average	0.417	2.242	5.365
Std Dev	0.031	0.238	0.298

Based on the results, a second freeze-drying experiment was conducted on 30 mock aluminum delay columns that were slurry loaded using a batch of environmentally benign delay formulation identical to the previous batch. Each mock delay column was dosed with 300 µL of the composite slurry. There were some difficulties related to the loading of the syringe which caused some columns to be under- or over-loaded. Freeze-drying of the mock delay columns occurred by freezing the columns for 7 h at 14 °F (-10 °C) before the applying vacuum (0.44 to 0.65 Torr) for 40 h. The columns were then warmed to room temperature under vacuum and consolidation occurred according to the previously specified procedure at 30 ksi. The results indicated that six columns failed to ignite during combustion tests. Failure analysis of columns 1 and 2 indicated that there was still water present in the columns after freeze-drying. For some freeze-drying applications, an additional drying step may be required to remove any residual water. Before testing the remaining columns, drying of the remaining mock delay columns occurred at 194 °F (90 °C) for 2 h followed by storage in a desiccator for more than 70 h. After the secondary drying step, 4 columns still failed to ignite. Visual inspection of the top of the columns indicated that the A-1A transition charge had become covered with delay mixture during consolidation. Ignition of the unfired delay columns from the bottom further validated this hypothesis. The delay mixture covering the A-1A most likely scraped off the column walls during consolidation. For the next set of delay columns, the material was pre-consolidated by hand before the addition of the A-1A transition charge to ensure this problem does not occur.

Table 7.2. *Consolidation height, burn time, and IBR data for the second batch of freeze-dried columns (10 columns were prepared with powder loaded dried material as a baseline, which yielded an IBR of 4.05 sec/in with a standard deviation of 0.24 sec/in).*

Column	Height (in)	Burn time (s)	Inverse Burn Rate (s/in)
1	0.38820	No ignition	
2	0.23230	No ignition	
3	0.36500	2.008	5.501
4	0.39550	1.968	4.976
5	0.42200	2.216	5.251
6	0.38950	1.816	4.662
7	0.39100	No ignition	
8	0.41340	1.874	4.533
9	0.38440	2.122	5.520
10	0.39670	2.058	5.188
11	0.40300	1.794	4.452
12	0.38320	2.042	5.329
13	0.38650	2.218	5.739
14	0.38600	2.162	5.601
15	0.38200	2.048	5.361
16	0.38400	No ignition	
17	0.39850	1.992	4.999
18	0.60340	2.584	4.282
19	0.30670	1.736	5.660
20	0.39250	2.040	5.197
21	0.38080	No ignition	
22	0.38370	2.040	5.317
23	0.38220	No ignition	
24	0.40850	2.224	5.444
25	0.38120	2.348	6.159
26	0.35500	1.892	5.330
27	0.45170	2.404	5.322
28	0.39110	2.132	5.451
29	0.39300	2.036	5.181
30	0.39470	1.956	4.956
Minimum	0.232	1.736	4.282
Maximum	0.603	2.584	6.159
Range	0.371	0.848	1.877
Average	0.391	2.071	5.226
Std Dev	0.054	0.197	0.430

Based on the results of the freeze-drying experiments up to this point, another batch of environmentally benign delay formulation was prepared. The composite slurry loaded mock delay columns and the excess composite material were frozen at -22 °F (-30 °C) for 72 h before freeze-drying at 23 °F (-5 °C) for 24 h under vacuum (maximum vacuum 0.76 Torr). After freeze-drying the samples, a secondary drying step was applied to remove any residual water 302 °F (150 °C) for 4 hours followed by cooling and storage in a desiccator for a minimum of 16 h. The excess material was sieved, and powder loaded into mock delay columns as a baseline for the material characterization. In Table 7.3 the consolidation height, burn time, and IBR data are listed for the third batch of slurry loaded freeze-dried columns.

Table 7.3. *Consolidation height, burn time, and IBR data for third batch of slurry loaded freeze-dried columns.*

Column	Height (in)	Burn time (s)	Inverse Burn Rate (s/in)
1	0.41700	2.308	5.535
2	0.41400	2.324	5.614
3	0.40820	2.332	5.713
4	0.42720	2.540	5.946
5	0.40860	2.468	6.040
6	0.41730	2.628	6.298
7	0.40150	2.448	6.097
8	0.40320	2.456	6.091
9	0.41200	2.296	5.573
10	0.41160	2.52	6.122
11	0.40230	2.480	6.165
12	0.41240	2.496	6.052
13	0.41640	2.576	6.186
14	0.40970	2.448	5.975
15	0.40600	2.456	6.049
16	0.41360	2.560	6.190
17	0.40680	2.584	6.352
18	0.40670	2.612	6.422
19	0.40930	2.668	6.518
20	0.40120	2.604	6.491
Minimum	0.401	2.296	5.535
Maximum	0.427	2.668	6.518
Range	0.026	0.372	0.984
Average	0.410	2.490	6.071
Std Dev	0.006	0.111	0.287

The data in the table above indicates that slurry loading of the columns yielded a consistent loading. The use of a pre-consolidation step of the material to remove any residual material from the sides of the column eliminated the previously observed misfires. The burn time/IBR data for the columns are very consistent and indicate that this technique should work to produce M201A1 delay columns.

The next dosing experiment consisted of a 50 g batch ($SrMoO_4$ 67.4 wt%, Al 6.8 wt%, Si 15.8 wt%, D.E. 4.7 wt%, SiO_2 5.0 wt%, and ADP 0.4 wt%) mixed in 12.4 mL of water. The viscosity of the prepared mixture was thick, close to cake batter, and settling of the constituents during processing was minimal. There were four processing and performance parameters that were investigated as part of this dosing experiment:

1. Requirement of A-1A transition charge;
2. Feasibility of freeze-drying M201A1 columns;
3. Use of Al-Bi2O3 nanothermite granules as a ZPP output charge replacement;
4. Use of slurry dosing for the formation of M201A1 delay columns.

Prior to dosing, each M201A1 delay column was loaded with an aluminum-bismuth trioxide nanothermite pellet (approximately 40 mg) for the output charge. The composite slurry was prepared using the Resodyn LabRAM. After mixing, 400 µL of the composite slurry was dosed into each delay column using a positive displacement pipette. The M201A1 columns were then

frozen at -22 °F (-30 °C) for 72 hours followed by freeze drying for 24 hours at 23 °F (-5 °C) and 0.8 Torr. After freeze drying, the columns were split into 2 batches. Batch 1 (qty: 20 columns) was placed in a convection oven at 194 °F (90 °C) for 4 hours for a secondary drying step prior to storage in a desiccator. Batch 2 (qty: 15) was placed directly into the desiccator. The different drying procedures were used to determine if a secondary drying step, at an elevated temperature, is required after freeze drying. All columns were stored in the desiccator for 48 hours before consolidation. After drying in the desiccator, the 35 prepared M201A1 delay columns were processed as follows:

- Columns 1-5: No A-1A transition charge and consolidated at 30 ksi (dried at 194 °F (90 °C));
- Columns 6-35: 30 mg of A-1A as the transition charge and consolidated at 30 ksi.
    - Columns 6-20 dried at 194 °F (90 °C) and
    - Columns 21-35 only dried in a desiccator).

Primers were then inserted and crimped into M201A1 columns following developed procedures. All 35 columns were inserted into M201A1 housings and fired. Results of columns 1-5 (no A-1A transition charge) indicated the primer itself is inconsistent, but capable of igniting delay mix (1 out of 5 ignited). The burn time results of columns 6-35 are presented in Table 7.4 and Table 7.5. The use of the nanothermite granules as the output charge led to inconsistencies in both the column consolidation height and burn time as the placement of the granules within the column was not consistent. For all future experiments, the nanothermite will be loaded into the columns in powder form.

Table 7.4. *Consolidation height, burn time, and IBR data for slurry loaded and freeze dried M201A1 delay columns with a secondary drying process at* 194 °F (90 °C) *("na" – no burn time was determined due to an error in the timing setup – column functioned properly).*

Column	Height (in)	Burn time (s)	Inverse Burn Rate (s/in)
6	0.53800	1.700	3.160
7	0.58700	1.600	2.726
8	0.35090	1.100	3.135
9	0.54660	1.700	3.110
10	0.59480	1.733	2.914
11	0.56320	1.500	2.663
12	0.61600	1.667	2.706
13	0.59210	na	na
14	0.60460	1.433	2.371
15	0.56420	1.500	2.659
16	0.60320	1.667	2.763
17	0.57220	1.600	2.796
18	0.59020	1.600	2.711
19	0.47280	na	na
20	0.57750	1.667	2.886
Minimum	0.351	1.100	2.371
Maximum	0.616	1.733	3.160
Range	0.265	0.633	0.789
Average	0.558	1.574	2.815
Std Dev	0.065	0.162	0.215

Table 7.5. *Consolidation height, burn time, and IBR data for slurry loaded and freeze dried M201A1 delay columns with no secondary drying process and only desiccator storage ("na" – column did not ignite).*

Column	Height (in)	Burn time (s)	Inverse Burn Rate (s/in)
21	0.55060	2.400	4.359
22	0.54000	2.367	4.383
23	0.55040	na	na
24	0.53700	2.267	4.221
25	0.54540	1.967	3.606
26	0.54800	1.867	3.406
27	0.54400	1.600	2.941
28	0.55200	na	na
29	0.53560	2.567	4.792
30	0.54800	1.933	3.528
31	0.55720	1.867	3.350
32	0.54720	2.200	4.020
33	0.54300	1.967	3.622
34	0.53400	1.867	3.496
35	0.55420	na	na
Minimum	0.534	1.600	2.941
Maximum	0.557	2.567	4.792
Range	0.023	0.967	1.851
Average	0.546	2.072	3.810
Std Dev	0.007	0.271	0.516

The data indicates that slurry loading of the M201A1 column is possible. However, due to the increased processing time associated with this effort, additional focus was not continued.

7.4. IPA Mixing

Due to inconsistent burn rates and problems with sustained propagation demonstrated in deliverables for Task 13 the entire process was investigated. One of the key issues discovered was that $SrMoO_4$ was slightly soluble in water. It was hypothesized that during the mixing process using water the $SrMoO_4$ morphology was changing. The delay properties when dried was evidence of this. When the delays were compared side by side after drying the water mixed delay was hard and difficult to sieve, as opposed to the IPA mixed delay that was talc-like powder which was easily sieved. The resulting delay presented a much tighter standard deviation in both open columns and M213/M228 fuzes. The IPA mixed delay was also slightly faster than its comparable water mixed delay. This is believed to be caused by better mixing of constituents. This investigation led to the ability to use polymeric binders that were previously not viable.

The processing using IPA is similar to water processing:

1. Program the control software to mix the materials using the following procedure: 2 minutes at 50 g acceleration force, and 20 min at 75 g acceleration force;
2. Weigh out the required constituents and add the powders to the Resodyn LabRAM mixing container;
3. Add the required amount of water to the Resodyn LabRAM mixing container to achieve 75% solids loading concentration;
4. Secure the mixing container in the Resodyn LabRAM and start cooling water < 50 °F (10 °C);
5. Start pre-dispersing step at set-point of 50 g acceleration force for 2 min;
6. Ramp-up set-point to 75 g acceleration force for 20 min;

The drying procedure for the formation of the composite powder used for powder loading is as follows:

1. Pour the mixture onto a tray coated with a conductive Teflon sheet and spread it as thin as possible to facilitate drying;
2. Dry the delay mixture in a convection air dryer for 5-10 minutes under ambient conditions;
3. Sieve the delay mixture using a US #200 (70 µm) sieve;
4. Dry the delay mixture in a convection oven at 140 °F (60 °C) for 16 hours;
5. Place delay mixture in desiccator to cool;

7.5. Mixing Improvements

This testing was done with respect to a T-10 replacement. However, all processing and loading techniques were the same as the delay used for M213/M228 fuzes. All delay compositions used in this study were prepared utilizing RAM mixing technology and the same SOP. The delay composition used in all 10 mixtures were made using an identical formulation to IMP-B092716-V1 except utilizing IPA as the processing liquid.

- 25 to 75 fuel to oxidizer ratio;
- 30 to 70 aluminum to silicon ratio;
- Fumed silica dilution was 5 wt%;
- Solids loading of 75% (25 g batch with 8.5 g IPA).

The test consisted of ten individual delay mixes. From each prepared and dried delay mix ten open columns were manufactured and tested at 70 °F. During the pressing there were two separate operators making open columns. The manufacture of the open column testing was conducted as follows:

- All layers were pressed at 30 ksi for approximately 15 second dwell;
- 25 mg A-1A for output charge pressed and measured;
- Three layers of 230 mg delay composition;
- 50 mg A-1A ignition charge.

All layers were measured, the output charge was subtracted from the final delay layer. This method ensures that only the delay was included in the IBR.

Delay compositions were mixed consecutively using the same RAM recipe. This recipe mixes the slurry for 22 minutes at 50 and 75g's. All compositions demonstrated slurry formations at similar points, approximately 13 minutes, into the mixing process (see Figure 1). The slurry formation was illustrated in the RAM Viewer.

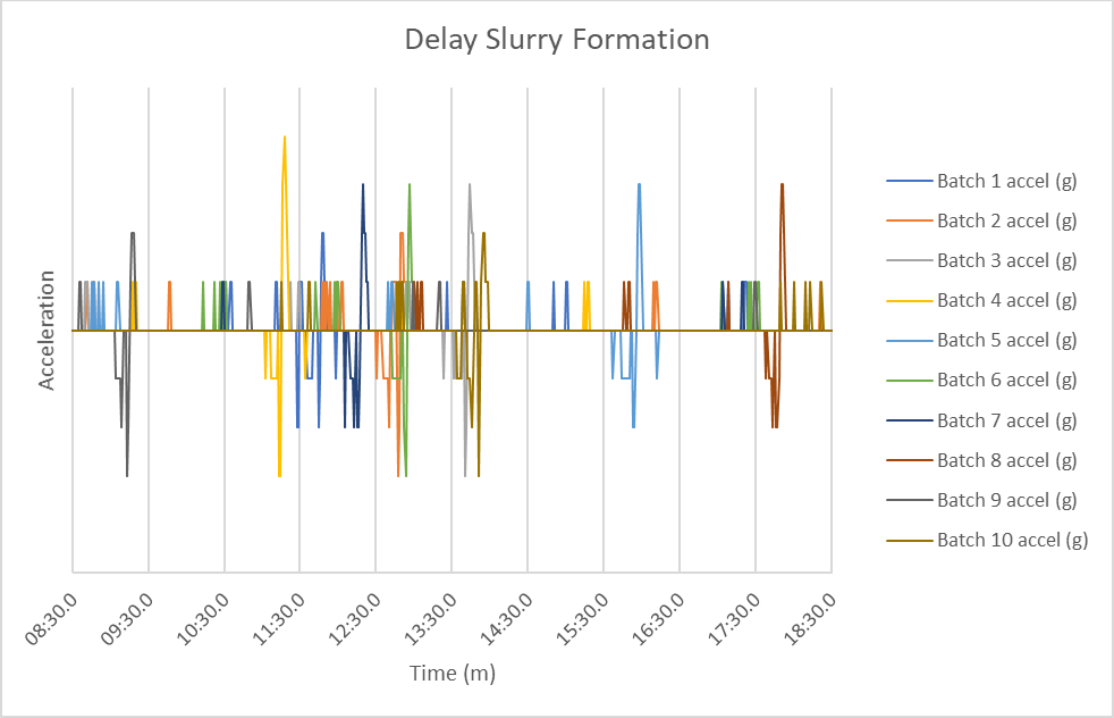

Figure 7.10. *Combined RAM mixing logs demonstrating slurry formation at average mix time near 13 minutes. This is the point in the recipe when components are adequately wetted to form a slurry.*

Table 7.6. *Batch to batch open column testing results batch 1 through 10 were new batches. Batch 1A and 2A were previously reported testing data. Batch 6 and 7 remade for uniform press operator.*

Batch	Average IBR (s/in)	Standard Deviation	Coefficient of Variation %
1	3.38	0.10	3.01
2	3.36	0.06	1.87
3	3.34	0.05	1.55
4	3.35	0.06	1.69
5	3.37	0.06	1.65
6	3.31	0.10	2.98
7	3.36	0.05	1.41
8	3.45	0.07	2.03
9	3.37	0.04	1.18
10	3.35	0.05	1.51
1A	3.34	0.04	1.27
2A	3.30	0.07	1.97
112 Open Delays Overall Results	3.36	0.07	2.21

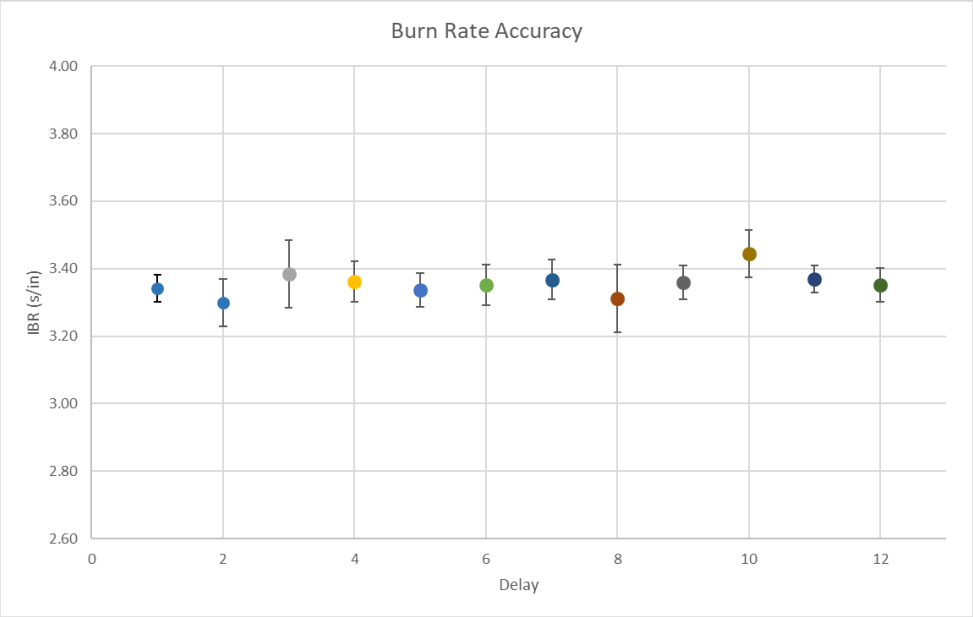

Figure 7.11. *Points depict average batch IBR and error bars represent standard deviation. Batch 1 and 2 (1A & 2A) were previously reported data. Batch 3 begins the new batches.*

Although this test was for T-10, it is applicable to both T-10 and tungsten / barium chromate replacement due to the entire process and the formulations being the same. All tested delays met the requirements for the Mk 4 MOD 2 testing requirements in open columns. The testing demonstrates 112 open delay columns from twelve batches performed well within the accuracy required of open columns in MIL-D-85306A(AS) *Military Specification, Delay Composition, T-10* and customer requirements under N00174-17-D-0008, Statement of Work for *Evaluation and Characterization of Strontium Molybdate Delay Composition*. These references require 3.31 to 3.35 s/in IBR and a CV% of less than 5.0%. All the data collected from this experiment, demonstrates this mixing process exceeds all requirements. IMP can confidently conclude the proposed mixing process utilizing RAM technology exceeds requirements set for this project.

7.6. Loading Improvements

Using the delay material developed under this project and IMP IRAD funded dispensing system, during year four of this effort a new technology in loading was investigated to provide a substantial improvement in slurry loading of the delay material. This development investigated the use of auger type valves rather than the piston driven valves, as previously investigated. The advancement provided a continuous flow of delay slurry capable of loading an entire fuze. This technique can be seen in Figure 7.12.

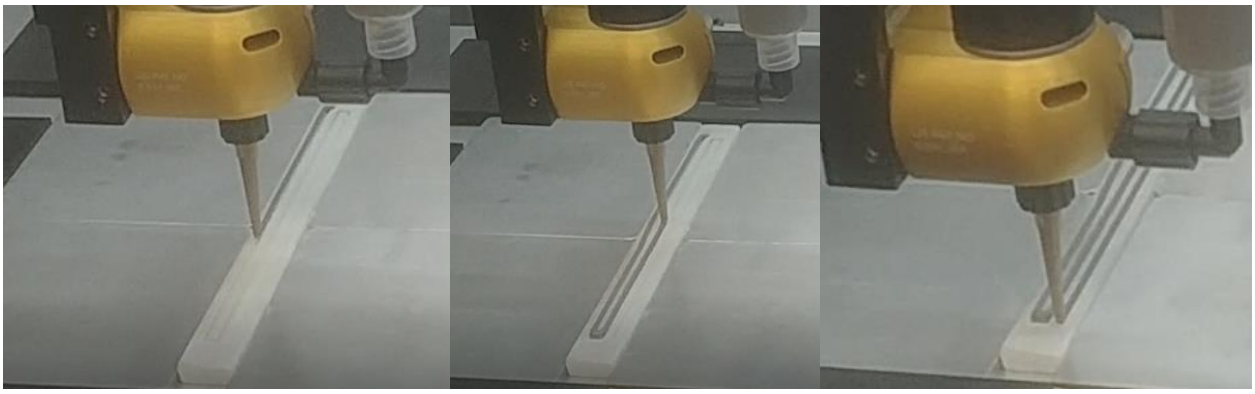

Figure 7.12. *Depositing delay slurry onto substrate for new dispensing technology investigation.*

Although this testing was highly successful (see Figure 7.13), there remains much to be determined regarding slurry optimization for use in this type of loading technique. The slurry is currently being studied for proper polymeric binder concentration and viscosity requirements. The solids loading ratios must be optimized to meet loading objectives. The viscosity must also be considered when developing this methodology. It has been noted that the flowability of the slurry is crucial to filling voids in fuze housings. Another crucial element to this development is the long-term stability of the delay with the polymeric binder necessary for this technique to be viable.

Figure 7.13. *Image of combustion experiment of deposited delay slurry.*

The early application of this technique has led to some encouraging results. Although not fully understood why, the burn time of the delay slurry is nearly double that of the same delay without the binder additive. This binder has also showed the same result when sieved and tested in open columns. Because of this, the binder may also prove to be an excellent manufacturing aid to prevent segregation when using legacy loading techniques.

8. Task 4 – Manufacturing and testing of ten fully assembled M201A1 delay elements

8.1. Development Attempts

An environmentally benign delay formulation with a composition of: $SrMoO_4$ 63.13 wt%, Al 8.12 wt%, Si 18.96 wt%, Diatomaceous Earth (DE) 4.77 wt%, and Bentonite 5.02 wt% was prepared using the water-based mixing technique in the Resodyn LabRAM I. This delay material was processed by removing water by convective drying at 70 °F in low humidity for 2 h, sieved to 425 μm, and finally dried at 250 °F for 4 h to remove any remaining water. From this mixture, 150 mock aluminum delay columns were prepared for characterization. The mock aluminum delay columns were volumetrically loaded with this delay formulation and 30 mg of A-1A prior to consolidation of the materials at 30 ksi. The average height of the delay columns was 0.30" with a standard deviation of 0.015". The columns were put into groups of ten. These groups were then randomly tested at the required temperatures for a total of 50 delay columns at each temperature. The burn time results, for the columns tested at -25 ^{o}F, 70 ^{o}F, and 160 ^{o}F, were 1.35 s with a standard deviation of 0.11 s, 1.38 s with a standard deviation of 0.11 s, and 1.26 s with a standard deviation of 0.12 s, respectively. Upon completion of the tests, the environmentally benign delay mixture was loaded into five M201A1 delay columns with 30 ± 5 mg of zirconium-potassium perchlorate (ZPP) as the output charge and 30 ± 5 mg of A-1A as the transition charge. The materials were consolidated at 30 ksi in one pressing step. After consolidation, a M39A1C primer was inserted into the delay column and the top of the column crimped. The complete column was inserted into the M201A1 fuze assembly housing as shown in Figure 8.1. The five prepared delay columns were fired, and the burn times were determined through video analysis. The columns had an average burn time of 1.2 s with an average column height of 0.37", indicating that the material is burning faster within the M201A1 delay column than in the open column.

The faster burn rate in the M201A1 delay columns indicated that a new delay formulation with lower aluminum concentration to slow down the burn time should be used. The composition of the new environmentally benign delay formulation was: $SrMoO_4$ 63.13 wt%, Al 5.42 wt%, Si 21.65 wt%, DE 4.77 wt%, and Bentonite 5.02 wt%. This environmentally benign delay formulation was tested in ten mock aluminum delay columns each at -25 ^{o}F and 70 ^{o}F. The burn time results were 2.21 s with a standard deviation of 0.21 s and 2.04 s with a standard deviation of 0.13 s, respectively.

Figure 8.1. *Photograph of M201A1 environmentally benign delay column with M39A1C primer crimped and inserted in the grenade delay column housing.*

The adjusted formulation was tested in fully assembled M201A1 fuze assemblies and provided an average measured burn time of 1.9 seconds with a column height of 0.31 inches. However, during the characterization of 100 fully assembled M201A1 fuze assemblies at ambient conditions, incomplete combustion of the delay mixture within the column led to a failure of the output charge ignition in several columns. Failure analysis on the delay columns was conducted and it was determined that the change in formulation had generated a reactive mixture that did not consistently maintain a self-sustained combustion. In an attempt to ensure self-sustained combustion, new formulations were explored. The concentration of aluminum was increased, the particle size of the silicon, which was 30 microns, was decreased, and/or the binder (Bentonite) was removed from the system. Environmentally benign delay formulations, with the adjusted compositions, were prepared for testing in the mock aluminum delay columns. The compositions of the four formulations prepared are presented in Table 8.1. Each formulation was tested in 75 mock delay columns under ambient conditions.

Table 8.1. *Identified environmentally benign delay formulations (DE, ADP).*

Formulation	Wt% $SrMoO_4$	Wt% Al	Wt% 30 µm Si	Wt% 1-5 µm Si	Wt% DE	Wt% Bentonite	Wt% ADP
1	66.3	5.7	22.7	0.0	5.0	0.0	0.3
2	66.3	5.7	0.0	22.7	5.0	0.0	0.3
3	62.9	6.8	0.0	20.3	4.7	5.0	0.3
4	62.9	6.8	20.3	0.0	4.7	5.0	0.3

The consolidated mock delay columns had an average height of 0.298 inches with average inverse burn rates of 8.02, 6.69, 5.03, and 6.09 s/in for formulations 1-4, respectively. However, it is important to note that during the burn tests of formulation 1, the ignition of the output charge did not occur in two of the delay columns. The large particle size distribution of the Mil-Spec silicon powder was identified as most likely cause of the quenching and it was decided to replace it with 1-5 micron silicon powder from the same manufacturer for preparation of future formulations. Analysis of the results indicated that a delay formulation composition in between Formulations 2 and 3, listed above, and with a binder would provide an optimal inverse burn rate with desired reliability. The delay composition selected for use in the environmentally benign M201A1 delay

columns (tested next in the SAT fixture for Task 4) was: $SrMoO_4$ 63.18 wt%, Al 6.09 wt%, Si 20.98 wt%, DE 4.75 wt%, and Bentonite 5 wt%.

The selected environmentally benign delay formulation was then tested in M201A1 delay columns without a primer, open to the atmosphere, to determine the required height of the delay formulation within the column. In this configuration the delay formulation provided an inverse burn rate of approximately 5.5 seconds per inch. Therefore, a column height of 0.23 inches should be required to provide a delay column burn time of 1.25 s. Five M201A1 fully assembled fuzes were prepared for testing. The M201A1 fuze assemblies were loaded with 0.36 g of delay formulation and the material was consolidated at 30 ksi for an average column height of 0.228". Video analysis indicated a burn time of 0.822 s with a standard deviation of 0.08 s. This was much faster than was expected. To determine the reason, additional tests in fully assembled M201A1 fuzes were conducted with varying delay column heights. The data indicates that the burn rate of the selected delay formulation was affected by the pressure within the sealed fuze assembly. The higher the height of the consolidated delay formulation, the higher the pressure was within the fuze when the primer was fired. This yielded the faster inverse burn rate.

Based on the collected data, a column height of 0.54" was selected for the M201A1 fuze assemblies that were prepared for testing in the SAT fixture. Subsequently, 60 M201A1 delay columns were prepared. The columns were consolidated at 30 ksi and had an average consolidation height of 0.545". Of the 60 columns prepared, 15 columns were selected using a random number generator for shipment to EBA&D for testing in the SAT fixture on June 7th and 8th, 2016. The remaining 45 M201A1 fuze assemblies were tested and burn times determined through video analysis. The average burn time for the M201A1 fuze assemblies was 1.54 s with a standard deviation of 0.046 s with no misfires being recorded. The 15 fully assembled M201A1 fuze assemblies were shipped to EBA&D on May 19th, 2016.

8.2. Test Results at EBA&D

The sub-assembly test fixture, designed and fabricated by EBA&D, was used for the characterization of the M201A1 fuze assemblies. The SAT fixture was characterized through the ignition of ten commercial M201A1 delay columns purchased from AMTEC. The data collected from the SAT fixture, for both the commercial M201A1 and the environmentally benign M201A1 fuze assemblies, is presented in Figure 8.2.

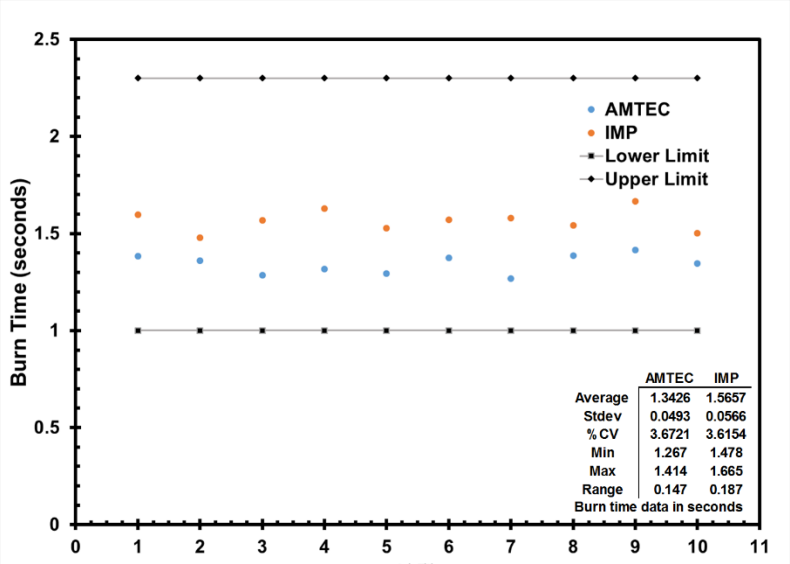

Figure 8.2. *Measured burn time results for commercially available M201A1 delay columns tested at ambient temperature (70 °F) in the sub-assembly test fixture.*

The environmentally benign M201A1 delay columns tested in the SAT fixture met the specified requirements of the M201A1 fuze assemblies (see Table 8.2).

Table 8.2. *Burn times of commercially available M201A1 and environmentally benign M201A1 fuze assemblies tested at ambient temperature (70 °F) in the SAT fixture at EBA&D.*

Column	AMTEC (s)	IMP (s)
1	1.382	1.598
2	1.361	1.478
3	1.285	1.567
4	1.316	1.629
5	1.295	1.527
6	1.374	1.57
7	1.267	1.579
8	1.386	1.541
9	1.414	1.665
10	1.346	1.503
Average	1.34	1.57
Std Dev	0.0493	0.057

9. Task 6 – Determination of reaction kinetics and thermal conductivity

9.1. Method

The thermal conductivity of the selected environmentally benign delay formulation was determined using a Hot Disk™ thermal constants analyzer located at the SDSM&T. The equipment used is shown in Figure 9.1. The material was tested as an unreacted 1 in diameter pellet consolidated at 30 ksi and in the reacted form after cooling.

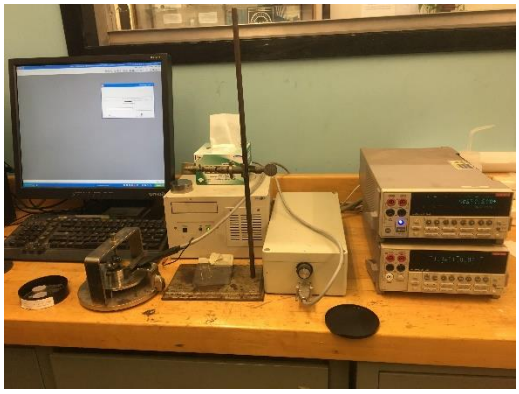

Figure 9.1. *Photograph of Hot Disk™ thermal constants analyzer located at the SDSM&T.*

The Boddington reaction kinetics measurement setup used the combustion temperature profile of the pellet of the environmentally benign delay formulation. The pellet had the following characteristics: 2.5 cm diameter, 2.0 cm in height, consolidated at 30 ksi, with a pellet density of approximately 2.23 g/mL. Kinetics tests were conducted by placing a pellet in a container with two type C thermocouples made of tungsten and rhenium alloys. The two thermocouples were inserted into the pellet through small holes drilled into the sides of the pellet to a minimum depth of 1.25 cm at two different axial positions. The thermocouples were routed to a data acquisition unit and processed through DasyLab software installed on a PC. Approximately 50 mg of A-1A was placed on top of the pellet as an ignition charge. A bare nickel chromium resistance wire (60% nickel, 16% chromium) was connected to a power source for hot wire ignition of the A-1A charge (see Figure 9.2).

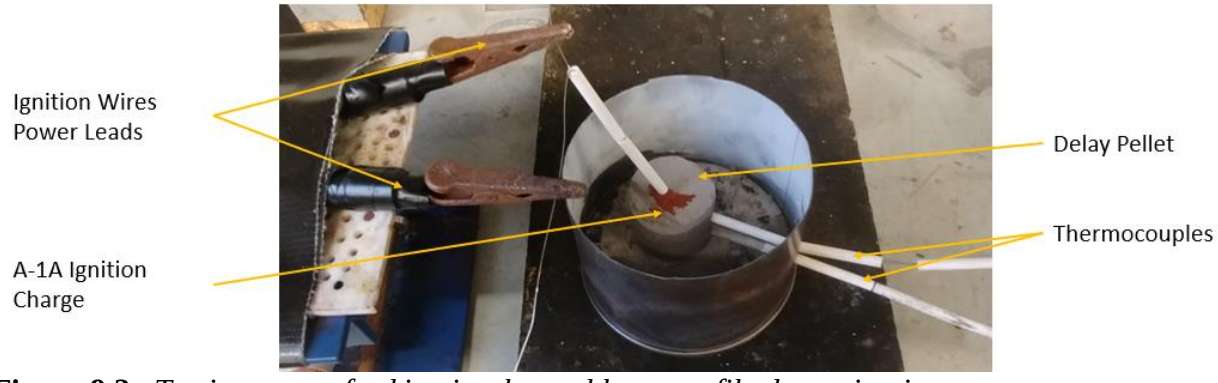

Figure 9.2. *Testing set-up for kinetics thermal burn profile determination.*

This data was collected as part of Task 6 - Determination of reaction kinetics and thermal conductivity and were used for the development of the mathematical model in Task 9 - Mathematical Modeling.

9.2. Results

Data acquisition and analysis was completed for kinetics modeling. Temperature profiles are illustrated in Figure 9.3 through Figure 9.12. 390 °F (200 °C) to ensure sufficient data capture that is required for determination of kinetic constants needed for modeling studies. The temperature profiles presented below depict a portion of the data collected (starting just before the thermal peak with an approximate 34 s duration). The gray line is the raw recorded data and the red overlay shows smoothing, calculated using a moving average of 10 samples per point.

Five experiments were conducted with varied fuel to oxidizer ratios, with the binary fuel concentration constant at 30:70 aluminum to silicon ratio. The samples were as follows:

- Samples 1 and 2 25 wt% fuel
- Samples 3 and 4 20 wt% fuel
- Samples 5 and 6 40 wt% fuel
- Samples 7 and 8 35 wt% fuel
- Samples 9 and 10 30 wt% fuel

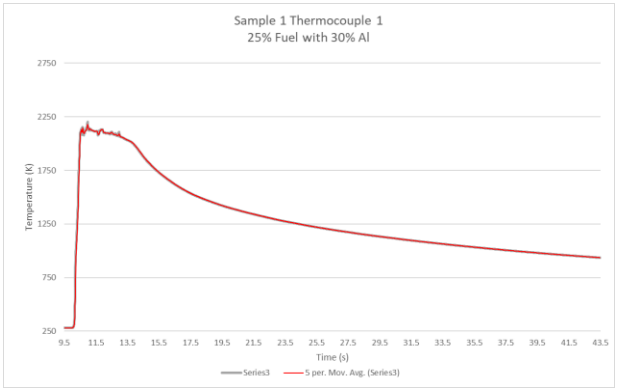

Figure 9.3. *Sample 1 (25 wt% fuel with 30/70 Al/Si ratio). Thermocouple 1 temperature profile for a 34 second burn interval.*

Data captured for Sample 1 burn experiment, using thermocouple 2, was not properly recorded due to reversed polarity of thermocouple during construction. Additional steps were added to pretest the polarity prior to running the next experiments.

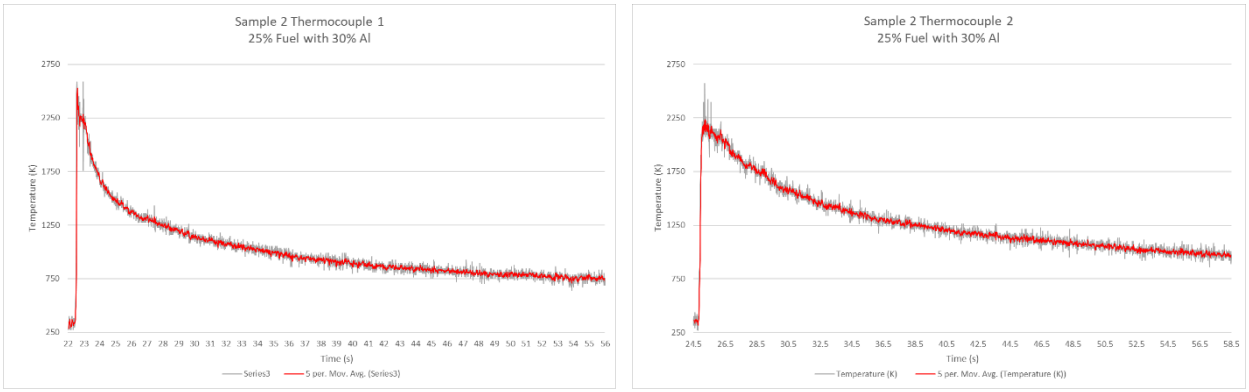

(a) *(b)*

Figure 9.4. *Sample 2 (25 wt% fuel with 30/70 Al/Si ratio). (a) Thermocouple 1 temperature profile for a 34 second burn interval. (b) Thermocouple 2 temperature profile for 34 second burn interval.*

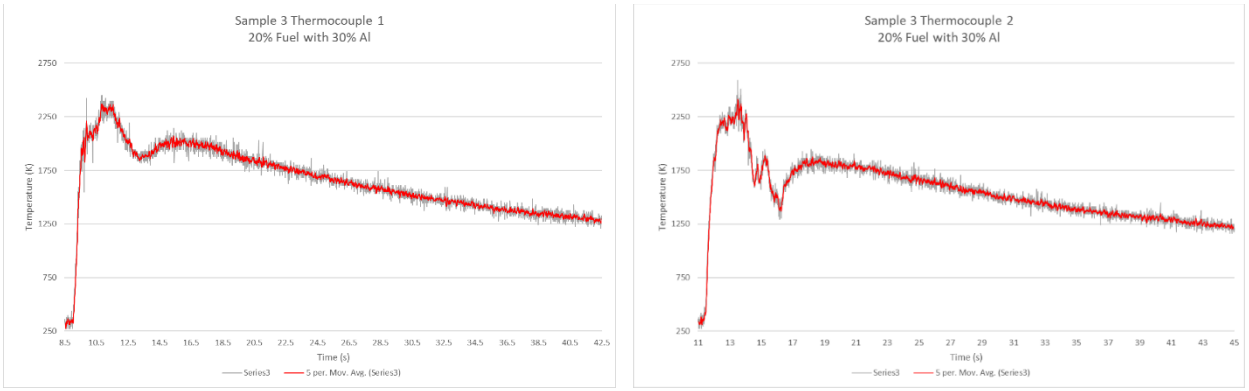

(a) *(b)*

Figure 9.5. *Sample 3 (20 wt% fuel with 30/70 Al/Si ratio). (a) Thermocouple 1 temperature profile for a 34 second burn interval. (b) Thermocouple 2 temperature profile for a 34 second burn interval.*

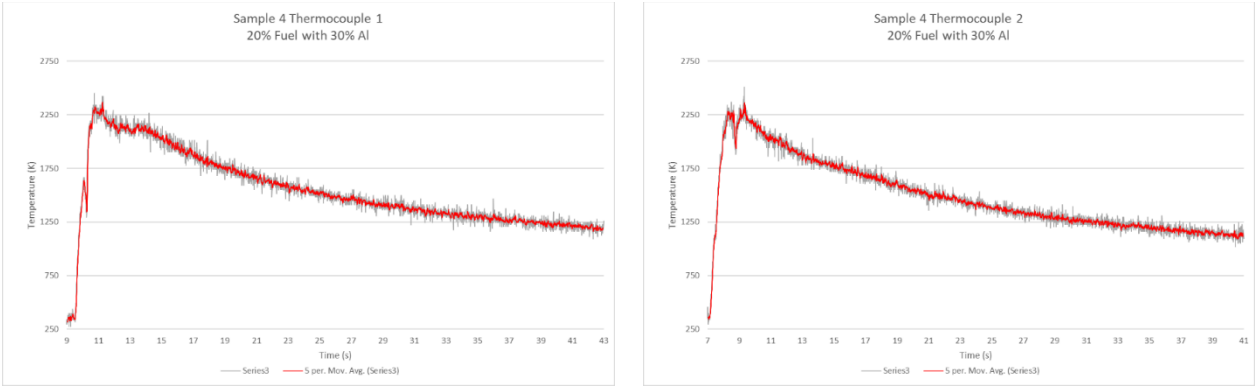

(a) *(b)*

Figure 9.6. *Sample 4 (20 wt% fuel with 30/70 Al/Si ratio). (a) Thermocouple 1 temperature profile for a 34 second burn interval. (b) Thermocouple 2 temperature profile for a 34 second burn interval.*

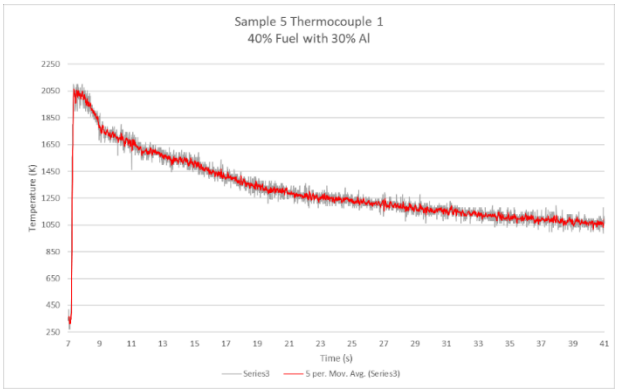

(a)

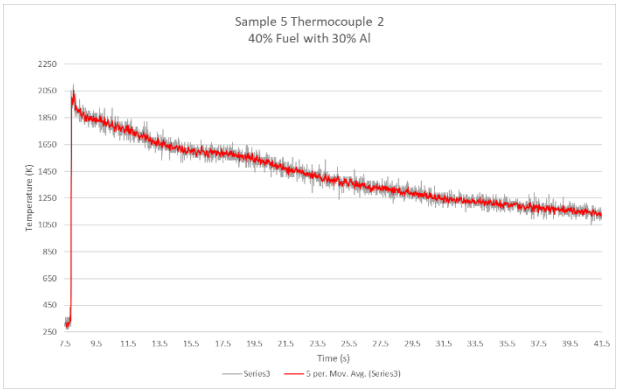

(b)

Figure 9.7. *Sample 5 (40 wt% fuel with 30/70 Al/Si ratio). (a) Thermocouple 1 temperature profile for a 34 second burn interval. (b) Thermocouple 2 temperature profile for a 34 second burn interval.*

Data from Sample 6 burn experiment using thermocouple 1 was not usable due to excessive noise observed.

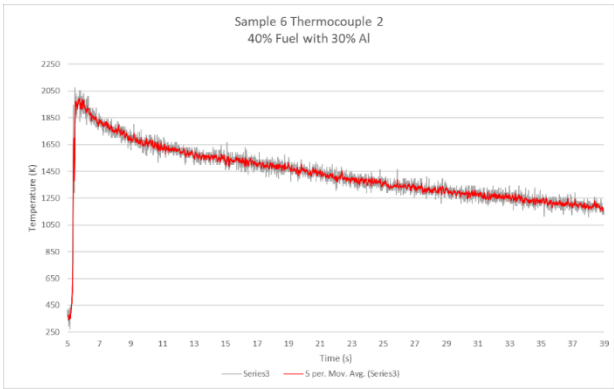

Figure 9.8. *Sample 6 (40 wt% fuel with 30/70 Al/Si ratio). Thermocouple 2 temperature profile for a 34 second burn interval.*

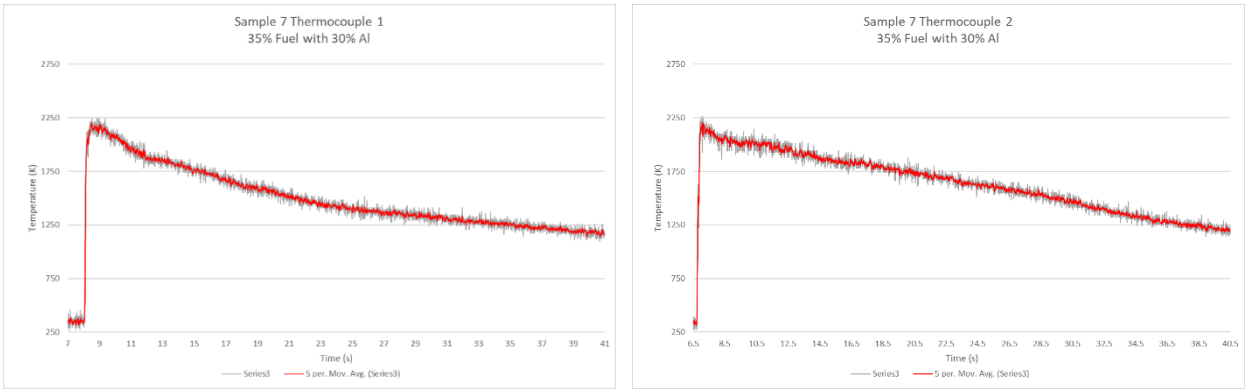

(a) *(b)*

Figure 9.9. *Sample 7 (35 wt% fuel with 30/70 Al/Si ratio). (a) Thermocouple 1 temperature profile for a 34 second burn interval. (b) Thermocouple 2 temperature profile for a 34 second burn interval.*

The data collected from Sample 8 burn experiment using thermocouple 1 was not usable due to excessive noise observed in the data. IMP suspects a bad thermocouple as the root cause of the excessive noise.

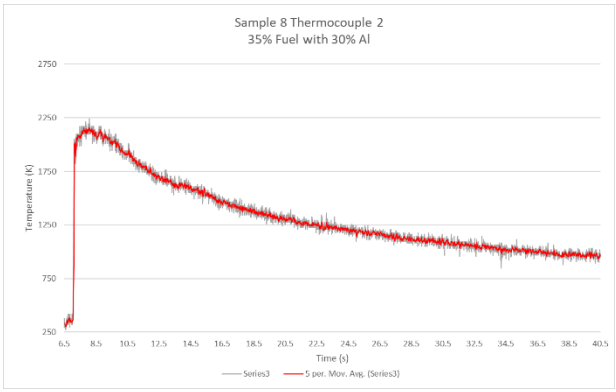

Figure 9.10. *Sample 8 (35 wt% fuel with 30/70 Al/Si ratio). Thermocouple 2 temperature profile for a 34 second burn interval.*

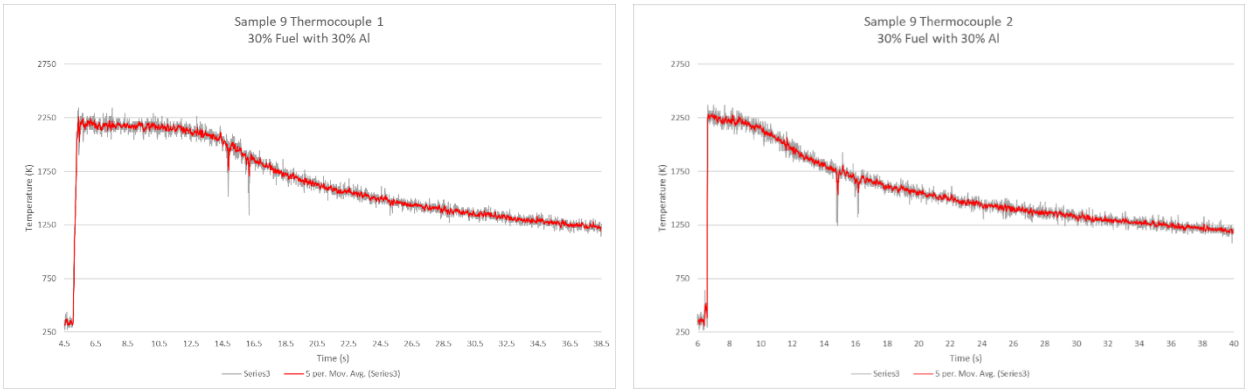

(a) *(b)*

Figure 9.11. *Sample 9 (30 wt% fuel with 30/70 Al/Si ratio). (a) Thermocouple 1 temperature profile for a 34 second burn interval. (b) Thermocouple 2 temperature profile for a 34 second burn interval.*

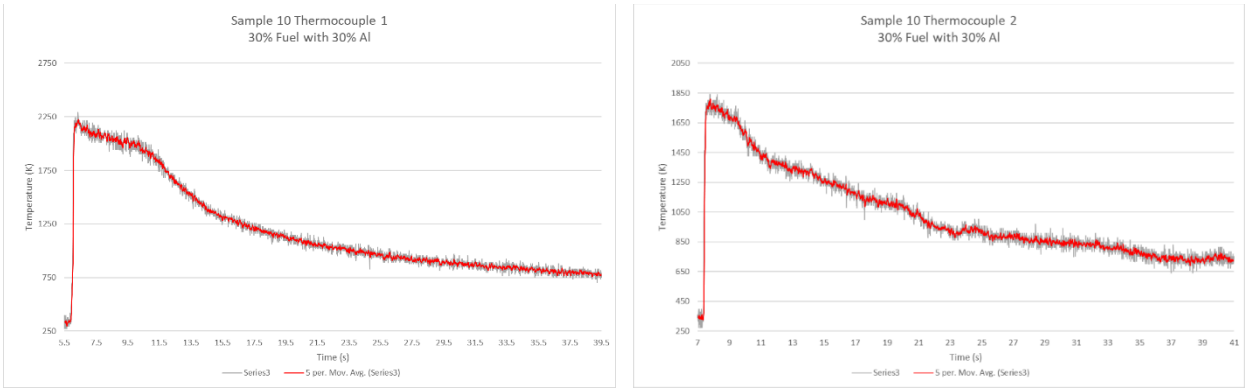

(a) *(b)*

Figure 9.12. *Sample 10 (30 wt% fuel with 30/70 Al/Si ratio). (a) Thermocouple 1 temperature profile for a 34 second burn interval. (b) Thermocouple 2 temperature profile for a 34 second burn interval.*

The combusted Samples 1 through 10 from burn experiments are depicted in Figure 9.13 through Figure 9.17.

Figure 9.13. *Post reaction material from samples 1 (left) and 2 (right).*

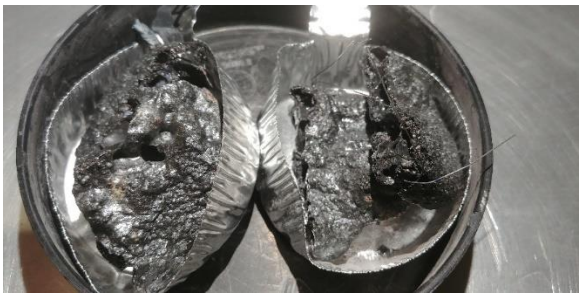

Figure 9.14. *Post reaction material from sample 3 (left) and 4 (right).*

Figure 9.15. *Post reaction material from sample 5(left) and 6 (right).*

Figure 9.16. *Post reaction material from sample 7 (left) and 8 (right).*

Figure 9.17. *Post reaction material from sample 9 (left) and 10 (right).*

The average thermal conductivities for the samples before and after combustion was determined to be 0.42 W/m·K and 0.28 W/m·K, respectively. The entire temperature dynamic profile was used to determine the pre-exponential coefficient, k_0 and activation energy, E, using the Boddington method. The values of E and ko were determined at 159.7 kJ/mol and 4.109•105 s-1, respectively. These values were used in 2D modeling studies to analyze combustion characteristics in actual hardware assembly.

10. Task 7 – Manufacturing and testing of a minimum of thirty fully assembled M201A1 delay elements at -65 °F, 70 °F, and 160 °F

10.1. Manufacturing

M201A1 fuze assemblies were prepared using the selected environmentally benign delay formulation (IMP-B092716-V1) consisting of: $SrMoO_4$ 67.4 wt%, Al 6.8 wt%, Si 15.8 wt%, DE 4.7 wt%, SiO_2 5.0 wt%, and ADP: 0.3 wt%. A sample population 150 fuze assemblies were manufactured. Each delay column was loaded with approximately 40 mg of aluminum-bismuth trioxide nanothermite output charge, 670 mg of delay formulation, 30 mg of A-1A ignition charge, and then consolidated at 30 ksi. The M201A1 fuze assemblies were split into 3 batches for temperature conditioning prior to characterization. Batch 1 consisted of 90 M201A1 fuzes that were conditioned at -65 ^{o}F for 16 hours. The delay column production specifications and burn time data for Batch 1 are presented in Table 10.1. Batch 2 consisted of 30 M201A1 fuzes conditioned at 160 ^{o}F for 16 hours. Note: Column 98 functioned properly, but there was an error in the recording and the burn time was not determined. The delay column production specifications and burn time data for Batch 2 are presented in Table 10.2(a). Batch 3 consisted of 30 M201A1 fuzes tested at ambient conditions. The delay column production specifications and burn time data for Batch 3 are presented in Table 10.2(b). The burn time data for all 3 batches is compiled for comparison in
Figure 10.1 There were no failures and all fuze assemblies performed within the required specifications.

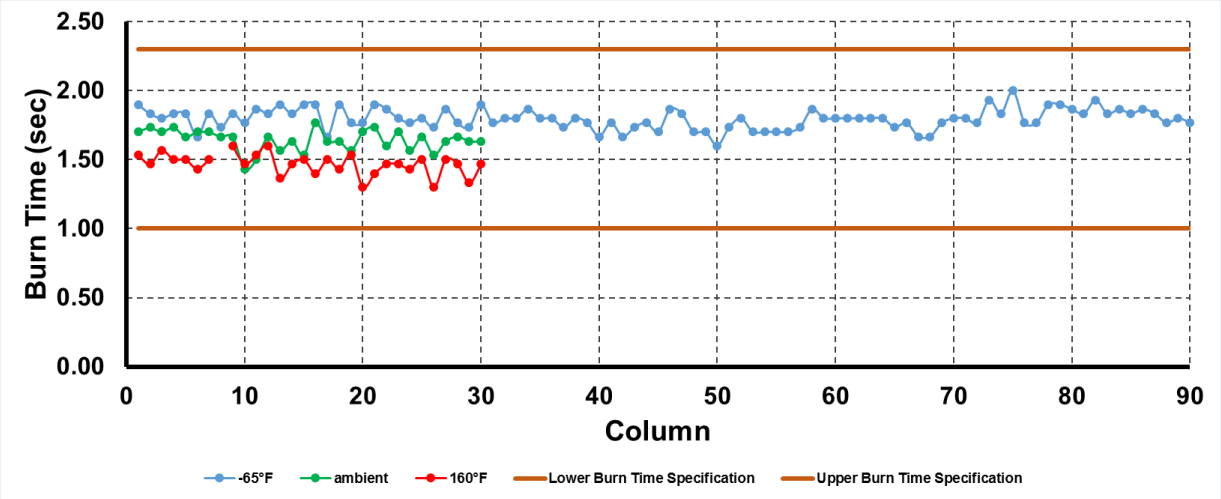

Figure 10.1. *Burn times for 150 M201A1 fuze assemblies tested at -65 ^{o}F, ambient, and 160 ^{o}F.*

Table 10.1. *Consolidation height, burn time, and IBR data for Batch 1 M201A1 fuze assemblies at -65 °F.*

Column	Height (in)	Burn time (s)	Inverse Burn Rate (s/in)	Column	Height (in)	Burn time (s)	Inverse Burn Rate (s/in)	Column	Height (in)	Burn time (s)	Inverse Burn Rate (s/in)
1	0.46500	1.900	4.086	31	0.41800	1.767	4.226	61	0.42500	1.800	4.235
2	0.44510	1.833	4.119	32	0.40840	1.800	4.407	62	0.40520	1.800	4.442
3	0.44760	1.800	4.021	33	0.40950	1.800	4.396	63	0.43700	1.800	4.119
4	0.42460	1.833	4.318	34	0.43300	1.867	4.311	64	0.42950	1.800	4.191
5	0.42720	1.833	4.292	35	0.43550	1.800	4.133	65	0.42700	1.733	4.059
6	0.44130	1.667	3.777	36	0.41400	1.800	4.348	66	0.43400	1.767	4.071
7	0.44570	1.833	4.113	37	0.41720	1.733	4.155	67	0.43130	1.667	3.864
8	0.43300	1.733	4.003	38	0.41020	1.800	4.388	68	0.41950	1.667	3.973
9	0.44600	1.833	4.111	39	0.40600	1.767	4.351	69	0.41800	1.767	4.226
10	0.43820	1.767	4.032	40	0.40350	1.667	4.131	70	0.43250	1.800	4.162
11	0.46000	1.867	4.058	41	0.41550	1.767	4.252	71	0.42900	1.800	4.196
12	0.44230	1.833	4.145	42	0.43020	1.667	3.874	72	0.43000	1.767	4.109
13	0.44500	1.900	4.270	43	0.42000	1.733	4.127	73	0.45300	1.933	4.268
14	0.43850	1.833	4.181	44	0.43020	1.767	4.107	74	0.46600	1.833	3.934
15	0.44760	1.900	4.245	45	0.41600	1.700	4.087	75	0.47150	2.000	4.242
16	0.45730	1.900	4.155	46	0.44450	1.867	4.199	76	0.41950	1.767	4.211
17	0.42050	1.667	3.964	47	0.43700	1.833	4.195	77	0.43500	1.767	4.061
18	0.43520	1.900	4.366	48	0.42070	1.700	4.041	78	0.46260	1.900	4.107
19	0.42940	1.767	4.114	49	0.40550	1.700	4.192	79	0.46850	1.900	4.055
20	0.42850	1.767	4.123	50	0.43150	1.600	3.708	80	0.46600	1.867	4.006
21	0.44240	1.900	4.295	51	0.43630	1.733	3.973	81	0.44700	1.833	4.101
22	0.43250	1.867	4.316	52	0.43800	1.800	4.110	82	0.44900	1.933	4.306
23	0.43540	1.800	4.134	53	0.43120	1.700	3.942	83	0.44400	1.833	4.129
24	0.42650	1.767	4.142	54	0.43400	1.700	3.917	84	0.46050	1.867	4.054
25	0.43100	1.800	4.176	55	0.43000	1.700	3.953	85	0.44100	1.833	4.157
26	0.43520	1.733	3.983	56	0.42250	1.700	4.024	86	0.45850	1.867	4.071
27	0.41950	1.867	4.450	57	0.39600	1.733	4.377	87	0.46100	1.833	3.977
28	0.41350	1.767	4.272	58	0.46350	1.867	4.027	88	0.43100	1.767	4.099
29	0.41120	1.733	4.215	59	0.43050	1.800	4.181	89	0.47220	1.800	3.812
30	0.43240	1.900	4.394	60	0.44400	1.800	4.054	90	0.45020	1.767	3.924
Minimum	0.396	1.600	3.708								
Maximum	0.472	2.000	4.450								
Range	0.076	0.400	0.742								
Average	0.434	1.796	4.136								
Std Dev	0.017	0.074	0.151								

Table 10.2. (a) *Consolidation height, burn time, and IBR data for Batch 2 M201A1 fuze assemblies at 160 °F. Note: Column 98 functioned properly, but there was an error in the recording and the burn time was not determined. (b) Consolidation height, burn time, and IBR data for Batch 3 M201A1 fuze assemblies at ambient conditions.*

Column	Height (in)	Burn time (s)	Inverse Burn Rate (s/in)
91	0.43500	1.533	3.525
92	0.44120	1.467	3.324
93	0.43130	1.567	3.632
94	0.47280	1.500	3.173
95	0.44150	1.500	3.398
96	0.41820	1.433	3.427
97	0.43240	1.500	3.469
98	0.45630		
99	0.45660	1.600	3.504
100	0.42150	1.467	3.480
101	0.42750	1.533	3.587
102	0.47320	1.600	3.381
103	0.43050	1.367	3.175
104	0.41620	1.467	3.524
105	0.43150	1.500	3.476
106	0.43100	1.400	3.248
107	0.45200	1.500	3.319
108	0.39950	1.433	3.588
109	0.47200	1.533	3.249
110	0.43220	1.300	3.008
111	0.41100	1.400	3.406
112	0.43150	1.467	3.399
113	0.41670	1.467	3.520
114	0.41950	1.433	3.417
115	0.46000	1.500	3.261
116	0.42150	1.300	3.084
117	0.41350	1.500	3.628
118	0.43500	1.467	3.372
119	0.43800	1.333	3.044
120	0.42150	1.467	3.480
Minimum	0.400	1.300	3.008
Maximum	0.473	1.600	3.632
Range	0.074	0.300	0.625
Average	0.435	1.467	3.383
Std Dev	0.019	0.075	0.167

(a)

Column	Height (in)	Burn time (s)	Inverse Burn Rate (s/in)
121	0.45100	1.700	3.769
122	0.44350	1.733	3.908
123	0.43950	1.700	3.868
124	0.44850	1.733	3.865
125	0.42720	1.667	3.901
126	0.44500	1.700	3.820
127	0.43850	1.700	3.877
128	0.44500	1.667	3.745
129	0.42500	1.667	3.922
130	0.40700	1.433	3.522
131	0.41950	1.500	3.576
132	0.44500	1.667	3.745
133	0.44150	1.567	3.549
134	0.41250	1.633	3.960
135	0.44300	1.533	3.461
136	0.48500	1.767	3.643
137	0.43750	1.633	3.733
138	0.43400	1.633	3.763
139	0.43500	1.567	3.602
140	0.44700	1.700	3.803
141	0.45050	1.733	3.848
142	0.45900	1.600	3.486
143	0.44350	1.700	3.833
144	0.42400	1.567	3.695
145	0.43500	1.667	3.831
146	0.43950	1.533	3.489
147	0.42750	1.633	3.821
148	0.43300	1.667	3.849
149	0.40650	1.633	4.018
150	0.41700	1.633	3.917
Minimum	0.407	1.433	3.461
Maximum	0.485	1.767	4.018
Range	0.079	0.333	0.557
Average	0.437	1.642	3.761
Std Dev	0.016	0.075	0.151

(b)

10.2. M201A1 Fuze Results

The M201A1 fuzes met the required burn time, and additional 238 M201A1 fuze assemblies were prepared. The M201A1 fuze assemblies were loaded with 20-25 mg of ZPP, 670 mg of delay formulation, 30 mg of A-1A, and then consolidated at 30 ksi. A complete build sheet for all 238 M201A1 fuze assemblies is presented in Appendix B. From the 238 prepared M201A1 fuze

assemblies, columns were randomly selected for batch qualification testing. The qualification tests were conducted at ambient (qty: 8), -65 °F (qty: 10), and 160 °F (qty: 10). The results of the qualification tests are presented in Table 10.3.

Table 10.3. *(a) Consolidation height, burn time, and IBR data for random sample of 8 deliverable M201A1 fuze assemblies at ambient conditions. (b) Consolidation height, burn time, and IBR data for random sample of 10 deliverable M201A1 fuze assemblies at -65 °F. (c) Consolidation height, burn time, and IBR data for random sample of 10 deliverable M201A1 fuze assemblies at 160 °F.*

Column	Height (in)	Burn time (s)	Inverse Burn Rate (s/in)
18	0.40300	1.600	3.970
38	0.41050	1.633	3.979
39	0.41400	1.600	3.865
57	0.40600	1.600	3.941
59	0.41250	1.600	3.879
151	0.43100	1.700	3.944
198	0.42950	1.633	3.803
203	0.42350	1.600	3.778
Minimum	0.403	1.600	3.778
Maximum	0.431	1.700	3.979
Range	0.028	0.100	0.201
Average	0.416	1.621	3.895
Std Dev	0.010	0.033	0.071

(a)

Column	Height (in)	Burn time (s)	Inverse Burn Rate (s/in)
6	0.41450	1.833	4.423
13	0.41200	1.767	4.288
23	0.42800	1.800	4.206
25	0.44500	1.900	4.270
60	0.41200	1.867	4.531
62	0.41100	1.667	4.055
135	0.41550	1.700	4.091
180	0.42250	1.733	4.103
181	0.43450	1.833	4.219
215	0.40750	1.767	4.335
Minimum	0.408	1.667	4.055
Maximum	0.445	1.900	4.531
Range	0.038	0.233	0.476
Average	0.420	1.787	4.252
Std Dev	0.011	0.070	0.143

(b)

Column	Height (in)	Burn time (s)	Inverse Burn Rate (s/in)
9	0.44100	1.600	3.628
14	0.41950	Primer Fail	
19	0.40850	Primer Fail	
61	0.41500	1.567	3.775
88	0.43000	1.633	3.798
108	0.41000	1.600	3.902
118	0.42600	1.567	3.678
128	0.40000	1.500	3.750
147	0.44900	Fired - No video	
186	0.44800	Primer Fail	
Minimum	0.400	1.500	3.628
Maximum	0.449	1.633	3.902
Range	0.049	0.133	0.274
Average	0.425	1.578	3.755
Std Dev	0.016	0.042	0.088

(c)

The data for burn tests at 160 °F indicated 3 misfires (columns 14, 19, and 186). The root cause analysis of the failures was determined. The operator had initially set the temperature conditioning chamber to 160 °C instead of 160 °F (71.1 °C) for the first 4 hours of conditioning of the entire sample set. Disassembly of the delay columns indicated that the primer failed to function in all 3 cases. The delay columns were ignited with a NiCr wire and all 3 functioned properly. In addition, column 147 functioned properly; however, the time was not determined due to an error in the video recording setup.

The remaining 210 prepared columns were split into 6 batches of 35 columns each. Batches 1-3 went through temperature & humidity conditioning according to MIL-STD-331C Fuze Test Standards Appendix C Test 1 in order to simulate storage conditions. Batches 4-6 did not go through the temperature and humidity characterization. Following conditioning, Batches 1 & 4 were tested at -65 °F, Batches 2 & 5 were tested at ambient conditions, and Batches 3 & 6 were tested at 160 °F.

Upon receipt of the environmentally benign M201A1 fuze assemblies, EBA&D sealed the primers with the required varnish lacquer. A photograph of a selected batch after sealing is presented in Figure 10.2. In addition to the sealing of the primers, EBA&D x-rayed each column to ensure that

there were no defects or damage to the columns during the shipment. A photograph of an x-rayed columns is shown in Figure 10.3.

Figure 10.2. *Photograph of M201A1 fuze assemblies after varnishing with the required lacquer.*

Figure 10.3. *Photograph of M201A1 fuze assembly x-ray.*

IMP personnel (Dr. Zac Doorenbos and Mr. Daniel Perkins Jr.) traveled to the EBA&D facility in Simsbury, CT to witness the testing of the manufactured environmentally benign M201A1 delay columns. For this characterization, the lot was split into 6 batches of 35 columns each. The conditioning for each batch was:

- Batch 1: Temperature and humidity conditioned per the *MIL-STD-331C Appendix C* procedure followed by a minimum of 2 h temperature conditioning at -65 ^{o}F and fired within 70 s of being removed from the conditioning chamber;
- Batch 2: Temperature and humidity conditioned per the *MIL-STD-331C Appendix C* procedure followed by a minimum of 2 h temperature conditioning at ambient conditions and fired;
- Batch 3: Temperature and humidity conditioned per the *MIL-STD-331C Appendix C* procedure followed by a minimum of 2 h temperature conditioning at 160 ^{o}F and fired within 70 s of being removed from the conditioning chamber;

- Batch 4: Conditioned at -65 ^{o}F for a minimum of 2 h and fired within 70 s of being removed from the conditioning chamber;
- Batch 5: Fired at ambient conditions;
- Batch 6: Conditioned at 160 ^{o}F for a minimum of 2 h and fired within 70 s of being removed from the conditioning chamber.

The testing was completed over a 2-day period (December 12th and 13th, 2016) at the EBA&D facility in Simsbury, CT. The results of the testing are summarized in Table 10.4. All tested assembled systems performed without misfires. Commercially available M201A1 fuze assemblies were purchased from AMTEC and split into 6 batches and exposed to the same conditioning conditions and fired. The environmentally benign M201A1 delay columns all performed within the required DoD burn time specifications of 1 – 2.3 s.

Table 10.4. *Burn time data for M201A1 delay fuzes (IMP environmentally benign & AMTEC commercial fuzes).*

	Temperature & Humidity Conditioned					
	Batch 1	Batch 2	Batch 3	Batch 4	Batch 5	Batch 6
	IMP M201A1 Delay Fuzes					
Average Burn Time (s)	1.81	1.68	1.59	1.76	1.66	1.56
Burn Time Standard Devation (s)	0.07	0.08	0.05	0.05	0.06	0.05
% CV	3.65	4.70	3.15	3.09	3.48	3.46
Temperature Coefficient (s/^{o}F)		0.0010			0.0009	
	DoD M201A1 LAT Data					
Average Burn Time (s)				1.77	1.68	1.53
Burn Time Standard Devation (s)				0.08	0.07	0.06
% CV				4.49	3.98	4.00
Temperature Coefficient (s/^{o}F)					0.0011	
	AMTEC Commercial M201A1 Delay Fuzes					
Average Burn Time (s)	2.07	1.95	1.53	1.86	1.57	1.38
Burn Time Standard Devation (s)	0.23	0.20	0.12	0.21	0.16	0.14
% CV	11.22	10.51	7.87	11.35	9.93	10.07
Temperature Coefficient (s/^{o}F)		0.0024			0.0021	

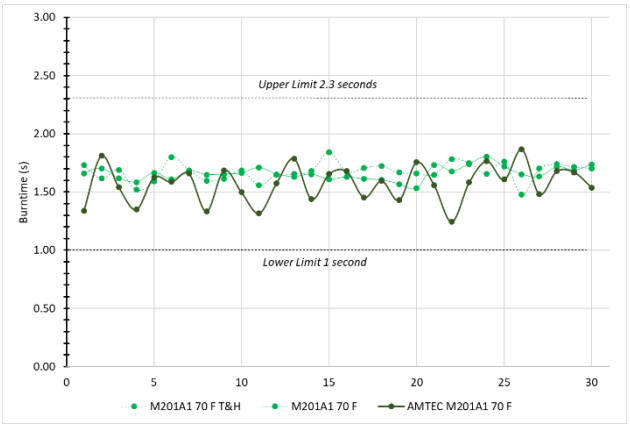

(a)

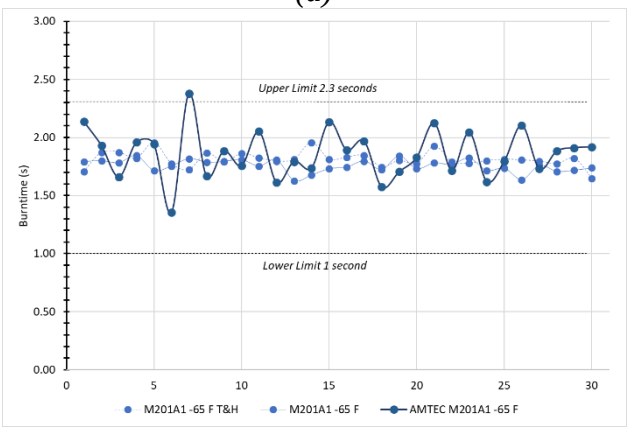

(b)

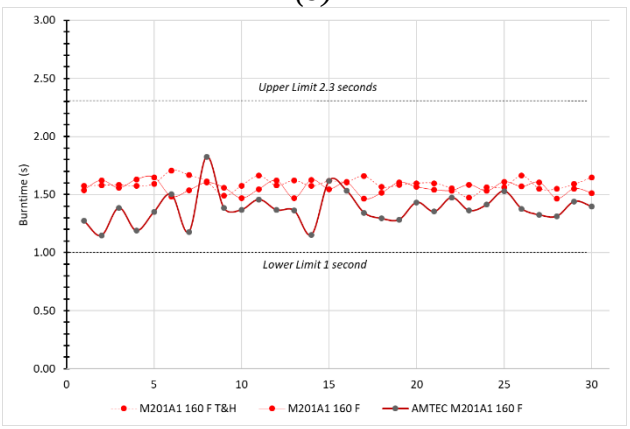

(c)

Figure 10.4. *Illustration of test results versus commercially available M201A1 Delay Fuzes. (a) 70 °F, (b) -65 °F, (c) 160 °F.*

10.3. Conclusions

The data shows that the environmentally benign delay formulation had a lower burn time range and better consistency than the current commercial M201A1 fuzes (see Figure 10.4) and it was in line with the Lot Acceptance Testing (LAT) data from the DoD. The testing of the M201A1 fuzes has met the requirements for the completion of project Task 7 ahead of the planned schedule.

11. Task 8 – Development of environmentally acceptable input transition and output charges

11.1. Development and Testing

Task 8 was focused on the development of an environmentally acceptable replacement for the Zirconium Potassium Perchlorate (ZPP) output charge used in the M201A1 delay columns. An aluminum/bismuth trioxide nanothermite was identified as a possible replacement for the ZPP. The nanothermite material was tested in the M201A1 delay columns with positive results. In addition, PEP2100 equilibrium calculations software (developed by the Navy at China Lake) was used to identify the desired concentration of possible gas generating additives to increase the pressure output. The software indicated that an aluminum/bismuth trioxide nanothermite, with the addition of 10 wt% HMX, would provide a similar gas output to ZPP.

Closed bomb pressure analysis was conducted on the nanothermite and ZPP, see Figure 11.1. The results from dynamic pressure tests indicated that the pure nanothermite material provided a lower pressure output than the ZPP. The nanothermite composition was further tuned by the addition of HMX to increase the pressure output. The results of the closed bomb tests are presented in Figure 11.2. The results indicated that the material with 10 wt% HMX provided a similar peak pressure but, had a lower sustained pressure when compared to ZPP.

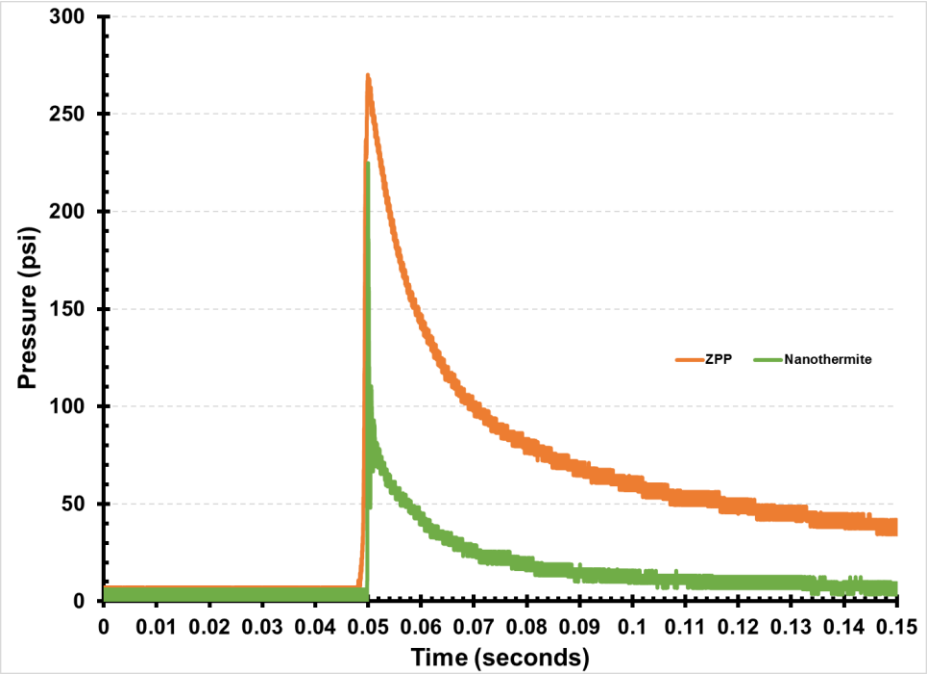

Figure 11.1. *Dynamic pressure curves for 60 mg of ZPP and nanothermite ignited in a 15 cc closed bomb.*

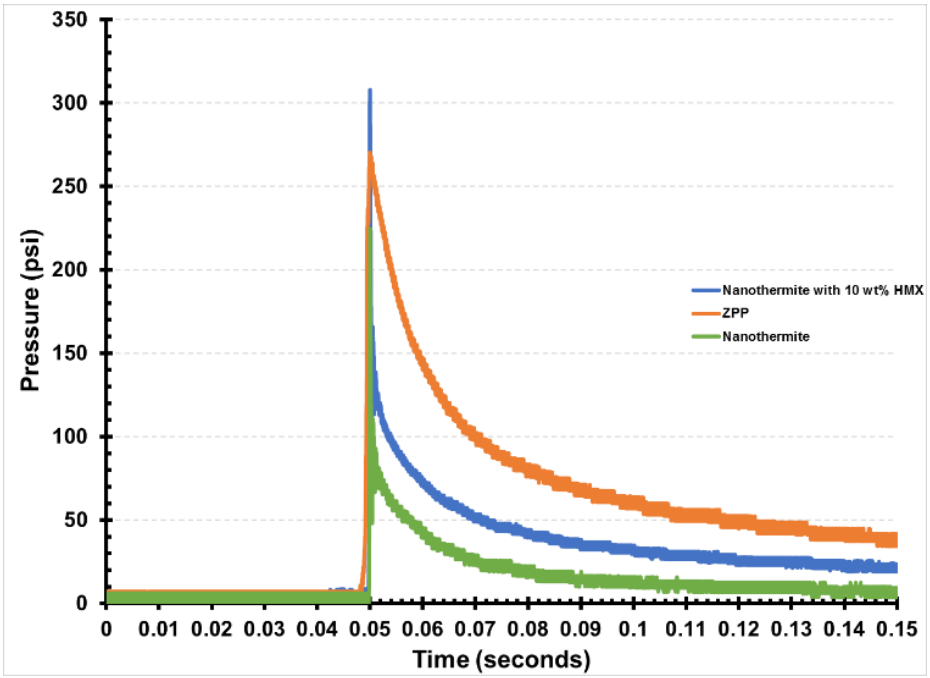

Figure 11.2. *Dynamic pressure curves for 60 mg of nanothermite with 10 wt% HMX, ZPP, and pure nanothermite ignited in a 15 cc closed bomb.*

11.2. Conclusions

It has been concluded that using 10 wt% HMX as a pressure generator provided suitable output pressure to be used as an output charge for the M201A1 fuze.

12.Task 9 – Development of Mathematical Model

12.1. Background

Mathematical modeling of a combustion front propagation in delay columns has several benefits. These benefits include saving time and providing a better understanding of combustion front stability in the presence of heat losses and extreme initial temperatures. It also provides a tool for new designs and improvements.

To determine the phase composition of the combustion by-products, X-ray diffraction crystallography (XRD) was conducted. The SEM-EDS analysis of the combustion products was completed as a supplement to XRD data. The SEM EDS was done utilizing a Zeiss Supra40 variable-pressure field-emission SEM with an Oxford AztecEnergy advanced system for X-ray microanalysis and electron backscattered diffraction. XRD analysis and phase identification was conducted at the South Dakota School of Mines and Technology on a Rigaku Ultima-Plus X-Ray Diffractometer. A tested sample was prepared by grinding the combusted delay composition in a mortar and pestle to a fine powder, approximately 200 µm particle size. The sample was then placed on a slide and placed into the XRD instrument. The sample preparation for the SEM-EDS included: removing the lower portion of a fuze body containing combustion products with a band saw, pressing the fired fuze into a phenolic resin puck, and polishing to a 1 µm finish (see Figure 12.1). Table 12.1 presents certificate of analysis (CoA) for all constituents to define what other materials are present within the lot.

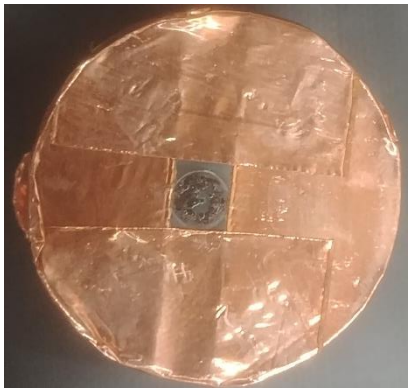

Figure 12.1. *Stem of an M213/M228 fuze with combusted delay residue pressed into phenolic resin puck for SEM EDS mapping.*

Table 12.1. *Delay composition constituents and impurities compiled from certificates of analysis of the used lots. Diatomaceous earth lot used was from a naturally occurring DE and COA was not available.*

Alfa Aesar - Strontium Molybdenum (I27X015) COA	
Strontium Molybdenum ($SrMoO_4$)	99.9%
Barium (Ba)	<0.3%
Sulfate	<0.02%
Chloride	<0.02%
Phosphate	<0.01%
Valimet – Spherical Aluminum Powder H-5 (15-6053) COA	
Aluminum (Al)	99.8%
Iron (Fe)	0.10%
AEE – Silicon Metal Powder SI-100 (1705542) COA	
Silicon (Si)	99%
Iron (Fe)	<0.01%
Aluminum (Al)	<0.2%
Calcium (Ca)	<0.01%
Chromium (Cr)	<0.001%
Copper (Cu)	<0.001%
Chlorine (Cl)	<0.01%
Titanium (Ti)	<0.003%
Silicon (IV) Oxide, Amorphous Fumed, S.A. 85-115 $m^2 g^{-1}$ (I20W038) COA	
SiO_2	100%
AEE - Diatomaceous Earth MIL-D-20550 Rev B (1502518) https://www.diatomaceousearthonline.com.au/analysis/	
Silica (Si02)	> 70%
Calcium (Ca)	1.00%
Magnesium (Mg)	0.60%
Manganese (Mn)	0.50%
Phosphorus (P)	0.01%
Potassium (K)	0.20%
Iron (Fe)	4.00%
Cobalt (Co)	5mg/kg
Molybdenum (Mo)	5mg/kg
Sulphur (S)	42mg/kg
Zinc (Zn)	42mg/kg

12.2. Combustion By-Product Phase Identification

The quantitative XRD analysis demonstrated that by weight, 63% of the combustion products were amorphous materials and were not identifiable using this analysis procedure. The phases that were identified are as follows:

- Molybdenum (Mo), Figure 12.2 and Figure 12.3;
- Silicon (Si), Figure 12.2 and Figure 12.3;
- Strontium Molybdate ($SrMoO_4$), Figure 12.2 and Figure 12.3;
- Molybdenum Silicide ($MoSi_3$), Figure 12.2 and Figure 12.3;
- Molybdenum Silicide ($MoSi_2$), Figure 12.3;
- Quartz (SiO_2), Figure 12.3.

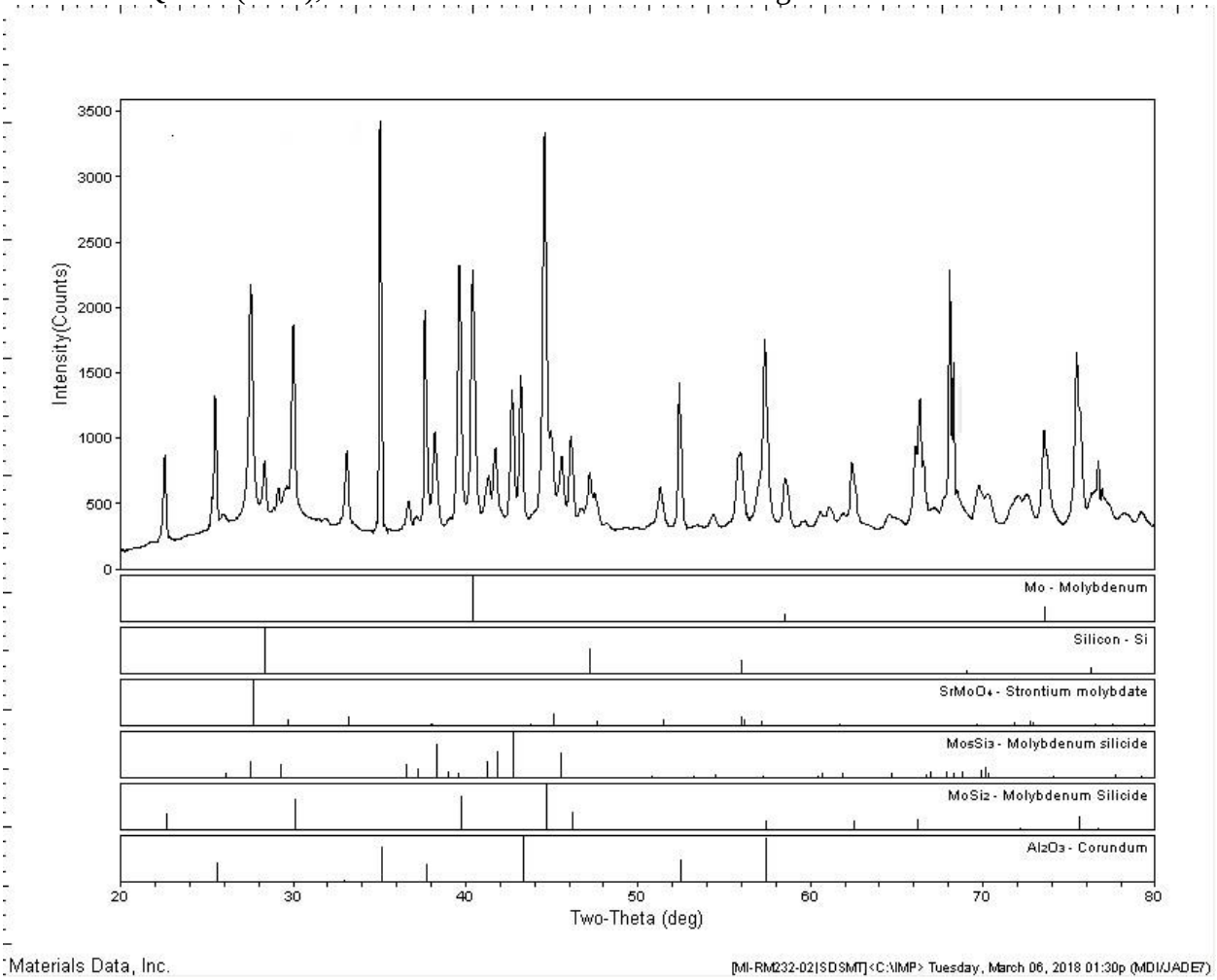

Figure 12.2. *XRD spectrum of delay combustion products. With Al_2O_3 (corundum) baseline additive.*

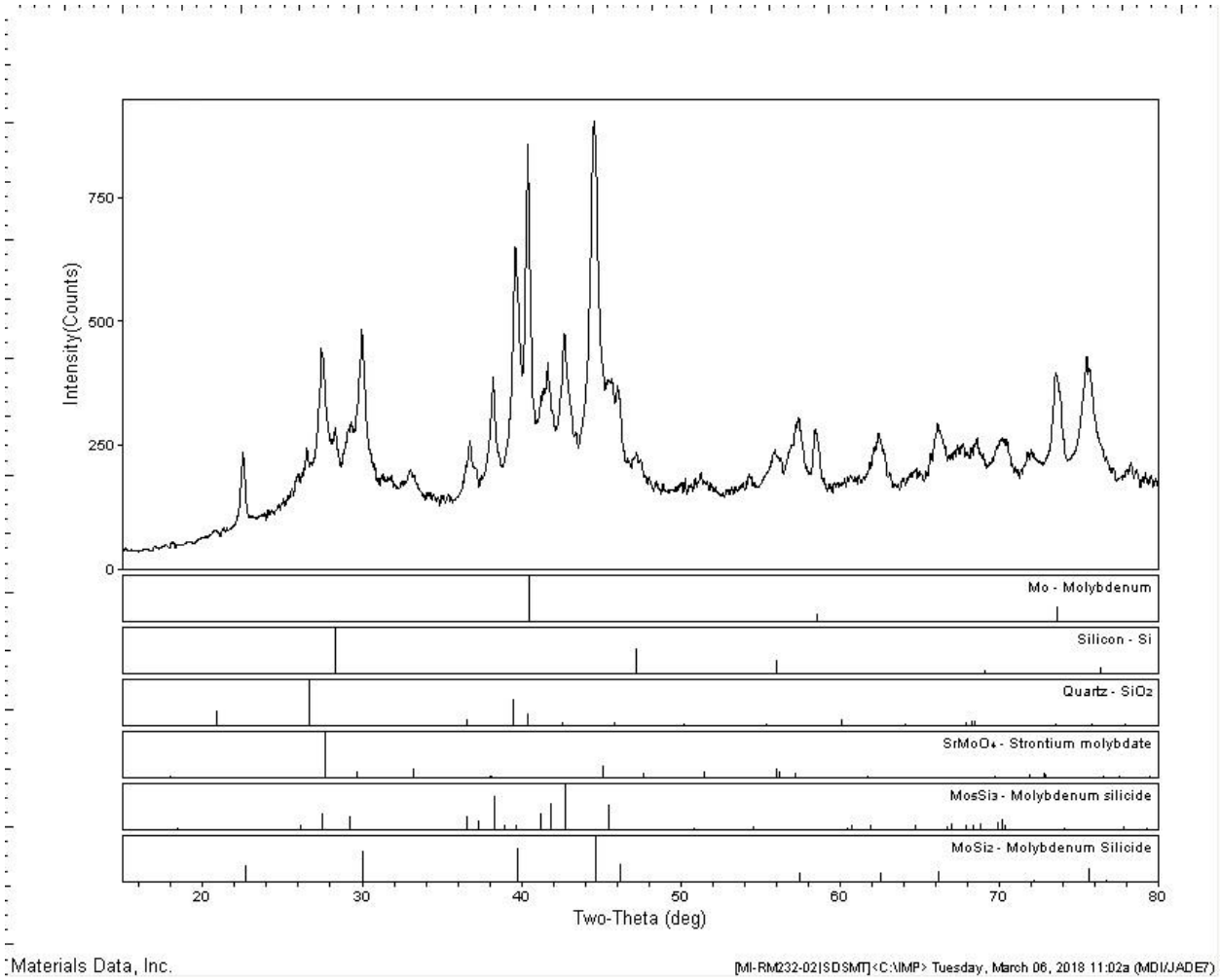

Figure 12.3. *XRD spectrum of delay combustion products. Without Al_2O_3 (corundum) baseline additive.*

Due to the high amount of amorphous materials and the lack of aluminum (Al) found in the combustion products using the XRD analysis method, SEM-EDS was conducted to supplement the data set. Four sites were tested in the prepped sample. Table 12.2 identifies each site and constituents found at that site. Table 12.3 identifies the phases identified at each analyzed site. It is important to note that site 4 contained unreacted delay composition, located between the outside edge of the combusted material and the zinc fuze wall.

Table 12.2. *Constituents identified in the EDS maps.*

Constituent	Site 1	Site 2	Site 3	Site 4
Oxygen (O)	X	X	X	X
Aluminum (Al)	X	X	X	X
Silicon (Si)	X	X	X	X
Carbon (C)		X		
Strontium (Sr)	X	X	X	X
Sulphur (S)				X
Molybdenum (Mo)	X		X	
Thallium (Tl)	X			
Zinc (Zn)	X		X	
Sodium (Na)	X		X	X
Potassium (K)	X			
Tungsten (W)		X		
Barium (Ba)		X		

Table 12.3. *Phases identified in the EDS maps.*

Constituent	Site 1	Site 2	Site 3	Site 4
SrSiAlO	X	X	X	
MoSiO			X	X
SiO			X	X
SrAlSiO			X	
SrSiMoO			X	X
AlO				X

Site 1

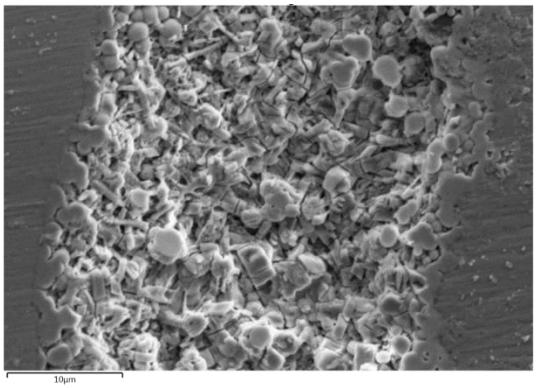

Figure 12.4. *SEM image of site 1.*

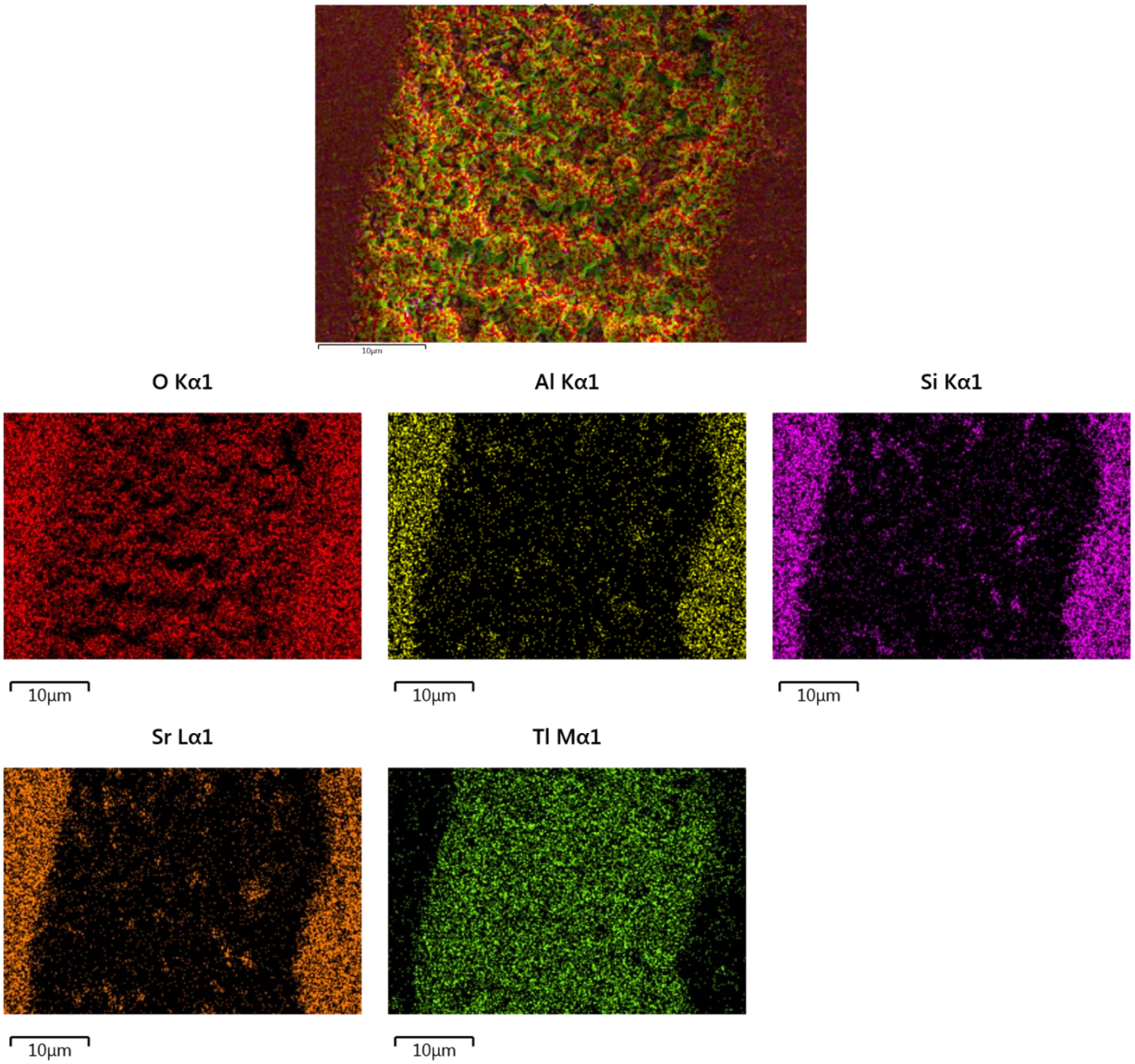

Figure 12.5. *EDS image of site 1, with color mapping.*

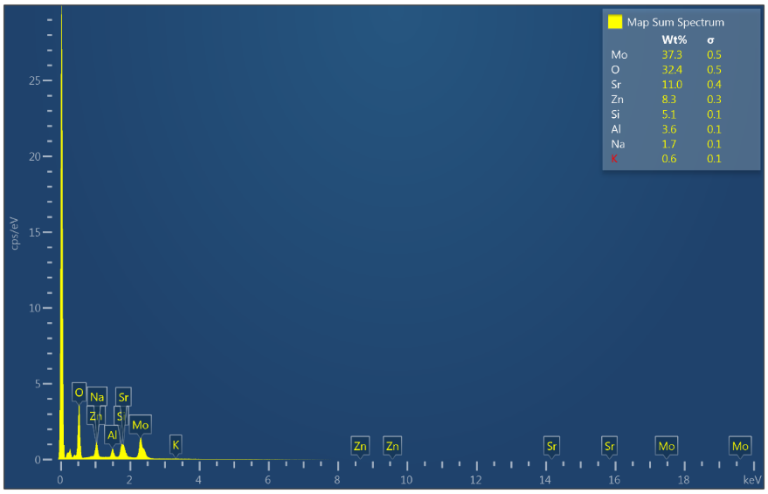

Figure 12.6. *EDS results map sum spectrum of site 1.*

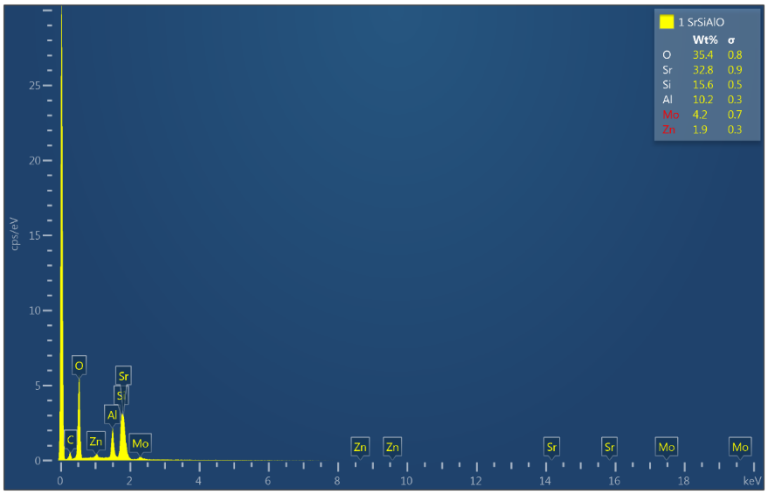

Figure 12.7. *EDS SrSiAlO phase result spectrum site 1.*

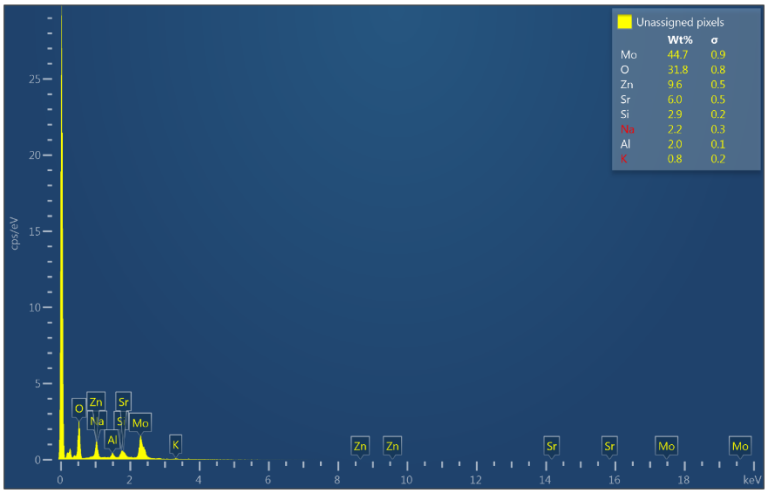

Figure 12.8. *EDS unassigned pixels phase result spectrum site 1.*

Site 2

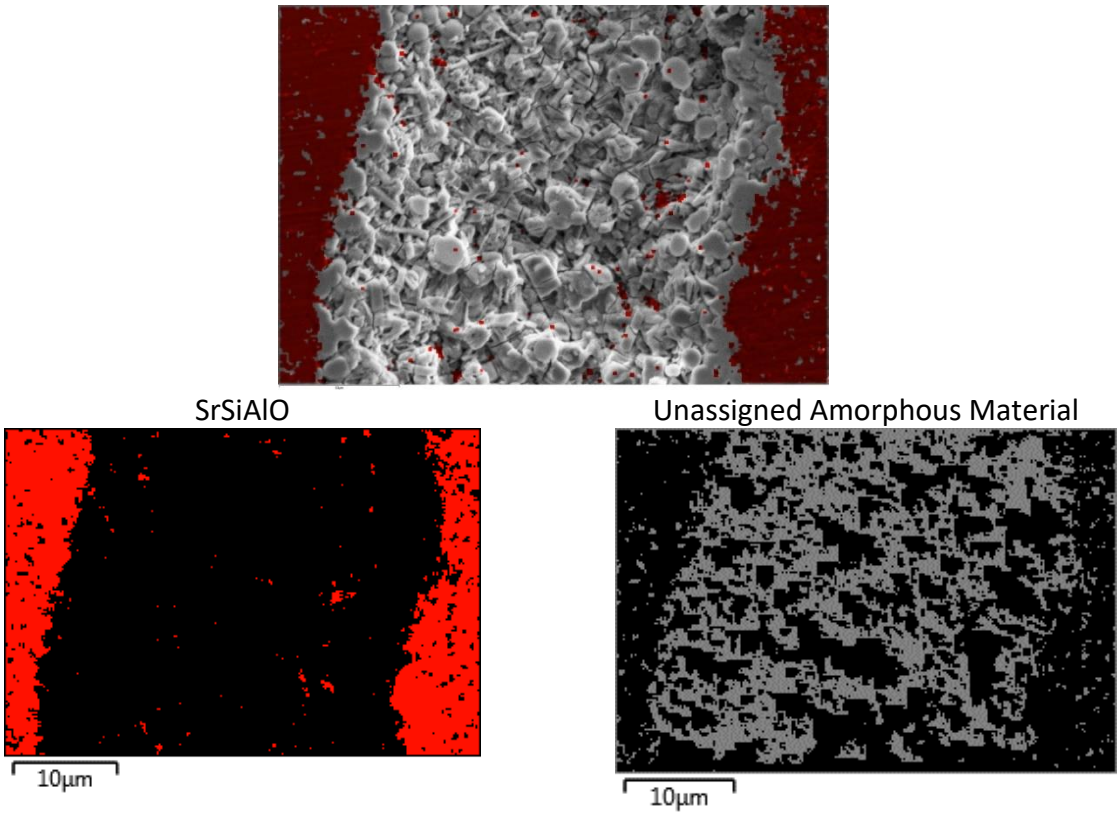

Figure 12.9. *EDS Phase map of site 1.*

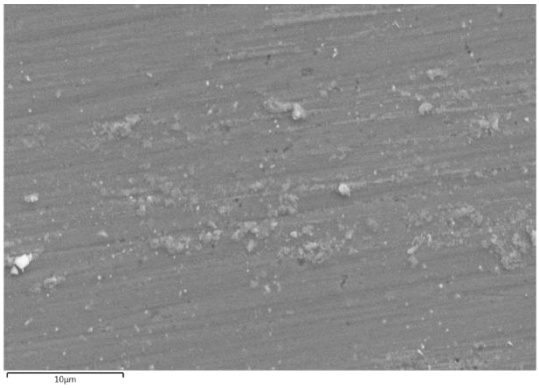

Figure 12.10. *SEM image of site 2.*

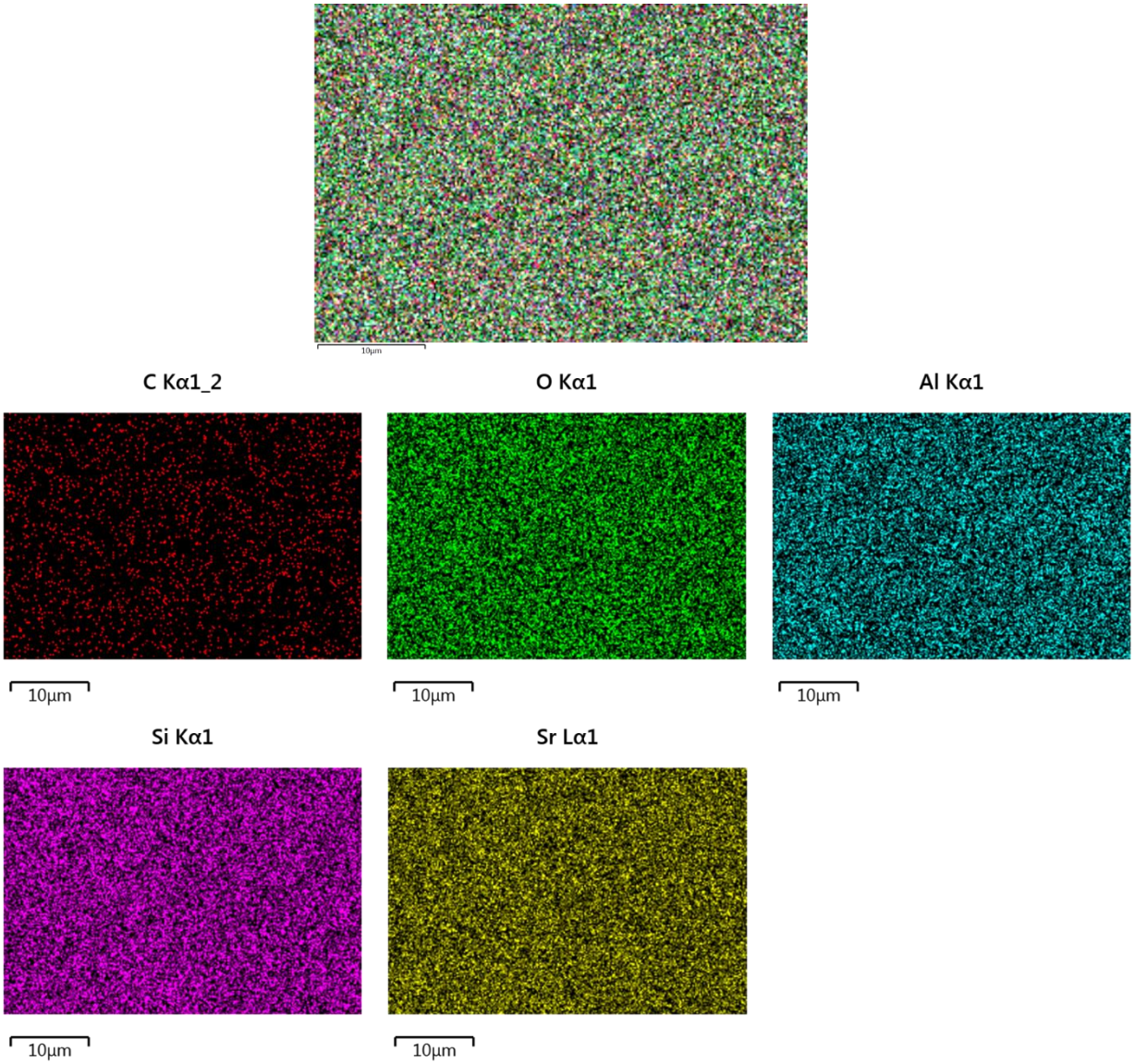

Figure 12.11. *EDS image of site 2, with color mapping.*

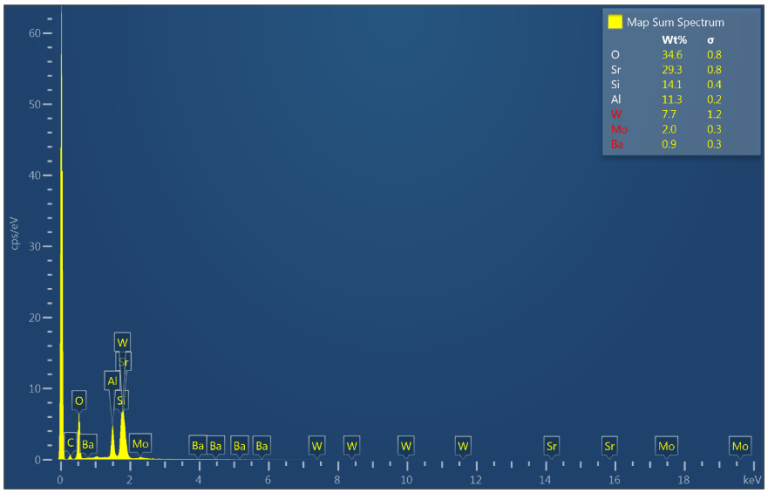

Figure 12.12. *EDS results map sum spectrum of site 2.*

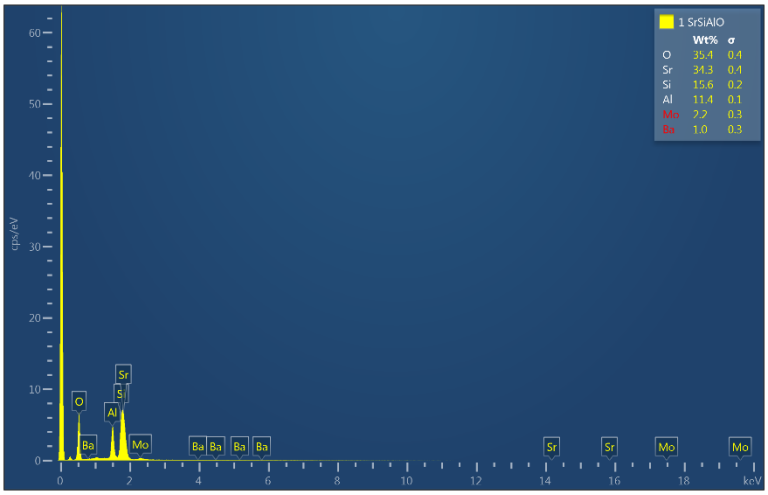

Figure 12.13. *EDS SrSiAlO phase result spectrum site 2.*

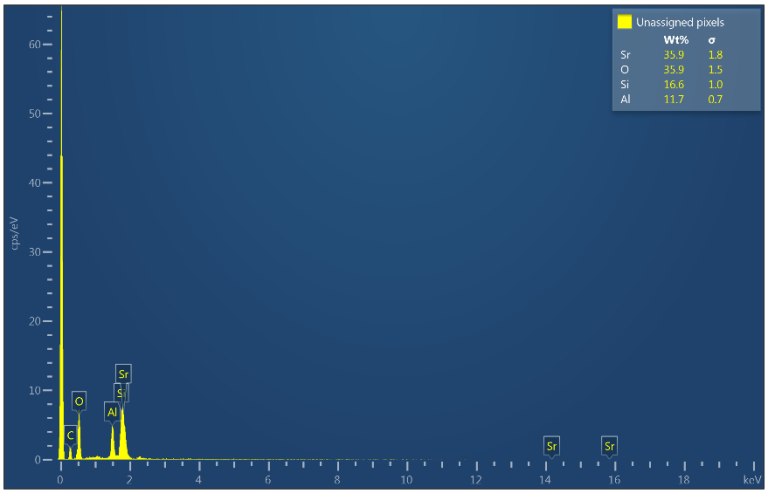

Figure 12.14. *EDS unassigned pixels phase result spectrum site 2.*

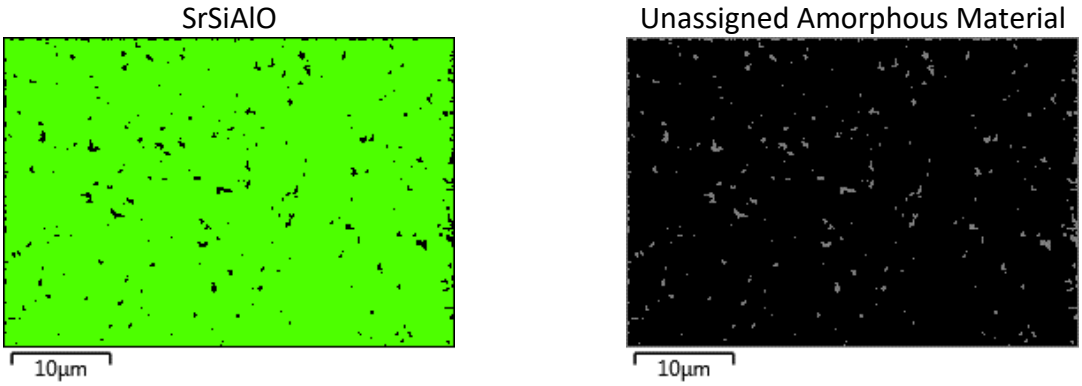

Figure 12.15. *EDS Phase map of site 2.*

Site 3

Figure 12.16. *SEM image of site 3.*

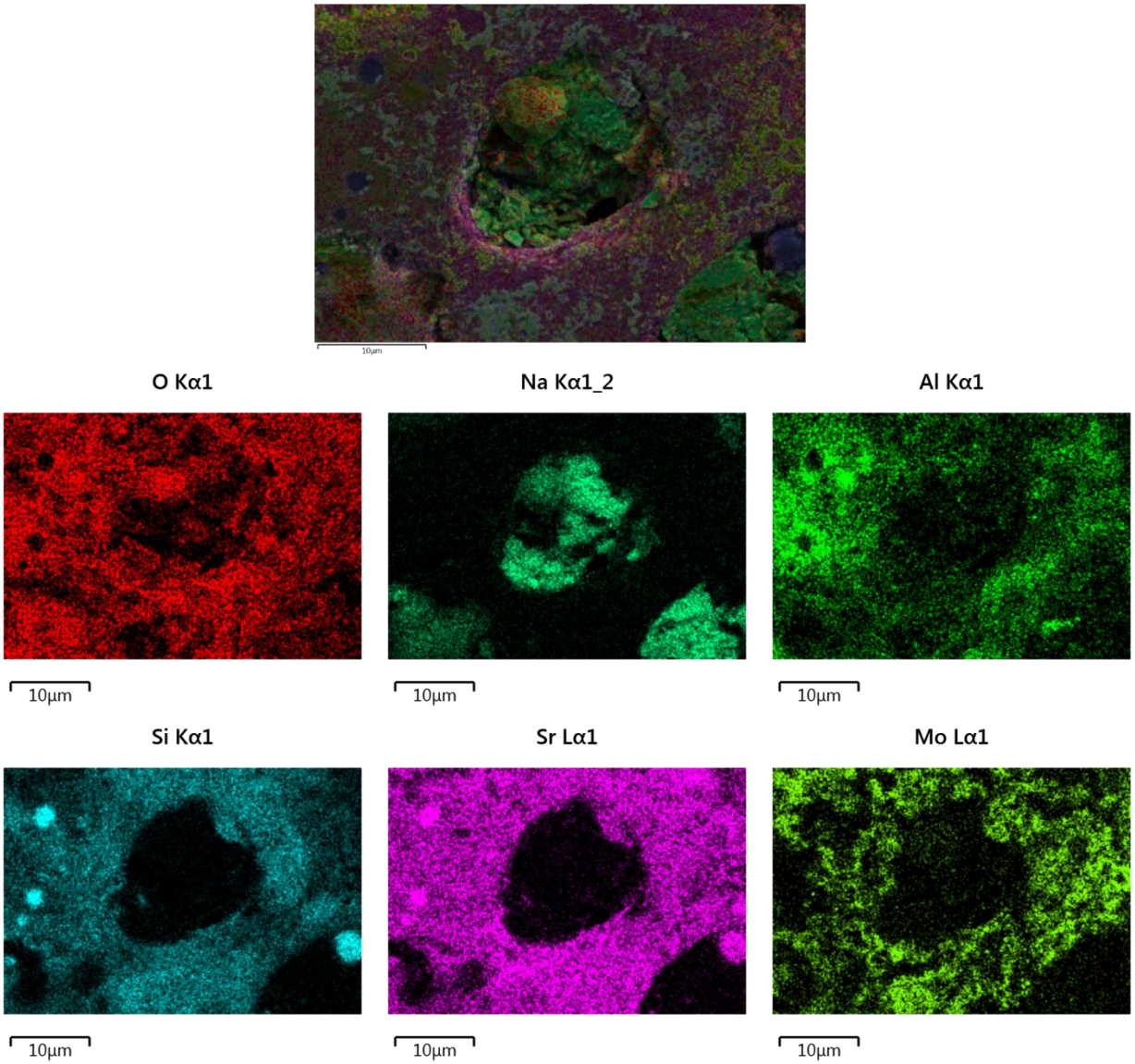

Figure 12.17. *EDS image of site 3, with color mapping.*

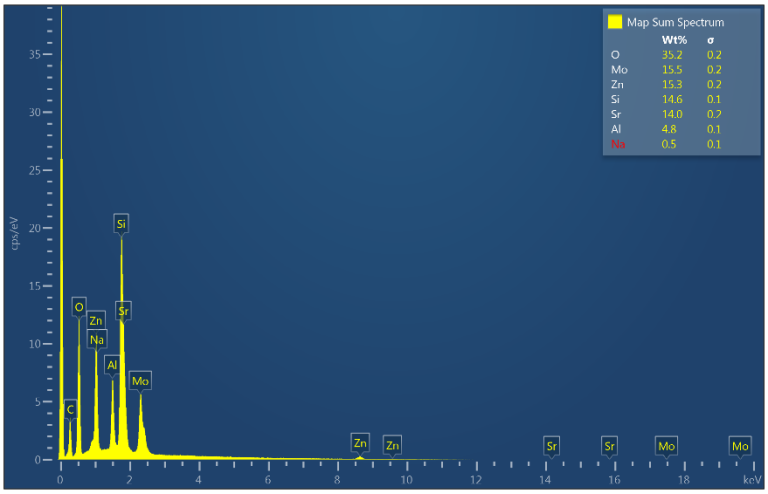

Figure 12.18. *EDS results map sum spectrum of site 3.*

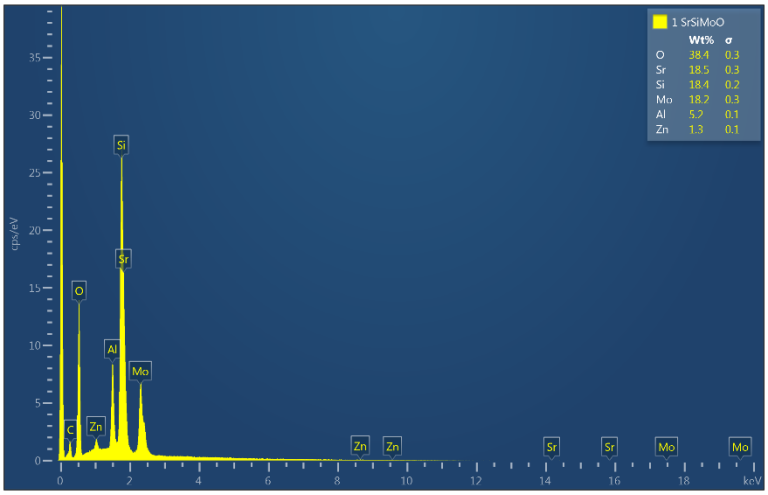

Figure 12.19. *EDS SrSiMoO phase result spectrum site 3.*

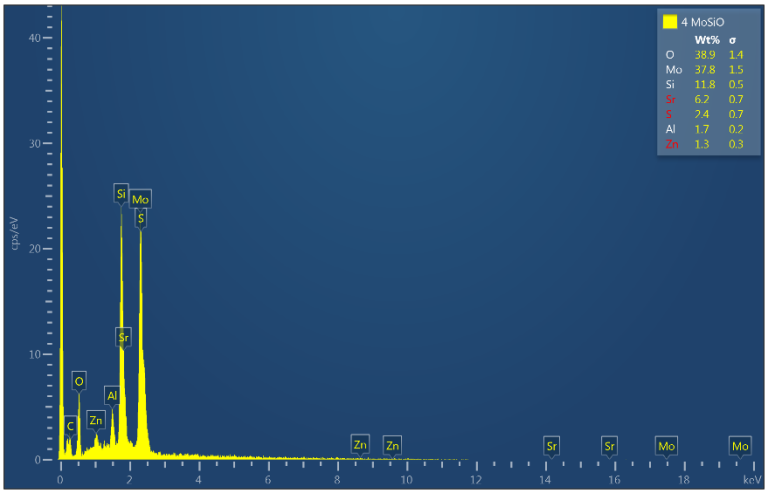

Figure 12.20. *EDS MoSiO phase result spectrum site 3.*

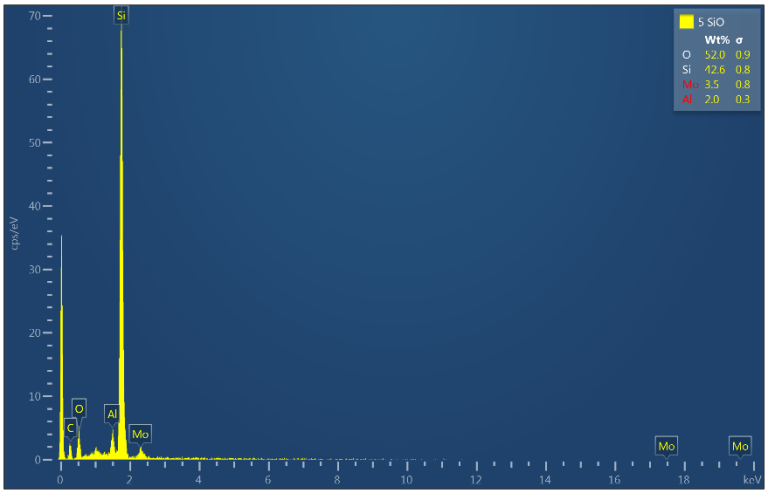

Figure 12.21. *EDS SiO phase result spectrum site 3.*

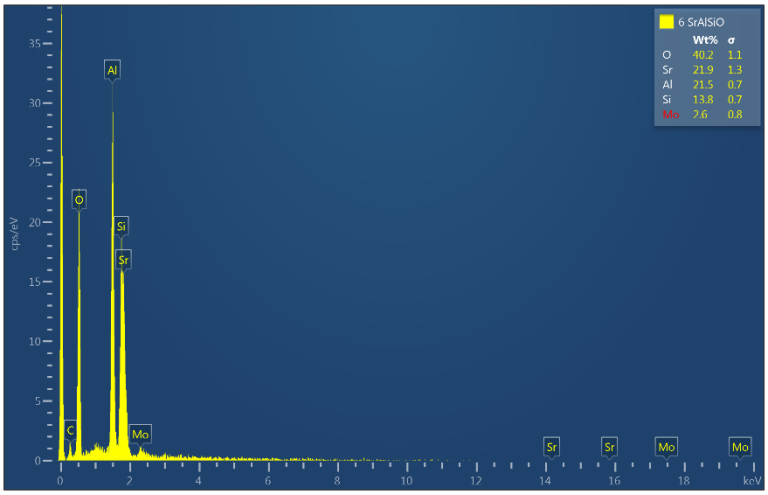

Figure 12.22. *EDS SrAlSiO phase result spectrum site 3.*

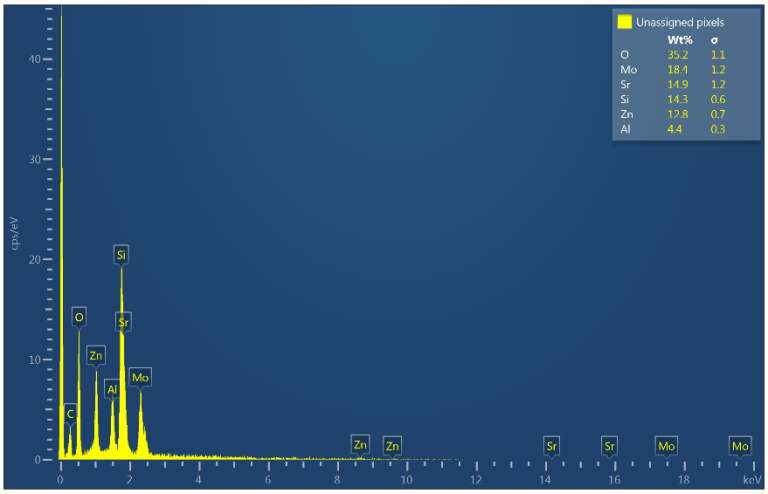

Figure 12.23. *EDS unassigned pixels phase result spectrum site 3.*

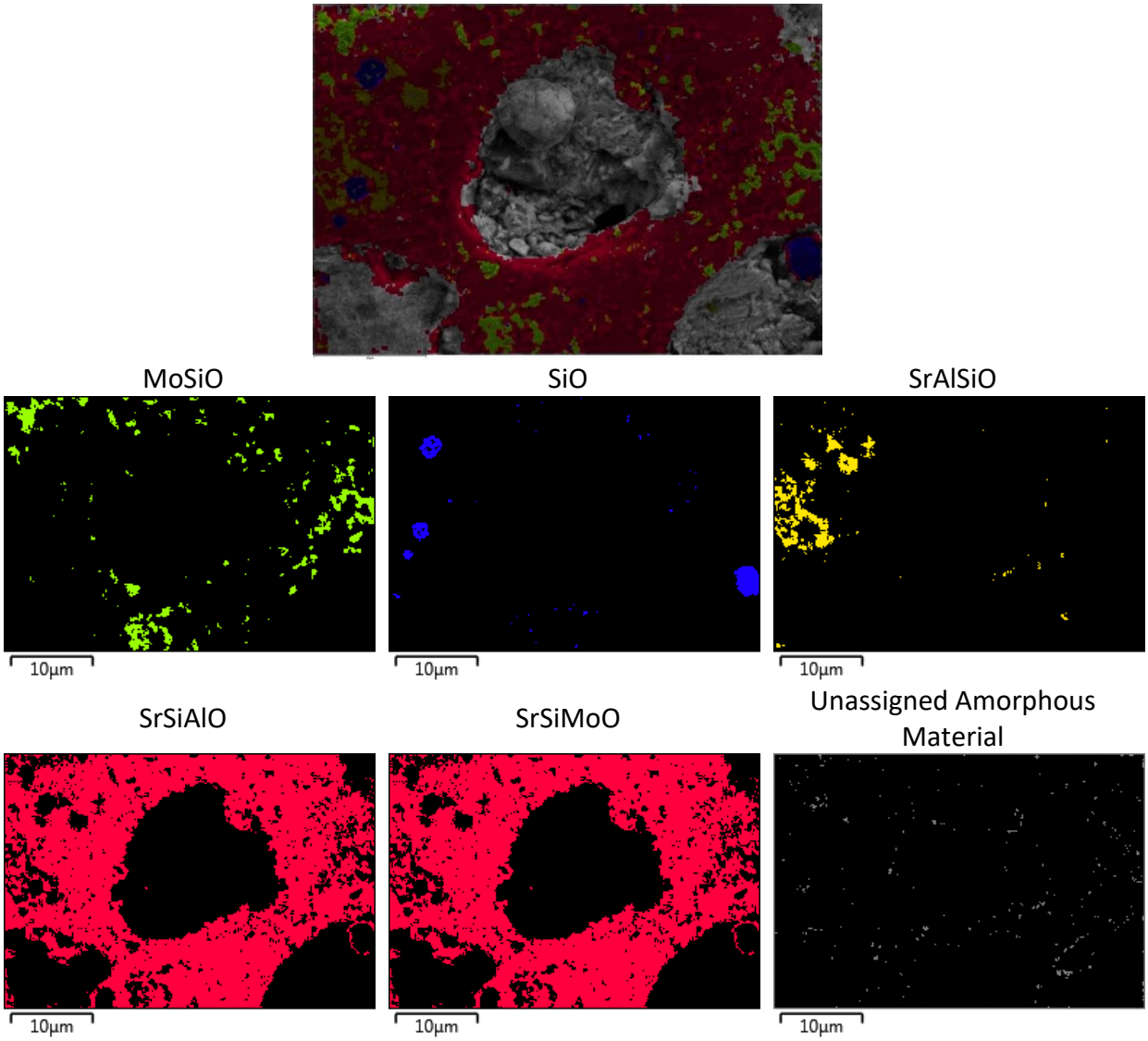

Figure 12.24. *EDS Phase map of site 3.*

Site 4

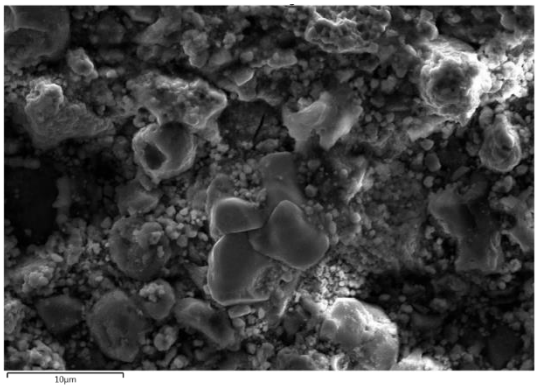

Figure 12.25. *SEM image of site 4, un-reacted material located near fuze wall.*

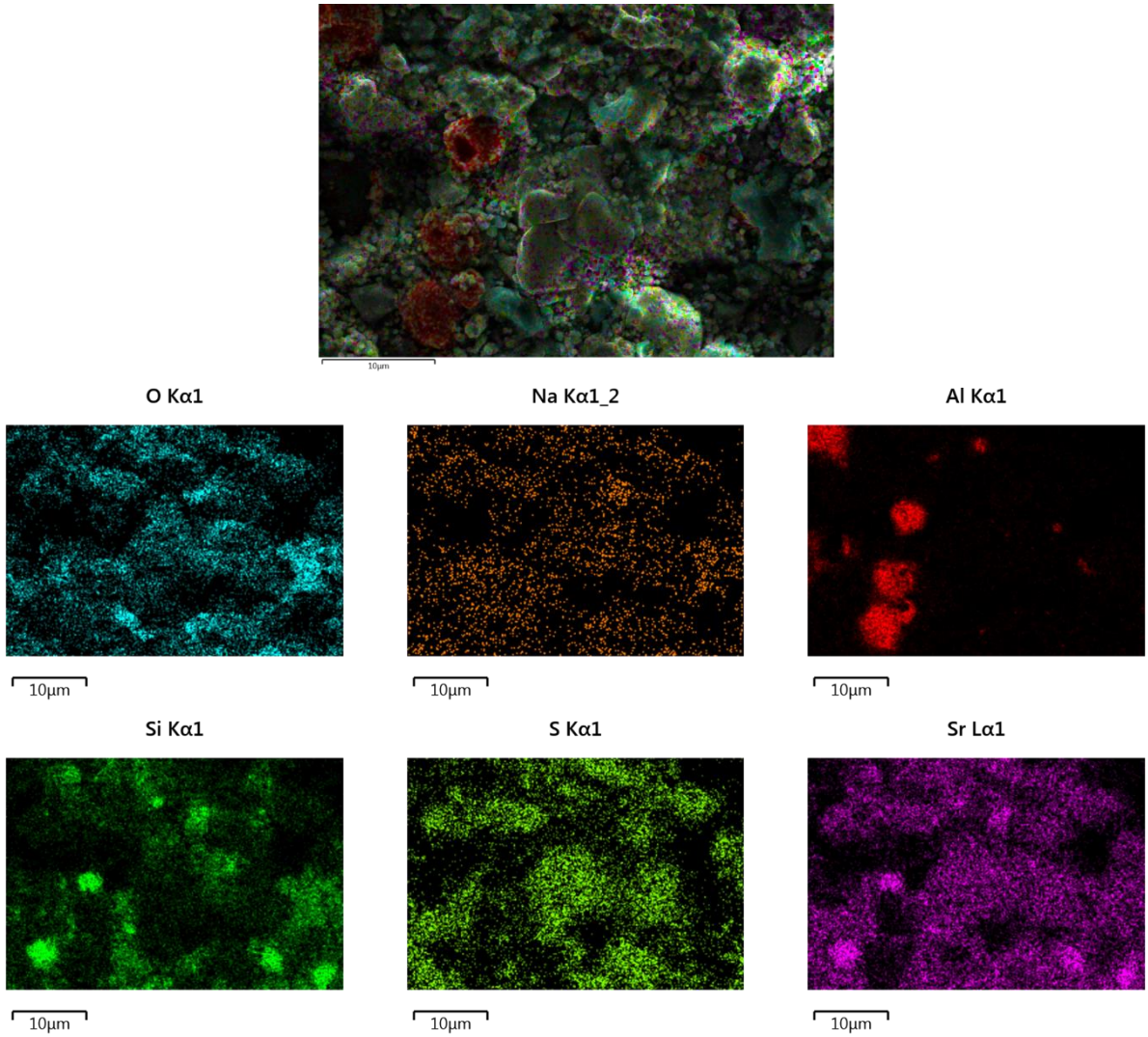

Figure 12.26. *EDS image of site 4, with color mapping.*

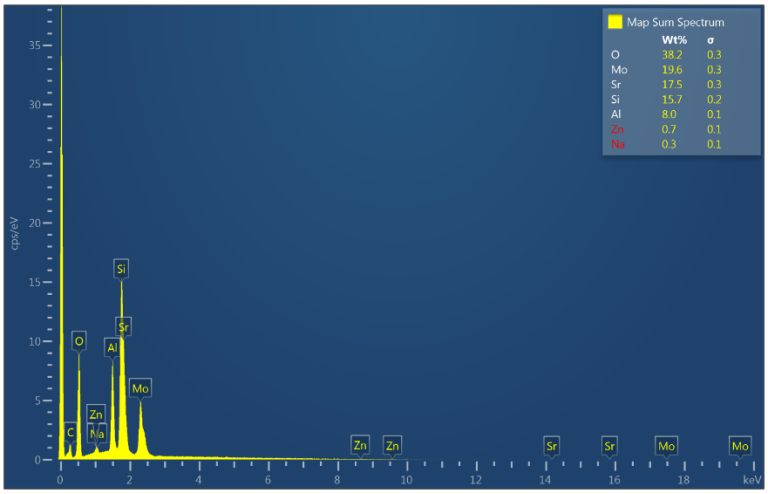

Figure 12.27. *EDS results map sum spectrum of site 4.*

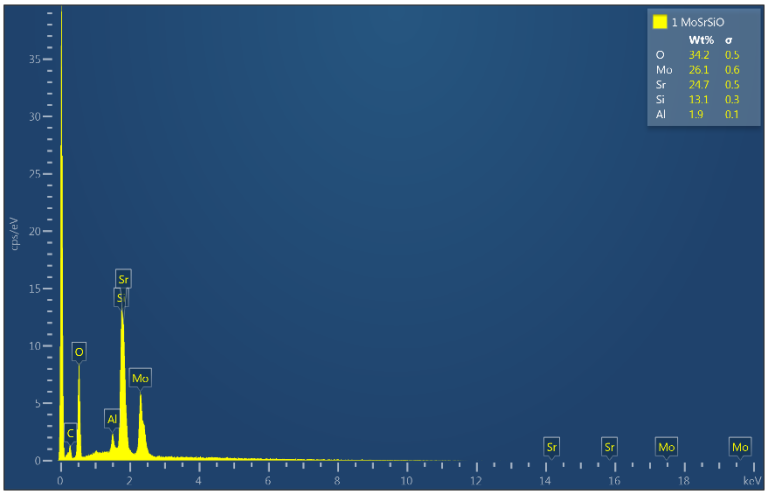

Figure 12.28. *EDS MoSrSiO phase result spectrum site 4.*

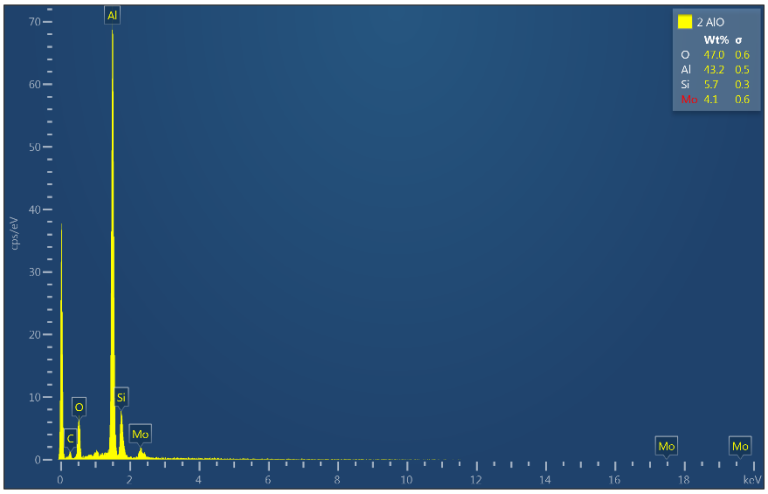

Figure 12.29. *EDS AlO phase result spectrum site 1.*

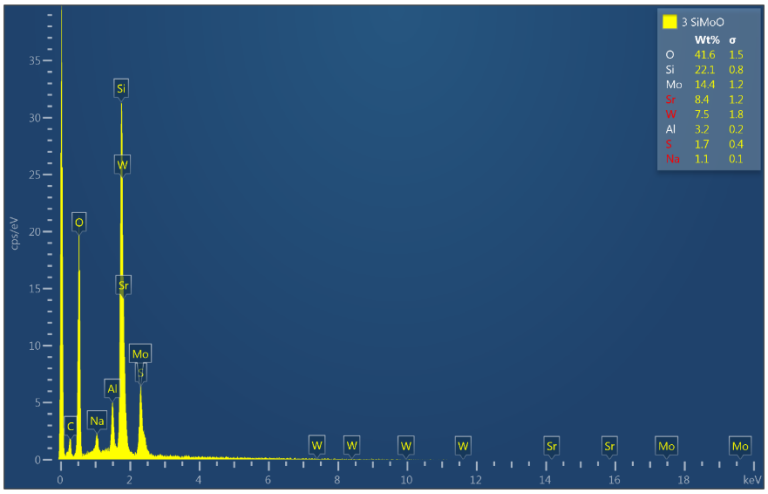

Figure 12.30. *EDS SiMoO phase result spectrum site 4.*

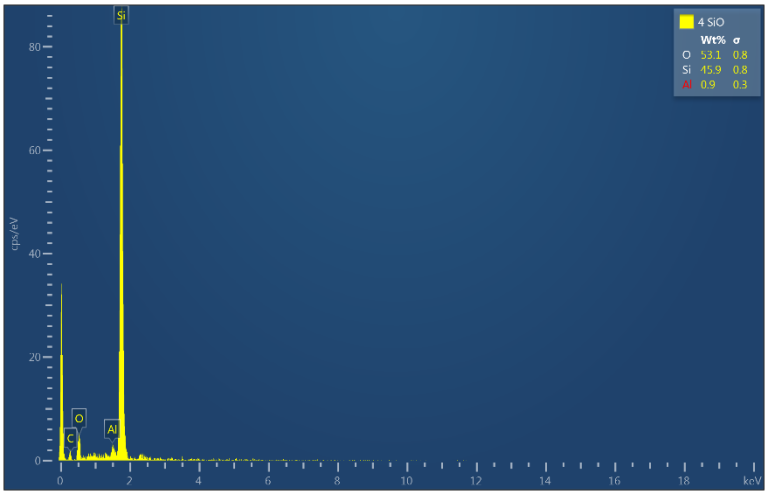

Figure 12.31. *EDS SiO phase result spectrum site 4.*

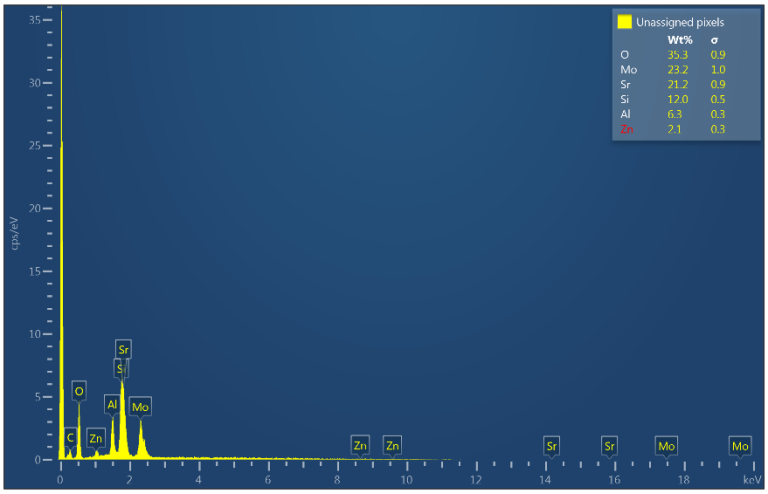

Figure 12.32. *EDS unassigned pixels phase result spectrum site 4.*

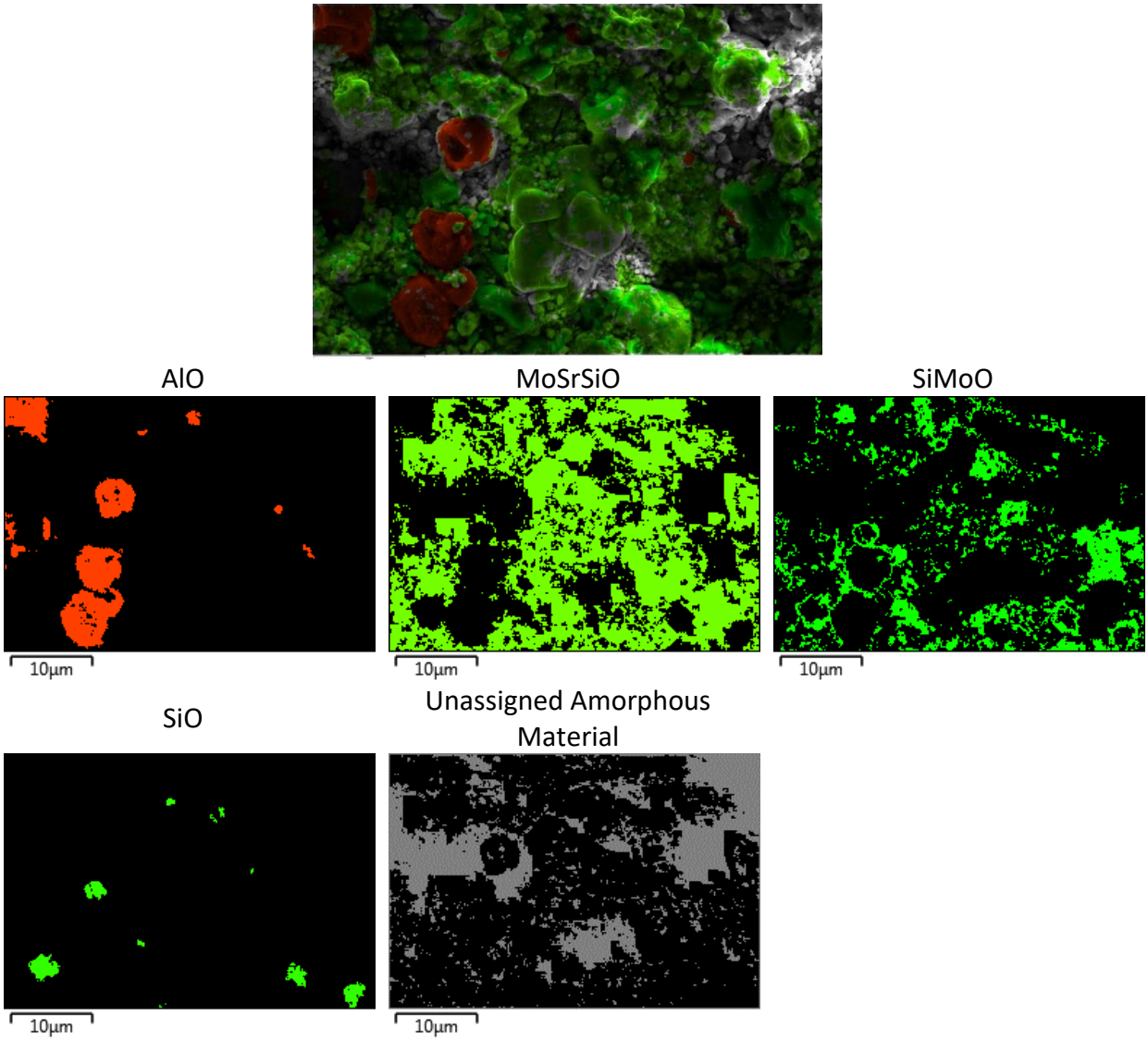

Figure 12.33. *EDS Phase map of site 4.*

12.3. Mathematical modeling

In this particular mathematical analysis, a 2-D model was selected due to a system symmetry. A schematic of the hardware used is shown in Figure 12.34.

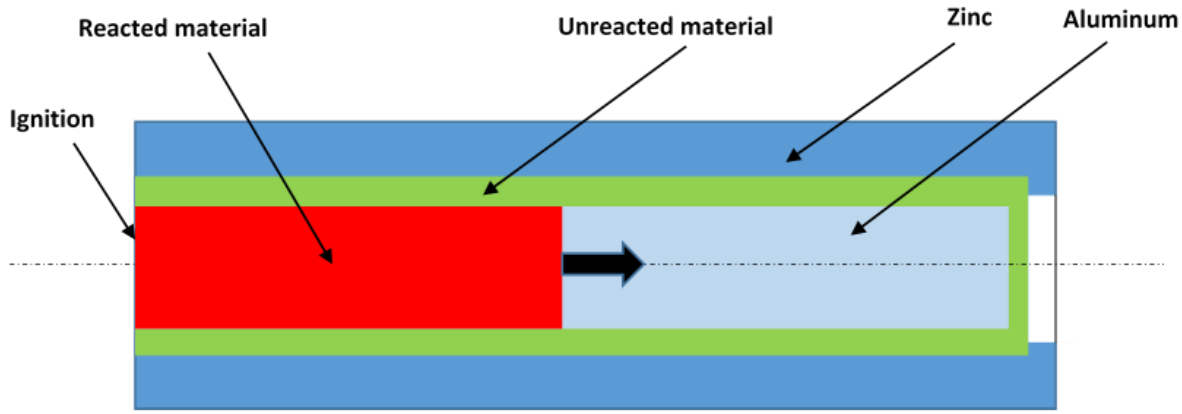

Figure 12.34. *Schematics of the hardware used in mathematical modeling of a combustion front propagation.*

The governing mathematical model equations of gasless combustion in a cylindrical coordinate system reads:

$$\rho C_p \frac{\partial T}{\partial t} = \lambda\left(\frac{\partial^2 T}{\partial x^2} + \frac{1}{r}\frac{\partial T}{\partial r}\right) + (-\Delta H_R)\rho(-r_A)$$

$$\frac{\partial \eta}{\partial t} = (-r_A); \qquad \text{where:} \qquad -r_A = k_o e^{-E/RT}(1-\eta)$$

Symbols in these equations are:
T – temperature in K; t – time in s; ρ – density of consolidated delay mixture in kg/m^3; C_p – specific heat of the delay mixture in J/kg•K; x – axial coordinate in m; r – radial coordinate in m; ($-\Delta H_r$) – heat of reaction in J/kg; λ – thermal conductivity in W/m•K; $-r_A$ – reaction rate in 1/s; η – conversion; k_o frequency factor in 1/s; E – activation energy in J/mol; R – universal gas constant in J/mol•K.

Governing equations describing the combustion front propagation were solved simultaneously with partial equations describing heat transfer by conduction on metal tubes containing the reactive mixture. All governing equations were solved using COMSOL software version 5.3a. Each 2-D domain was discretized using triangular finite elements.

The chemical reaction equation for the condensed reaction used in M201A1 hardware was determined by conducting thermodynamic calculations (HSC Chemistry software) and XRD analysis of the resulting product. Based on these results it was deduced that the overall molar reaction, for Al concentration in the binary fuel Al/Si=30/70 by weight and fuel to oxidizer ratio F/O=25/75 by weight, should read:

$$0.249Al + 0.55945Si + 0.272SrMoO_4 + 0.162SiO_2 =$$
$$0.272SrO + 0.38325SiO_2 + 0.125MoSi_2 + 0.1245Al_2O_3 + 0.0294Mo_5Si_3$$

The adiabatic combustion temperature for this reaction was conducted using HSC Chemistry software. The value of this adiabatic temperature is 2368 K, the activation energy, E, and the frequency factor, k_o, were determined using the Boddington method. The temperature profiles required for the evaluation were measured on larger pellets using W-W/Rh thermocouples. The determined values of E and k_o were 159.7 kJ/mol and $4.109 \cdot 10^5$ s^{-1}, respectively. Thermal conductivities of the reacting mixture before and after reaction were also determined experimentally and the average value of 0.65 W/m•K was used in modeling studies. Thermal conductivity was slightly adjusted to obtain comparable combustion front velocities with experimental data.

Mathematical modeling studies conducted using COMSOL software with a heat transfer module under both adiabatic and nonadiabatic conditions. The results of 1-D transient simulations at 70 ^oF are shown in Figure 12.35. The simulation was conducted with 60,000 nodes and the transient temperature profiles indicate that this particular reaction propagates slightly in an oscillatory mode, which is typical for very exothermic reactions with higher activation energy[7]. Additional simulations conducted at -65 ^oF and 160 ^oF revealed that the combustion front propagates approximately 10% slower at lower temperature while the propagation is faster by approximately the same factor at higher temperature.

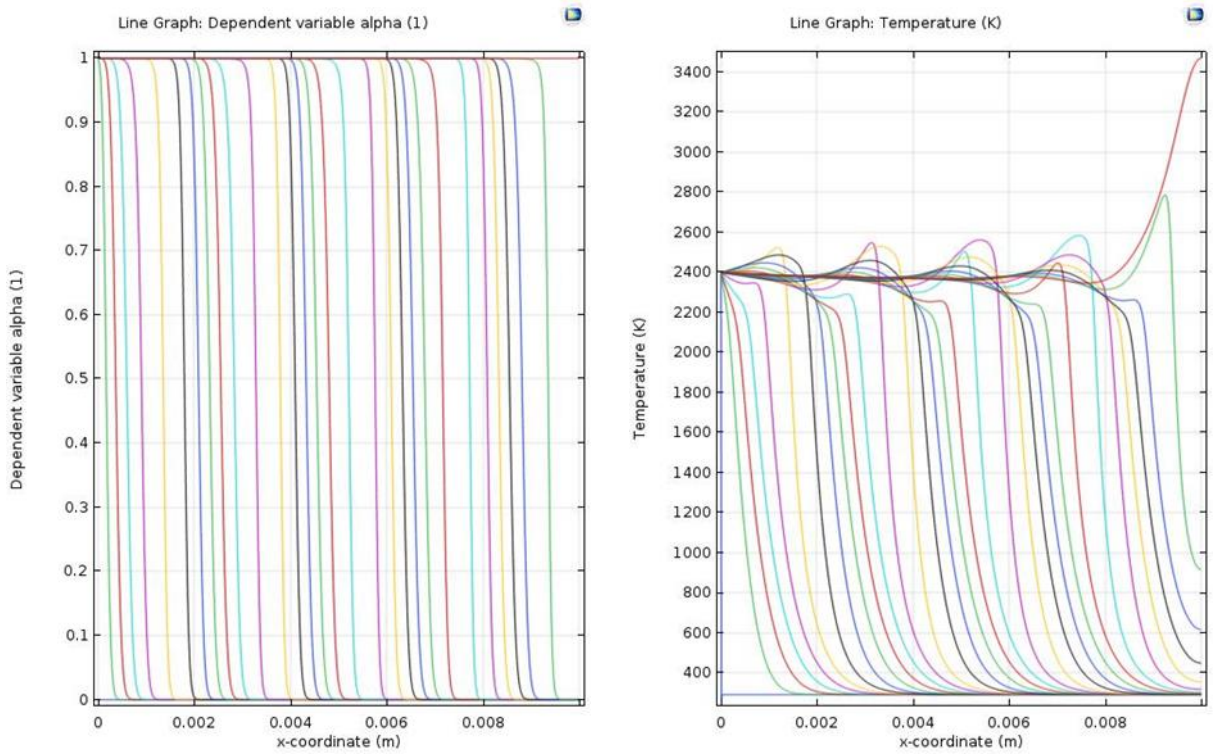

(a) (b)

Figure 12.35. *Simulated 1-D transient conversion (a) and temperature (b) profiles under adiabatic conditions. Conversion and temperature profiles are printed at intervals of 0.05 s*

2-D modeling studies were conducted under nonadiabatic conditions as shown schematically in Figure 12.34. In this case over 1 million free triangular finite elements were used to adequately model this highly nonlinear system. As can be seen from Figure 12.35, heat transfer from the reacting mixture to aluminum tube has caused preheating of the delay mixture ahead of the combustion front causing faster propagation after the initial slow propagation period. This effect has been significantly suppressed in the case when aluminum tube was replaced with less thermally conductive material, e.g. stainless steel.

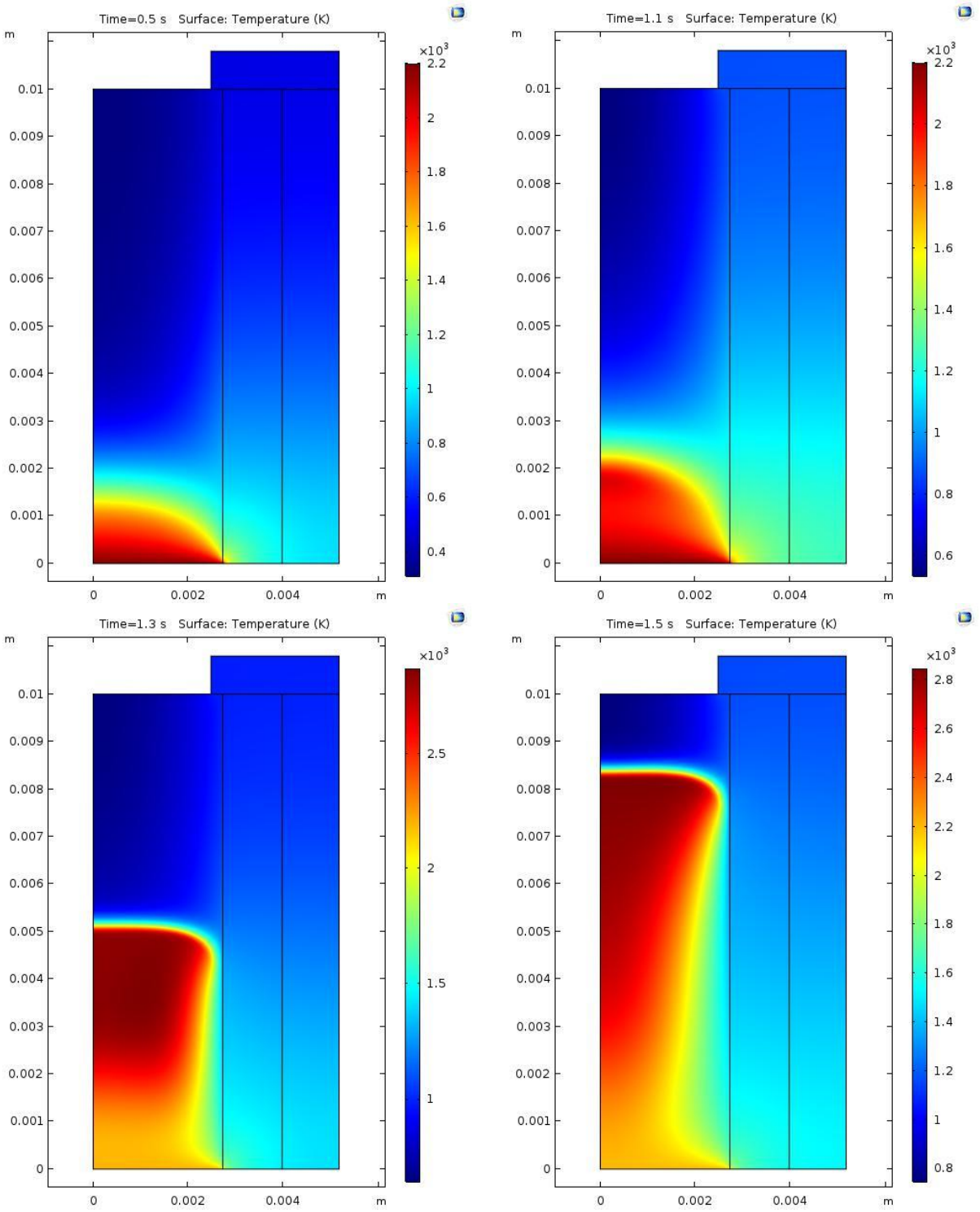

Figure 12.36. *2-D temperature profiles at 0.5 s, 1,1 s, 1.3 s, and 1.5 s. The schematic of the delay configuration is shown in Figure 12.34*

Both stability and numerical results have shown that experimentally determined activation energy is responsible for slight oscillations of the combustion front velocity. However, parametric studies have shown that the change in the value of activation energy by 10% stabilizes the combustion front. It should be emphasized that the value of measured activation energy and the assumption of the first order kinetics might be responsible for inaccurate representation of the overall reaction.

12.4. Heat Flow in M213/M228 Fuzes

Using the data generated in the previous sections a SolidWorks Heat Flow simulation was developed. This model was developed to provide insight into what is happening to heat within the M213/M228 fuze. The complex geometry and specific material present unique heat flow issues. The heat generated by the primer, ignition charge, and the pyrotechnic delay is vital to the self-sustaining burn front of the delay. It was noticed during failure investigations that when the delay did not fully propagate through the fuze, the point of failure was at the same place in the fuze in nearly 99% of the failures. This point was where the stem of the fuze and the threaded section of the fuze met (see Figure 12.37). It was hypothesized that excess heat was being removed from the delay at this point in the combustion causing extinction. It can be clearly identified in the heat flow simulation Figure 12.38 at the 1.5 to 3 s that this point in the fuze does in fact act as a "heat-brake". This is where a large amount of heat is absorbed into the fuze body. This prediction can be used to develop future hardware that doesn't present this failure concern.

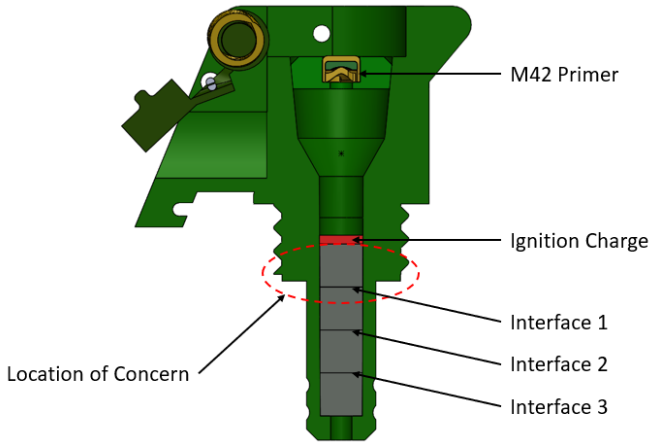

Figure 12.37. *M213/M228 fuze system failure schematics.*

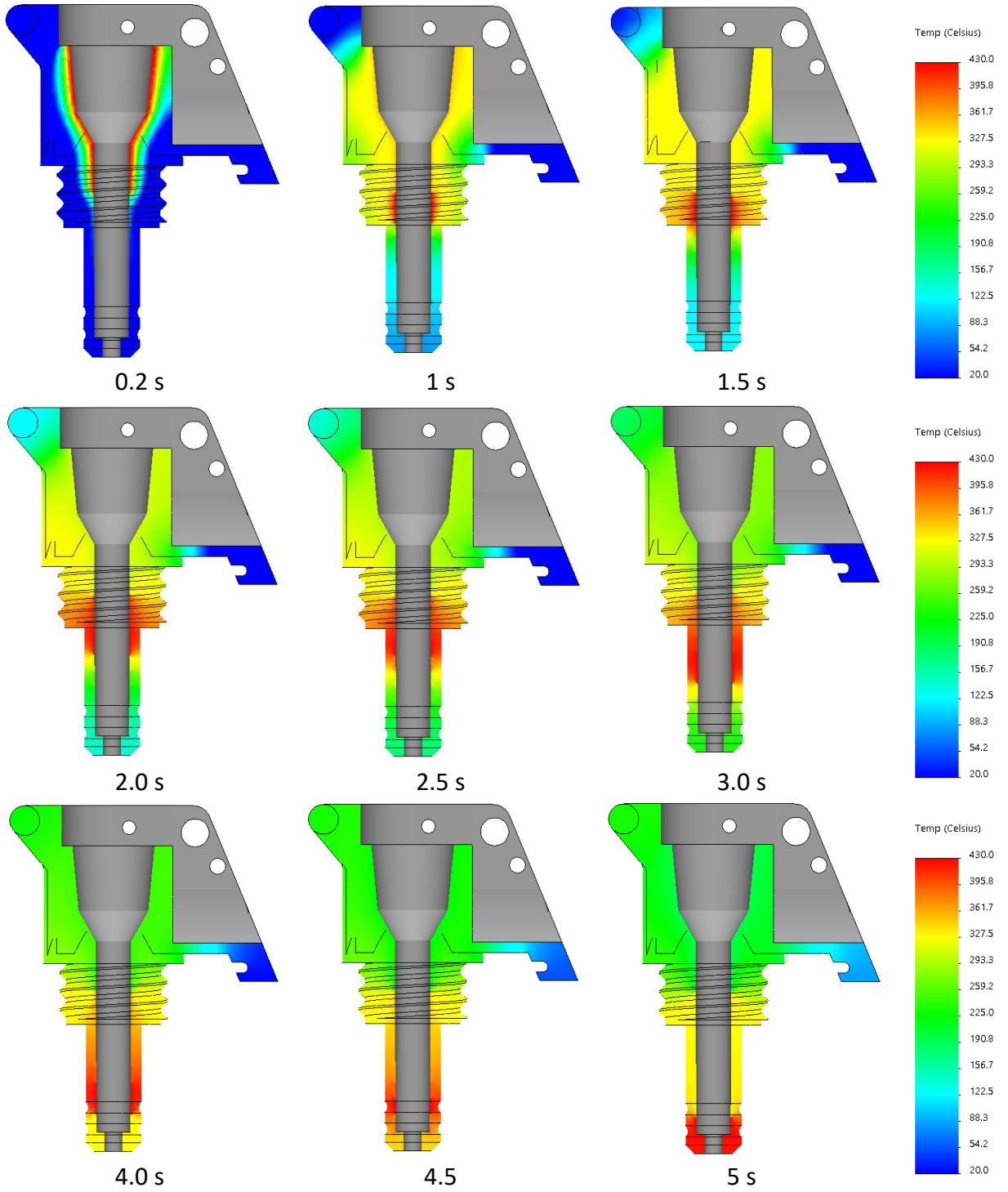

Figure 12.38. *Thermal simulation of M213/M228 fuze using SolidWorks Simulation software. Illustrating the heat transfer from the delay composition combustion to fuze body.*

Table 12.4. *SolidWorks Simulation Report. Detailing the thermal simulation parameters.*

Model Information

Solid Bodies		
Document Name and Reference	**Treated As**	**Volumetric Properties**
Split Line1 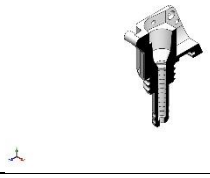	**Solid Body**	**Mass:0.114852 lb** **Volume:0.47449 in^3** **Density:0.242053 lb/in^3** **Weight:0.114774 lbf**

Study Properties

Study name	Thermal 2
Analysis type	Thermal (Transient)
Mesh type	Solid Mesh
Solver type	FFEPlus
Solution type	Transient
Total time	5 Seconds
Time increment	0.1 Seconds
Contact resistance defined?	No

Units

Unit system:	English (IPS)
Length/Displacement	in
Temperature	Celsius
Angular velocity	Hertz
Pressure/Stress	psi

Material Properties

Model Reference	Properties		Components
	Name: Model type: Default failure criterion: Thermal conductivity: Specific heat: Mass density:	Zinc AC41A Alloy, As Cast Linear Elastic Isotropic Unknown 0.00145651 BTU/(in.s.F) 0.100334 Btu/(lb.F) 0.242053 lb/in^3	SolidBody 2(Split Line1)(M213&M228 Fuze Body)

Mesh information

Mesh type	Solid Mesh
Mesher Used:	Standard mesh
Automatic Transition:	On
Include Mesh Auto Loops:	Off
Jacobian points	4 Points
Element Size	0.0399871 in
Tolerance	0.00199935 in
Mesh Quality Plot	High

Mesh information - Details

Total Nodes	112095
Total Elements	72516
Maximum Aspect Ratio	653.87
% of elements with Aspect Ratio < 3	96.9
% of elements with Aspect Ratio > 10	0.182
% of distorted elements (Jacobian)	0

Model name:M213&M228 Fuze Body
Study name:Thermal 2(-Default-)
Mesh type: Solid Mesh

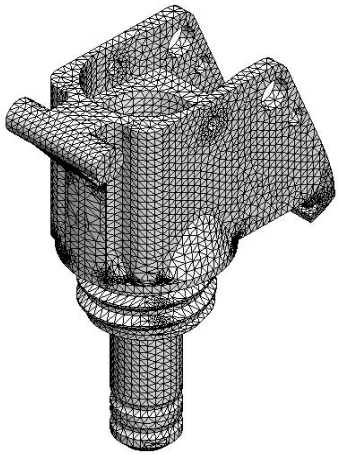

13.Task 11 – Basic Technology Assessment for Scale-Up

A scale-up assessment was conducted by Ensign Bickford Aerospace and Defense for the process developed by IMP. This document was submitted to SERDP as: *Environmentally Benign Pyrotechnic Formulation: Development Process Scale-Up*[4] and is included in Appendix E of this report.

14.Task 12 – ESD, BAM Friction, and BAM Impact Characterization

14.1. BAM Impact Sensitivity

BAM Impact characterization of the proposed M201A1 delay composition consisting of: $SrMoO_4$ 67.4 wt%, Al 6.8 wt%, Si 15.8 wt%, DE 4.7 wt%, SiO_2 5.0 wt%, and ADP: 0.4 wt% was conducted using the procedure specified in the UN "Recommendations on Transport of Dangerous Goods - Manual of Tests and Criteria" and the BAM impact testing apparatus shown in Figure 14.1. For this characterization, each test apparatus was loaded with 30 to 35 mg of the delay mix inside the guide ring in between two cylinders. The sample test fixture was placed in the BAM impact device and a drop weight of 1, 5, or 10 kg was dropped from a predetermined height (< 60 cm). After impact, the test apparatus was disassembled, and the results of each test were determined visually. The results of each test were assessed as: 1) no-reaction, 2) decomposition/partial reaction, and 3) explosion. The threshold of ignition (TOI) was determined at the point where six consecutive tests are observed with the results categorized as "no-reaction" or "decomposition".

Figure 14.1. *Photograph showing the BAM impact sensitivity tester at Innovative Materials and Processes, LLC (Purchased from Chilworth Technology Ltd.).*

14.2. BAM Friction Sensitivity

BAM Friction characterization of the delay composition was conducted using the procedure specified in the UN Recommendations on Transport of Dangerous Goods - Manual of Tests and Criteria, the BAM friction tester shown in Figure 14.2. The test consisted of placing approximately 30-35 mg of the composite material on a porcelain plate and placing the porcelain pin in contact with the sample. The desired load was then placed onto the arm and the actuator was activated for one revolution. The results of each test were assessed as: 1) no reaction, 2) decomposition (change of color), 3) gasses evolved, and 4) explosion. Testing was repeated at the selected energy levels until the TOI energy level was determined. The TOI was determined at the point where six consecutive tests were observed with the results categorized as "no-reaction" or "decomposition".

Figure 14.2. *Photograph showing BAM friction sensitivity tester at Innovate Materials and Processes, LLC (Purchased from Chilworth Technology Ltd.).*

14.3. Electrostatic Discharge Sensitivity

Electrostatic Discharge (ESD) characterization of the delay composition was conducted using the procedure specified in the MIL-STD-1751 A, "Safety and Performance Test for Qualification of Explosives", for solid substances and a MIL-SPEC Model 931D electrostatic discharge simulator with a blast chamber purchased from Electrotech Systems Inc. (see Figure 14.3). For each experiment, 30 – 35 mg of the delay mix was loaded in the sample holder, covered with mylar tape, and placed under the ignition pin. For all ESD characterization tests, the height of the sample plate was adjusted until the discharge needle pierced the mylar tape. The blast chamber door was then closed, the capacitor was charged, and the electricity was discharged into the sample. After the electrical discharge, the blast chamber door was opened, and the sample holder was analyzed to determine if ignition occurred. The results of each test can be assessed as: 1) no reaction, 2) decomposition (change of color), 3) gasses evolved, and 4) explosion. The TOI was determined at the point where 20 consecutive tests were observed with the results categorized as "no-reaction" or "decomposition".

Figure 14.3. *Photograph showing the electrostatic discharge tester with blast chamber at Innovative Materials and Processes, LLC (The manufacturer is Electro-Tech Systems Inc. Model 931).*

14.4. Results

Testing has indicated that the delay composition in powder form is very insensitive to friction, impact, and ESD stimuli. A summary of these tests results is presented in Table 14.1 along with HMX B5 as a reference material (conducted under DOTC-17-01-INIT0932 project).

Table 14.1. *BAM friction, BAM impact, and ESD testing sensitivity data of the proposed M201A1 delay mixture.*

Test Type	Input Energy	Number of Tests	Results	Reference (HMX)
BAM Friction	360 N	6	Negative	80 N
BAM Impact	60 J	6	Negative	6.8 J
ESD	250 mJ	20	Negative	To be determined

- The BAM Impact TOI for the delay composition was determined to be greater than 60 J (the maximum limit of equipment).
- The BAM Friction TOI for the delay composition was determined to be greater than 360 N (the maximum limit of equipment).
- The ESD TOI for the delay composition was determined to be greater than 250 mJ (the maximum limit of equipment).

The results of the characterization tests show the TOI for the environmentally benign delay composition is considered insensitive in accordance with UN "Recommendations on Transport of Dangerous Goods - Manual of Tests and Criteria" for impact and friction, and in accordance with MIL-STD-1751 A for ESD.

15. Task 13 -- Manufacturing and testing of sixty fully assembled M228 and M213 delay elements at -65 °F, 70 °F, and 160 °F

15.1. M213/M228 Fuze System Manufacture and Testing

The hardware developed is based on the specifications provided by the DoD. The loading and consolidation die were developed to allow for ten fuzes to be loaded at a time. A photograph of the consolidation die is shown in Figure 15.1.

Figure 15.1. *Photograph of M213/M228 fuzes in the consolidation die.*

In addition to the traditional flat punch used for the consolidation of the material within the fuze housing, a custom punch was developed to deglaze and relieve material stresses located at the interfaces between the consolidated layers of delay formulation in the M213/M228 fuzes. A picture of the deglazing punch is shown in Figure 15.2.

Figure 15.2. *Photograph of the deglazing punch developed for the disruption of the material within the column to deglaze and relieve material stresses located at the press interfaces.*

The crimping process was conducted after the primed primer holder assembly was inserted into the fuze housing. The primer holder assembly was pressed into the fuze to flush insertion depth

with the top of the fuze housing at pressures ranging from 9.8 to 10 ksi. The primer holder assembly was then crimped with a 0.542 in diameter die (see Figure 15.3 left) at pressures ranging from 9.8 to 10 ksi. The primer was then crimped into the primer holder assembly using a 0.200 in diameter die (see Figure 15.3 right) at pressures ranging from 3.4 to 3.8 ksi.

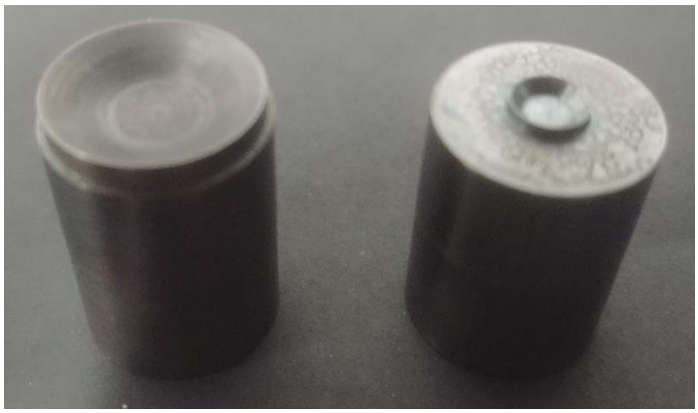

Figure 15.3. *M213/M228 fuze primer holder assembly crimping die (left) and M42 primer crimping die (right).*

M213/M228 fuzes are manufactured using the following method:

1. Use a volumetric or gravimetric method to measure the required amount of delay mixture for the first loading increment and add it to the M213/M228 housing;
2. Consolidate the loaded delay composition using the selected consolidation punch at 25 ksi pressure with a dwell time of 5 s;
3. Record the consolidation height;
4. Using the deglazing punch, lower to the pressed layer surface, with approximately 40 psi, rotate punch five 180° turns, and remove from the fuze;
5. Repeat steps 1-4 for total of four loading increments;
6. For the fourth increment, measure the required amount of delay mixture and add it to the M213/M228 housing;
7. Insert the stepped punch and lightly tap delay down until surface holds the stepped shape.
8. Use a volumetric spoon to measure 200 ± 5 mg IMP A-1A and add it to the M213/M228 delay housing;
9. Consolidate the loaded energetic material at 25 ksi using the flat punch and record the final consolidation height;
10. Insert the M42 primer into the M213/M228 primer holders using the arbor press (Figure 15.4);
11. Install primed primer assemblies into the charging well of the fuze body (see Figure 15.5). Install primer holder into the M213/M228 housing using the pneumatic press until insertion depth is flush (Figure 15.6).
12. Crimp the primer assembly within the fuze body;
13. Crimp the primer within the primer assembly.

Figure 15.4. *Photograph of M42 primers inserted into M213A1/M228A1 primer holders.*

Figure 15.5. *Inserting primed primer assemblies into fuze bodies during manufacturing process.*

Figure 15.6. *Photograph of a completed M213/M228 fuze assembly.*

The testing apparatus developed for fuze testing features a Kistler 8742A5 shock accelerometer which identifies primer initiation (t=0) by measuring the shock developed when the fuze anvil strikes the primer. The testing fixture is pictured in Figure 15.7. To identify the final fuze function time, a photo diode is attached to the apparatus via a fiber optics cable. The fuze's light output was measured when the fuze burns through to the end of the delay formulation for identification of final time (t_f) (see Figure 15.8).

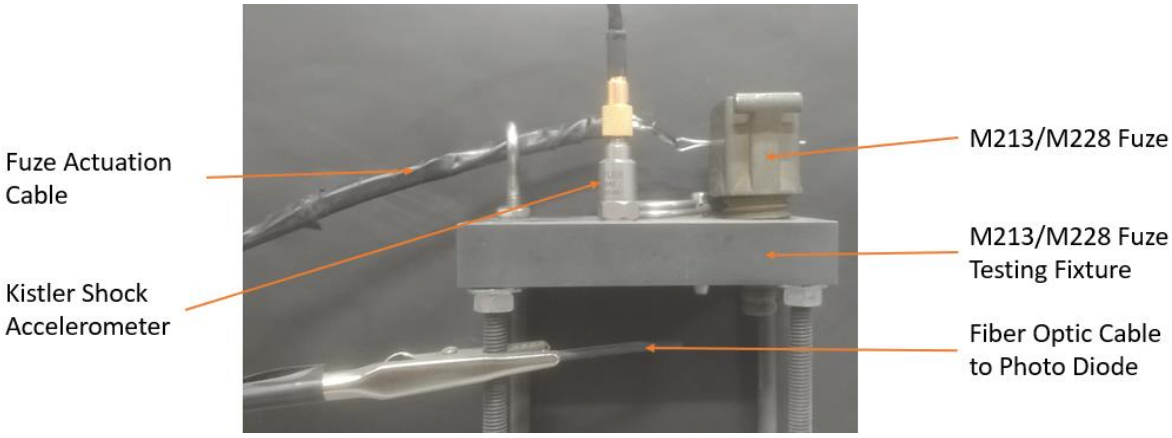

Figure 15.7. *Photograph of M213/M228 fuze in testing fixture at IMP.*

Figure 15.8. *Testing a M213/M228 fuze at IMP R&D Lab*

15.2. Primer Configuration Testing (Olin, MIC, and DBX-1)

M42 primers used in the M213/M228 fuzes currently contain lead styphnate. These primers are produced commercially by Olin. Two alternative M42 primer configurations tested were MIC and DBX-1. Comparisons are presented here.

Olin M42 Primers

Figure 15.11 shows data from a M213/M228 fuze built, using legacy lead-based Olin primers. This was conducted for a comparison to DBX-1 based primer testing. The fuzes with Olin primers produced an average IBR of 4.79 s/in, with a standard deviation of 0.053 s. The resulting coefficient of variation was 1.09%. It could also be noted that no breaches or bulging were observed on fired primers.

The following pressure output graphs display the pressure outputs of legacy lead-based Olin M42 primers (see Figure 15.9 and Figure 15.10), demonstrating a high and low primer brisance.

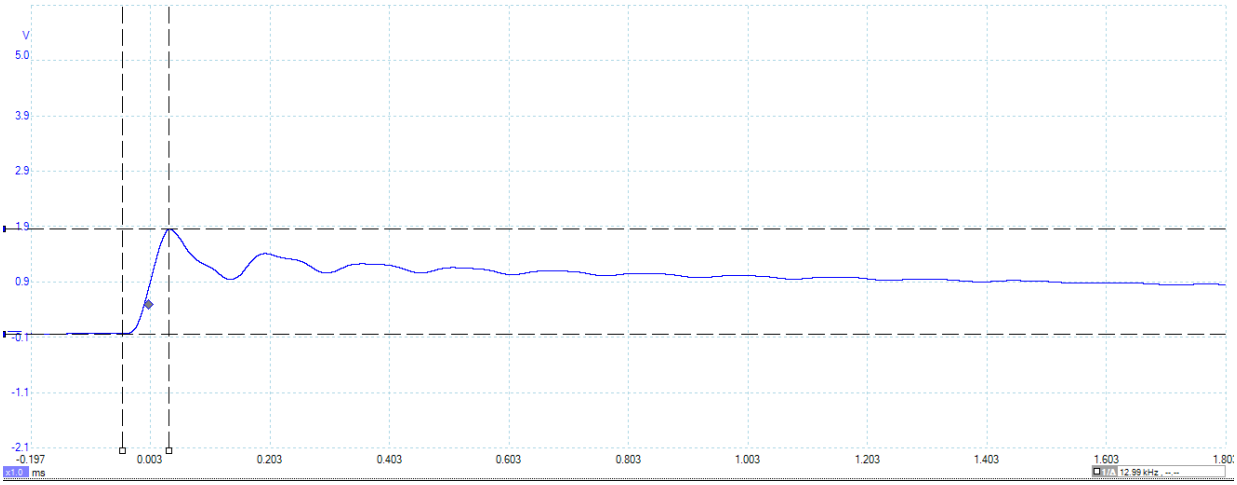

Figure 15.9. *Pressure output profile for an Olin lead based M42 primer lot number WCC09F002-029 (to calculate pressure, 1 V = 1000 PSI).*

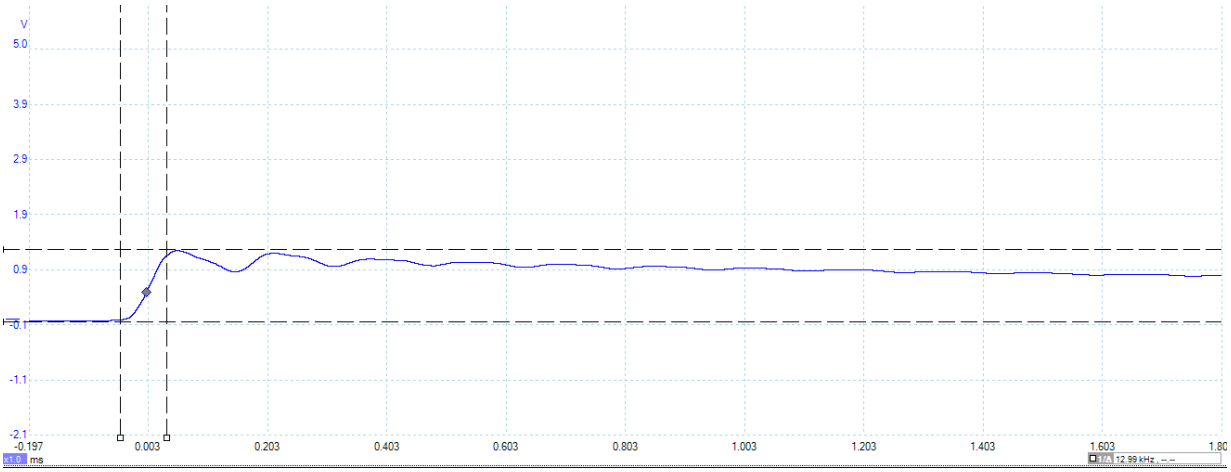

Figure 15.10. *Pressure output profile for an Olin lead based M42 primer lot number WCC09F002-029 (to calculate pressure, 1 V = 1000 PSI).*

Column	Height (in)	Burn time (s)	Inverse Burn Rate (s/in)
1	0.86150	4.200	4.875
2	0.84300	4.033	4.784
3	0.85400	4.167	4.879
4	0.83000	4.000	4.819
5	0.85750	4.067	4.742
6	0.84500	4.000	4.734
7	0.82300	3.900	4.739
8	0.83750	3.967	4.736
9	0.84350	4.033	4.782
10	0.85800	4.133	4.817
Minimum	0.823	3.900	4.734
Maximum	0.862	4.200	4.879
Range	0.039	0.300	0.145
Average	0.845	4.050	4.791
Std Dev	0.012	0.089	0.053

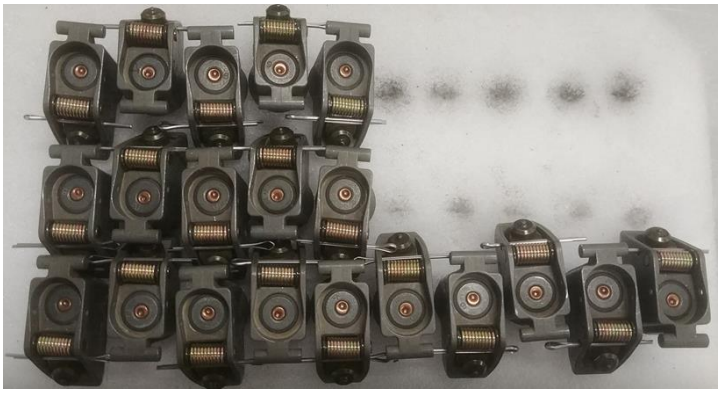

Figure 15.11. *M213/M228 fuze testing data using legacy lead-based Olin M42 primers maintained at 68 °F (20 °C). Accompanied by post testing pictures (right). This configuration produced a coefficient of variance of 1.09.*

DBX-1 Based Primer Testing

Following is testing data and pressure outputs for DBX-1 based primers for comparison to currently used Olin M42 primers. The following pressure output graphs display the pressure outputs of DBX-1 M42 primers (see Figure 15.12 and Figure 15.13) produced as part of work under DOTC-15-01-INIT411 project and utilizing the U.S. Army developed green primer formulation. The pressure output graphs illustrate the consistency of pressure output of DBX-1 based primers at 1 ksi and legacy primers to be between 1 and 1.9 ksi.

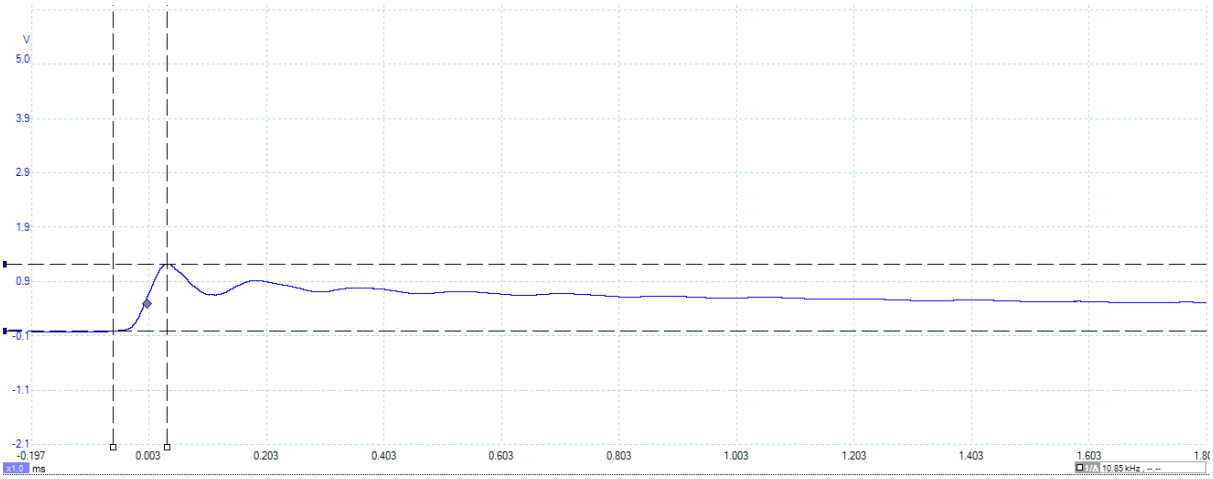

Figure 15.12. *Pressure output profile for a DBX-1 based primer, batch IMP-B060617 (to calculate pressure, 1 V = 1000 PSI).*

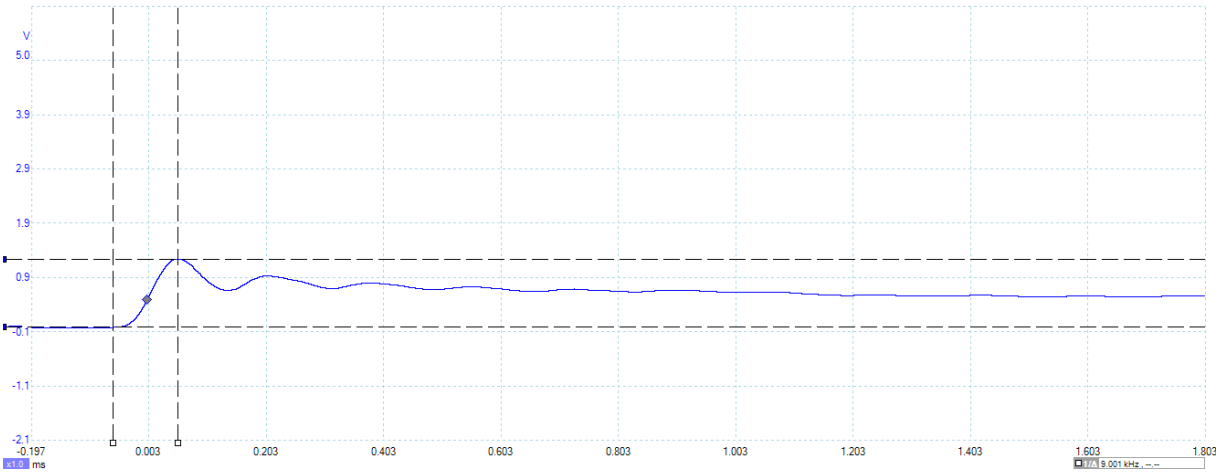

Figure 15.13. *Pressure output profile for a DBX-1 based primer, batch IMP-B060617 (to calculate pressure, 1 V = 1000 PSI).*

Initial testing of DBX-1 based primers displayed no breaches or abnormal bulging of the primer cup. Figure 15.14 illustrates that the primer cups did not breach when tested at 68 °F (20 °C). The #41 primer cups also did not display bulging at the anvil strike.

Column	Height (in)	Burn time (s)	Inverse Burn Rate (s/in)
41-1	0.91500	4.567	4.991
41-2	0.89550	4.600	5.137
41-3	0.90800	4.567	5.029
41-4	0.91950	4.567	4.966
41-5	0.89500	4.433	4.953
Minimum	0.895	4.433	4.953
Maximum	0.920	4.600	5.137
Range	0.025	0.167	0.183
Average	0.907	4.547	5.015
Std Dev	0.010	0.058	0.066
CV			1.316

Figure 15.14. *M213/M228 fuze testing data using DBX-1 based primers maintained at 68 °F (20 °C). Accompanied by post testing pictures (right).*

Testing of DBX-1 primers was conducted at the hot, cold, and ambient temperature conditions (see Figure 15.15 throughFigure 15.17).

Column	Height (in)	Burn time (s)	Inverse Burn Rate (s/in)
1	0.62950	4.118	6.542
2	0.63350	4.022	6.349
3	0.61900	3.947	6.376
4	0.61350	3.918	6.386
5	0.62100	4.081	6.572
6	0.62200	3.980	6.399
7	0.61100	4.001	6.548
8	0.60200	3.879	6.444
9	0.62250	3.879	6.231
10	0.63850	3.968	6.215
11	0.58600	3.734	6.372
12	0.59550	3.713	6.235
13	0.59050	3.736	6.327
14	0.59800	3.813	6.376
15	0.60500	3.929	6.494
Minimum	0.586	3.713	6.215
Maximum	0.639	4.118	6.572
Range	0.053	0.405	0.357
Average	0.613	3.915	6.391
Std Dev	0.015	0.120	0.110
C/V			1.72

Figure 15.15. *Results of M213/M228 fuze built with DBX-1 based IMP built primers tested at 160 °F (71 °C) accompanied by image of corresponding fired fuzes.*

Column	Height (in)	Burn time (s)	Inverse Burn Rate (s/in)
16	0.59450	4.789	8.056
17	0.58100	4.578	7.880
18	0.58850	4.751	8.073
19	0.58300	4.705	8.070
20	0.59500	4.780	8.034
21	0.57750	4.520	7.827
22	0.56950	4.448	7.810
23	0.56400	4.515	8.005
24	0.57300	4.683	8.173
25	0.58650	4.813	8.206
26	0.58350	4.787	8.204
27	0.57550	4.814	8.365
28	0.60250	4.944	8.206
29	0.59300	4.826	8.138
30	0.60500	4.841	8.002
Minimum	0.564	4.448	7.810
Maximum	0.605	4.944	8.365
Range	0.041	0.496	0.555
Average	0.585	4.720	8.070
Std Dev	0.011	0.138	0.148
C/V			1.84

Figure 15.16. *Results of M213/M228 fuze built with DBX-1 based IMP built primers tested at -60 °F (-54 °C) accompanied by image of corresponding fired fuzes.*

Column	Height (in)	Burn time (s)	Inverse Burn Rate (s/in)
31	0.54350	4.259	7.836
32	0.54050	4.113	7.610
33	0.52850	4.118	7.792
34	0.55000	4.322	7.858
35	0.55050	4.309	7.827
36	0.55700	4.344	7.799
37	0.56350	4.354	7.727
38	0.56800	4.461	7.854
39	0.56350	4.219	7.487
40	0.56800	4.368	7.690
41	0.56050	4.402	7.854
42	0.55600	4.426	7.960
43	0.55450	4.295	7.746
44	0.56100	4.409	7.859
45	0.54250	4.300	7.926
Minimum	0.529	4.113	7.487
Maximum	0.568	4.461	7.960
Range	0.040	0.348	0.473
Average	0.554	4.313	7.788
Std Dev	0.011	0.099	0.118
C/V			1.52

Figure 15.17. *Results of M213/M228 fuze built with DBX-1 based IMP built primers tested at 70 °F (22 °C) accompanied by image of corresponding fired fuzes.*

MIC based M42 Primer Testing

MIC based M42 primers, developed and manufactured at IMP under the DOTC-16-01-INIT0598 project, were also tested in the M213/M228 fuze configuration see Figure 15.18. It was thought in previous testing that the MIC primer was responsible for the failure to sustain combustion in the fuze, due to lower pressure output of the primer. However, results from improved interface processing prompted a reevaluation of the MIC primers with outstanding results (see Figure 15.19 through Figure 15.21). There were no observed breaches nor were there any bulging of the primer cups.

Figure 15.18. *Plot of IBR from fuzes tested with MIC based M42 primers.*

Column	Height (in)	Burn time (s)	Inverse Burn Rate (s/in)
1	0.91840	4.633	5.045
2	0.93400	4.633	4.961
3	0.90600	4.567	5.040
4	0.93210	4.600	4.935
5	0.92130	4.600	4.993
6	0.93605	4.600	4.914
7	0.91490	4.533	4.955
8	0.93805	4.667	4.975
9	0.89400	4.500	5.034
10	0.90990	4.567	5.019
Minimum	0.894	4.500	4.914
Maximum	0.938	4.667	5.045
Range	0.044	0.167	0.131
Average	0.920	4.590	4.987
Std Dev	0.014	0.047	0.044
CV			0.881

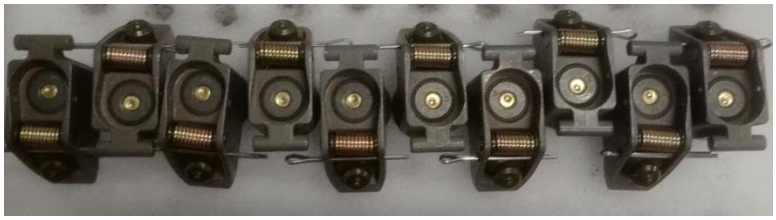

Figure 15.19. *Data from M213/M228 fuze testing using MIC M42 primers maintained at 68 °F (20 °C). Accompanied by post testing pictures (right).*

Column	Height (in)	Burn time (s)	Inverse Burn Rate (s/in)
1	0.98050	5.267	5.371
2	0.94550	4.867	5.147
3	0.99450	5.100	5.128
4	0.98500	5.200	5.279
5	0.96950	5.033	5.192
6	0.97300	5.233	5.379
7	0.99050	5.200	5.250
8	0.92350	4.933	5.342
9	0.96750	5.000	5.168
10	0.94100	4.933	5.243
Minimum	0.924	4.867	5.128
Maximum	0.995	5.267	5.379
Range	0.071	0.400	0.250
Average	0.967	5.077	5.250
Std Dev	0.022	0.136	0.087
CV			1.662

Figure 15.20. *Data from M213/M228 fuze testing using MIC M42 primers maintained at -65 °F (-54 °C). Accompanied by post testing pictures (right).*

Column	Height (in)	Burn time (s)	Inverse Burn Rate (s/in)
1	1.02600	4.667	4.548
2	1.03200	4.667	4.522
3	1.04300	4.533	4.346
4	1.02600	4.567	4.451
5	1.02550	4.600	4.486
6	1.02500	4.433	4.325
7	1.03050	4.467	4.334
8	1.03500	4.533	4.380
9	1.04350	4.533	4.344
10	1.03550	4.467	4.314
Minimum	1.025	4.433	4.314
Maximum	1.044	4.667	4.548
Range	0.019	0.233	0.235
Average	1.032	4.547	4.405
Std Dev	0.007	0.076	0.084
CV			1.903

Figure 15.21. *Data from M213/M228 fuze testing using MIC M42 primers maintained at 160 °F (71 °C). Accompanied by post testing pictures (right).*

15.3. Delay Formulation Optimization

Numerous delay formulations were previously evaluated for their performance characteristics. However, due to the long burn time (4 to 5.5 s), fuze housing material (Zinc), and the non-linear geometry of the M213/M228 fuze, it proved challenging to identify a formulation using the 2 to 3 µm (H-2) aluminum particle size. Characterization of H-3 (3-4.5 µm) and H-5 (4.5 to 7 µm) spherical aluminum provided promising results. Two formulations were used with successful function in M213/M228 fuzes; 1) a formulation of 25:75 fuel to oxidizer with a 30/70 H-3 particle size aluminum to silicon (IMP-B050818-V2), and 2) a formulation of 30:70 fuel to oxidizer ratio with a 32.5/68.5 H-5 particle size aluminum to silicon. Both formulations were tested and yielded proper burn time results. Additionally, consolidation heights were tuned for required burn times using both formulations.

Table 15.1 shows that using H-2 particle size required an excessively tall consolidation height to attain the required burn times.

Table 15.1. *M213/M228 delay fuze testing data, using MIC based primers and 4-layer consolidation process.*

Column	Height (in)	Burn time (s)	Inverse Burn Rate (s/in)
1	0.97700	5.200	5.322
2	0.92700	4.300	4.639
3	0.95800	4.533	4.732
4	0.95500	4.667	4.887
5	0.91850	4.900	5.335
6	0.77900	4.800	6.162
7	0.78050	4.600	5.894
8	0.84300	4.233	5.022
9	0.92550	5.133	5.547
Minimum	0.779	4.233	4.639
Maximum	0.977	5.200	6.162
Range	0.198	0.967	1.523
Average	0.896	4.707	5.282
Std Dev	0.072	0.317	0.490

Testing was conducted and compared to previously tested fuzes with the same formulation and configuration. Previous delay mixtures with Valimet H-2 aluminum, had average IBRs of 4.48 s*in-1. Using the same pyrotechnic mixture, with only an adjustment of aluminum's particle size to H-3, increased the average IBR by 0.29 s*in-1 (see Table 15.2).

Table 15.2. *Valimet H-3 Aluminum particle size testing data.*

Column	Height (in)	Burn time (s)	Inverse Burn Rate (s/in)
1	0.35750	1.700	4.755
2	0.37850	1.810	4.782
3	0.37800	1.840	4.868
4	0.37800	1.770	4.683
5	0.35650	1.780	4.993
6	0.39750	1.820	4.579
7	0.36700	1.710	4.659
8	0.40700	1.960	4.816
9	0.36850	1.740	4.722
10	0.35400	1.700	4.802
Minimum	0.354	1.700	4.579
Maximum	0.407	1.960	4.993
Range	0.053	0.260	0.414
Average	0.374	1.783	4.766
Std Dev	0.017	0.076	0.110
C/V			2.31

Initial data produced from testing of the H-5 aluminum-based formulation (25:75 by weight fuel to oxidizer ratio and 30:70 by weight Al to Si binary fuel ratio) demonstrated very consistent burn times within the required range. It produced an IBR near 6.4 s*in-1 tested at 68 °F (20 °C) (see Table 15.5) and 7.3 s*in-1 tested at -65 °F (-54 °C) (see Table 15.3). The IBRs of the fuzes provided the ability to reduce the consolidation height to 0.60 in. This consolidation height is ideal for manufacturing of the fuzes. After reliability testing of the composition, it was found that some fuzes failed to sustain combustion propagation. Additionally, the range of burn times at the temperature extremes were also an issue. After testing of fuzes at -65 °F (-54 °C), 5.5% failed to sustain combustion propagation and the average burn times produced at 160 °F (71°C) (see Table 15.4) were 5.4 s and 4.1 s respectively. This mixture would have a high probability of generating burn times that were outside of the requirements when considering the standard deviation is 0.11 s at -65 °F (-54 °C) and 0.10 s at 160 °F (71°C).

Table 15.3. *Consolidation height, burn time, and IBR data from testing of a delay mixture comprised of a 25:75 by weight fuel to oxidizer ratio and 30:70 by weight Al to Si ratio utilizing H-5 aluminum at -65 °F (-54 °C).*

Column	Height (in)	Burn time (s)	Inverse Burn Rate (s/in)	Column	Height (in)	Burn time (s)	Inverse Burn Rate (s/in)	Column	Height (in)	Burn time (s)	Inverse Burn Rate (s/in)
1	0.68000	5.067	7.451	31	0.70600	FTF		61	0.68050	6.233	9.160
2	0.68600	4.900	7.143	32	0.68450	6.200	9.058	62	0.68250	6.133	8.987
3	0.68800	5.067	7.364	33	0.66800	6.067	9.082	63	0.67250	6.200	9.219
4	0.68400	5.067	7.407	34	0.67300	5.900	8.767	64	0.68250	6.067	8.889
5	0.68600	5.100	7.434	35	0.67500	FTF		65	0.68150	6.067	8.902
6	0.68850	4.933	7.165	36	0.68250	6.167	9.035	66	0.72800	6.433	8.837
7	0.67700	4.933	7.287	37	0.67900	6.000	8.837	67	0.68200	6.067	8.895
8	0.67200	4.967	7.391	38	0.68900	6.100	8.853	68	0.68800	6.133	8.915
9	0.67050	4.900	7.308	39	0.66950	5.600	8.364	69	0.70200	6.167	8.784
10	0.69450	5.100	7.343	40	0.67000	5.833	8.706	70	0.68350	6.300	9.217
11	0.69300	5.133	7.407	41	0.71500	5.500	7.692	71	0.69800	6.167	8.835
12	0.69550	5.067	7.285	42	0.70150	5.400	7.698	72	0.69200	6.167	8.911
13	0.69400	5.233	7.541	43	0.69550	5.267	7.572	73	0.69800	6.133	8.787
14	0.70100	5.100	7.275	44	0.69700	5.167	7.413	74	0.70450	6.367	9.037
15	0.68450	5.033	7.353	45	0.70100	5.267	7.513	75	0.68400	6.000	8.772
16	0.69300	5.100	7.359	46	0.69150	5.100	7.375	76	0.69900	6.333	9.259
17	0.69750	5.133	7.360	47	0.70200	5.267	7.502	77	0.69900	6.200	8.870
18	0.69100	5.133	7.429	48	0.71400	5.267	7.376	78	0.69250	6.233	9.001
19	0.70800	5.200	7.345	49	0.70850	5.333	7.528	79	0.70100	6.033	8.607
20	0.69950	5.167	7.386	50	0.71900	5.367	7.464	80	0.69850	FTF	
21	0.72400	5.400	7.459	51	0.67150	5.833	8.687	81	0.71300	6.033	8.462
22	0.72200	5.367	7.433	52	0.67150	5.900	8.786	82	0.69850	6.100	8.733
23	0.71700	5.467	7.624	53	0.68950	FTF		83	0.68500	6.000	8.759
24	0.73100	5.467	7.478	54	0.71950	6.033	8.385	84	0.69450	6.100	8.783
25	0.73350	5.500	7.498	55	0.68750	5.933	8.630	85	0.70350	6.033	8.576
26	0.71350	5.133	7.195	56	0.69100	5.733	8.297	86	0.69200	5.767	8.333
27	0.72150	FAD (Camera issue)		57	0.70550	FTF		87	0.70050	5.933	8.470
28	0.73150	5.367	7.337	58	0.69350	5.900	8.508	88	0.68950	5.967	8.654
29	0.72350	5.167	7.141	59	0.68900	5.733	8.321	89	0.69900	5.867	8.393
30	0.72600	5.333	7.346	60	0.72000	6.033	8.380	90	0.70900	5.867	8.275
								Minimum	0.668	4.900	7.141
								Maximum	0.734	6.433	9.259
								Range	0.066	1.533	2.118
								Average	0.696	5.649	8.127
								Std Dev	0.016	0.459	0.708
								C/V			8.71

Table 15.4. *Consolidation height, burn time, and IBR data from testing of a delay mixture comprised of a 25:75 fuel to oxidizer ratio and 30:70 Al to Si ratio utilizing H-5 aluminum at 160 °F (71°C)*

Column	Height (in)	Burn time (s)	Inverse Burn Rate (s/in)
1	0.70350	4.802	6.826
2	0.70350	4.831	6.867
3	0.68750	4.738	6.892
4	0.68550	4.609	6.724
5	0.70200	4.729	6.736
6	0.70000	4.698	6.711
7	0.68400	Measure Fail	
8	0.68800	4.685	6.810
9	0.65250	4.662	7.145
10	0.72000	4.801	6.668
11	0.67750	4.620	6.819
12	0.68500	4.614	6.736
13	0.69500	4.670	6.719
14	0.69900	4.745	6.788
15	0.69950	4.832	6.908
16	0.72150	4.833	6.699
17	0.68650	Primer Blow-out	
18	0.67450	4.595	6.812
19	0.69200	4.659	6.733
20	0.67700	4.548	6.718
21	0.68850	4.515	6.558
22	0.68550	4.555	6.645
23	0.67400	4.386	6.507
24	0.69900	4.630	6.624
25	0.69550	4.751	6.831
26	0.69850	4.605	6.593
27	0.67000	4.425	6.604
28	0.68950	4.468	6.480
29	0.68900	4.598	6.673
30	0.67350	4.388	6.515
Minimum	0.653	4.386	6.480
Maximum	0.722	4.833	7.145
Range	0.069	0.447	0.665
Average	0.690	4.643	6.726
Std Dev	0.014	0.127	0.139
C/V			2.07

Table 15.5. *Consolidation height, burn time, and IBR data from testing of a delay mixture comprised of a 25:75 fuel to oxidizer ratio and 30:70 Al to Si ratio utilizing aluminum H-5 at 68 °F (20 °C).*

Column	Height (in)	Burn time (s)	Inverse Burn Rate (s/in)
1	0.59250	4.333	7.314
2	0.58800	4.667	7.937
3	0.60200	4.633	7.697
4	0.60400	Primer Blow-out	
5	0.61900	4.833	7.808
6	0.61000	4.533	7.432
7	0.59100	4.433	7.501
8	0.58800	4.367	7.426
9	0.59450	4.400	7.401
10	0.59850	4.400	7.352
Minimum	0.588	4.333	7.314
Maximum	0.619	4.833	7.937
Range	0.031	0.500	0.623
Average	0.599	4.511	7.541
Std Dev	0.010	0.159	0.207
C/V			2.75

This delay formulation proved to be unreliable and further testing was conducted on a formulation with increased aluminum content to decrease variance and increase combustion propagation sustainability.

Testing of a delay formulation containing 25:75 by weight fuel to oxidizer ratio and 32.5:67.5 by weight H-5 aluminum to silicon ratio was conducted. This adjustment to the formulation adds 0.4 g of Al to the overall 75 g mixture in an effort to eliminate failures, decrease the burn time variance at different testing temperatures, and maintain acceptable fuze consolidation height (see Table 15.6 through Table 15.8)

Table 15.6. *Consolidation height, burn time, and IBR data from testing of a delay mixture comprised of a 25:75 fuel to oxidizer and 32.5:67.5 Al to Si. Tested at -65 °F (-54 °C). Fuze number 1 functioned as designed, an error with test equipment set-up occurred.*

Column	Height (in)	Burn time (s)	Inverse Burn Rate (s/in)
1	0.81150	FAD	
2	0.84650	6.203	7.328
3	0.81800	5.922	7.240
4	0.83200	5.978	7.185
5	0.82350	6.034	7.327
6	0.83050	5.959	7.175
7	0.82300	6.175	7.503
8	0.85650	6.662	7.778
9	0.92000	5.884	6.396
10	0.81900	5.978	7.299
Minimum	0.812	5.884	6.396
Maximum	0.920	6.662	7.778
Range	0.109	0.778	1.383
Average	0.838	6.088	7.248
Std Dev	0.030	0.227	0.349
C/V			4.82

Table 15.7. *Consolidation height, burn time, and IBR data from testing of a delay mixture comprised of a 25:75 fuel to oxidizer ratio and 32.5:67.5 Al to Si ratio utilizing H-5 aluminum at 68 °F (20 °C)*

Column	Height (in)	Burn time (s)	Inverse Burn Rate (s/in)
1	0.71100	4.952	6.965
2	0.69450	4.859	6.996
3	0.69800	4.888	7.003
4	0.69000	4.856	7.038
5	0.70000	4.890	6.986
6	0.72350	5.102	7.052
7	0.69600	4.904	7.046
8	0.70000	4.890	6.986
9	0.68700	4.891	7.119
10	0.69000	4.886	7.081
Minimum	0.687	4.856	6.965
Maximum	0.724	5.102	7.119
Range	0.037	0.246	0.155
Average	0.699	4.912	7.027
Std Dev	0.010	0.068	0.046
C/V			0.66

Table 15.8. *Consolidation height, burn time, and IBR data from testing of a delay mixture comprised of 25:75 fuel to oxidizer ratio and 32.5:67.5 Al to Si ratio utilizing H-5 aluminum at 68 °F (20 °C).*

Column	Height (in)	Burn time (s)	Inverse Burn Rate (s/in) at 22 °C	Column	Height (in)	Burn time (s)	Inverse Burn Rate (s/in)
1	0.60300	4.735	7.852	31	0.59350	4.660	7.852
2	0.60100	4.745	7.895	32	0.58600	4.701	8.022
3	0.61150	4.836	7.908	33	0.61300	4.908	8.007
4	0.59500	4.798	8.064	34	0.60750	4.829	7.949
5	0.62800	4.954	7.889	35	0.61050	4.723	7.736
6	0.61400	4.812	7.837	36	0.59900	4.708	7.860
7	0.58100	4.589	7.898	37	0.58950	4.766	8.085
8	0.60700	4.795	7.900	38	0.60400	4.752	7.868
9	0.60950	4.915	8.064	39	0.61050	4.835	7.920
10	0.60100	4.787	7.965	40	0.60950	4.779	7.841
11	0.60600	4.794	7.911	41	0.60250	4.864	8.073
12	0.59200	4.850	8.193	42	0.60500	4.739	7.833
13	0.60650	4.776	7.875	43	0.58800	4.775	8.121
14	0.60300	4.874	8.083	44	0.60200	4.756	7.900
15	0.58550	4.576	7.816	45	0.59900	4.811	8.032
16	0.61800	4.938	7.990	46	0.61600	4.787	7.771
17	0.60850	4.808	7.901	47	0.60450	4.726	7.818
18	0.60300	4.860	8.060	48	0.59900	4.756	7.940
19	0.60500	4.899	8.098	49	0.59700	4.792	8.027
20	0.60300	4.815	7.985	50	0.60250	4.664	7.741
21	0.62000	4.863	7.844	51	0.59950	4.819	8.038
22	0.62250	4.815	7.735	52	0.61650	4.870	7.899
23	0.60700	4.758	7.839	53	0.60250	4.811	7.985
24	0.61700	4.925	7.982	54	0.59550	5.238	8.796
25	0.62500	4.851	7.762	55	0.58450	4.696	8.034
26	0.61850	4.860	7.858	56	0.59750	4.703	7.871
27	0.60800	4.801	7.896	57	0.60700	4.958	8.168
28	0.59650	4.757	7.975	58	0.60800	4.832	7.947
29	0.60400	4.840	8.013	59	0.60000	4.756	7.927
30	0.60000	4.730	7.883	60	0.58500	4.709	8.050
				Minimum	0.581	4.576	7.735
				Maximum	0.628	5.238	8.796
				Range	0.047	0.662	1.061
				Average	0.604	4.801	7.951
				Std Dev	0.010	0.097	0.153
				C/V			1.92

Using the optimized delay formulation, fuzes were consolidated to 0.63 ± 0.01 inch. Table 15.9 and Table 15.12 illustrate that fuzes tested in hot and ambient temperatures were within specifications. However; from the fuzes tested in cold temperature, seven samples were above the 5.5 second burn time limit (see Table 15.10 and Table 15.11). Table 15.13 and Table 15.14 show that when the fuze height was adjusted to 0.61 ± 0.05, all samples were within the specified burn time range.

Table 15.9. *Consolidation height (in), burn time (s), and inverse burn rate (s*in^{-1}) for M213/M228 fuze reliability testing. Samples were soaked at 68 °F (20 °C).*

Column	Height (in)	Burn time (s)	Inverse Burn Rate (s/in)
1	0.63000	4.743	7.529
2	0.62500	4.842	7.747
3	0.62450	4.924	7.885
4	0.62500	4.751	7.602
5	0.62400	4.643	7.441
6	0.63150	4.836	7.658
7	0.63950	4.950	7.740
8	0.63400	4.802	7.574
9	0.62800	4.812	7.662
10	0.63400	4.771	7.525
Minimum	0.624	4.643	7.441
Maximum	0.640	4.950	7.885
Range	0.016	0.307	0.444
Average	0.630	4.807	7.636
Std Dev	0.005	0.085	0.124
C/V			1.62

Table 15.10. *Consolidation height (in), burn time (s), and inverse burn rate (s*in^{-1}) for M213/M228 fuze reliability testing. Samples were soaked at -60 °F (-54 °C).*

Column	Height (in)	Burn time (s)	Inverse Burn Rate (s/in)
11	0.63150	5.388	8.532
12	0.63250	5.283	8.353
13	0.62900	5.590	8.887
14	0.63100	5.347	8.474
15	0.63950	5.363	8.386
16	0.63450	5.724	9.021
17	0.63000	5.535	8.786
18	0.63950	5.699	8.912
19	0.63400	5.431	8.566
20	0.63800	5.517	8.647
Minimum	0.629	5.283	8.353
Maximum	0.640	5.724	9.021
Range	0.011	0.441	0.669
Average	0.634	5.488	8.656
Std Dev	0.004	0.143	0.221
C/V			2.56

Table 15.11. *Consolidation height (in), burn time (s), and inverse burn rate (s*in^{-1}) for M213/M228 fuze reliability testing. Samples were soaked at -60 °F (-54 °C) set 2.*

Column	Height (in)	Burn time (s)	Inverse Burn Rate (s/in)
21	0.63100	5.359	8.493
22	0.63500	5.534	8.715
23	0.62800	5.304	8.446
24	0.62750	5.414	8.628
25	0.62900	5.436	8.642
26	0.63350	5.367	8.472
27	0.63600	5.505	8.656
28	0.63000	5.323	8.449
29	0.62800	5.421	8.632
30	0.62450	5.413	8.668
Minimum	0.625	5.304	8.446
Maximum	0.636	5.534	8.715
Range	0.012	0.230	0.269
Average	0.630	5.408	8.580
Std Dev	0.003	0.070	0.097
C/V			1.14

Table 15.12. *Consolidation height (in), burn time (s), and inverse burn rate (s*in^{-1}) for M213/M228 fuze reliability testing. Samples were soaked at 160 °F (71 °C).*

Column	Height (in)	Burn time (s)	Inverse Burn Rate (s/in)
31	0.62600	4.454	7.115
32	0.63500	4.467	7.035
33	0.63050	4.494	7.128
34	0.62650	4.470	7.135
35	0.63050	4.453	7.063
36	0.63400	4.415	6.964
37	0.63150	4.451	7.048
38	0.63200	4.438	7.022
39	0.63050	4.460	7.074
40	0.62900	4.440	7.059
Minimum	0.626	4.415	6.964
Maximum	0.635	4.494	7.135
Range	0.009	0.079	0.171
Average	0.631	4.454	7.064
Std Dev	0.003	0.020	0.050
C/V			0.70

Table 15.13. *Consolidation height (in), burn time (s), and inverse burn rate (s*in^{-1}) for M213/M228 fuze reliability testing. Samples were consolidated to 0.61 inch and soaked at 160 °F (71 °C).*

Column	Height (in)	Burn time (s)	Inverse Burn Rate (s/in)
41	0.61350	4.405	7.180
42	0.60900	4.405	7.233
43	0.61400	4.386	7.143
44	0.60800	4.345	7.146
45	0.60950	4.381	7.188
Minimum	0.608	4.345	7.143
Maximum	0.614	4.405	7.233
Range	0.006	0.060	0.090
Average	0.611	4.384	7.178
Std Dev	0.002	0.022	0.033
C/V			0.46

Table 15.14. *Consolidation height (in), burn time (s), and inverse burn rate (s*in^{-1}) for M213/M228 fuze reliability testing. Samples were consolidated to 0.61 inch and soaked at -60 °F (-54 °C).*

Column	Height (in)	Burn time (s)	Inverse Burn Rate (s/in)
46	0.60800	5.270	8.668
47	0.61050	5.282	8.652
48	0.61200	5.292	8.647
49	0.60900	5.491	9.016
50	0.61650	5.354	8.685
Minimum	0.608	5.270	8.647
Maximum	0.617	5.491	9.016
Range	0.009	0.221	0.369
Average	0.611	5.338	8.734
Std Dev	0.003	0.082	0.142
C/V			1.63

15.4. EBA&D M213/M228 Characterization

For completion of Tasks 13, Manufacturing and Testing of Sixty Fully Assembled M228 and M213 Delay Elements at -65 °F, 70 °F, and 160 °F, EBA&D altered the SAT for the characterization of the developed environmentally benign fuze assemblies. Key features of the SAT include:

- Remote operation;
- Convenient and quick fuze testing;
- Emulate the percussion of real grenades at the primer;
- Ability to test multiple fuze designs (M201A1, M213/M228).

The device was equipped with an accelerometer that detects the impact of the firing pin on the primer. The photo diode was utilized to measure the fuzes output light signal to determine the combustion time of the fuze. The signals were fed directly to an oscilloscope where they were

saved and analyzed. A photograph of the sub-assembly test fixture is presented in Figure 15.22. The procedure for the testing of the fuze assemblies, within the SAT, is as follows:

1. Ensure the accelerometer and photo diode are hooked up and functioning properly;
2. Place the selected fuze assembly in test block;
3. Install the sleeve assembly with firing pin;
4. Place the drop tube on top of the sleeve assembly and insert both the primary and secondary pins;
5. Insert the ball in the drop tube, remove the secondary pin, and close the blast chamber;
6. Set the scope to record and pull the primary pin;
7. Analyze the data from the accelerometers and determine the burn time;
8. Repeat the steps above for each test that must be conducted.

If the device does not fire, the fixture is not opened for a minimum of 5 min to ensure the safety of the operator. If the fuze is temperature conditioned it must be fired within 70 s after being removed from the conditioning chamber.

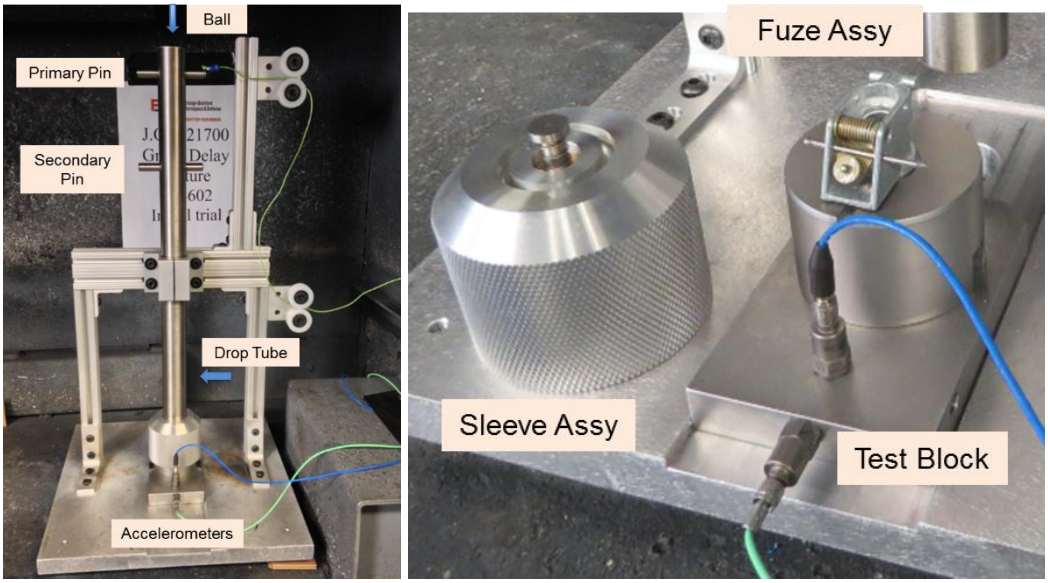

Figure 15.22. *Photographs of the M201A1 SAT fixture built at EBA&D.*

IMP has a well-established expertise in the field of processing and development of lead-free primers and found it to be of value added to the development of the completely environmentally benign fuze systems. With the main goal of replacing perchlorates and hexavalent chromates the added value is to also eliminate the legacy lead-based primer with a lead-free alternative.

The primers that were tested in this effort were:

- Legacy Olin M42 primers currently used in M213/M228 fuzes;
- MIC M42 primers currently in development at IMP, a nanothermite based lead free primer;
- DBX-1 M42 primers, also in development at IMP, a DBX-1 based lead-free primer.

MIC and DBX-1 M42 primers were used in deliverable manufacturing of M213/M228 fuzes tested at EBA&D.

- 105 M213/M228 fuzes using formulation IMP-B050818-V2 were tested utilizing MIC M42 primers
  - 35 were characterized at -65 °F (-54 °C)
  - 35 were characterized at 160 °F (71 °C)
  - 35 were characterized at 68 °F (20 °C)
- 5 M213/M228 fuzes were tested utilizing DBX-1 M42 primers with an M67 booster characterized at 68 °F (20 °C).

The DBX-1 based C70 detonator is being developed in a current partnership effort with ARDEC, EBA&D, and IMP. This testing was conducted to demonstrate function of a complete environmentally benign fuze system for a grenade application. The testing was done simultaneously with Task 13 Manufacturing and testing of sixty fully assembled M228 and M213 delay elements at -65 °F, 70 °F and 160 °F at EBA&Ds energetics testing lab.

15.5. M213/M228 fuze testing at EBA&D

M213/M228 fuze testing conducted at EBA&D was witnessed by Matt Puszynski and Dan Perkins. The following tests were conducted for Task 13 evaluation.

- 35 IMP MIC environmentally benign delay fuzes tested at 160 °F (71 °C);
- 35 IMP MIC environmentally benign delay fuzes tested at 68 °F (20 °C);
- 35 IMP MIC environmentally benign delay fuzes tested at -65 °F (54 °C);
- 35 Chemring current production legacy fuzes tested at 160 °F (71 °C);
- 35 Chemring current production legacy fuzes tested at 68 °F (20 °C);
- 35 Chemring current production legacy fuzes tested at -65 °F (54 °C);

Results from EBA&D's thermal conditioning testing of Chemring M213/M228 fuzes are shown in Figure 15.23. Results from the IMP produced environmentally benign M213/M228 fuzes are shown in Figure 15.24. Complete data from the M213/M228 testing at EBA&D is included in Appendix C.

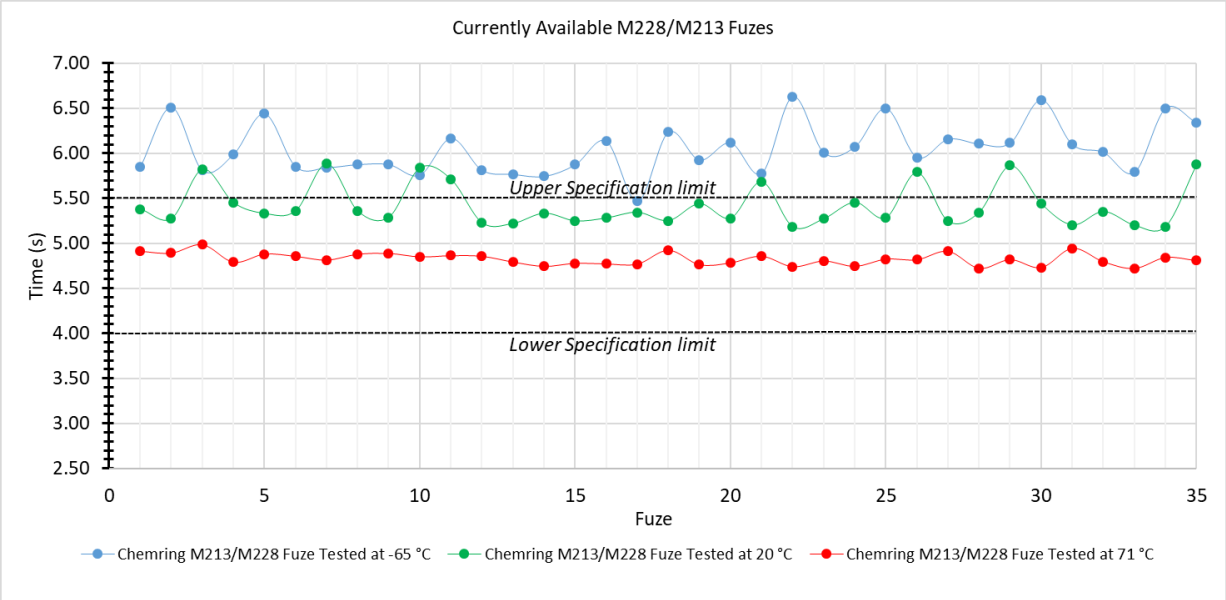

Figure 15.23. *Results from EBA&D testing of M213/M228 fuzes currently produced for DoD M67 Grenades. Upper limit burn time is 5.5 s and lower limit burn time is 4 s.*

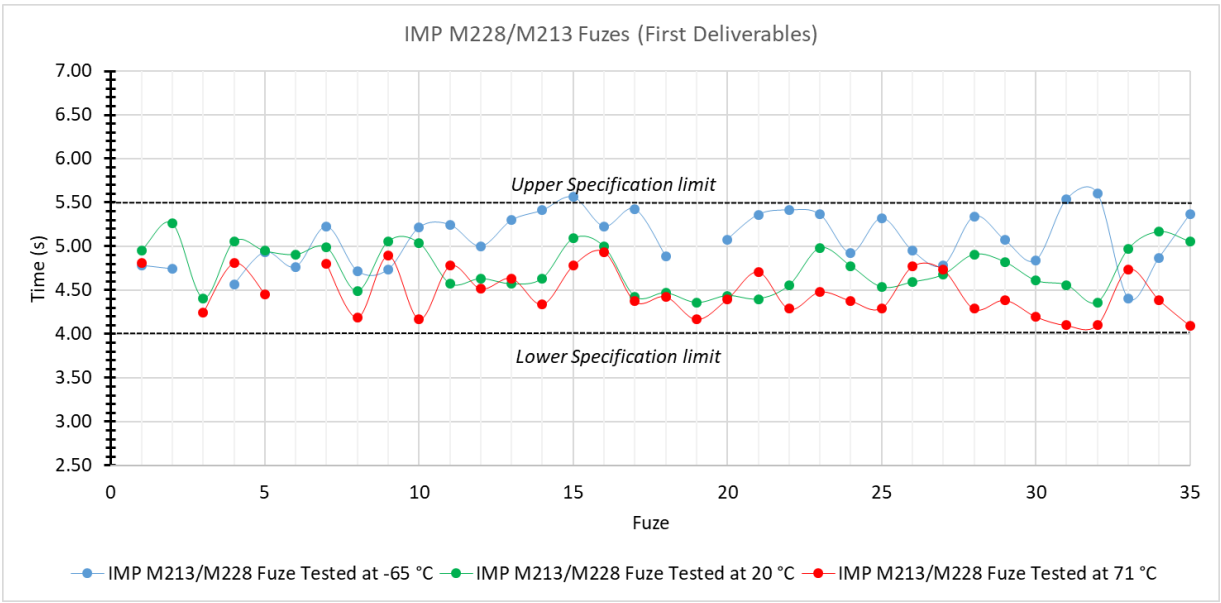

Figure 15.24. *Results from EBA&D testing of IMP developed environmentally benign M213/M228 fuzes. Upper limit burn time is 5.5 s and lower limit burn time is 4 s.*

During the testing, fuzes 72 and 76 failed to function at 160 °F (71 °C). X-ray analysis revealed the M42 primer failed to function leaving the A-1A charge undisturbed. Off center hits of the primer firing pin were observed on both misfired samples. The fuzes were re-fired using an anvil and spring instead of the SAT ball drop method of ignition. The anvil and spring caused one of the fuzes to function as designed, but the other did not. It can be inferred that the primer ignition device was responsible for the primer misfires and not the primer itself. Fuzes 3 and 19 failed at -65 °F (-54 °C) (see Figure 15.25). These fuzes primer and transition charge functioned properly, but the delay composition quenched at the interface between the first and second pressing interval.

IMP addressed these issues responsible for the fuze failures during subsequent no-cost extension reporting period.

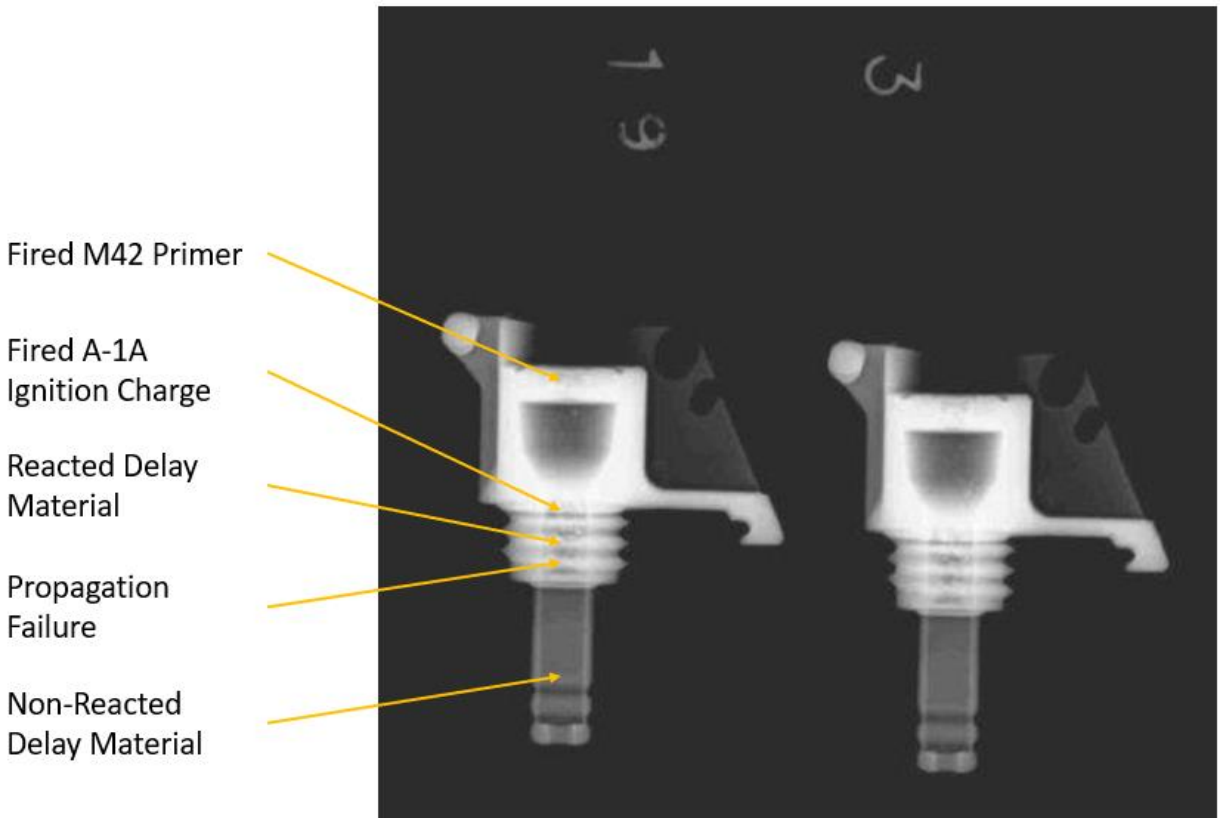

Figure 15.25. *Failure analysis using x-ray, courtesy of EBA&D. X-ray identified the M42 primer functioned and ignited the A-1A transition charge thereby igniting the delay material of both fuzes 3 and 19. The x-ray also identifies the location the propagation front failed.*

15.6. No Cost Extension R&D due to demonstration failure

Because of the failures demonstrated in the deliverable testing at EBA&D a 1-year No-Cost Extension to this SERDP project was proposed and approved. The deliverable quantity was increased to 150 fuzes, tested at IMP R&D Lab. The fuzes would be tested with zero failures and thermally conditioned 50 fuzes tested at -65, 70, and 160 °F.

The resulting extension provided time to investigate the entire M213/M228 delay mixing process. Specifically, the mixing fluid was investigated. This investigation discovered that the solubility of $SrMoO_4$ in water was enough that it was causing issues within the mixing process. To mitigate this the use of Isopropanol Alcohol (IPA) was substituted for water. The resulting mixture demonstrated an improvement in the sieving process. The sieve size was reduced from #40 (425 µm) to a #80 (180 µm). The finer particles provided an improvement in packing density and consistent density throughout the layer during consolidation.

The mixing process itself was investigated back to the initial steps. It was found that the pre-blending of the constituents in a particular order was vital to the final mixture success. This process

includes weighing the constituents and combining Al, Si, $SrMoO_4$, and DE. The key process is, prior to adding the fuel/oxidizer blend, the IPA and SiO_2 be blended to form a paste. Once the SiO_2 paste is formed the fuels, oxidizer, and DE are then combined until all are wetted. This process substantially improved the accuracy of the burn rate.

To ensure the A-1A did not separate from the delay material during ignition transfer to the delay, especially in cold testing, the loading procedure was perfected. It was found the matrix developed during consolidation of the last increment of delay powder and ignitor material was substantial enough to hold the different density powders together during the ignition event.

An investigation into the importance of solids loading in the slurry during mixing was also conducted. It was discovered that if the solids loading was too low the slurry demonstrated stratification. Through visual inspection of the delay material this can be observed that the finer particles of Si were floating on top of the slurry. This observation was also translated into the burn rate. The lower solids loading demonstrated a half second faster burn rate in open columns. This was substantially reduced or eliminated by increasing the solids loading to 75%.

Also developed to substantially improve the overall M213/M228 process was a funnel. These funnels were designed to expand the loading void so that the fuzes could accept a taller consolidation height (see Figure 15.26). The problem presented itself as; when loading loose powder, it would protrude above the stem where the delay resides. This made consolidation of the delay difficult and limited the A-1A installation to after the delay was consolidated. The increased volume of the stem provided the room for mire delay material which allowed for an increase in aluminum concentration in the delay formulation. The aluminum content is key to the stability of the burn front of the self-sustaining propagation of the delay. It also provided the opportunity to consolidate the A-1A with the last increment of delay material creating a matrix of delay and ignition material.

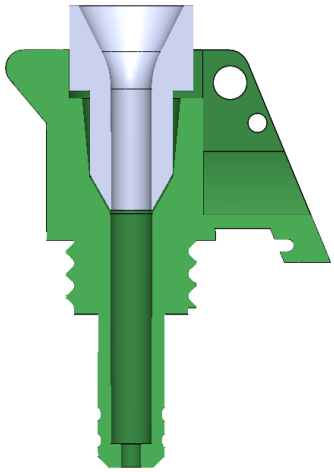

Figure 15.26. *SolidWorks rendering of funnel used for delay consolidation installed on M213/M228 fuze.*

The results of the deliverable delays far exceeded expectations. There were more than 200 fuzes built including confidence testing. There were zero failures for all fuzes tested with this delay and

improved manufacturing method. (see Figure 15.27). Notice all fuzes functioned within the specified burn time requirements of 4 to 5.5 s. This is in contrast to the currently produced M213/M228 fuzes which demonstrated only hot temperature conditioned fuzes remained within the specification limits previously presented. The data analysis from the second round of deliverable M213/M228 testing is presented in Tables 15.15 to 15.17, for the three conditioning temperatures. The complete data from the testing is included in Appendix D.

Table 15.15. *IMP deliverable M213/M228 fuze statistics from testing at -65 °F from a sample set of 50 fuzes.*

Consolidation stats		Burn Time Stats		IBR Stats	
Min	0.843	**Min**	4.810	**Min**	5.446
Max	0.923	**Max**	5.260	**Max**	5.806
Range	0.080	**Range**	0.450	**Range**	0.360
Avg	0.894	**Avg**	5.054	**Avg**	5.651
Std Dev	0.018	**Std Dev**	0.115	**Std Dev**	0.075
		CV%	2.271	**CV%**	1.333

Table 15.16. *IMP deliverable M213/M228 fuze statistics from testing at 70 °F from a sample set of 50 fuzes.*

Consolidation stats		Burn Time Stats		IBR Stats	
Min	0.862	**Min**	4.279	**Min**	4.768
Max	0.923	**Max**	4.770	**Max**	5.334
Range	0.062	**Range**	0.491	**Range**	0.566
Avg	0.904	**Avg**	4.589	**Avg**	5.079
Std Dev	0.013	**Std Dev**	0.123	**Std Dev**	0.113
		CV%	2.674	**CV%**	2.227

Table 15.17. *IMP deliverable M213/M228 fuze statistics from testing at 160 °F from a sample set of 50 fuzes.*

Consolidation stats		Burn Time Stats		IBR Stats	
Min	0.872	**Min**	4.238	**Min**	4.711
Max	0.923	**Max**	4.525	**Max**	4.958
Range	0.051	**Range**	0.287	**Range**	0.247
Avg	0.901	**Avg**	4.368	**Avg**	4.846
Std Dev	0.010	**Std Dev**	0.067	**Std Dev**	0.056
		CV%	1.535	**CV%**	1.155

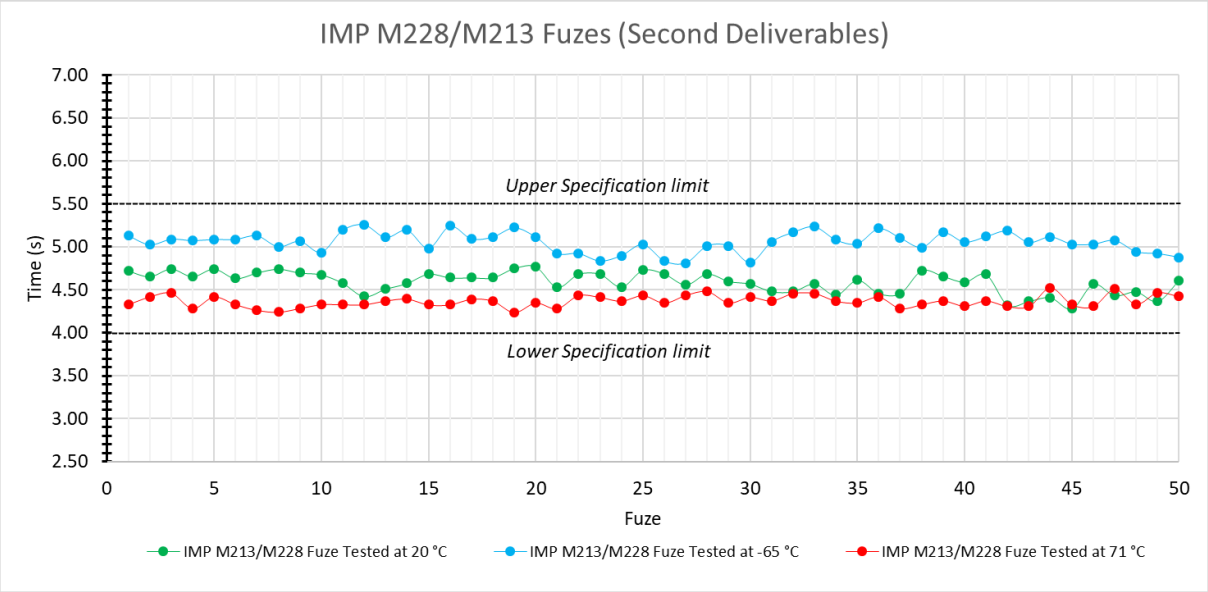

Figure 15.27. *Graph of data from testing of M213/M228 fuzes. 50 fuzes tested at -65 °F, 70 °F, and 160 °F. Upper limit burn time is 5.5 s and lower limit burn time is 4 s.*

15.7. SERDP Value added Research and Development

In addition to M213/M228 fuze testing, a fully environmentally benign fuze proof-of-concept was alsodemonstrated. These fuzes consisted of the following components:

- DBX-1 based C70 detonators was tested for the first time ever. Three out of five of the assemblies fired without defect. The two misfired fuzes were analyzed with x-ray and it was determined that the same root cause was responsible for the failure to function as observed in cold for fuzes 3 and 19 previously reported earlier in this section.
- Lead-free M42 primers proved, using both MIC based and DBX-1 based formulations which are both lead-free and demonstrated exceptional viability.
- Chromium (IV) free environmentally benign delay formulation.

This testing provided the first ever fully environmentally benign firing train of the M67 grenade.

Results and Discussion

During the course of this SERDP funded project many accomplishments were made. The strategic mission of the SERDP program to reduce the impact of DoD energetics effect on the environment has been met in all aspects of this project. Pyrotechnic delay formulations and primer constituents currently used are environmentally hazardous due to the presence of potassium perchlorate, barium chromate (containing hexavalent chromium), and/or lead compounds. The most hazardous compound used in the currently used pyrotechnic delay is chromium (VI). The National Institute for Occupational Safety and Health considers all chromium (VI) compounds to be occupational carcinogens and Occupational Safety and Health Administration has established a permissible exposure level of 0.5 µg/m^3, [3] which is 100 times less than lead which is 50 µg/m^3 [4]. Based on this data, the replacement of the chromium (VI) based delay formulation is important to sustainability of the material for the DoD.

Leveraging parallel R&D efforts in the removal of environmentally hazardous energetic compounds, IMP has merged its expertise in primer development with fuze development. This has infused an entirely new level of 'green initiative' into this project that wasn't conceived until year 2 of the effort. This development laid the foundation for the use of the following components of the investigated fuzes integrated into this SERDP program:

- Lead-free primers (DBX-1 and MIC based primers) in M213/M228 fuzes;
- Perchlorate-free M201A1 output charge (MIC);
- Lead azide and lead styphnate-free C70 detonators (DBX-1 based booster charge).

IMP found the benefits not only in the environmental aspects of the project but in the overall precision, accuracy, and reliability of the entire fuze system.

The integral elements of the overall project and key R&D results obtained in the individual tasks are described below:

Task 1

The microcalorimeter output data shown in Figure.16.1 confirms long term chemical compatibility of the proposed environmentally acceptable delay formulation. This figure shows that any reactions/interactions for key individual reactants and the entire formulation are decreasing in rate. In addition, these tests indicate that any reactions that may occur are not accelerating with time at increased temperature. The compatibility criterion was also calculated in accordance with STANAG 4147 Test 2 – The Heat Flow Calorimetry Test. This calculation also shows no compatibility issues. According to STANAG 4147 the material is considered compatible (D=0.69 which is significantly less than critical parameter D_{cr}=2).

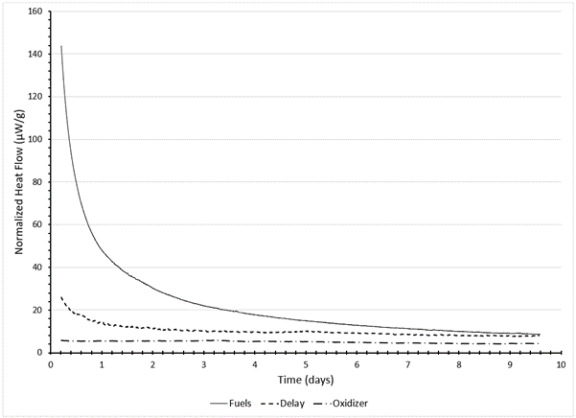

Figure.16.1. *Microcalorimeter report from delay composition compatibility analysis.*

Task 2

Figure 16.2 shows the effect of fuel to oxidizer ratio, at the constant ratio of aluminum-to-silicon in the binary fuel (30:70 by weight), on IBR. These measurements were conducted in an open column configuration and each point indicates the average IBR of ten open delay column tests. As can be observed in this graph, the IBR can be varied at 70 °F from approximately 3.5 to 11 s/in. The IBR at -65 °F and 160 °F are consistently lower and higher, respectively.

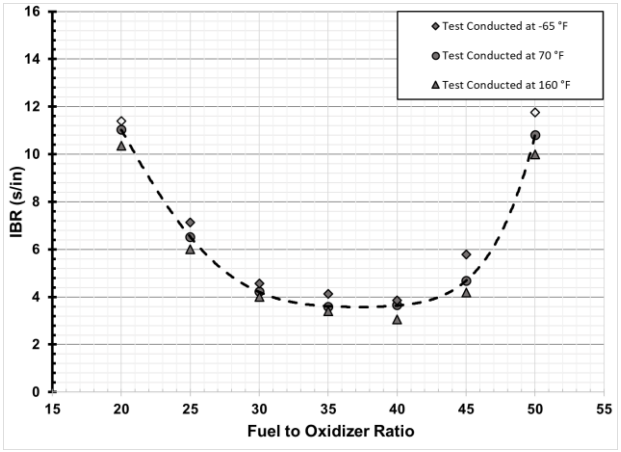

Figure 16.2. *IBR as a function of fuel-to-oxidizer ratio at constant concentration of aluminum in the binary fuel (Al(H-2)/Si=30/70 by weight). Each point indicates the average IBR of ten open delay column tests. Note: Data shown with an empty point failed to maintain combustion propagation.*

The results indicate a wide range of tunability for this particular formulation.

Task 3

During the course of the project it was determined that IPA gives slightly better and more consistent results than water as a processing liquid. This might be caused by elimination of a slight solubility of strontium molybdate in water and the subsequent formation of "harder" agglomerates after drying. In general, processing using IPA is similar to water processing:

1. Program the control software to mix the materials using the following procedure: 2 minutes at 50 g acceleration force, and 20 min at 75 g acceleration force;

2. Weigh out the required constituents and add the powders to the Resodyn LabRAM mixing container;
3. Add the required amount of IPA to the Resodyn LabRAM mixing container to achieve 75% solids loading concentration;
4. Secure the mixing container in the Resodyn LabRAM and start cooling water < 50 °F (10 °C);
5. Start pre-dispersing step at set-point of 50 g acceleration force for 2 min;
6. Ramp-up set-point to 75 g acceleration force for 20 min;

The drying procedure for the formation of the composite powder used for powder loading is as follows:

1. Pour the mixture onto a tray coated with a conductive Teflon sheet and spread it as thin as possible to facilitate drying;
2. Dry the delay mixture in a convection air dryer for 5-10 minutes under ambient conditions;
3. Sieve the delay mixture using a US #200 (70 µm) sieve;
4. Dry the delay mixture in a convection oven at 140 °F (60 °C) for 16 hours;
5. Place delay mixture in desiccator to cool;

Task 4

The sub-assembly test fixture, designed and fabricated by EBA&D, was used for the characterization of the M201A1 fuze assemblies. The SAT fixture was characterized through the ignition of ten commercial M201A1 delay columns purchased from AMTEC. The data collected from the SAT fixture, for both the commercial M201A1 and the environmentally benign M201A1 fuze assemblies, is presented in Figure 16.3.

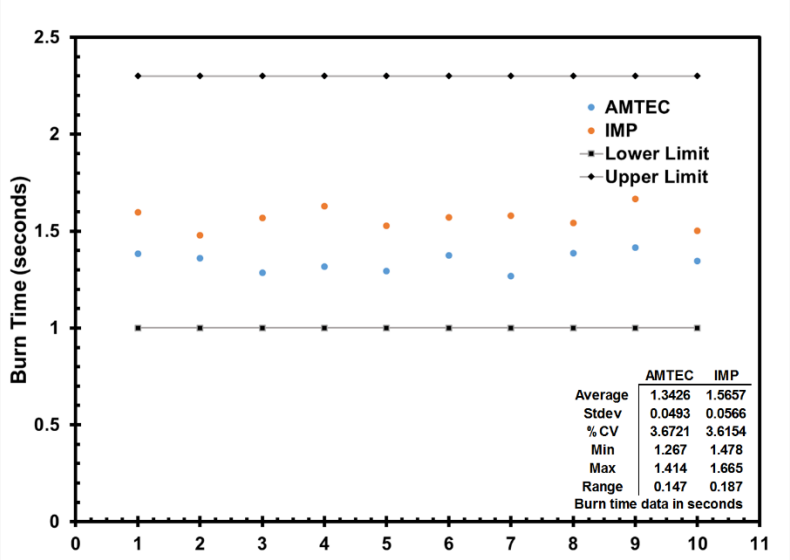

Figure 16.3. *Measured burn time results for commercially available M201A1 delay columns tested in the sub-assembly test fixture.*

Task 6

The average thermal conductivities for the samples before and after combustion was determined to be 0.42 W/m·K and 0.28 W/m·K, respectively. The entire temperature dynamic profile was used to determine the pre-exponential coefficient, k_0 and activation energy, E, using the Boddington method, which is the very reliable method of kinetic constants determination in exothermic systems, with higher ignition temperatures. In this case, the DSC method was tried but was not suitable due to high temperature limit of instrument (1,500^{o}C maximum). The values of E and ko were determined at 159.7 kJ/mol and 4.109•105 s-1, respectively. These values were used in 2D modeling studies to analyze combustion characteristics in actual hardware assembly.

Task 7

The collected data from the testing shows that the environmentally benign delay formulation had a lower burn time range and better consistency than the current commercial M201A1 fuzes (see Figure 16.4) and it was in line with the Lot Acceptance Testing (LAT) data from the DoD. The testing of the M201A1 fuzes has met the requirements for the completion of project Task 7 ahead of the planned schedule.

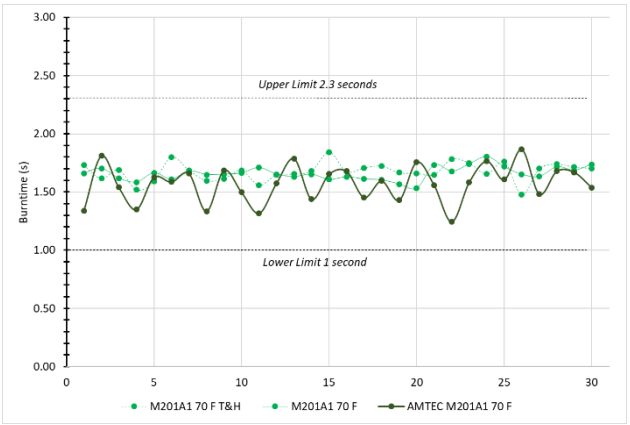

(a)

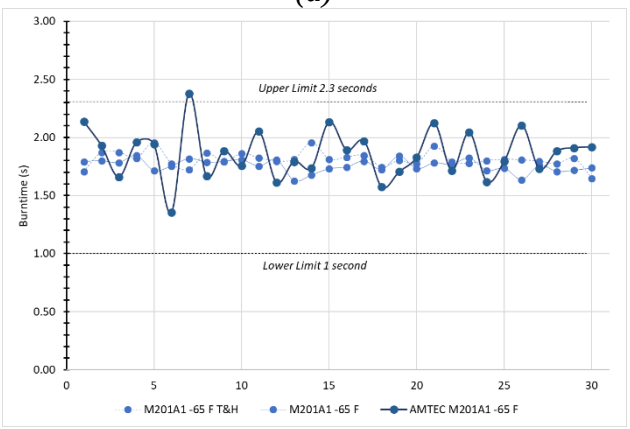

(b)

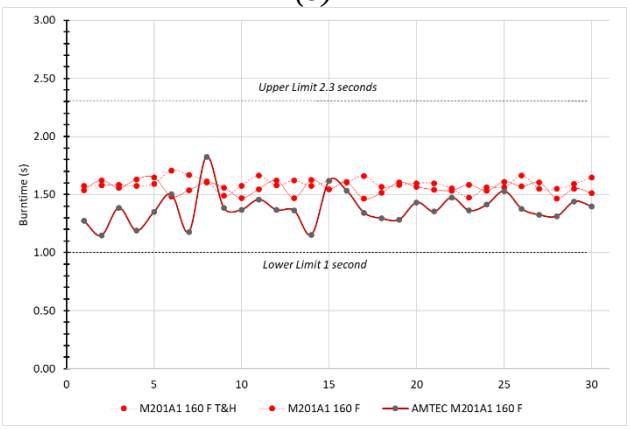

(c)

Figure 16.4. *Illustration of test results versus commercially available M201A1 Delay Fuzes. (a) 70 °F, (b) -65 °F, (c) 160 °F.*

Task 8

It has been concluded that using MIC material with 10 wt% of HMX as a pressure generator additive provided suitable performance to be used as an output charge for the M201A1 fuze (see Figure 16.5).

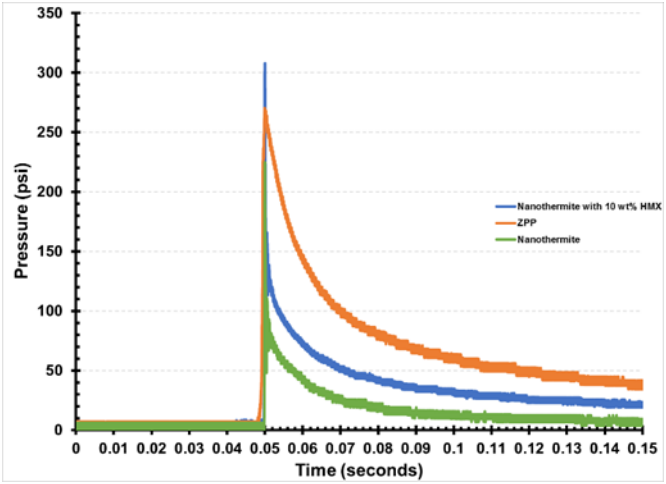

Figure 16.5. *Dynamic pressure curves for 60 mg of nanothermite with 10 wt% HMX, ZPP, and pure nanothermite ignited in a 15 cc closed bomb.*

Task 9

In this particular mathematical analysis, a 2-D model was selected due to a system symmetry (see Figure 16.6). Based on these results it was deduced that the overall molar reaction, for Al concentration in the binary fuel Al/Si=30/70 by weight and fuel to oxidizer ratio F/O=25/75 by weight, should read:

$$0.249Al + 0.55945Si + 0.272SrMoO_4 + 0.162SiO_2 =$$
$$0.272SrO + 0.38325SiO_2 + 0.125MoSi_2 + 0.1245Al_2O_3 + 0.0294Mo_5Si_3$$

The adiabatic combustion temperature for this reaction was conducted using HSC Chemistry software. The value of this adiabatic temperature is 2368 K, the activation energy, E, and the frequency factor, k_o, were determined using the Boddington method. The temperature profiles required for the evaluation were measured on larger pellets using W-W/Rh thermocouples. The determined values of E and k_o were 159.7 kJ/mol and $4.109 \cdot 10^5$ s^{-1}, respectively. Thermal conductivities of the reacting mixture before and after reaction were also determined experimentally and the average value of 0.65 W/m•K was used in modeling studies. Thermal conductivity was slightly adjusted to obtain comparable combustion front velocities with experimental data.

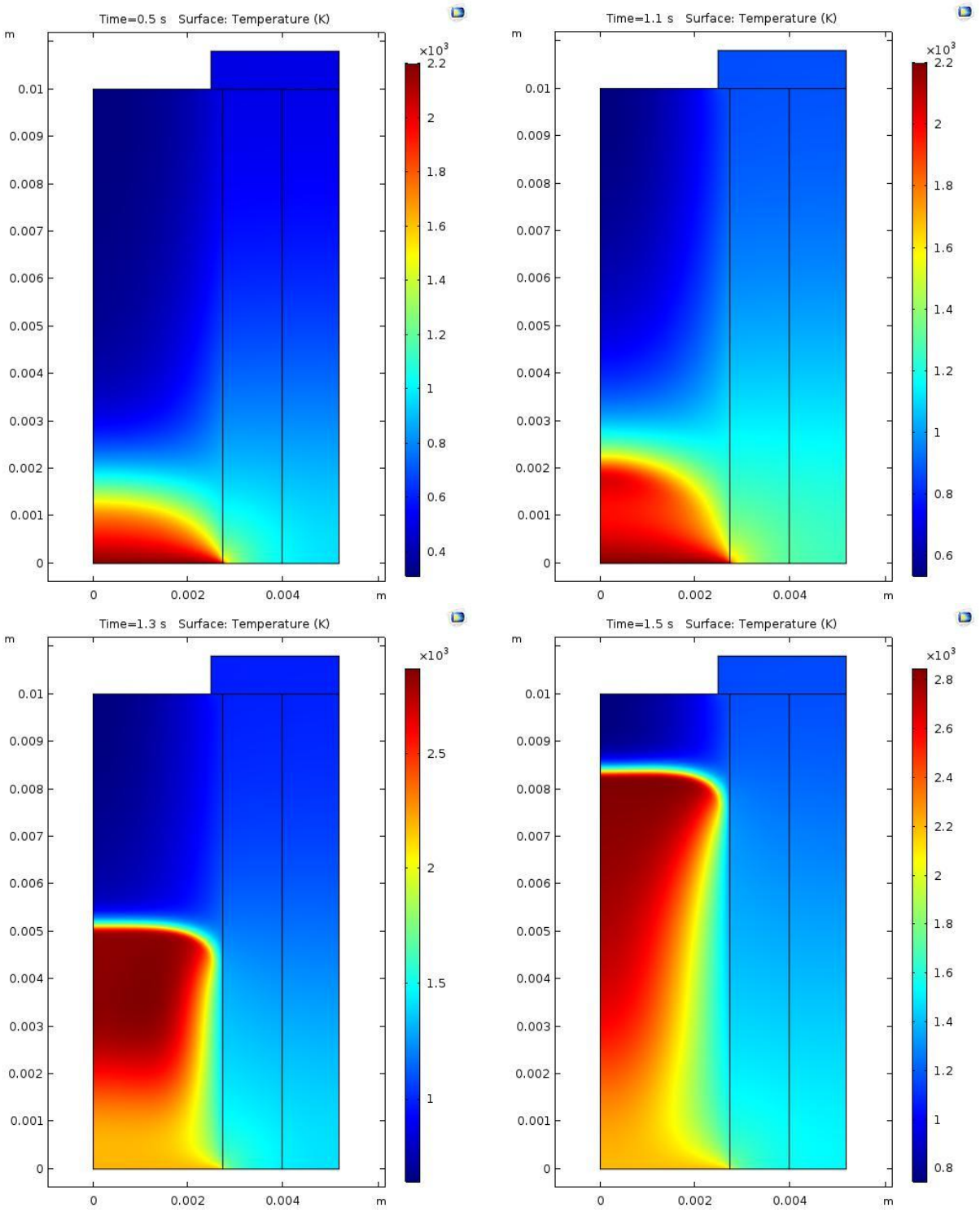

Figure 16.6. *2-D temperature profiles at 0.5 s, 1,1 s, 1.3 s, and 1.5 s. The schematic of the delay configuration is shown in Figure 12.34*

Mathematical modeling studies conducted using COMSOL software with a heat transfer module under both adiabatic and nonadiabatic conditions. The results of 1-D transient simulations at 70 ^{o}F are shown in Figure 16.7. The simulation was conducted with 60,000 nodes and the transient

temperature profiles indicate that this particular reaction propagates slightly in an oscillatory mode, which is typical for very exothermic reactions with higher activation energy[7]. Additional simulations conducted at -65 ^{o}F and 160 ^{o}F revealed that the combustion front propagates approximately 10% slower at lower temperature while the propagation is faster by approximately the same factor at higher temperature.

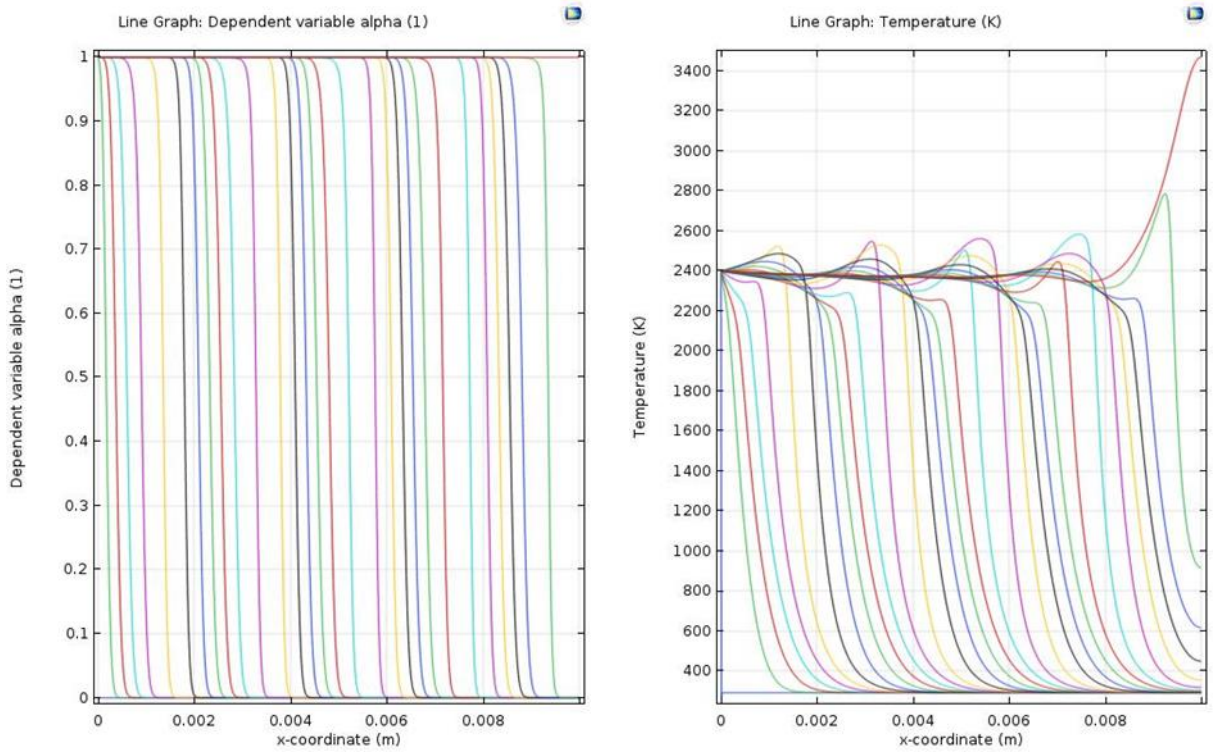

(a) (b)

Figure 16.7. *Simulated 1-D transient conversion (a) and temperature (b) profiles under adiabatic conditions. Conversion and temperature profiles are printed at intervals of 0.05 s*

Task 11

A scale-up assessment was conducted by Ensign Bickford Aerospace and Defense Company for the process developed by IMP. This document was submitted to SERDP as: Environmentally Benign Pyrotechnic Formulation: Development Process Scale-Up, and is included in Appendix E.

Task 12

The BAM Impact TOI for the delay composition was determined to be greater than 60 J (the maximum limit of equipment).

- The BAM Friction TOI for the delay composition was determined to be greater than 360 N (the maximum limit of equipment).
- The ESD TOI for the delay composition was determined to be greater than 250 mJ (the maximum limit of equipment).

The results of the characterization tests show the TOI for the environmentally benign delay composition is considered insensitive in accordance with UN "Recommendations on Transport of

Dangerous Goods - Manual of Tests and Criteria" for impact and friction, and in accordance with MIL-STD-1751 A for ESD.

Task 13

The results of the deliverable delay fuzes far exceeded expectations. There were more than 200 fuzes built including initial confidence testing. There were zero failures for all fuzes tested with this delay material and improved manufacturing method, (see Figure 16.8). Notice all fuzes functioned within the specified burn time requirements of 4 to 5.5 s. This is in contrast to the currently produced M213/M228 fuzes which demonstrated only hot temperature conditioned fuzes remained within the specification limits.

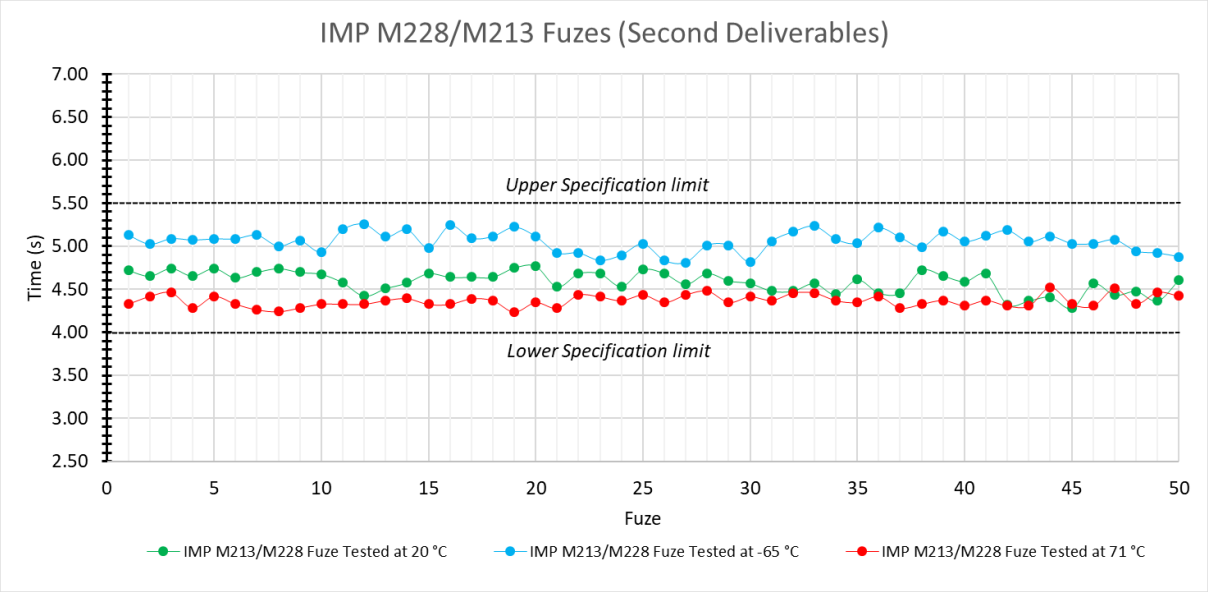

Figure 16.8. *Graph of deliverable M213/M228 Fuzes. 50 fuzes tested at -65 °F, 70 °F, and 160 °F. Upper limit burn time is 5.5 s and lower limit burn time is 4 s.*

Conclusions and Implications for Future Research/Implementation

Lead chromate, barium chromate, and potassium perchlorate are used as oxidizers in the pyrotechnic delay formulations currently utilized in the M201A1 and M213/M228 fuzes. Lead and chromate contamination within the ground water and soil is highly regulated by the EPA with levels set as low as 1-2 parts per billion in some states. The currently used fuze systems costs are mounting due to containment and clean up at commercial and DoD training ranges. The effect of these costs has an impact on DoD readiness as well as an impact on the environment. This project focused on the development of an environmentally benign pyrotechnic delay formulation that meets the environmental concerns. This research has provided a near drop-in replacement for legacy manufacturing of M201A1, M213, and M228 fuzes.

IMP has developed a new environmentally benign delay fuze system, as well as, demonstrated that the M201A1 and M213/M228 fuzes can be a functioned properly using this material. A novel mixing procedure for manufacturing of this material was developed as part of this work effort. The delay formulation was shown to be insensitive from impact, friction, and electrostatic discharge sensitivity standpoint. The constituents of the formulation have been determined to be compatible with each other using microcalorimetry. IMP has shown that the M42 primer along with the M201A1 and M213/M228 fuze, including the C70 detonator, can fully function with a compete removal of the toxic constituents currently used in these systems. Additionally, the US Army possesses a patent describing an adapter, in which the M39A1C primer can be replaced with an M42 primer. Due to limited application of the M39A1C primer the option of using a reliable M42 lead free primer is optimal and very desirable. IMP is confident that a lead-free option could be installed in the M39A1C primer to replace the lead thiocyanate-based formulation. This effort would remove all environmentally hazardous compounds from the M201A1 fuze system.

During initial testing of the M213/M228 fuzes at EBA&D, there were a few misfires observed. Changes to the processing of the delay material, loading improvements, and minor changes to the delay formulation have provided outstanding results. The environmentally benign delay demonstrated zero failures and 100% function within specified timing requirements. The currently produced fuze have shown to only produce 60% of fuzes to be within specified timing requirements, with zero failures, but not environmentally benign.

This R&D project has moved to the next level and matured into one current ESTCP project with Naval Surface Warfare Center - Indian Head and Naval Air Warfare Center - China Lake research facilities. Currently, this environmentally benign delay is being tuned to demonstrate the possibility of replacing T-10 in the MK 4 MOD 2 and CCU-47/A cartridges that reside in the CAD/PAD aircrew egress systems. Also proposed is an ESTCP in conjunction with the US Army CCDC-AC at Picatinny Arsenal to demonstrate the viability of this delay material in the M213/M228 fuze with an environmentally benign DBX-1 based primer and C70 detonator.

Due to the success of this environmentally benign delay project relying on slurry processing technique utilizing RAM technology, this formulation is also proposed in an ESTCP effort for additive manufacturing of novel delay elements. The future work efforts might be extended to print this formulation using a multi-axis printer. This approach requires significantly more development, such as long-term storage studies of this slurry to ensure its viability when combined

with a polymeric binder. However, preliminary results obtained by IMP and other laboratories are highly encouraging. Using this novel approach new designs for delays with increased level of reliability, as well as, vastly improved safety to operators and significant reduction in health hazards during production of this pyrotechnic delay is a viable path forward. The automated loading of delays will also improve the accuracy, precision, and reliability of the systems that use this environmentally benign pyrotechnic delay.

Literature Cited

[1] Comyn, *DOFL Technical Report No. TR-1015, Pyrotechnic Research at DOFL Part II. Pyrotechnic Delays*, 15 February 1962.

[2] Eck, W.S., Toxicology Report No. S.0032635-15, Department of Defense, Strategic Environmental Research and Development Program (SERDP), *Toxicology Assessment for SERDP Project WP-2518 Gasless Delay Element,* December 2018.

[3] Puszynski, J.A. and Hlavacek, V. *Synthesis and Processing of Ceramic Materials***,** Ind. Eng. Chem. Res. 1996, 35, 349-77.

[4] Dufrane, Ensign Bickford Aerospace and Defense Company, SUBWP2519: Task 4, *Environmentally Benign Pyrotechnic Formulation: Development Process Scale-Up*, 2018.

[5] United States Department of Labor, Occupational Safety and Health Administration; CFR 1910.1025(c)(1); Lead; https://www.osha.gov/laws-regs/regulations/standardnumber/1910/1910.1025; Accessed Mar 2019.

[6] United States Department of Labor, Occupational Safety and Health Administration; CFR 1910.1026(a)(4); Chromium (VI), https://www.osha.gov/laws-regs/regulations/standardnumber/1910/1910.1026, Accessed Mar 2019.

[7] United States Environmental Protection Agency, National Primary Drinking Water Regulations, https://www.epa.gov/ground-water-and-drinking-water/national-primary-drinking-water-regulations#one, Accessed May 2019.

[8] ASTM E2552-16, *Standard Guide for Assessing the Environmental and Human Health Impacts of New Compounds for Military Use*, ASTM International, West Conshohocken, PA, 2016, www.astm.org, 2019.

[9] North Atlantic Treaty Organization (NATO) STANAG 4147 (Edition 2), *Chemical Compatibility of Ammunition Components, with Explosives (Non-Nuclear Applications),* Test 2 – The Heat Flow Calorimetry Test, Pg. D-25, 5 June 2001.

Appendices:

Appendix A – List of Scientific/Technical Publications

D. Perkins, M. Puszynski and J. Puszynski, "Experimental and Modeling Studies of Environmentaly Benign Tunable Pyrotechnic Delay Systems," **Published and Presented** in *43rd International Pyrotechnics Society Seminar Proceedings*, Fort Collins, CO, Print and 2018.

D. Perkins, M. Puszynski and J. Puszynski, "A New Environmentally Benign Tunable Pyrotechnic System for a Potential Replacement of T-10 Delay Formulation," **Presented** in *Navy CAD/PAD Technical Workshop*, 2018.

D. Perkins, M. Puszynski and J. Puszynski, "Development of Novel Environmentally Benign Tubable Pyrotechnic Delay Systems," **Presented** in *50th International Annual Conference of the Fraunhofer ICT*, Karlsruhe, Germany, 2019.

Appendix B – Data produced from EBA&D M201A1 fuze testing IMP vs. AMTEC

Temperature and Humidity Conditioned -65 °F Tested M201A1 Fuzes

Serial Number	Bulid Date	Column	ZPP Charge Weight	Delay Mix (g) +-.03	A-1A (mg) +-.05	Consolidation Height (in)	Burn Time (s)	IBR (s/in)
1-01	4-Oct-16	127	22.3	0.67	30	0.39150	1.70700	4.36015
1-02	4-Oct-16	94	24.1	0.67	30	0.41900	1.87000	4.46301
1-03	4-Oct-16	24	21.6	0.67	30	0.42100	1.87300	4.44893
1-04	4-Oct-16	100	24.9	0.67	30	0.42900	1.82000	4.24242
1-05	4-Oct-16	17	26.7	0.67	30	0.41250	1.95700	4.74424
1-06	5-Oct-16	163	23.7	0.67	30	0.43000	1.77500	4.12791
1-07	4-Oct-16	92	24.4	0.67	30	0.38650	1.72300	4.45796
1-08	5-Oct-16	216	22.8	0.67	30	0.42300	1.86500	4.40898
1-09	4-Oct-16	50	20.6	0.67	30	0.40550	1.78900	4.41184
1-10	4-Oct-16	4	20.1	0.67	30	0.41100	1.86100	4.52798
1-11	4-Oct-16	12	23.1	0.67	30	0.42500	1.82500	4.29412
1-12	4-Oct-16	75	20.6	0.67	30	0.38250	1.79500	4.69281
1-13	5-Oct-16	165	21.2	0.67	30	0.43450	1.81300	4.17261
1-14	4-Oct-16	63	21.2	0.67	30	0.43400	1.95700	4.50922
1-15	4-Oct-16	84	22.1	0.67	30	0.40350	1.81300	4.49318
1-16	4-Oct-16	109	27.6	0.67	30	0.39650	1.83000	4.61538
1-17	5-Oct-16	189	25.5	0.67	30	0.43950	1.84500	4.19795
1-18	4-Oct-16	55	23.7	0.67	30	0.41200	1.74600	4.23786
1-19	5-Oct-16	209	25.3	0.67	30	0.42350	1.80200	4.25502
1-20	5-Oct-16	228	21.8	0.67	30	0.40070	1.77200	4.42226
1-21	5-Oct-16	160	23.4	0.67	30	0.44600	1.92600	4.31839
1-22	4-Oct-16	35	22.7	0.67	30	0.39550	1.79200	4.53097
1-23	4-Oct-16	113	24.9	0.67	30	0.39000	1.77900	4.56154
1-24	5-Oct-16	154	22.3	0.67	30	0.42950	1.80000	4.19092
1-25	5-Oct-16	211	23.6	0.67	30	0.40700	1.81200	4.45209
1-26	4-Oct-16	90	24.2	0.67	30	0.42000	1.80600	4.30000
1-27	5-Oct-16	226	22.0	0.67	30	0.41750	1.79500	4.29940
1-28	4-Oct-16	27	26.0	0.67	30	0.42550	1.77400	4.16921
1-29	5-Oct-16	205	23.7	0.67	30	0.42800	1.81900	4.25000
1-30	4-Oct-16	87	22.3	0.67	30	0.38550	1.64700	4.27237
1-31	4-Oct-16	114	21.6	0.67	30	0.41750	NA	NA
1-32	5-Oct-16	176	20.6	0.67	30	0.41500	NA	NA
1-33	4-Oct-16	65	22.2	0.67	30	0.43950	NA	NA
1-34	4-Oct-16	77	26.2	0.67	30	0.41000	NA	NA
1-35	5-Oct-16	156	22.3	0.67	30	0.46100	NA	NA

Consolidation stats		Burn Time Stats		IBR Stats	
Min	0.4	Min	1.64700	Min	4.12791
Max	0.4	Max	1.95700	Max	4.74424
Range	0.1	Range	0.31	Range	0.61634
Avg	0.4	Avg	1.81293	Avg	4.38096
Std Dev	0.0	Std Dev	0.06502	Std Dev	0.15782
CV%			3.586451		3.60235

Temperature and Humidity Conditioned 70 °F Tested M201A1 Fuzes

Serial Number	Bulid Date	Column	ZPP Charge Weight	Delay Mix (g) +-.03	A-1A (mg) +-.05	Consolidation Height (in)	Burn Time (s)	IBR (s/in)
2-01	5-Oct-16	187	21.1	0.70	30	0.43400	1.73000	3.98618
2-02	4-Oct-16	21	23.0	0.70	30	0.40800	1.61600	3.96078
2-03	5-Oct-16	224	21.3	0.70	30	0.42100	1.69000	4.01425
2-04	5-Oct-16	208	22.8	0.70	30	0.40850	1.51900	3.71848
2-05	5-Oct-16	193	22.0	0.70	30	0.40900	1.59200	3.89242
2-06	4-Oct-16	1	21.8	0.70	30	0.45050	1.79900	3.99334
2-07	4-Oct-16	124	21.1	0.70	30	0.39850	1.68700	4.23338
2-08	4-Oct-16	48	20.9	0.70	30	0.39000	1.59800	4.09744
2-09	5-Oct-16	238	25.1	0.70	30	0.41500	1.61500	3.89157
2-10	4-Oct-16	29	21.6	0.70	30	0.40800	1.68600	4.13235
2-11	4-Oct-16	53	22.6	0.70	30	0.38750	1.55900	4.02323
2-12	4-Oct-16	28	22.0	0.70	30	0.41750	1.64700	3.94491
2-13	5-Oct-16	190	22.0	0.70	30	0.42100	1.65400	3.92874
2-14	5-Oct-16	174	23.2	0.70	30	0.41550	1.68200	4.04813
2-15	5-Oct-16	149	23.5	0.70	30	0.45300	1.84200	4.06623
2-16	4-Oct-16	119	25.0	0.70	30	0.40000	1.67500	4.18750
2-17	5-Oct-16	204	23.9	0.70	30	0.45350	1.70700	3.76406
2-18	4-Oct-16	95	20.4	0.70	30	0.41550	1.72300	4.14681
2-19	4-Oct-16	11	22.2	0.70	30	0.42450	1.66600	3.92462
2-20	4-Oct-16	134	22.6	0.70	30	0.39300	1.66100	4.22646
2-21	5-Oct-16	210	23.7	0.70	30	0.40600	1.64900	4.06158
2-22	4-Oct-16	132	20.2	0.70	30	0.42650	1.78200	4.17819
2-23	4-Oct-16	129	22.0	0.70	30	0.42950	1.74800	4.06985
2-24	4-Oct-16	98	22.0	0.70	30	0.40200	1.65400	4.11443
2-25	4-Oct-16	140	22.1	0.70	30	0.41600	1.76000	4.23077
2-26	4-Oct-16	49	25.5	0.70	30	0.36700	1.47900	4.02997
2-27	5-Oct-16	219	20.7	0.70	30	0.42450	1.70100	4.00707
2-28	4-Oct-16	144	21.2	0.70	30	0.44350	1.73800	3.91883
2-29	5-Oct-16	200	20.8	0.70	30	0.41900	1.71500	4.09308
2-30	4-Oct-16	33	26.5	0.70	30	0.40750	1.70300	4.17914
2-31	5-Oct-16	212	22.5	0.70	30	0.42250	NA	NA
2-32	4-Oct-16	122	22.3	0.70	30	0.42100	NA	NA
2-33	5-Oct-16	172	27.3	0.70	30	0.43200	NA	NA
2-34	4-Oct-16	3	25.1	0.70	30	0.42850	NA	NA
2-35	4-Oct-16	34	27.3	0.70	30	0.41000	NA	NA

Consolidation stats		Burn Time Stats		IBR Stats	
Min	0.4	Min	1.47900	Min	3.71848
Max	0.5	Max	1.84200	Max	4.23338
Range	0.1	Range	0.363	Range	0.51489
Avg	0.4	Avg	1.67590	Avg	4.03546
Std Dev	0.0	Std Dev	0.077436	Std Dev	0.12755
CV%			4.620571		3.16076

Temperature and Humidity Conditioned 160 °F Tested M201A1 Fuzes

Serial Number	Bulid Date	Column	ZPP Charge Weight	Delay Mix (g) +-.03	A-1A (mg) +-.05	Consolidation Height (in)	Burn Time (s)	IBR (s/in)
3-01	5-Oct-16	161	21.3	0.67	30	0.42000	1.57700	3.75476
3-02	4-Oct-16	72	21.8	0.67	30	0.40600	1.58000	3.89163
3-03	4-Oct-16	80	21.5	0.67	30	0.40450	1.58400	3.91595
3-04	5-Oct-16	237	23.0	0.67	30	0.40750	1.57500	3.86503
3-05	4-Oct-16	67	20.6	0.67	30	0.42500	1.59300	3.74824
3-06	5-Oct-16	145	22.2	0.67	30	0.43500	1.70700	3.92414
3-07	5-Oct-16	148	20.7	0.67	30	0.45350	1.66700	3.67585
3-08	5-Oct-16	164	25.3	0.67	30	0.45100	1.61500	3.58093
3-09	4-Oct-16	133	20.3	0.67	30	0.40250	1.48900	3.69938
3-10	5-Oct-16	202	20.4	0.67	30	0.41850	1.57700	3.76822
3-11	4-Oct-16	143	23.2	0.67	30	0.42450	1.66200	3.91519
3-12	4-Oct-16	101	24.2	0.67	30	0.41050	1.57800	3.84409
3-13	5-Oct-16	206	24.0	0.67	30	0.43300	1.62200	3.74596
3-14	4-Oct-16	117	21.6	0.67	30	0.41550	1.57400	3.78821
3-15	5-Oct-16	167	20.4	0.67	30	0.44350	1.61700	3.64600
3-16	4-Oct-16	78	22.8	0.67	30	0.42350	1.60900	3.79929
3-17	5-Oct-16	234	26.9	0.67	30	0.43700	1.66000	3.79863
3-18	4-Oct-16	69	20.5	0.67	30	0.42350	1.56500	3.69540
3-19	5-Oct-16	229	21.6	0.67	30	0.41600	1.58200	3.80288
3-20	5-Oct-16	171	23.8	0.67	30	0.43500	1.59800	3.67356
3-21	5-Oct-16	179	20.5	0.67	30	0.43950	1.59800	3.63595
3-22	4-Oct-16	141	23.3	0.67	30	0.40800	1.55200	3.80392
3-23	4-Oct-16	45	24.7	0.67	30	0.39700	1.47400	3.71285
3-24	5-Oct-16	196	21.9	0.67	30	0.42150	1.56200	3.70581
3-25	5-Oct-16	177	22.5	0.67	30	0.40750	1.56200	3.83313
3-26	5-Oct-16	233	21.6	0.67	30	0.44000	1.66300	3.77955
3-27	4-Oct-16	89	25.5	0.67	30	0.41850	1.55100	3.70609
3-28	4-Oct-16	2	21.0	0.67	30	0.40500	1.54800	3.82222
3-29	5-Oct-16	150	22.8	0.67	30	0.43400	1.59000	3.66359
3-30	5-Oct-16	159	22.2	0.67	30	0.44950	1.64800	3.66630
3-31	4-Oct-16	5	21.6	0.67	30	0.42600	NA	NA
3-32	4-Oct-16	74	26.3	0.67	30	0.41700	NA	NA
3-33	4-Oct-16	26	20.7	0.67	30	0.39200	NA	NA
3-34	4-Oct-16	30	21.1	0.67	30	0.40400	NA	NA
3-35	5-Oct-16	146	21.4	0.67	30	0.43900	NA	NA

Consolidation stats		Burn Time Stats		IBR Stats	
Min	0.4	Min	1.47400	Min	3.58093
Max	0.5	Max	1.70700	Max	3.92414
Range	0.1	Range	0.233	Range	0.34321
Avg	0.4	Avg	1.59263	Avg	3.76209
Std Dev	0.0	Std Dev	0.049263	Std Dev	0.08893
CV%			3.093172		2.36389

-65 °F Tested M201A1 Fuzes

Serial Number	Bulid Date	Column	ZPP Charge Weight	Delay Mix (g) +-.03	A-1A (mg) +-.05	Consolidation Height (in)	Burn Time (s)	IBR (s/in)
4-01	4-Oct-16	105	22.5	0.70	30	0.42900	1.79100	4.17483
4-02	4-Oct-16	83	20.4	0.70	30	0.40400	1.80000	4.45545
4-03	5-Oct-16	183	24.0	0.70	30	0.41050	1.78300	4.34348
4-04	4-Oct-16	16	22.3	0.70	30	0.42600	1.84400	4.32864
4-05	4-Oct-16	44	24.9	0.70	30	0.41300	1.71500	4.15254
4-06	4-Oct-16	123	25.2	0.70	30	0.38450	1.75300	4.55917
4-07	5-Oct-16	175	22.4	0.70	30	0.43250	1.81800	4.20347
4-08	5-Oct-16	207	24.4	0.70	30	0.41950	1.78700	4.25983
4-09	4-Oct-16	37	25.2	0.70	30	0.42750	1.79300	4.19415
4-10	4-Oct-16	51	26.4	0.70	30	0.41800	1.80900	4.32775
4-11	5-Oct-16	217	22.9	0.70	30	0.40400	1.75300	4.33911
4-12	4-Oct-16	70	22.4	0.70	30	0.41450	1.80900	4.36429
4-13	4-Oct-16	46	23.5	0.70	30	0.39800	1.62700	4.08794
4-14	4-Oct-16	20	26.1	0.70	30	0.39350	1.67600	4.25921
4-15	5-Oct-16	182	23.2	0.70	30	0.40850	1.73000	4.23501
4-16	4-Oct-16	43	30.0	0.70	30	0.41000	1.74400	4.25366
4-17	5-Oct-16	230	24.2	0.70	30	0.42800	1.79700	4.19860
4-18	4-Oct-16	107	26.6	0.70	30	0.40850	1.72200	4.21542
4-19	4-Oct-16	104	23.7	0.70	30	0.42900	1.84100	4.29138
4-20	5-Oct-16	218	21.1	0.70	30	0.40600	1.73100	4.26355
4-21	5-Oct-16	191	25.0	0.70	30	0.43050	1.78100	4.13705
4-22	4-Oct-16	131	22.1	0.70	30	0.42200	1.76700	4.18720
4-23	4-Oct-16	81	20.7	0.70	30	0.43400	1.82300	4.20046
4-24	4-Oct-16	52	20.7	0.70	30	0.40200	1.71500	4.26617
4-25	4-Oct-16	32	21.7	0.70	30	0.41850	1.73400	4.14337
4-26	4-Oct-16	22	25.1	0.70	30	0.39250	1.63600	4.16815
4-27	4-Oct-16	97	22.9	0.70	30	0.41650	1.75900	4.22329
4-28	4-Oct-16	47	20.2	0.70	30	0.37900	1.70700	4.50396
4-30	5-Oct-16	168	22.4	0.70	30	0.42600	1.71700	4.03052
4-31	4-Oct-16	68	21.6	0.70	30	0.41900	1.73800	4.14797
4-29	4-Oct-16	42	23.6	0.70	30	0.44850	na	NA
4-32	5-Oct-16	220	23.1	0.70	30	0.42450	NA	NA
4-33	5-Oct-16	178	21.2	0.70	30	0.42200	NA	NA
4-34	4-Oct-16	36	28.1	0.70	30	0.41000	NA	NA
4-35	4-Oct-16	79	21.8	0.70	30	0.39500	NA	NA

Consolidation stats		Burn Time Stats		IBR Stats	
Min	0.4	Min	1.62700	Min	4.03052
Max	0.4	Max	1.84400	Max	4.55917
Range	0.1	Range	0.217	Range	0.52865
Avg	0.4	Avg	1.75667	Avg	4.25052
Std Dev	0.0	Std Dev	0.053452	Std Dev	0.11458
CV%			3.042829		2.69576

70 °F Tested M201A1 Fuzes

Serial Number	Bulid Date	Column	ZPP Charge Weight	Delay Mix (g) +-.03	A-1A (mg) +-.05	Consolidation Height (in)	Burn Time (s)	IBR (s/in)
5-01	4-Oct-16	103	22.3	0.67	30	0.42650	1.66100	3.89449
5-02	4-Oct-16	121	20.2	0.67	30	0.43550	1.70200	3.90815
5-03	4-Oct-16	7	22.6	0.67	30	0.41900	1.61800	3.86158
5-04	4-Oct-16	54	21.1	0.67	30	0.40400	1.58500	3.92327
5-05	4-Oct-16	99	22.8	0.67	30	0.42250	1.66400	3.93846
5-06	5-Oct-16	194	20.8	0.67	30	0.40250	1.61000	4.00000
5-07	4-Oct-16	93	22.9	0.67	30	0.43000	1.68100	3.90930
5-08	4-Oct-16	58	22.1	0.67	30	0.41700	1.64900	3.95444
5-09	4-Oct-16	138	20.2	0.67	30	0.41350	1.65300	3.99758
5-10	4-Oct-16	112	20.6	0.67	30	0.41600	1.66300	3.99760
5-11	5-Oct-16	197	22.8	0.67	30	0.43600	1.70900	3.91972
5-12	4-Oct-16	10	22.4	0.67	30	0.42550	1.65300	3.88484
5-13	5-Oct-16	225	22.3	0.67	30	0.41750	1.63200	3.90898
5-14	5-Oct-16	169	29.0	0.67	30	0.44900	1.65200	3.67929
5-15	4-Oct-16	56	20.1	0.67	30	0.39200	1.60700	4.09949
5-16	4-Oct-16	91	20.7	0.67	30	0.39950	1.63000	4.08010
5-17	4-Oct-16	139	21.6	0.67	30	0.42650	1.61100	3.77726
5-18	5-Oct-16	166	26.4	0.67	30	0.41750	1.60300	3.83952
5-19	4-Oct-16	31	22.2	0.67	30	0.39450	1.56800	3.97465
5-20	5-Oct-16	231	20.1	0.67	30	0.42200	1.53100	3.62796
5-21	4-Oct-16	40	22.9	0.67	30	0.42200	1.73300	4.10664
5-22	4-Oct-16	96	25.5	0.67	30	0.40500	1.67800	4.14321
5-23	5-Oct-16	158	23.3	0.67	30	0.46400	1.74000	3.75000
5-24	5-Oct-16	236	22.8	0.67	30	0.45550	1.80400	3.96048
5-25	5-Oct-16	184	24.0	0.67	30	0.45200	1.71700	3.79867
5-26	4-Oct-16	8	25.4	0.67	30	0.42600	1.65000	3.87324
5-27	5-Oct-16	214	21.2	0.67	30	0.41350	1.63300	3.94921
5-28	4-Oct-16	82	21.7	0.67	30	0.42750	1.71500	4.01170
5-29	4-Oct-16	76	23.9	0.67	30	0.41800	1.68700	4.03589
5-30	5-Oct-16	153	22.5	0.67	30	0.44800	1.73700	3.87723
5-31	5-Oct-16	192	21.5	0.67	30	0.42400	NA	NA
5-32	5-Oct-16	221	25.6	0.67	30	0.42300	NA	NA
5-33	5-Oct-16	170	22.5	0.67	30	0.43800	NA	NA
5-34	5-Oct-16	155	24.4	0.67	30	0.43150	NA	NA
5-35	5-Oct-16	199	20.3	0.67	30	0.41850	NA	NA

Consolidation stats		Burn Time Stats		IBR Stats	
Min	0.4	Min	1.53100	Min	3.62796
Max	0.5	Max	1.80400	Max	4.14321
Range	0.1	Range	0.273	Range	0.51525
Avg	0.4	Avg	1.65920	Avg	3.92276
Std Dev	0.0	Std Dev	0.05674	Std Dev	0.11733
			3.41972		2.99090

160 °F Tested M201A1 Fuzes

Serial Number	Bulid Date	Column	ZPP Charge Weight	Delay Mix (g) +-.03	A-1A (mg) +-.05	Consolidation Height (in)	Burn Time (s)	IBR (s/in)
6-01	4-Oct-16	41	25.6	0.70	30	0.39600	1.53900	3.88636
6-02	5-Oct-16	213	23.3	0.70	30	0.43450	1.62300	3.73533
6-03	5-Oct-16	157	20.6	0.70	30	0.44500	1.55700	3.49888
6-04	5-Oct-16	222	22.8	0.70	30	0.42500	1.63000	3.83529
6-05	4-Oct-16	102	25.5	0.70	30	0.41100	1.64900	4.01217
6-06	4-Oct-16	86	20.2	0.70	30	0.39600	1.48300	3.74495
6-07	4-Oct-16	85	20.7	0.70	30	0.40550	1.53600	3.78792
6-08	5-Oct-16	173	23.9	0.70	30	0.43600	1.60300	3.67661
6-09	5-Oct-16	188	25.9	0.70	30	0.42900	1.56000	3.63636
6-10	4-Oct-16	120	22.7	0.70	30	0.39900	1.46800	3.67920
6-11	5-Oct-16	223	21.8	0.70	30	0.41500	1.54700	3.72771
6-12	4-Oct-16	73	20.1	0.70	30	0.41900	1.62100	3.86874
6-13	4-Oct-16	125	20.9	0.70	30	0.40300	1.46800	3.64268
6-14	4-Oct-16	137	25.0	0.70	30	0.44450	1.62600	3.65804
6-15	4-Oct-16	142	21.7	0.70	30	0.41900	1.54700	3.69212
6-16	5-Oct-16	195	26.5	0.70	30	0.44400	1.60300	3.61036
6-17	4-Oct-16	15	24.0	0.70	30	0.40400	1.46300	3.62129
6-18	5-Oct-16	162	23.2	0.70	30	0.43500	1.51400	3.48046
6-19	4-Oct-16	64	26.5	0.70	30	0.44150	1.60500	3.63533
6-20	5-Oct-16	227	21.5	0.70	30	0.40700	1.56500	3.84521
6-21	4-Oct-16	136	22.6	0.70	30	0.43150	1.54100	3.57126
6-22	5-Oct-16	201	26.5	0.70	30	0.41800	1.53400	3.66986
6-23	5-Oct-16	152	22.2	0.70	30	0.43900	1.58400	3.60820
6-24	4-Oct-16	126	20.3	0.70	30	0.41000	1.53100	3.73415
6-25	4-Oct-16	71	22.1	0.70	30	0.42950	1.61000	3.74854
6-26	4-Oct-16	130	25.9	0.70	30	0.41900	1.56900	3.74463
6-27	4-Oct-16	116	23.7	0.70	30	0.43050	1.60500	3.72822
6-28	4-Oct-16	111	23.8	0.70	30	0.40050	1.46600	3.66042
6-29	5-Oct-16	232	27.3	0.70	30	0.43750	1.55100	3.54514
6-30	5-Oct-16	185	23.2	0.70	30	0.42050	1.51200	3.59572
6-31	4-Oct-16	110	22.7	0.70	30	0.40700	NA	NA
6-32	4-Oct-16	106	22.5	0.70	30	0.40550	NA	NA
6-33	5-Oct-16	235	21.1	0.70	30	0.43450	NA	NA
6-34	4-Oct-16	115	25.0	0.70	30	0.40550	NA	NA
6-35	4-Oct-16	66	22.5	0.70	30	0.41100	NA	NA

Consolidation stats		Burn Time Stats		IBR Stats	
Min	0.4	Min	1.46300	Min	3.48046
Max	0.4	Max	1.64900	Max	4.01217
Range	0.0	Range	0.186	Range	0.53171
Avg	0.4	Avg	1.55700	Avg	3.69604
Std Dev	0.0	Std Dev	0.053032	Std Dev	0.11506
			3.406041		3.11311

Appendix C – Data produced from EBA&D M213/M228 testing IMP vs. Chemring

Serial Number M213-IMP-A-	Bulid Date	Batch	Build Sequence	Delay Mix (g) +-.002	A-1A (g) +-.007	MIC M42 Primer	Consolidation Height (in)	Burn Time (s)	IBR (s/in)
1	18-May-18	B050818	76	1.1800	0.0374	0.031	0.88700	4.784	5.39346
2	17-May-18	B050818	51	1.1800	0.0374	0.031	0.86650	4.744	5.47490
3	14-May-18	B050818	6	1.1800	0.0374	0.031	0.88300	FTF	
4	14-May-18	B050818	8	1.1800	0.0374	0.031	0.84200	4.566	5.42280
5	17-May-18	B050818	32	1.1800	0.0374	0.031	0.89550	4.936	5.51200
6	18-May-18	B050818	94	1.1800	0.0374	0.031	0.87350	4.767	5.45736
7	17-May-18	B050818	54	1.1800	0.0374	0.031	0.89250	5.226	5.85546
8	18-May-18	B050818	59	1.1800	0.0374	0.031	0.86550	4.721	5.45465
9	18-May-18	B050818	96	1.1800	0.0374	0.031	0.88050	4.736	5.37876
10	17-May-18	B050818	47	1.1800	0.0374	0.031	0.86650	5.214	6.01731
11	17-May-18	B050818	30	1.1800	0.0374	0.031	0.88100	5.248	5.95687
12	14-May-18	B050818	15	1.1800	0.0374	0.031	0.85500	5.001	5.84912
13	17-May-18	B050818	42	1.1800	0.0374	0.031	0.87250	5.297	6.07106
14	18-May-18	B050818	62	1.1800	0.0374	0.031	0.89050	5.411	6.07636
15	18-May-18	B050818	73	1.1800	0.0374	0.031	0.92800	5.562	5.99353
16	18-May-18	B050818	87	1.1800	0.0374	0.031	0.86500	5.228	6.04393
17	14-May-18	B050818	5	1.1800	0.0374	0.031	0.87050	5.425	6.23205
18	17-May-18	B050818	19	1.1800	0.0374	0.031	0.87450	4.887	5.58834
19	18-May-18	B050818	111	1.1800	0.0374	0.031	0.88000	FTF	
20	18-May-18	B050818	2	1.1800	0.0374	0.031	0.89450	5.079	5.67803
21	18-May-18	B050818	109	1.1800	0.0374	0.031	0.86900	5.362	6.17031
22	18-May-18	B050818	65	1.1800	0.0374	0.031	0.89900	5.413	6.02113
23	18-May-18	B050818	77	1.1800	0.0374	0.031	0.88250	5.364	6.07819
24	17-May-18	B050818	20	1.1800	0.0374	0.031	0.87900	4.925	5.60296
25	17-May-18	B050818	27	1.1800	0.0374	0.031	0.87450	5.322	6.08576
26	18-May-18	B050818	64	1.1800	0.0374	0.031	0.89100	4.95	5.55556
27	17-May-18	B050818	38	1.1800	0.0374	0.031	0.87700	4.784	5.45496
28	18-May-18	B050818	108	1.1800	0.0374	0.031	0.90250	5.34	5.91690
29	14-May-18	B050818	12	1.1800	0.0374	0.031	0.86350	5.072	5.87377
30	18-May-18	B050818	68	1.1800	0.0374	0.031	0.87600	4.842	5.52740
31	17-May-18	B050818	17	1.1800	0.0374	0.031	0.89900	5.538	6.16018
32	17-May-18	B050818	41	1.1800	0.0374	0.031	0.93300	5.604	6.00643
33	18-May-18	B050818	88	1.1800	0.0374	0.031	0.88100	4.409	5.00454
34	17-May-18	B050818	40	1.1800	0.0374	0.031	0.88000	4.872	5.53636
35	18-May-18	B050818	66	1.1800	0.0374	0.031	0.89150	5.366	6.01907

Serial Number M213-IMP-A-	Bulid Date	Batch	Build Sequence	Delay Mix (g) +-.002	A-1A (g) +-.007	MIC M42 Primer	Consolidation Height (in)	Burn Time (s)	IBR (s/in)
36	18-May-18	B050818	102	1.1800	0.0374	0.031	0.86750	4.953	5.70951
37	18-May-18	B050818	97	1.1800	0.0374	0.031	0.93150	5.263	5.65003
38	18-May-18	B050818	110	1.1800	0.0374	0.031	0.84200	4.407	5.23397
39	18-May-18	B050818	107	1.1800	0.0374	0.031	0.88600	5.056	5.70655
40	17-May-18	B050818	56	1.1800	0.0374	0.031	0.87200	4.948	5.67431
41	18-May-18	B050818	90	1.1800	0.0374	0.031	0.86850	4.905	5.64767
42	18-May-18	B050818	114	1.1800	0.0374	0.031	0.87600	4.988	5.69406
43	18-May-18	B050818	67	1.1800	0.0374	0.031	0.88400	4.487	5.07579
44	18-May-18	B050818	104	1.1800	0.0374	0.031	0.89000	5.057	5.68202
45	17-May-18	B050818	50	1.1800	0.0374	0.031	0.88950	5.041	5.66723
46	18-May-18	B050818	69	1.1800	0.0374	0.031	0.89150	4.575	5.13180
47	18-May-18	B050818	85	1.1800	0.0374	0.031	0.89750	4.631	5.15989
48	18-May-18	B050818	71	1.1800	0.0374	0.031	0.89450	4.571	5.11012
49	18-May-18	B050818	84	1.1800	0.0374	0.031	0.87750	4.634	5.28091
50	18-May-18	B050818	99	1.1800	0.0374	0.031	0.90400	5.09	5.63053
51	18-May-18	B050818	75	1.1800	0.0374	0.031	0.89150	4.998	5.60628
52	14-May-18	B050818	13	1.1800	0.0374	0.031	0.85450	4.427	5.18081
53	18-May-18	B050818	106	1.1800	0.0374	0.031	0.86900	4.468	5.14154
54	17-May-18	B050818	29	1.1800	0.0374	0.031	0.87650	4.356	4.96977
55	14-May-18	B050818	4	1.1800	0.0374	0.031	0.84700	4.436	5.23731
56	18-May-18	B050818	58	1.1800	0.0374	0.031	0.88100	4.399	4.99319
57	17-May-18	B050818	39	1.1800	0.0374	0.031	0.89000	4.553	5.11573
58	18-May-18	B050818	63	1.1800	0.0374	0.031	0.89750	4.982	5.55097
59	17-May-18	B050818	53	1.1800	0.0374	0.031	0.89450	4.776	5.33930
60	17-May-18	B050818	26	1.1800	0.0374	0.031	0.87950	4.535	5.15634
61	18-May-18	B050818	72	1.1800	0.0374	0.031	0.89550	4.591	5.12674
62	18-May-18	B050818	79	1.1800	0.0374	0.031	0.91700	4.677	5.10033
63	17-May-18	B050818	52	1.1800	0.0374	0.031	0.88550	4.909	5.54376
64	14-May-18	B050818	10	1.1800	0.0374	0.031	0.84900	4.822	5.67962
65	17-May-18	B050818	48	1.1800	0.0374	0.031	0.90600	4.609	5.08720
66	17-May-18	B050818	22	1.1800	0.0374	0.031	0.89600	4.558	5.08705
67	17-May-18	B050818	23	1.1800	0.0374	0.031	0.86400	4.361	5.04745
68	18-May-18	B050818	74	1.1800	0.0374	0.031	0.87450	4.97	5.68325
69	17-May-18	B050818	44	1.1800	0.0374	0.031	0.93500	5.169	5.52834
70	18-May-18	B050818	105	1.1800	0.0374	0.031	0.89500	5.056	5.64916

Serial Number M213-IMP-A-	Bulid Date	Batch	Build Sequence	Delay Mix (g) +-.002	A-1A (g) +-.007	MIC M42 Primer	Consolidation Height (in)	Burn Time (s)	IBR (s/in)
71	17-May-18	B050818	55	1.1800	0.0374	0.031	0.88800	4.806	5.41216
72	18-May-18	B050818	103	1.1800	0.0374	0.031	0.85750	Equipment Issue	
73	18-May-18	B050818	82	1.1800	0.0374	0.031	0.86650	4.246	4.90017
74	18-May-18	B050818	61	1.1800	0.0374	0.031	0.88200	4.812	5.45578
75	17-May-18	B050818	33	1.1800	0.0374	0.031	0.93250	4.455	4.77748
76	14-May-18	B050818	11	1.1800	0.0374	0.031	0.84000	Equipment Issue	
77	18-May-18	B050818	1	1.1800	0.0374	0.031	0.86250	4.797	5.56174
78	17-May-18	B050818	21	1.1800	0.0374	0.031	0.88100	4.19	4.75596
79	18-May-18	B050818	78	1.1800	0.0374	0.031	0.90900	4.896	5.38614
80	18-May-18	B050818	91	1.1800	0.0374	0.031	0.85600	4.17	4.87150
81	18-May-18	B050818	81	1.1800	0.0374	0.031	0.87800	4.778	5.44191
82	18-May-18	B050818	95	1.1800	0.0374	0.031	0.84300	4.517	5.35824
83	18-May-18	B050818	92	1.1800	0.0374	0.031	0.85950	4.636	5.39383
84	17-May-18	B050818	43	1.1800	0.0374	0.031	0.89350	4.34	4.85730
85	17-May-18	B050818	18	1.1800	0.0374	0.031	0.88750	4.781	5.38704
86	18-May-18	B050818	80	1.1800	0.0374	0.031	0.92300	4.937	5.34886
87	17-May-18	B050818	45	1.1800	0.0374	0.031	0.89300	4.372	4.89586
88	18-May-18	B050818	70	1.1800	0.0374	0.031	0.91500	4.428	4.83934
89	17-May-18	B050818	36	1.1800	0.0374	0.031	0.86150	4.167	4.83691
90	18-May-18	B050818	86	1.1800	0.0374	0.031	0.89600	4.4	4.91071
91	17-May-18	B050818	31	1.1800	0.0374	0.031	0.88850	4.71	5.30107
92	18-May-18	B050818	89	1.1800	0.0374	0.031	0.89750	4.287	4.77660
93	18-May-18	B050818	60	1.1800	0.0374	0.031	0.88250	4.482	5.07875
94	18-May-18	B050818	112	1.1800	0.0374	0.031	0.89700	4.379	4.88183
95	17-May-18	B050818	46	1.1800	0.0374	0.031	0.87200	4.296	4.92661
96	17-May-18	B050818	49	1.1800	0.0374	0.031	0.92400	4.771	5.16342
97	17-May-18	B050818	35	1.1800	0.0374	0.031	0.88950	4.733	5.32097
98	14-May-18	B050818	14	1.1800	0.0374	0.031	0.86100	4.287	4.97909
99	18-May-18	B050818	115	1.1800	0.0374	0.031	0.88650	4.388	4.94980
100	17-May-18	B050818	24	1.1800	0.0374	0.031	0.86200	4.199	4.87123
101	18-May-18	B050818	93	1.1800	0.0374	0.031	0.84800	4.099	4.83373
102	18-May-18	B050818	98	1.1800	0.0374	0.031	0.86250	4.105	4.75942
103	17-May-18	B050818	37	1.1800	0.0374	0.031	0.89150	4.739	5.31576
104	18-May-18	B050818	57	1.1800	0.0374	0.031	0.91050	4.389	4.82043
105	18-May-18	B050818	7	1.1800	0.0374	0.031	0.85700	4.096	4.77946

Chemring					
Chemring M213/M228 Fuze Tested at -65 °C		Chemring M213/M228 Fuze Tested at 20 °C		Chemring M213/M228 Fuze Tested at 71 °C	
1	5.852	**36**	5.382	**71**	4.913
2	6.513	**37**	5.274	**72**	4.893
3	5.811	**38**	5.827	**73**	4.987
4	5.991	**39**	5.453	**74**	4.791
5	6.442	**40**	5.332	**75**	4.882
6	5.854	**41**	5.361	**76**	4.856
7	5.843	**42**	5.889	**77**	4.815
8	5.877	**43**	5.358	**78**	4.88
9	5.878	**44**	5.29	**79**	4.889
10	5.761	**45**	5.843	**80**	4.851
11	6.169	**46**	5.715	**81**	4.864
12	5.814	**47**	5.227	**82**	4.857
13	5.769	**48**	5.22	**83**	4.793
14	5.747	**49**	5.334	**84**	4.745
15	5.875	**50**	5.248	**85**	4.779
16	6.137	**51**	5.281	**86**	4.772
17	5.468	**52**	5.345	**87**	4.77
18	6.237	**53**	5.251	**88**	4.925
19	5.927	**54**	5.441	**89**	4.763
20	6.119	**55**	5.28	**90**	4.784
21	5.779	**56**	5.687	**91**	4.858
22	6.632	**57**	5.183	**92**	4.741
23	6.009	**58**	5.273	**93**	4.805
24	6.074	**59**	5.456	**94**	4.745
25	6.501	**60**	5.284	**95**	4.826
26	5.957	**61**	5.792	**96**	4.819
27	6.159	**62**	5.244	**97**	4.913
28	6.106	**63**	5.345	**98**	4.722
29	6.116	**64**	5.867	**99**	4.82
30	6.595	**65**	5.441	**100**	4.731
31	6.099	**66**	5.202	**101**	4.947
32	6.014	**67**	5.354	**102**	4.796
33	5.791	**68**	5.199	**103**	4.722
34	6.5	**69**	5.186	**104**	4.844
35	6.341	**70**	5.878	**105**	4.809

Appendix D – Data produced from IMP M213/M228 final deliverable testing

Batch ID	Fuze Number	Consolidation Height (in)	Burn Time (s)	IBR (s/in)	Temperature
B082118-2	M213-16	0.913	5.132	5.624	-65°F
B082118-2	M213-17	0.923	5.024	5.446	-65°F
B082118-2	M213-18	0.888	5.089	5.734	-65°F
B082118-2	M213-19	0.897	5.073	5.659	-65°F
B082118-2	M213-20	0.906	5.087	5.618	-65°F
B082118-2	M213-21	0.901	5.087	5.649	-65°F
B082118-2	M213-22	0.910	5.130	5.637	-65°F
B082118-2	M213-23	0.902	5.000	5.546	-65°F
B082118-2	M213-24	0.906	5.065	5.591	-65°F
B082118-2	M213-25	0.888	4.935	5.561	-65°F
B082118-2	M213-26	0.912	5.195	5.696	-65°F
B082118-2	M213-27	0.909	5.260	5.790	-65°F
B082118-2	M213-28	0.902	5.109	5.664	-65°F
B082118-2	M213-29	0.915	5.195	5.678	-65°F
B082118-2	M213-30	0.905	4.983	5.509	-65°F
B082118-2	M213-31	0.918	5.243	5.714	-65°F
B082118-2	M213-32	0.893	5.094	5.704	-65°F
B082118-2	M213-33	0.905	5.116	5.653	-65°F
B082118-2	M213-34	0.908	5.224	5.753	-65°F
B082118-2	M213-35	0.908	5.116	5.637	-65°F
B121718-1	M213-1	0.867	4.921	5.679	-65°F
B121718-1	M213-2	0.875	4.921	5.627	-65°F
B121718-1	M213-3	0.843	4.832	5.735	-65°F
B121718-1	M213-4	0.858	4.897	5.711	-65°F
B121718-1	M213-5	0.894	5.027	5.626	-65°F
B121718-1	M213-6	0.851	4.832	5.681	-65°F
B121718-1	M213-7	0.854	4.810	5.632	-65°F
B121718-1	M213-8	0.889	5.010	5.639	-65°F
B121718-1	M213-9	0.876	5.010	5.719	-65°F
B121718-1	M213-10	0.852	4.815	5.651	-65°F
B121718-1	M213-11	0.893	5.059	5.668	-65°F
B121718-1	M213-12	0.909	5.170	5.691	-65°F
B121718-1	M213-13	0.914	5.236	5.732	-65°F
B121718-1	M213-14	0.887	5.081	5.732	-65°F
B121718-1	M213-15	0.893	5.037	5.644	-65°F
B121718-1	M213-16	0.898	5.214	5.806	-65°F
B121718-1	M213-17	0.908	5.104	5.624	-65°F
B121718-1	M213-18	0.892	4.993	5.598	-65°F
B121718-1	M213-19	0.907	5.166	5.699	-65°F
B121718-1	M213-20	0.905	5.055	5.589	-65°F
B121718-1	M213-21	0.906	5.120	5.651	-65°F
B121718-1	M213-22	0.900	5.185	5.761	-65°F
B121718-1	M213-23	0.893	5.052	5.661	-65°F
B121718-1	M213-24	0.900	5.117	5.689	-65°F
B121718-1	M213-25	0.913	5.031	5.510	-65°F
B121718-1	M213-26	0.891	5.031	5.650	-65°F
B121718-1	M213-27	0.898	5.075	5.651	-65°F
B121718-1	M213-28	0.878	4.942	5.632	-65°F
B121718-1	M213-29	0.895	4.921	5.498	-65°F
B121718-1	M213-30	0.888	4.876	5.491	-65°F
Consolidation stats		**Burn Time Stats**		**IBR Stats**	
Min	0.843	**Min**	4.810	**Min**	5.446
Max	0.923	**Max**	5.260	**Max**	5.806
Range	0.080	**Range**	0.450	**Range**	0.360
Avg	0.894	**Avg**	5.054	**Avg**	5.651
Std Dev	0.018	**Std Dev**	0.115	**Std Dev**	0.075
		CV%	2.271	**CV%**	1.333

Batch ID	Fuze Number	Consolidation Height (in)	Burn Time (s)	IBR (s/in)	Temperature
B121718-1	M213-31	0.912	4.722	5.178	70°F
B121718-1	M213-32	0.892	4.655	5.219	70°F
B121718-1	M213-33	0.915	4.744	5.185	70°F
B121718-1	M213-34	0.899	4.655	5.178	70°F
B121718-1	M213-35	0.908	4.744	5.225	70°F
B121718-1	M213-36	0.896	4.633	5.171	70°F
B121718-1	M213-37	0.915	4.698	5.137	70°F
B121718-1	M213-38	0.915	4.743	5.186	70°F
B121718-1	M213-39	0.907	4.698	5.183	70°F
B121718-1	M213-40	0.916	4.677	5.109	70°F
B121718-1	M213-21	0.883	4.579	5.186	70°F
B121718-1	M213-22	0.886	4.423	4.992	70°F
B121718-1	M213-23	0.897	4.510	5.031	70°F
B121718-1	M213-24	0.901	4.576	5.079	70°F
B121718-1	M213-25	0.904	4.685	5.185	70°F
B121718-1	M213-26	0.895	4.642	5.189	70°F
B121718-1	M213-27	0.906	4.642	5.126	70°F
B121718-1	M213-28	0.897	4.642	5.178	70°F
B121718-1	M213-29	0.891	4.750	5.334	70°F
B121718-1	M213-30	0.923	4.770	5.168	70°F
B121718-1	M213-31	0.883	4.531	5.131	70°F
B121718-1	M213-32	0.920	4.683	5.090	70°F
B121718-1	M213-33	0.920	4.683	5.090	70°F
B121718-1	M213-34	0.916	4.535	4.954	70°F
B121718-1	M213-35	0.923	4.730	5.127	70°F
B121718-1	M213-36	0.921	4.686	5.088	70°F
B121718-1	M213-37	0.888	4.559	5.137	70°F
B121718-1	M213-38	0.923	4.686	5.077	70°F
B121718-1	M213-39	0.905	4.600	5.086	70°F
B121718-1	M213-40	0.900	4.570	5.081	70°F
B121718-1	M213-41	0.900	4.481	4.982	70°F
B121718-1	M213-42	0.893	4.481	5.018	70°F
B121718-1	M213-43	0.891	4.570	5.132	70°F
B121718-1	M213-44	0.918	4.437	4.836	70°F
B121718-1	M213-45	0.910	4.614	5.070	70°F
B121718-1	M213-46	0.902	4.459	4.943	70°F
B121718-1	M213-47	0.910	4.459	4.900	70°F
B121718-1	M213-48	0.905	4.725	5.221	70°F
B121718-1	M213-49	0.919	4.659	5.072	70°F
B121718-1	M213-50	0.902	4.592	5.094	70°F
B121718-1	M213-51	0.920	4.679	5.086	70°F
B121718-1	M213-52	0.862	4.324	5.019	70°F
B121718-1	M213-53	0.895	4.367	4.882	70°F
B121718-1	M213-54	0.901	4.411	4.896	70°F
B121718-1	M213-55	0.898	4.279	4.768	70°F
B121718-1	M213-56	0.922	4.567	4.956	70°F
B121718-1	M213-57	0.894	4.434	4.960	70°F
B121718-1	M213-58	0.902	4.478	4.967	70°F
B121718-1	M213-59	0.883	4.367	4.946	70°F
B121718-1	M213-60	0.906	4.611	5.092	70°F

Consolidation stats		Burn Time Stats		IBR Stats	
Min	0.862	**Min**	4.279	**Min**	4.768
Max	0.923	**Max**	4.770	**Max**	5.334
Range	0.062	**Range**	0.491	**Range**	0.566
Avg	0.904	**Avg**	4.589	**Avg**	5.079
Std Dev	0.013	**Std Dev**	0.123	**Std Dev**	0.113
		CV%	2.674	**CV%**	2.227

Batch ID	Fuze Number	Consolidation Height (in)	Burn Time (s)	IBR (s/in)	Temperature
B121718-1	M213-41	0.891	4.330	4.860	160°F
B121718-1	M213-42	0.915	4.419	4.830	160°F
B121718-1	M213-43	0.915	4.463	4.878	160°F
B121718-1	M213-44	0.876	4.285	4.894	160°F
B121718-1	M213-45	0.909	4.419	4.861	160°F
B121718-1	M213-46	0.905	4.330	4.785	160°F
B121718-1	M213-47	0.881	4.264	4.840	160°F
B121718-1	M213-48	0.872	4.242	4.865	160°F
B121718-1	M213-49	0.892	4.285	4.807	160°F
B121718-1	M213-50	0.897	4.329	4.829	160°F
B121718-1	M213-51	0.897	4.329	4.826	160°F
B121718-1	M213-52	0.904	4.329	4.791	160°F
B121718-1	M213-53	0.897	4.372	4.877	160°F
B121718-1	M213-54	0.902	4.394	4.874	160°F
B121718-1	M213-55	0.900	4.327	4.810	160°F
B121718-1	M213-56	0.906	4.327	4.776	160°F
B121718-1	M213-57	0.904	4.392	4.858	160°F
B121718-1	M213-58	0.908	4.371	4.817	160°F
B121718-1	M213-59	0.893	4.238	4.746	160°F
B121718-1	M213-60	0.897	4.348	4.850	160°F
B121718-1	M213-61	0.907	4.283	4.725	160°F
B121718-1	M213-62	0.900	4.435	4.928	160°F
B121718-1	M213-63	0.902	4.414	4.896	160°F
B121718-1	M213-64	0.899	4.370	4.861	160°F
B121718-1	M213-65	0.904	4.435	4.906	160°F
B121718-1	M213-66	0.891	4.348	4.880	160°F
B121718-1	M213-67	0.905	4.437	4.905	160°F
B121718-1	M213-68	0.904	4.482	4.958	160°F
B121718-1	M213-69	0.886	4.350	4.912	160°F
B121718-1	M213-70	0.908	4.416	4.866	160°F
B121718-1	M213-1	0.905	4.373	4.835	160°F
B121718-1	M213-2	0.909	4.459	4.905	160°F
B121718-1	M213-3	0.905	4.459	4.927	160°F
B121718-1	M213-4	0.890	4.371	4.914	160°F
B121718-1	M213-5	0.903	4.349	4.819	160°F
B121718-1	M213-6	0.908	4.416	4.866	160°F
B121718-1	M213-7	0.910	4.285	4.711	160°F
B121718-1	M213-8	0.904	4.329	4.789	160°F
B121718-1	M213-9	0.897	4.373	4.875	160°F
B121718-1	M213-10	0.905	4.313	4.768	160°F
B121718-1	M213-11	0.904	4.373	4.837	160°F
B121718-1	M213-12	0.903	4.308	4.771	160°F
B121718-1	M213-13	0.884	4.308	4.873	160°F
B121718-1	M213-14	0.919	4.525	4.924	160°F
B121718-1	M213-15	0.897	4.330	4.830	160°F
B121718-1	M213-16	0.911	4.308	4.729	160°F
B121718-1	M213-17	0.920	4.508	4.900	160°F
B121718-1	M213-18	0.893	4.334	4.853	160°F
B121718-1	M213-19	0.923	4.468	4.843	160°F
B121718-1	M213-20	0.918	4.423	4.821	160°F
Consolidation stats		**Burn Time Stats**		**IBR Stats**	
Min	0.872	**Min**	4.238	**Min**	4.711
Max	0.923	**Max**	4.525	**Max**	4.958
Range	0.051	**Range**	0.287	**Range**	0.247
Avg	0.901	**Avg**	4.368	**Avg**	4.846
Std Dev	0.010	**Std Dev**	0.067	**Std Dev**	0.056
		CV%	1.535	**CV%**	1.155

Appendix E – Ensign Bickford Aerospace and Defense Technology Scale-Up Report

Ensign-Bickford Aerospace & Defense

RIGHT FOR YOUR MISSION

ENVIRONMENTALLY BENIGN PYROTECHNIC FORMULATION: DEVELOPMENT PROCESS SCALE-UP

Subcontract No. SUBWP2519: Task 4

Prepared By:
ENSIGN-BICKFORD AEROSPACE & DEFENSE COMPANY
Simsbury, Connecticut
Originator: R.M. Dufrane
September 27, 2018

1. SCOPE

1.1. This procedure defines the general requirements to achieve production levels of an environmentally benign pyrotechnic formulation to meet the quantities necessary to support the production levels of M201A1 and M213/M228 fuze assemblies.

2. SAFETY AND REGULATORY REQUIREMENTS:

2.1. Personnel Safety. Personnel working with materials, items or assemblies described by this document must have read and understood the pertinent "General Safety and Health" procedures governed by the facility, local, state and/or federal requirements.

2.2. Description of the Material, Item or Assembly. The pyrotechnic mixture consists of various fuels and oxidizers required to create an environmentally benign "gasless" delay formulation to be utilized in a M201A1 or M213/M228 fuze assembly with proper function over temperatures ranging from -65°F to +160°F.

2.3. Description of Function. The pyrotechnic material to be incrementally loaded and consolidated in either a M201A1 or M213/M228 fuze assembly. Initiation of material is induced by the pressure/heat output signal from a percussion primer.

2.4. Description of Sensitivity to Environments. The mixture is rather insensitive to ignition by heat, impact, friction, and electrostatic discharge (ESD). However, care should be taken to avoid these conditions when handling this product.

2.5. Listing of Personal Protective Equipment (PPE). Workers should follow requirements established at designated facility and in accordance with the material safety data sheet.

2.6. Quantity of Pyrotechnic, Propellant, or Explosive Per Batch, Item or Assembly. Present batch size is approximately 75g (of dried material). However this may be increased to meet demand as long as facility quantity and distance requirements are maintained.

2.7. Reactive Waste Material. Consult with the local, state and/or federal Safety and Regulatory Compliance Departments for proper waste handling and disposal.

2.8. Ozone Depleting Substances (ODS). Not Applicable.

2.9. The following safety and regulatory requirements may apply to this procedure and should be used as required.

2.9.1. Specifications

DoD 4145.26-M	DoD Contractors Safety Manual for Ammunition and Explosives, Mar 13, 2008
SW-010-AG-ORD-010	List of Explosives for Navy Munitions Rev 3, April16, 2001
NavOrd Report 6632	Electrostatic Spark Sensitivity of Bulk Explosives and Metal/Oxidant Mixtures
ARLCD-CR-80047	A Compilation of Hazard Test Data for Pyrotechnic Compositions Picatinny Arsenal Encyclopedia of Explosives and Related Items

Standards

MIL-STD-1751A	Safety and Performance Tests for the Qualification of Explosives (High Explosives, Propellants, and Pyrotechnics)
MIL-C-13739A	Detail Specification Composition, Delay

Code of Federal Regulations

29 CFR 1910.119	Occupational Safety and Health Standards – Process Safety Management of Highly Hazardous Chemicals

2.9.2. Other Documents

Safety Data Sheets (SDS); Obtain most recent SDS from appropriate supplier for all raw materials associated to the mixing process.

3. TOOLS, MATERIALS AND EQUIPMENT

3.1. Tools

3.1.1. Conductive scoops and spatulas

3.1.2. Dry pans non-stick coated (fitted to size of oven)

3.1.3. Sieve #200 (75 µm) and #325 (45 µm)

3.1.4. PPE

3.1.4.1. Eye protection

3.1.4.2. Respiratory protection

3.1.4.3. ESD protection

3.2. Materials: Pyrotechnic Mix

Material	Description	Supplier
Strontium Molybdate	99% Pure	Alfa Aesar PN 40238
Diatomaceous Earth	MIL-D-20550B	Atlantic Equipment Engineering/Micron Metals
Silicon (IV) Oxide	Amorphous Fumed, 85-115m^2/g	Alfa Aesar PN 42737
Aluminum Powder	Uncoated Atomized	Valimet, PN H2 and H5
Silicone Powder	1-5µm	Atlantic Equipment Engineering/Micron Metals, PN SI-100
Isopropyl Alcohol	Technical Grade	Acros Organics PN 444250050
Ammonium Dihydrogen Phosphate	99.9%, Extra Pure	Acros Organics, PN 193701000
Distilled Water		Fastenal, PN 1027462

3.3. Equipment

3.3.1. Weighing scale (0.1mg resolution)

3.3.2. Resodyn Labram Acoustic Mixer with water cooling jacket

3.3.3. Chiller attached to Resodyn water jacket, capable to 46°F

3.3.4. Convection oven

3.3.5. Vacuum pump capable to 25 inHg

3.3.6. HEPA (2 µm) filters and particle trap for vacuum pump

3.3.7. Convection air dryer

4. PYROTECHNIC SCALE-UP:

4.1. Process Mapping

4.1.1. Figure 4.1.1-1 depicts the general process flow to produce the applicable pyrotechnic mix.

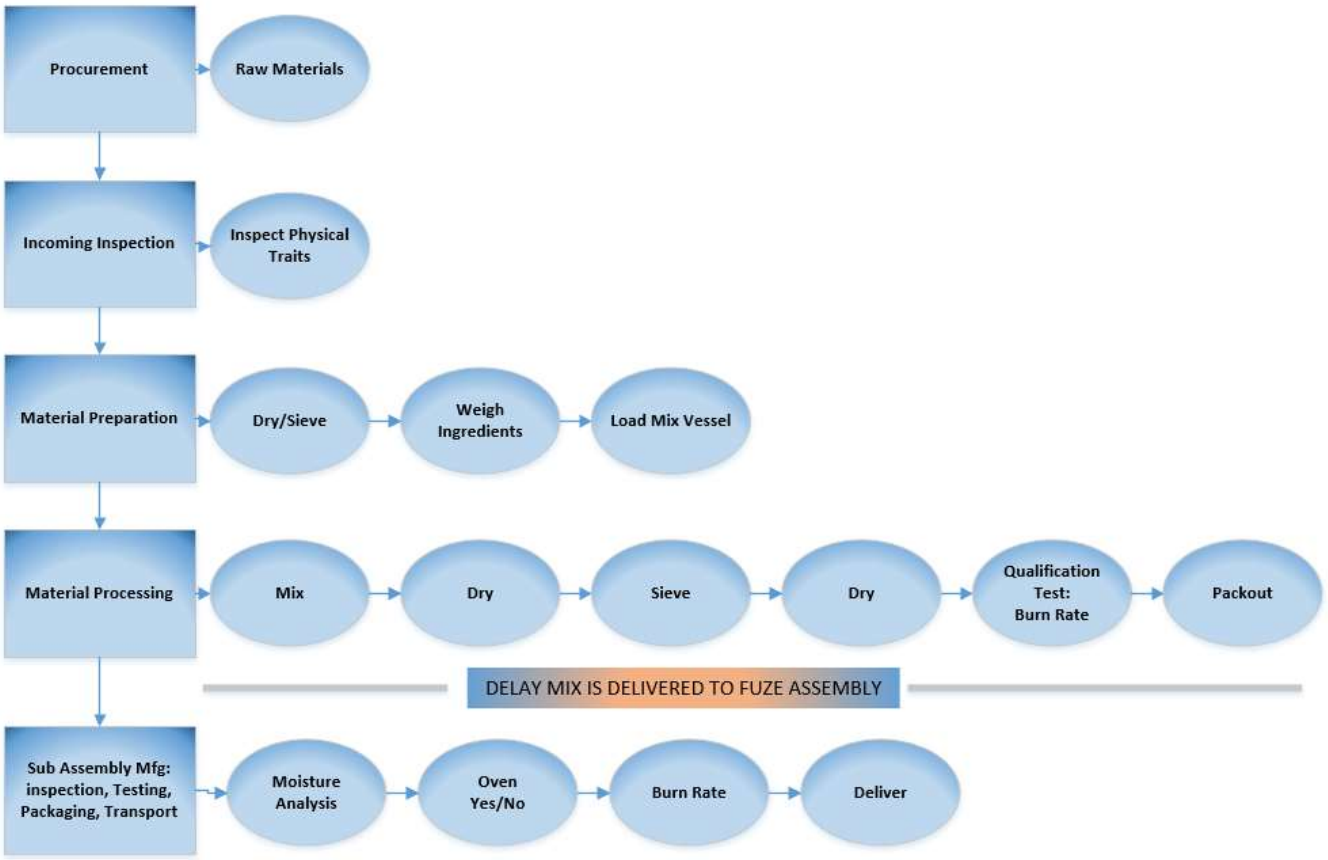

FIGURE 4.1.1-1: Process Map

5. PRE-STARTUP REVIEW

5.1. Assessment of Candidate Compositions

5.1.1. An initial process hazard analysis (PHA) or similar assessment shall be performed. The PHA shall identify, evaluate, and control the hazards involved in the process. The PHA team is responsible for:

a. Conducting and documenting the PHA in accordance with the PHA Facilitator's Guide;

b. Promptly addressing the PHA team's findings and recommendations;

c. Assuring that the recommendations are resolved in a timely manner and that the resolution is documented;

d. Documenting what actions are to be taken;

e. Developing a written schedule of when these actions are to be completed;

f. Communicating the actions to operating, maintenance, and other employees whose work assignments are in the process and who may be affected by the recommendation or actions;

g. One or more of the following methodologies, as deemed appropriate, is used to determine and evaluate the hazards of the process being analyzed:

What-If;

Failure Mode and Effects Analysis (FMEA);

Fault Tree Analysis;

An appropriate equivalent methodology.

5.1.2. The Process Hazard Analysis (PHA) addresses:

a. The hazards of the process;

b. The identification of any previous incident which had a likely potential for catastrophic consequences in the workplace;

c. Engineering and administrative controls applicable to the hazards and their interrelationships such as appropriate application of detection methodologies to provide early warning of releases. (Acceptable detection methods might include process monitoring and control instrumentation with alarms, and detection hardware such as hydrocarbon sensors);

d. Consequences of failure of engineering and administrative controls;

e. Facility siting;

f. Human factors;

g. A qualitative evaluation of a range of the possible safety and health effects of failure of controls on employees in the workplace.

5.1.3. The process hazard analysis is performed by a team with expertise in engineering and process operations, and the team includes:

a. At least one employee who has experience and knowledge specific to the process being evaluated;

b. At least one member of the team who is knowledgeable in the specific PHA methodology being used;

c. May include operating or maintenance personnel, if appropriate;

d. PHAs, updates, or revalidations for each Process Safety Management covered process as well as the documented resolution of recommendations will be retained for the life of the process.

5.2. Assessment: Manufacturing, Fixturing and Tooling (to accommodate Friction, Impact, Static and Heat)

5.2.1. Explosive and personnel limits should be posted in all operating buildings and shall not be exceeded, whenever possible, lesser quantities should be maintained. Remember to follow the cardinal safety rule (3M Rule):

In the explosives community, we handle ammunition and explosives using the cardinal principle…expose the fewest people – to the smallest amount of explosives – for the shortest time possible.

M – Minimize people
M – Minimize explosive quantity
M – Minimize exposure time

5.2.2. The tooling, fixturing and process should minimize any potential for friction, impact, static discharge and heat. Items should be identified and evaluated within the PHA.

5.2.3. Tooling and Equipment –Equipment is typically fixed and is a permanent or semi-permanent installation that comes in contact with energetic materials such as presses and mixers. Tooling is typically a work aid that come in contact with energetic materials such as a powder puck, spatula, or scoop. Tooling and Equipment approved to be used in specific operations shall be defined in Manufacturing Instructions.

5.2.3.1. The following are guidelines for tools and items which are approved for use in areas with specified static electricity controls that may include but not limited to conductive floors, table tops and mats, wrist straps, grounded equipment, tooling and recommended controlled humidity levels.

a. Tooling made of conductive materials such as metal or conductive plastic;

b. Tooling made of non-sparking materials;

c. Containers made of conductive/non-sparking materials such as conductive totes, conductive part holding trays, metal trays and pans and conductive or static dissipative bags;

d. Clipboards, books, notebooks, loose sheets of paper, etc., used to read or record data or follow instructions (this manual included), must be kept at least 1 meter (3.3 ft.) from ESD sensitive items or must be placed in ESD-safe bags or totes. Materials specifically made and verified to be safe in an ESD area are exempt from this requirement;

e. Electronic equipment used in the manufacturing process such as computers, flat screens, tablets, scan guns, and other equipment which can potentially generate a static charge must keep at least a 1-meter separation distance between the location where ESD sensitive material is handled and the equipment;

f. ESD safe or static dissipative tape, containers or transferring fixtures.

5.2.4. Conductive – A material is generally considered conductive if it has a bulk resistivity less than 10^4 Ω-cm. The point-to-point resistance of a conductive item varies depending on the size of the object and where the measurements are taken but is generally less than 10kΩ. Common conductive materials are metals like copper, steel, and aluminum.

5.2.5. Static dissipative – A materials is generally considered static dissipative if it has a bulk resistivity greater than 10^4 Ω-cm and less than 10^{10} Ω-cm. The point-to-point resistance of a static dissipative item varies depending on the size of the object and where the measurements are taken but is generally in the 10kΩ to 10GΩ range. Most static dissipative materials are specially fabricated plastics that contain conductive particles like metal or carbon.

All processes which utilize dry explosive and/or pyrotechnic powders shall be performed in appropriate electrostatic discharge controlled areas utilizing conductive floors, mats, grounded equipment, shoes, gloves and wrist straps. As a secondary electrostatic discharge control method, the minimum humidity values should be established. ESD sensitivity of metal powders varies greatly with particle size. Consult with your cognizant safety personnel when selecting humidity level.

6. HANDLING – PERSONNEL AND MANUFACTURING HYGIENE

6.1. All employees shall wear PPE required as posted for the area; the posting will override all paragraphs within this section.

6.2. All employees must, as a minimum, wear company supplied safety glasses with side shields in manufacturing buildings, test sites/labs, magazines, docks when loading/unloading trucks and chemical laboratories.

6.3. All employees must wear company approved safety shoes when working in manufacturing buildings, test sites/labs, storage buildings, and laboratories. All safety shoes shall have no exposed metal (nails, clips, or tramp metal) on the soles and heels. PPE posting will override all paragraphs within this section. Conductive footwear must be clearly posted in areas where it is required and shall be worn where required.

6.4. When respirators are required, they must be company approved. Consult with your cognizant safety personnel with any questions on respirators or dust mask requirements.

6.5. When wrist straps and conductive footwear are required, they must be company approved. Conductive shoes shall be checked and logged upon first entering the conductive area and re-tested and logged upon reentering the area if the employee has left the building and walked outside with the conductive shoes or has removed the shoes and put them back on.

6.6. When working in ESD sensitive areas, producers shall not wear static producing clothing (nylon or synthetic garments). As a minimum, producers shall wear 50% cotton undergarments, socks and outer garment (such as a lab coat) and conductive footwear.

6.7. Housekeeping

6.7.1. Personnel exits, walkways, aisles and traffic areas shall be kept clear at all times.

6.7.2. Floors, traffic areas, operating areas, and equipment shall be kept clean to prevent accumulation of explosive materials and/or sensitizing materials (sand, grit, etc).

6.7.3. Explosive contaminated material is hazardous waste. All waste materials must be placed in designated waste containers. All waste must be collected regularly and be taken to the proper waste pick-up areas. All holding containers for waste will be properly marked for segregation as to the type of waste. Each waste container must be kept securely covered at all times, unless adding to or removing waste.

6.7.4. All wastewater (mop water) must be placed in the properly designated container.

6.7.5. See Section 9. Cleanup, for methods to handle spills of explosive/pyrotechnic materials.

7. MANUFACTURING PROCESS ASSESSMENT

7.1. Preliminary Manufacturing Instructions – Development Level

7.1.1. The following are general guidelines and recommendations used to produce a mix of 75g of dried material. The associated ratios may be used in the scale-up from the present mix size to that required to meet the demand of M201A1 or M213/M228 fuze production.

7.1.2. Storage of materials should meet recommendations of manufacturer and that proposed within this document.

7.1.3. Prior to mixing, the raw materials should be tested to insure materials consistently meet specifications. Once several different lots of material have been analyzed and consistent results have been obtained, then scaling back on the tests should be considered. See recommended tests depicted in Table 7.1.3-1.

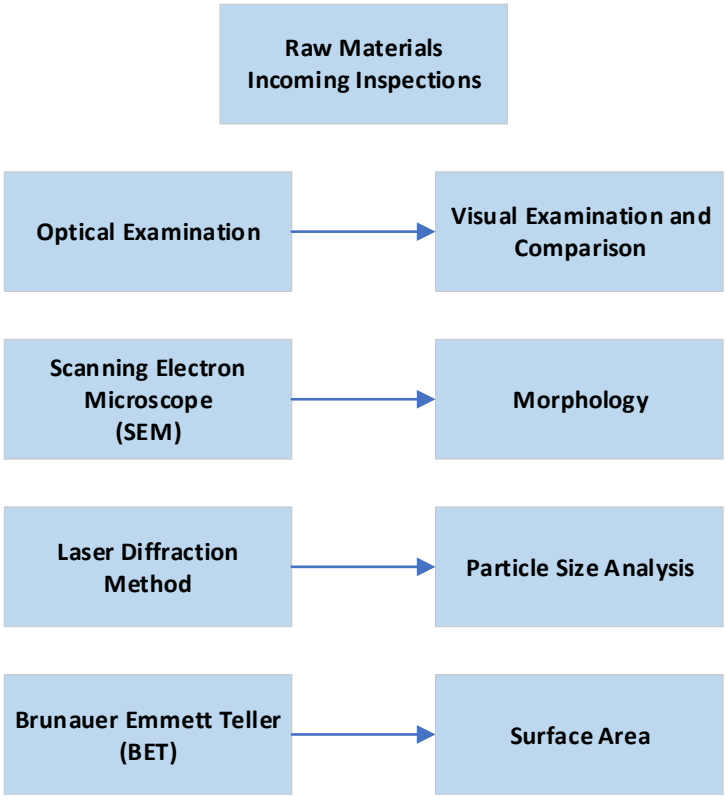

Table 7.1.3-1: Recommended Testing for Incoming Raw Materials

7.1.4. The addition of the raw materials to the mix should follow the material flow chart depicted in 7.1.4-1.

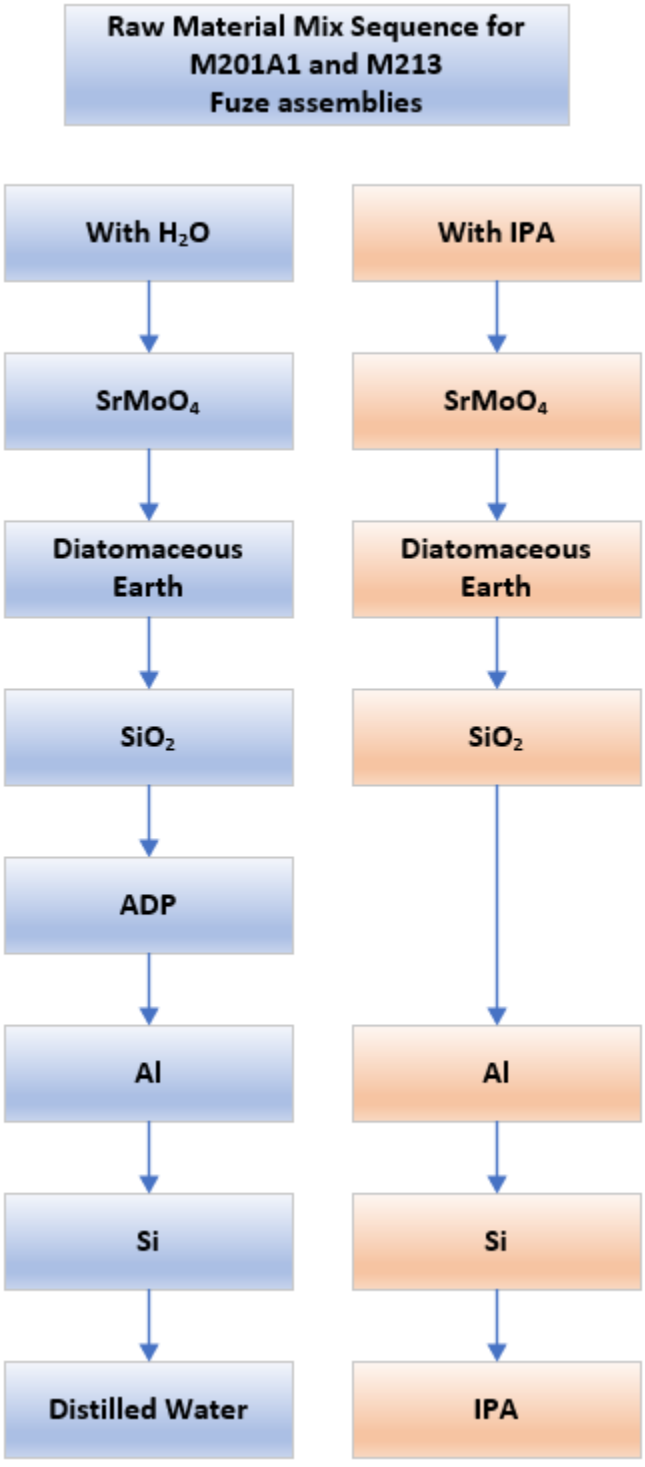

Table 7.1.4 -1: Raw Material Mix Sequence

7.1.5. Below is an estimate of quantity per mix to meet a monthly demand of 10K, 30K or 60K of the associated fuze assemblies. This may fluctuate since it is dependent to the final burn-speed per mix. The estimate is based on the present mix formula that utilizes 0.7g/1.15g for the associated M201A1/M213 fuze, respectively. See Table 7.1.5-1.

M201A1 Assembly Quantity/Month		M213 Assembly Quantity/Month	
Fuzes	lbs/mnth	Fuzes	lbs/mnth
10000	15	10000	25
30000	46	30000	76
60000	93	60000	152

Table 7.1.5-1: Quantity of Mix per Demand

7.1.6. Below is an estimate of raw materials required per mix to meet a monthly demand of 10K (15 or 25lbs), 30K (46 or 76lbs) or 60K (93 or 152lbs) fuze assemblies. This may fluctuate since it is dependent to the final burn-speed per mix. The estimate is based on the present mix formula that utilizes 0.7g/1.15g for the associated M201A1/M213 fuze, respectively. See Table 7.1.6-1 and 7.1.6-2.

M201A1 Assemblies

		w/ H_2O RM: lbs/mnth					w/ IPA RM: lbs/mnth		
RMs	% Mix	15	46	93	RMs	% Mix	15	46	93
$SrMoO_4$	67.24%	10.38	31.13	62.26	$SrMoO_4$	67.50%	10.13	31.05	62.78
DE	4.98%	0.77	2.31	4.61	DE	5.00%	0.75	2.30	4.65
SiO_2	4.98%	0.77	2.31	4.63	SiO_2	5.00%	0.75	2.30	4.65
ADP	0.39%	0.06	0.18	0.36	ADP	-	0.00	0.00	0.00
Al	6.72%	1.04	3.11	6.22	Al	6.75%	1.01	3.11	6.28
Si	15.69%	2.42	7.26	14.53	Si	15.75%	2.36	7.25	14.65

Table 7.1.6-1: M201A1 Raw Materials Required per Demand

M213 Assemblies

RMs	% Mix	w/ H_2O 25	w/ H_2O 76	w/ H_2O 152	RMs	% Mix	w/ IPA 25	w/ IPA 76	w/ IPA 152
$SrMoO_4$	67.20%	10.37	31.11	62.22	$SrMoO_4$	67.50%	10.13	31.05	62.78
DE	5.00%	0.77	2.31	4.63	DE	5.00%	0.75	2.30	4.65
SiO_2	5.00%	0.77	2.31	4.63	SiO_2	5.00%	0.75	2.30	4.65
ADP	0.40%	0.06	0.19	0.37	ADP	-	0.00	0.00	0.00
Al	7.80%	1.20	3.61	7.22	Al	7.90%	1.19	3.63	7.35
Si	14.60%	2.25	6.76	13.52	Si	14.60%	2.19	6.72	13.58

Table 7.1.6-2: M213 Raw Materials Required per Demand

NOTE: The above formulations have been determined from production and testing of small batches of the associated mix. A Resodyn LabRAM acoustic mixer was used to produce a homogenous mix with a final weight of approximately 75g dried material from a mixing cycle time of 22 minutes. Production of larger batches to meet a greater demand should be generated using the same mix ratio's and tested for comparison on uniformity and burn rate to ensure homogeneity and burn-speed meets specifications.

7.1.7. The batch size will be determined by the size of the mixer. The development process utilized 15% of the capacity of the mix vessel. Any scale-up to a larger vessel should consider using same ratio and test to ensure mix meets required physical and burn-speed properties. Table 7.1.7-1 is an estimate for the M201A1 fuze assembly that depicts: 1) estimates for the number of mix cycles, 2) hours of mixing per month, and 3) larger mixers. Estimates are to meet the demand of 10K, 30K and 60K assemblies per month (or 15/46/93 lbs/month). Table 7.1.7.-2 shows same for the M213/M228 fuze assemblies.

%mix /capacity	Type	Vessel Size (lbs)	Mixing min/cycle	Mixing g/mix	RM: lbs/mnth 15	RM: lbs/mnth 46	RM: lbs/mnth 93	
15	LabRAM	1.1		75	93	280	560	cycles/mnth
			22		34	103	205	hrs/mnth
15	LabRAM II	2.2		150	47	140	281	cycles/mnth
			22		17	51	103	hrs/mnth
15	OmniRAM	11		748	9	28	56	cycles/mnth
			22		3	10	21	hrs/mnth
15	RAM5	80		5443	1	4	8	cycles/mnth
			22		0	1	3	hrs/mnth

Table 7.1.7-1: Estimated Cycles and Mix Hours/Month/M201A1

%mix /capacity	Type	Vessel Size (lbs)	Mixing min/cycle	Mixing g/mix	RM: lbs/mnth 25	RM: lbs/mnth 76	RM: lbs/mnth 152	
15	LabRAM	1.1		75	151	460	919	cycles/mnth
			22		55	169	337	hrs/mnth
15	LabRAM II	2.2		150	76	230	461	cycles/mnth
			22		28	84	169	hrs/mnth
15	OmniRAM	11		748	15	46	92	cycles/mnth
			22		6	17	34	hrs/mnth
15	RAM5	80		5443	2	6	13	cycles/mnth
			22		1	2	5	hrs/mnth

Table 7.1.7-2: Estimated Cycles and Mix Hours/Month/M213/228

7.2. Produce Mix

7.2.1. Flow Chart 7.2.1-1 shows the general process flow for the mix preparation.

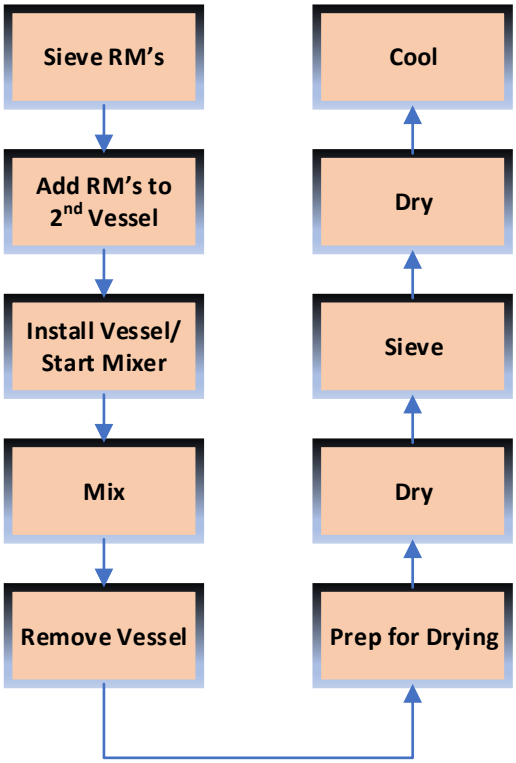

Flow Chart 7.2.1-1: Mix Preparation

7.2.2. All raw materials should be sieved prior to adding to mix vessel. A #200 (75µm) should be used for the $SrMoO_4$ material. All other raw materials utilize a #325 (45µm) size sieve.

7.2.3. Add constituents to 8 oz LabRAM mix vessel in the same flow as shown in Table 7.1.4.1.

7.2.4. Quantities per ingredients should mirror the percentages shown in Table 7.1.6-1 and 7.1.6-2. Constituents should be weighed using a scale with a 0.1mg resolution.

7.2.5. Load and secure mix vessel according to the supplier recommendations (LabRAM I with cooling jacket fixture). See Photograph 7.2.5-1.

Photograph 7.2.5-1: Vessel with Cooling Jacket Secured to Mixer

7.2.6. The vessel shall be wrapped in a cooling jacket with a maintained temperature set at 46°F, using appropriate chiller (Lytron RC011), capable of 32 L/hr flow. Photograph 7.2.6-1 shows the layout of the process cell used for this mix operation.

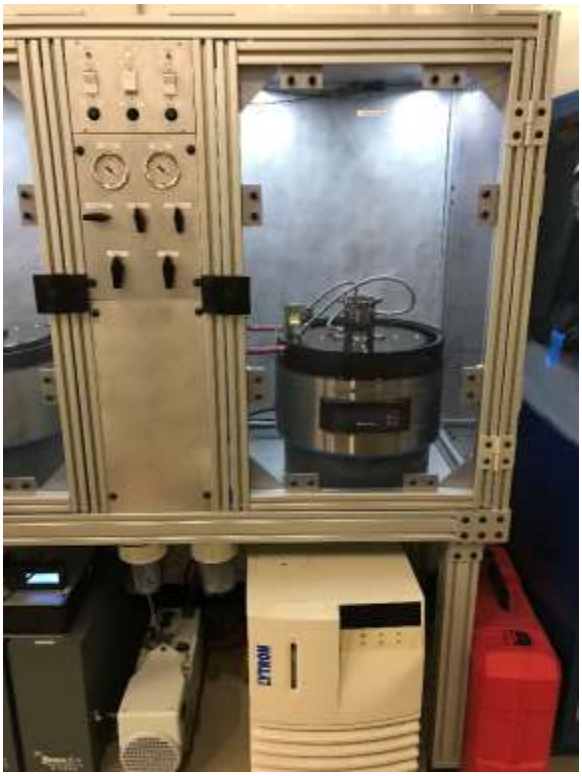

Photograph 7.2.6-1: Layout of Mixing Process Cell

7.2.7. The mix cycle should be set for an acceleration of 50g's for 2 minutes followed by a ramp-up to 75g's for 20 minutes with 25 inHg of vacuum applied at 10 minutes into the second step (after phase change occurs), using an appropriate vacuum pump (Edwards RV8). Particle filters need to be installed before vacuum pump (2 µm HEPA).

NOTE: The vacuum process is not required during the mix operation for the Isopropyl alcohol (IPA) process. This is due to the volatility with a high evaporation rate of the IPA that will alter the processing liquid to solids ratio during mixing.

7.2.8. Once mix cycle is complete, remove the vessel and scoop the mix onto appropriate drying trays (conductive Teflon sheets). Spread the material into a thin layer to prevent gravitational segregation (approximately 0.10 inches thick).

7.2.9. Dry material in a convective air dryer at 68°F temperature for 2 hours, at 30% relative humidity or less.

7.2.10. Remove powder from oven and screen material through a #40 (425µm) sieve.

7.2.11. Spread powder onto a tray and insert into oven set to a temperature of 302°F for 3 hours minimum.

7.2.12. Remove powder from oven and scoop or pour into appropriate container and allow to cool in a desiccator at less than 1% relative humidity until all materials reach room temperature.

7.2.13. Packaging is dependent on if mixing is performed at point of use. If this is the case, then conductive plastic containers with a secure snapping lid may be used to store the powder. Containers should remain in either a desiccator or heated storage until use. Size of container may also be dependent on method to transfer powder at the next level of fuze assembly. If mix is required to be shipped offsite, then follow CFR 49, Parts 100 – 199.

8. QUALIFICATION

8.1. General quality assurance provisions should adhere as specified in the contract and/or purchase order.

8.2. Recommended Tests: Methods should be defined in contract and/or purchase order.

8.2.1. Burn-speed: should be performed to ensure timing results meet associated requirements. Testing may be performed per MIL-C-13739A or similar method. Typically this is performed by loading/pressing the mix into the fuze body per the prescribed pressures and increments (quantity of load/press cycles) to meet specifications (e.g. charge height, density, etc…).

8.2.2. Moisture: Perform required method to determine percent moisture per mix. Samples should be collected at various locations within the mix.

8.2.3. Composition: Perform required tests to determine percent composition of each raw material. Samples should be collected at various locations within the mix.

9. CLEANUP

9.1. Spill Cleanup

Spills of explosives, pyrotechnics (delays), propellants, or materials containing explosives or pyrotechnics (delays) or propellants, shall be cleaned up immediately. Spill response activities shall follow the requirements specified within the facilities action plans. Consult with your cognizant safety personnel with any questions.

NOTE: The following represent guidelines for the various types of spills that could be encountered. The manufacturer's SDS should be consulted for all spills. When any doubt exists, the product vendor should be consulted by using the telephone number on the applicable SDS.

9.1.1. Responsibilities of second operator if spill is outside of the machine:

a) Acknowledge to the operator that you heard that a spill occurred. Obtain from the operator what spilled, amount and general area of the spill;
b) Do not step near the energetic spill;
c) Protect or guard the area so no one inadvertently enters the area;
d) Notify Area Supervisor and the Response Coordinator.

9.1.2. Responsibilities of operator who has spilled material and is utilizing a Man Down radio.

a) STOP;
b) DO NOT MOVE;
c) Wait until assistance arrives to the area;
d) If Anyone Comes By, Warn Them To Stay Clear Of The Spill Area;
e) Emergency Response Team members will then follow proper instructions per Spill Containment Clean up procedure.

9.1.3. Prior to initiating a clean-up a clean-up procedure will be developed based on the material spilled, the quantity of material spilled and the location of the spill. Only properly trained personnel can perform the spill clean-up.

9.1.4. Solvent: If the solvent is spilled anywhere, provide ventilation to a spill area. Gloves and adequate ventilation or a respirator is required.

9.1.5. Solvent-wet mix: If a wet mix is spilled anywhere, cordon off the area and remove any ignition sources. Add water or oil as needed to keep the material wet. Collect the material in a static-proof bag and seal. Consult with Regulatory Compliance for disposal of material.

WARNING: Dry material is susceptible to ignition. Failure to wet down material prior to clean up may result in ignition causing injury.

9.1.6. Dry mix: If a dry mix is spilled anywhere, cordon off the area and remove any ignition sources. Dry mix should be wet down with water until completely saturated. Collect the

material in a static proof bag and seal. Consult with Regulatory Compliance for disposal of material.

9.1.7. Operational Cleanup - Instructions on operational cleanup should be developed and specific to raw materials, the mixture (of raw materials), associated tooling and equipment.

9.2. WASTE DISPOSAL

9.2.1. Prepare all hazardous waste materials for disposal per Regulatory Compliance department guidelines.